CIVIL ENGINEERING STUDIES
STRUCTURAL RESEARCH SERIES NO. 126

DEVELOPMENT OF PROCEDURES FOR RAPID COMPUTATION OF DYNAMIC STRUCTURAL RESPONSE

By
JOHN W. MELIN

Approved by
N. M. NEWMARK

FINAL REPORT FOR THE PERIOD
1 JULY 1955 to 30 JUNE 1956
CONTRACT NO. AF 33(600)-24994
for
PHYSICAL VULNERABILITY DIVISION
DIRECTORATE OF INTELLIGENCE
U. S. AIR FORCE

UNIVERSITY OF ILLINOIS
URBANA, ILLINOIS

UNIVERSITY OF ILLINOIS

DEPARTMENT OF CIVIL ENGINEERING

URBANA, ILLINOIS

DEVELOPMENT OF PROCEDURES FOR RAPID COMPUTATION OF DYNAMIC STRUCTURAL RESPONSE

by

John W. Melin

Approved by

N. M. Newmark

Final Report
for the Period from
1 July 1955 to 30 June 1956

Contract No. AF 33(600)-24994

for
Physical Vulnerability Division
Deputy Director for Targets
Directorate of Intelligence
Headquarters, USAF
Washington 25, D. C.

ACKNOWLEDGMENT

This report is a final report for the period from 1 July 1955 to 30 June 1956 of a research project conducted in the Engineering Experiment Station of the University of Illinois, Department of Civil Engineering, and sponsored by the Physical Vulnerability Division of the Directorate of Intelligence, USAF, under Contract AF33(600)-24994. This report includes the results of the third year of investigation. The work of the first two years has been previously reported in the Final Reports of 1 July 1954 and 1 July 1955.

This investigation is under the general direction of N. M. Newmark, Research Professor of Structural Engineering and under the immediate supervision of John W. Melin, Research Assistant in Civil Engineering. The studies described in this report were conducted by Charles D. Bigelow, Samuel Stucliffe, Research Assistants in Civil Engineering and John Melin. Assistance in this work was also given by William H. Beutjer, an undergraduate in Civil Engineering.

Of invaluable aid in the preparation of the many tapes for use on the ILLIAC and in the performance of other clerical requirements was Mrs. Florence M. Bauer, Computer Teletype Operator.

The author wishes to acknowledge the fine cooperation of the Digital Computer Laboratory in the performance of the many numerical studies on the ILLIAC, the digital computer at the University of Illinois. Of particular help was the advice and assistance of John P. Nash, Research Professor of Applied Mathematics.

CONTENTS

	Page
ACKNOWLEDGMENT	i
LIST OF FIGURES	iii
INTRODUCTION	1
Objectives of Program	1
Phases of Investigation	2
SIMPLE STRUCTURAL SYSTEMS	5
Single-Degree-of-Freedom System	5
Structural Parameters	6
External Force Parameter	8
Equation of Motion	10
Maximum Response Charts	12
Time of Maximum Response	13
Delayed Rise Pulse Study	14
Damage Pressure Level	17
MULTISTORY STRUCTURAL ANALYSIS	22
Shear Beam	22
Natural Frequency	23
Bent Analysis	24
SUMMARY	26
NOMENCLATURE	27
REFERENCES	30
INDEX FOR FIGURES	31
FIGURES	34
DISTRIBUTION	137

LIST OF FIGURES

Figure No.	Title
1	Single-Degree-of Freedom System
2	Resistance Functions
3	Applied Forces
4-8	Maximum Response of Mass-Spring System to Initial Peak Triangular Pulse with Initial Impulse
9-13	Time of Maximum Response to Initial Peak Triangular Pulse with Impulse
14-33	Time of Maximum Response to Delayed Rise Triangular Force Pulse of Fig. 3c with Two Impulses
34-38	Maximum Response versus Rise Time for Delayed Rise Triangular Force Pulse with Elasto-Plastic Resistance
39	Maximum Response versus Rise Time for Delayed Rise Triangular Force Pulse with Impulses
40-49	Maximum Response versus Rise Time for Delayed Rise Triangular Force Pulse with Various Second Resistances
50	Unstable Bilinear Resistance
51	Energy Level versus Displacement for Unstable Bilinear Resistance

DEVELOPMENT OF PROCEDURES FOR RAPID COMPUTATION OF DYNAMIC STRUCTURAL RESPONSE

INTRODUCTION

Objectives of Program

This program is concerned primarily with the behavior of structures, structural elements, and complicated assemblages of elements subjected to the dynamic forces arising from air blast or ground shock. This behavior is measured by deflection or stress, permanent deformation, damage, or collapse. The general objectives are:

1. Development of charts or of rapid "rule-of-thumb" methods for the prediction of critical levels of blast intensity to produce severe damage or collapse of specific structural types.

2. Construction of charts or other rapid procedures for the rapid determination of the magnitude of response of specific structural types to various levels of intensity of blast or shock.

3. Critical examination of the accuracy of predictions of critical levels of force, or of magnitude of response, in terms of the uncertainties in values of blast parameters, structural characteristics, and material parameters.

4. Survey of the present state of knowledge relative to those items in Objective 3 which cause the greatest uncertainty in the predictions, and preparation of plans for further study of these items.

5. Development of methods of calculation suitable for the accurate solution of problems of dynamic response in complicated structures using high speed automatic digital computers; preparation of basic

codes for the determination of dynamic response of important classes of structures; and where necessary, calculation of responses for a range of values of structural parameters and of blast parameters.

Thus far the primary studies have been directed toward the development of general methods for determining and interpreting the response of simple structures. This has been accomplished by computing charts of maximum response for an extensive range of both structural and force parameters.

Approximate procedures for predicting critical pressure levels for simple structural systems have been developed and the results of such procedures have been compared with more exact data. The exact data have been presented in charts, and were obtained from solutions using the ILLIAC, the University of Illinois automatic digital computer. The application of the necessary methods of analysis on the automatic computer was accomplished by this project.

Present emphasis has been directed toward extension of knowledge of dynamic structure behavior. The approximate methods found applicable to simple structures are being used to analyze more complex structures. Numerical methods of analysis using ILLIAC have been developed for complex structural systems. Extensive studies of critical areas of response of simple structural systems are being conducted.

Phases of Investigation

The study of simple structures has been directed towards establishing general trends for dynamic response under transient forces. For analysis, the structure's mass has been concentrated at the top of

the columns and the shearing stiffness of all of the columns has been replaced by an equivalent spring, forming a single-degree-of-freedom system. The transient forces acting on the model have been representative of net equivalent forces which would act on the actual structure and the resistance function accounts for the inelastic action of the columns. This model has been used in response calculations for a large range in both blast parameters and resistance parameters, the results of which have been represented in numerous charts.

Approximate methods of predicting damage pressure level have been developed and extended to a point where it is possible to predict the damage pressure level for most of the types of blast force pulses acting on a structure with a completely general resistance function. Some effort has been directed toward increasing the generality of the type of force pulse applicable to the approximate damage pressure level formula.

A general study of the effects of variation of parameters was conducted and special emphasis was directed towards critical ranges of the parameters. Studies of this nature will be continued in an effort to further establish our knowledge of dynamic behavior of structures.

Many structures do not behave as a simple single-degree-of-freedom system but rather as a series of masses with interconnecting springs. Even these complex systems generally respond in one general mode thus making an approximate simple analysis possible. Several codes for analysis of complex systems using the ILLIAC have been developed in order to establish trends, and to obtain more exact solutions for checking purposes. The development of analogies between simple systems and complex systems is still in the initial stages with several codes

for complex analysis having just been completed. Preliminary studies indicate that the methods of anaylsis used on simple systems may be applied to complex structural systems to a slightly lesser degree of accuracy.

The multi-degree-of-freedom studies, because of their inherent complexities, are not conducive to detailed studies similar to the extensive studies of simple systems. With the knowledge of simple structural response, it is possible for the critical parameter ranges of complex systems to be established and studied in closer detail.

SIMPLE STRUCTURAL SYSTEMS

The Single-Degree-of-Freedom System

The single mass-spring replacement system is used primarily because of its comparative simplicity. Although structures respond to dynamic forces in an infinite number of degrees of freedom, for the most part only one mode is predominant. Thus the simple analogy yields a good approximation of the dynamic response of actual structures.

The mass-spring system is especially adaptable to the analysis of single story structures where the mass of the actual structure is concentrated at the top of the columns. The shearing stiffness of all the columns is taken equivalent to the single spring of the analogy. Thus the period of vibration of the replacement systems equals the period of the fundamental mode of vibration of the structure for small displacements. The weight of the structure plus the transient forces acting on top of the structure cause an overturning moment which increases linearily with displacement. These effects plus the effects of damping are accounted for in the analysis.

The single story industrial mill building shown in Fig. 1 is a good example of a single-degree-of-freedom system. The weight of such a structure is concentrated in the roof system which is generally very stiff compared to the lateral stiffness of the columns. The roof acts as a rigid body with very little differential displacement. There is little or no vertical motion accompanying the lateral motion caused by the dynamic forces. The columns are assumed to yield in a manner such that their total shearing force may be expressed as a multi-linear

function of displacement. From the forces acting on the entire structure it is necessary to compute the net force acting as a function of time on the concentrated mass.

This project is concerned primarily with the establishment of the dynamic characteristics of the analogous structure and the effects of each parameter on the response and damage pressure levels for the replacement structure. The application of the characteristics of the replacement structure to the analysis of actual structures under actual loads is being conducted by Armour Research Foundation under Contract AF33(600)-25734.

Structural Parameters

Ideally the replacement system should have a resistance identical to the actual structure during the loading cycle. That is, the replacement resistance should account for possible yielding of the columns and the resulting permanent set after unloading, or elastic unloading if yielding does not occur. Such a replacement system would be limited to the analysis of only one structure however.

Therefore in order to study the response characteristics of large groups of structures it has been necessary to choose a replacement resistance which approximates a large number of structures and then study the effects on response caused by minor changes in this resistance function. In this manner it has been possible in many cases to demonstrate that two seemingly unsimilar structures have essentially the same response characteristics.

For example, consider a single bay mill building with a flexible roof system. The bases of the columns may yield first as the structure is loaded and then the tops of the columns may yield later resulting in a constant resistance for larger displacements. It has been shown that a bilinear replacement resistance which has an equivalent energy level for any displacement greater than the yield displacement of the tops of the columns will have very similar response characteristics to the actual structure which has a trilinear resistance. Thus all of the response knowledge for a bilinear resistance function may be used directly in the analysis of the actual structure.

The bilinear resistance function has been found to be easily comparable to the resistance of almost all simple structures. This replacement resistance is shown graphically in Fig. 2. Figure 2a shows the resistance in terms of the actual structure, that is, in terms of the numerical value of yield resistance (q_y) and yield displacement (x_y). Figure 2b demonstrates the dimensionless form of the bilinear resistance which has been used in all of the studies of this project. Thus all the results may be applied to any structure.

The value of the yield resistance of a structure is known to be a function of the strain rate of loading. Although the analysis does not take cognizance of the strain rate or evaluate the yield resistance during the solution, the range of effect of this and similar phenomena may be obtained directly from charts prepared by this project.

The resistance which has been used in computing response by means of the ILLIAC is similar to the bilinear resistance shown in

Fig. 2, except for unloading which follows the initial elastic slope of the resistance. In this way the permanent set due to inelastic strain is accounted for in the analysis. Codes are available for finding the response when the resistance function can not be approximated with a bilinear replacement. For such a structure the resistance may be expressed by n straight lines. These codes have been used to establish general relationships between bilinear resistance and n-line resistance, and for the analysis of specific structures.

The natural period of vibration of the structure may not necessarily be equal to that of the replacement system. The initial stiffness of the replacement is chosen primarily in order to balance the energy level of the systems and also the actual mass may not equal the effective mass of the structure. Both of the above factors affect the ratio of the periods of the model and the original structure.

The nomenclature pertaining to the resistance parameters is presented in a section following the text of this report. Both the regular and dimensionless forms are given.

External Force Parameter

As in the case of the resistance parameters, an exact replacement force function would not be practical. The effective force function is controlled by numerous factors. The weapon size and position, in addition to the physical characteristics of the structure, have a direct influence on the forces. The overall dimensions, the permanence of the walls, and the drag coefficients influence the

magnitude of the forces. Primarily only triangular force pulses have been studied. The relationship between the highly erratic actual effective force and the generalized triangular pulse is difficult to evaluate exactly. However many basic principles and good approximations have been developed. The continued development along such lines is considered to be one of the primary studies of this project.

From the studies it has been possible in many cases to establish what are the most important factors of the force pulse parameters and also what errors are involved when certain irregularities in the actual pulse are neglected.

In the general studies performed using the ILLIAC, the force function has been expressed as a linear function of time with very sharp short duration peaks being represented by impulses. All of the force pulses have been expressed in terms of the yield resistance and the period of vibration of the structure to facilitate more general application.

Figure 3a shows the replacement representation of the initial peak triangular force pulse. The study of the initial peak triangular force pulse was presented in the Final Report of 1 July 1954 of this project and has been extended and clarified in both the Final Report of 1 July 1955 and this report.

The study of dynamic response to a force pulse with precursor, Fig. 3b, was discussed with charts in the 1 July 1954 Final Report of AF 24994. This study is presently being considered for extension to more critical ranges of parameters.

The study of response to delayed rise triangular force pulses has been extended to rise times equivalent to static loading for the general class of structural resistances. The delayed rise pulse is depicted in Fig. 3c and 3d. Figure 3d gives the dimensionless form which was used in these studies. The response study for delayed rise force pulses with and without impulses has been presented in the 1 July 1955 Final Report and the 1 January 1956 interim report with the corresponding time of maximum response charts appearing in this report.

The nomenclature used is given in the nomenclature section following the text of this report. The particular force pulses used in various studies are described in more detail under the headings of the individual studies.

Equation of Motion

The equation for the replacement system shown in Fig. 1 is:

$$m\ddot{x} + q(x) = p(t) \qquad (1)$$

where m is the mass

$\ddot{x}$ is the acceleration

$q(x)$ is the shear resistance expressed as a function of displacement

$p(t)$ is the external force which is a function of time.

The solution of the above by integration from time zero until such time as a maximum response occurs, has been stated in the previous Final Reports of this project. Also the numerous codes previously developed for solution of the problem using the ILLIAC has been outlined.

Briefly the procedure used is as follows:

The acceleration at a short time (Δt) in the future is approximated by assuming that only the external forces change. Integration of the acceleration twice by means of Newmark's β method, which is described in detail in reference 3, yields a new displacement. The acceleration is then recalculated taking account of both internal and external forces. The resulting acceleration is again integrated to obtain a new displacement. This iterative procedure is repeated until the acceleration assumed equals the calculated acceleration. Then the process is started again, for a time (Δt) further in the future. It is thus possible to plot response versus time, thereby obtaining the maximum response of the system.

In this way the differential equation of motion may be solved for inelastic dynamic response problems to an accuracy greater than that required for general engineering work, provided the actual structure behaves like the model.

The effects of other parameters may be included in the analysis and solved by the same means. The effects of damping, static and transient vertical loads are included in the following equation:

$$m\ddot{x} + c\dot{x} + q(x) = p(t) + \frac{x}{h}\left[v(t) + w\right] \qquad (2)$$

where c is the damping coefficient

$v(t)$ is the transient vertical force

w is the static vertical load

h is the height of the mass

The effect of impulse is accounted for by changing the velocity instantaneously at the time that impulse occurs.

Maximum Response Charts

As part of the objective of this project numerous charts have been developed for the rapid computation of dynamic structure response. These charts have been made from data computed using the ILLIAC. The response charts for the initial peak triangular force pulse study with impulse and the delayed rise triangular force pulse studies have been prepared using the same pattern of parameters. The response charts for the initial peak triangular force pulse study and the delayed rise triangular force pulse study with a rise time of one-half the period of vibration were presented in the 1 July 1955 Final Report of this project while the response charts for the delayed rise triangular force pulse studies for rise times of one, one and one-half, and twice the natural period of the structure were printed in the 1 January 1956 Interim Report of this project.

The parameters were as follows:

One chart was prepared for each of five second slopes of the bilinear resistance function. The ratio of second slopes to first slope equaled +0.1, +0.02, 0.0, -0.02, -0.04. This resistance function is shown in Fig. 2a and 2b.

Two equal impulses were applied to the structure one at time zero, and one at the time of maximum peak pressure. For the initial peak study this was equivalent to two impulses at time zero. The

relative values of the impulses were varied from +0.5, including +0.25, +0.05, +0.0, -0.05, -0.25, to -0.5.

In this report the response charts for the initial peak triangular force pulse study have been replotted and extended. There is one set of charts for each value of second slope of the bilinear resistance function and one chart in each set for a constant value of impulse. The value of second slope, and impulse is given on each chart and also in the Index of Figures preceeding the charts. On every chart the response in terms of yield displacement (x_m/x_y) is plotted against pulse duration in terms of the period of the system (t_d/T). There are lines of constant peak pressure in terms of yield resistance covering the entire range of applicable pressures. The dashed line indicates that the maximum response was negative. The study data are presented in Figs. 4 through 8.

Time of Maximum Response

As an integral part of the response studies for initial peak and delayed rise force pulses, the time of maximum response has been obtained. The charts of time of maximum response for both studies are presented in this report in Figs. 9 through 33. The study includes one group of charts for each rise time, t_1/T = 0, 0.5, 1.0, 1.5, 2.0. A group contains one set of charts for values of second slope of the bilinear resistance of +0.1, +0.02, 0.0, -0.02, -0.04. Within a set, there is one chart for each of the following maximum peak pressures in terms of the yield resistance p_m/q_y = 10, 5, 2, 1.0, 0.5, 0.0. The

charts are plotted with lines of constant impulse for times of maximum response versus duration of the force pulse. Both the time of maximum and the duration are expressed in terms of the natural period of vibration of the system. The dashed lines of the chart are the times of maximum for response maximums which are negative. The discontinuities between dashed lines and solid lines are due to the lag in time between the time of maximum negative response and the time of maximum positive response. The time lines are cut off when the maximum response exceeds the boundaries of the maximum response study.

Delayed Rise Pulse Study

A set of charts have been prepared for response versus rise time in an effort to demonstrate directly the effect of rise time of the delayed rise triangular force pulse on response of the single-degree-of-freedom system. The results are presented in Figs. 34 through 49. This study cross checks the previous delayed rise studies which have been published in the 1 July 1955 Final Report and the 1 January 1956 Interim Report of this project. By correlating the two studies it is possible to predict approximately the response levels for any rise time up to twice the natural period of vibration.

The response versus rise time study demonstrates directly the range of errors in predicting response and the approximate response for rise times up to that for which the response is nearly static. The study was conducted in two phases.

For the first phases an elasto-plastic resistance was subjected to delayed rise triangular force pulses with the total duration (t_d/T) constant. The response was plotted against rise time for lines of constant ratio of peak pressure over yield resistance. The total pulse durations used were t_d/T = 2.0, 5.0, 10, 100, 1000.

The second phase demonstrates the effect of variation of the second slope of the bilinear resistance. The ratio of second stiffness to initial stiffness was varied from +0.1 including +0.02, 0, -0.02, to -0.04. The pulse duration is constant for each chart. For one set the duration is 10 times the period and for the other the duration equals 100 times the period of vibration.

For an example of the establishment of response range, consider a rise time of about 1.3 times the natural period. Let the resistance be elasto-plastic, the duration of the force pulse equal 8 times the natural period, and the peak pressure equal the yield resistance.

From chart 35 of this report the response equals 1.28 for a duration of 5 and from chart 36 the response equals 1.5 for a duration of 10. Thus the response when the duration is 8 equals about 1.4 times the yield displacement. It is very important that the structural analyst continue his study beyond this point and establish the range of response errors. For example, if the error in predicting yield resistance is 20 per cent and in predicting peak pressure is also 20 per cent, it is thus possible for the ratio of peak pressure to yield resistance to range from 1.4 to 0.6. From the charts it can be

shown that the corresponding response varies from elastic to about sixty times the yield displacement. For most structures collapse would occur before the ductility factor reached 60. Therefore the response varies from elastic to collapse depending upon the direction of the errors in predicting resistance and peak pressure. It is thus necessary for the analyst not to establish a response but rather a range of response.

The damage pressure level presents a much better criterion for design in that it is a more stable parameter than response. It is still necessary to establish a range in damage pressure before any confidence may be placed upon the results obtained.

Maximum response versus rise time for the triangular pulse with impulse, shown in Fig. 39, vividly demonstrates the erratic effect of impulses. In this chart is shown that the studies of delayed rise triangular force pulse with constant rise time presented in the 1 July 1955 Final Report and the 1 January 1956 Interim Report must be used with caution when impulses are considered. Notice in Fig. 39 that the response maximums for a pulse without impulse are out of phase with the maximum for a pulse with impulses. For instance if one assumed that the maximum of the maximum responses for rise times between one and two times the period occurred when the rise time equals 1.5 times the period of vibration, the result taken from the chart would actually be closer to a minimum if an impulse of about 0.05 $q_y T$ accompanied the force pulse.

Damage Pressure Level Approximate Formula

An approximate equation for predicting the peak pressure level of initial peak triangular force pulse necessary to cause a given response for a structure having any resistance displacement relationship, has been developed by Dr. Newmark. The procedure is based on the principle of balancing the external force energy with the internal resistance energy and was presented in an ASCE paper.(4) The formula was generalized further in the 1 July 1954 Final Report of AF 24994 and redefined for the unstable resistance functions in both the 1 July 1955 Final Report and the 1 January 1956 Interim Report of this project.

The formula was developed from two classical exact solutions for damage pressure level. The exact solutions exist for force durations which are infinitely long or very short. The approximate formula for damage pressure level for a force pulse with a duration between the two limits was obtained by adding the two exact solutions with an empirical factor which makes the prediction correct at the two limits of pulse duration.

For a short duration pulse with impulse the initial kinetic energy must balance the work. Thus in dimensionless form the pressure level equals the effective resistance minus the effect of the impulse.

$$p'_m/q_y = \frac{T}{\pi t_d}\left[\left(\frac{2\mu q_{ave}}{q_y}\right)^{1/2} - B\right] = \frac{T}{\pi t_d}\left(A^{1/2} - B\right) \qquad (3)$$

where p'_m is the short duration pulse pressure level

q_y is the yield resistance

T is the period of vibration

t_d is the duration of the pulse

$q_{ave} = \frac{1}{x_m} \int_0^{x_m} q\, dx$ is the average resistance

$\mu = x_m/x_y$ is the ductility factor

$B = \frac{2\pi\, p_i t_i}{q_y T}$ is the effect of initial impulse

For a long duration force pulse with impulse the damage pressure level equals the average resistance minus the initial impulse factor

$$p''_m/q_y = q_{ave}/q_y - B^2/2\mu \qquad (4)$$

where p''_m is the damage pressure level for long duration force pulses.

For any pulse duration the approximate equation for damage pressure level is:

$$p'_m/q_y = p'_m/q_y + \frac{p''_m/q_y}{1 + \frac{0.7T}{t_d}} \qquad (5)$$

The above form is applicable for any resistance function for which the resistance does not decrease after yield. The unstable case is defined by a resistance which decreases after yielding occurs.

The following example of the damage pressure level for unstable bilinear resistance was given by Dr. N. M. Newmark. The energy level for any displacement is shown in Fig. 51 by curve AG. The energy level of resistance for this case follows two parabolic curves, one with an origin at A and the other originating at G. The parabolas are tangent at B the yield displacement.

The pressure for the long duration pulse shown in Fig. 50b appears as a sloping line on the energy diagram. Thus the damage pressure level necessary for a given response may be obtained directly as the slope of a line drawn from E_1, the initial energy level due to the impulse, to D, the energy level of resistance for the given displacement x'_m. The maximum pressure level necessary for any displacement greater than x_γ is obtained by drawing a line tangent at E to the resistance energy level AG from E_1, the impulse energy level. The maximum pressure level is defined as p_γ and the corresponding maximum energy level as E_γ at a displacement x_γ. For any given displacement x''_m greater than x_γ, the damage pressure level is p_γ and not the p_m obtained by constructing a line from E_1 to F. It is therefore apparent that x_γ is an important parameter against which any given x_m must be compared. The equation for x_γ is obtained from geometric relationships.

The energy level for yield displacement equals the area under the resistance diagram Fig. 50a up to x_y. Similarly the maximum resistance available is equal to the area under the entire resistance function. The latter is also equal to the energy level of an impulse required to cause collapse.

$$E_y = \frac{1}{2} q_y x_y \tag{6}$$

$$\frac{I_o^2}{2m} = E_o = \frac{1}{2} q_y x_o \tag{7}$$

where I_o equals the impulse necessary to cause collapse. The energy level for any displacement between x_y and x_o is equal to maximum energy

level minus a constant times square of the difference x_o and the given x.

$$E_x = E_o - c\,(x_o - x)^2 \tag{8}$$

The constant is evaluated to be equal to the difference in maximum and yield energy levels divided by the square of the maximum ductility factor by letting $x = x_y$

$$E_y = E_o - c\,(x_o - x_y)^2 \tag{9}$$

or

$$c = \frac{E_o - E_y}{(x_o - x_y)^2}$$

Substitution of equation 6, 7, 9, in 8 yields

$$E_x = \frac{1}{2} q_y \left[x_o - \frac{(x_o - x)^2}{(x_o - x_y)} \right] \tag{10}$$

p_γ is the first derivative of equation 10 evaluated at x_γ

$$\left.\frac{\partial E}{\partial x}\right|_{x=x_\gamma} = p_\gamma = q_y \left(\frac{x_o - x_\gamma}{x_o - x_y} \right) \tag{11}$$

From the geometry of parabolas $h_1 = h_2$, thus average of E' and E_γ equals E_o since

$$E' = E_1 + p_\gamma x_o \text{ and } E_\gamma = E_1 + p_\gamma x_\gamma$$

Substitution of (11) yields

$$E_1 + q_y \left(\frac{x_o - x_\gamma}{x_o - x_y} \right) \frac{x_o + x_\gamma}{2} = \frac{1}{2} q_y x_o = E_o \tag{12}$$

Therefore solving for x_γ

$$x_\gamma^2 = \frac{E_1}{E_o} (x_o^2 - x_o x_y) + x_o x_y \tag{13}$$

Remembering that

$$E_1 = \frac{I_1^2}{2m} \quad \text{and } E_o = \frac{I_o^2}{2m}, \; \mu_o = \frac{x_o}{x_y}$$

then

$$x_\gamma = \frac{I_1}{I_o} \sqrt{x_o^2 - x_o x_y} + \sqrt{x_o x_y} \tag{14}$$

or

$$\mu_\gamma = x_\gamma / x_y = \mu_o^{1/2} \left[1 + \frac{I_1}{I_o} (\mu_o - 1)^{1/2} \right] \tag{15}$$

After the critical response x_γ is known then the damage pressure level may be found according to the following limits set by x_γ for the unstable bilinear resistance

For

$$x_m < x_y \quad p_m/q_y = p_m'/q_y + \frac{p_m''/q_y}{1 + \frac{0.7T}{t_d}} \tag{16}$$

or for

$$x_m > x_\gamma \quad p_m/q_y = p_m'/q_y + \frac{p_\gamma/q_y}{1 + \frac{0.7T}{t_d}} \tag{17}$$

A similar derivation is possible for more general resistance functions, and has been discussed in the two previous annual reports.

MULTISTORY STRUCTURAL ANALYSIS

Shear Beam

The initial study of dynamic response of multistory structures was presented in the 1 July 1955 Final Report of this project. This study was devoted to the analysis of three story shear beam structures subjected to initial peak triangular force pulse loads. The shear beam resistance by definition assumes the floor systems of the structure to be infinitely stiff. The relative stiffness of the columns was varied from 1.0, 0.3, 0.2 where the same column extends over the entire height of the structure to a stiffness comparable to an earthquake design for which relative lateral stiffness varied in a ratio of 1, 1.1, 1.2 from top spring to bottom spring. The typical design probably would have about a constant lateral stiffness over the height. Thus this study although brief has covered the range of lateral shearing stiffnesses for a three story structure.

Two general trends were observed from the results of this study.

1) The lower story of the structure receives the most damage from impulse type loads. That is a fairly good estimate of damage pressure level may be obtained by assuming the upper two stories to be rigid thereby reducing the structure to a simple system to which the damage pressure level approximate formula may be applied.

2) For long duration loads the story which would be critical under static loads would also be critical under dynamic loads.

This study will have to be extended before any further observations will be warranted. The extension of this study is presently being outlined.

Natural Frequency

In cooperation with the extension of multistory inelastic dynamic structural analysis to methods which consider the flexibility of floors or girders it has been necessary to find the natural frequencies of bents with flexible floor systems. As a by-product of the work on methods and codes for dynamic analysis of bents using the ILLIAC, a code was found which automatically computes the stiffness matrix for a multistory multibay bent, the stiffness matrix being defined for the structure with n stories as a symmetrical array of n^2 constants of which the rth column represents the static forces necessary for equilibrium when a unit lateral displacement is given to the rth story and all other displacements are zero. For example, if for a three story structure, $n = 3$, the first floor ($r = 1$) is given a unit displacement and the resulting fixed ended moments are distributed by a moment distribution method, then the sum of the final moments for each story divided by the story height equals the shear in that story. From these shears, the forces acting on each floor level necessary to hold the structure in this configuration may be calculated. Similarly, if the second story ($r = 2$) is given a unit displacement, then the three forces ($n = 3$) for equilibrium of this configuration may be obtained. Following the same procedure for the

third story yields the last three forces, thus the stiffness matrix of nine forces ($n^2 = 9$) is obtained. It is equivalent to the sidesway forces computed for a moment distribution problem.

The stiffness matrix is not only very useful in static analysis but also forms the "A" matrix for natural frequency evaluation using the University of Illinois code No. M-5 which determines the solution for a set of matrix equations of the form $[A - \lambda D] = 0$ where λ is a function of natural frequency and D is a function of the mass of the structure. The stiffness matrix code is presently being revised for use both in static analysis and for evaluating natural frequencies.

Bent Analysis

In an effort to achieve a more exact analysis for the inelastic dynamic response problem a method which accounts for the flexibility of floor systems has been developed and coded for solution using the ILLIAC. Several problems have been solved to test the validity of the method. A more detailed description of this analysis will appear in a special report to be issued by this project.

The initial assumptions made in the analysis are similar to the shear beam analysis. The mass of each story is concentrated at the floor level and the forces act directly on the masses. The shear springs have been replaced with an elastic bent which is analyzed to obtain shearing forces. Only the changes in shear are computed. In this way inealsticity is achieved. A hinge placed at the end of any member will cause the moment to remain constant at the end of the

member until the relative rotation of the hinge changes direction. The hinge is then removed accounting for elastic unloading and the permanent set due to inelastic strain.

Preliminary investigations are now in progress on the development of a multistory dynamic response study using the ILLIAC. The preliminary study will be primarily concerned with the detection of the effect of the ratio of girder stiffness to column stiffness on the dynamic response characteristics of multistory structures.

SUMMARY

During the past year the study of simple structures has been extended while new methods of analysis for the multistory structure were developed. The codes for analysis of simple systems on the ILLIAC have been extended to more complex force and resistance functions.

Charts for maximum response of a single-degree-of-freedom system to a delayed rise triangular force pulse with impulse have been completed for rise times of 1.0, 1.5, 2.0 times the period of vibration of the structure. The time of maximum response charts for these and previous studies have been published. A cross study using rise time as a direct study variable has been presented.

The damage pressure level formula has been redefined for the case where the resistance function is unstable. Both equations and graphical methods have been used to clarify the unstable case.

Methods for analysis of the inelastic dynamic response for multistory structures with flexible girders have been developed and coded for solution using the ILLIAC.

It is planned to extend present data by approximate methods and charts to define response or damage pressure level for more general force pulses. Exploratory studies of multi-degree-of-freedom systems are presently being planned in an effort to establish general response characteristics.

NOMENCLATURE

Dimensional Quantity	Analogous Dimensionless Quantity
x = displacement of mass of single-degree-of-freedom system.	-
$q(x)$ = resistance of spring displacement x.	$q(x)/q_y$
x_y = "yield" displacement of spring at the point where the resistance function changes slope.	-
q_y = "yield" resistance of the spring at the point where the resistance function changes slope.	-
k_1 = initial, elastic slope of resistance function. $q_y = k_1 x_y$.	-
k_2 = second, inelastic slope of resistance function.	$k_2 k_1 = k$
x_m = maximum displacement of mass	$x_m/x_y = \mu$
x_o = "collapse" displacement of mass at the point where $q(x) = 0$ for $x \neq 0$ and for k_2 negative.	$x_o/x_y = \mu_o$
t = time.	t/T
Δt = time interval used for numerical integration.	$\Delta t/T$
$p(t)$ = pressure at time t.	$p(t)/q_y$
t_d = total duration of applied force.	t_d/T
t_1 = rise time of applied force; also, time of second impulse in Figs. 3c and 3d.	t_1/T

Dimensional Quantity	Analogous Dimensionless Quantity
p_m = peak force; damage pressure level; critical pressure level.	p_m/q_y
I, I_o, I_1 = impulses for applied forces of Figs. 3c and 3d.	$I_i/q_y T$
m = magnitude of mass.	-
$\dot{x}$ = velocity of mass.	$\Delta t\dot{x}/x_y$
c = coefficient of damping.	$c\Delta t/M$
$\ddot{x}$ = acceleration of mass.	$(\Delta t)^2\ddot{x}/x_y$
h = height of centroid of mass.	x_y/h
$v(t)$ = vertical transient pressure at time t.	$v(t)/q_y$
w = vertical static load.	w/q_y
T = period of vibration for small deflections. $T = 2\pi(m/k_1)^{1/2}$	-
p'_m = peak pressure required to produce a given maximum deflection x_m for loads of short duration.	p'_m/q_y
p''_m = peak pressure required to produce a given maximum deflection x_m for loads of infinite duration.	p''_m/q_y
p_γ = maximum value of p''_m; limiting value of p''_m.	p_γ/q_y

Dimensional Quantity	Analogous Dimensionless Quantity
q_{ave} = average resisting force from zero to maximum deflection.	q_a/q_y
x_γ = deflection at which p''_m is a maximum.	$\mu_\gamma = x_\gamma/x_y$
A = dimensionless quantity in approximate formula for p_m/q_y. For bilinear resistance $A = 2\mu-1 + k(\mu-1)^2$.	-
B = dimensionless quantity in approximate formula for p_m/q_y. $B = 2\pi I/q_y T$.	-

REFERENCES

1. Brooks, Nancy B., "Development of Procedures for Rapid Computation of Dynamic Structural Response," Civil Engineering Studies, Structural Series No. 83, University of Illinois, July 1954.

2. Brooks, N. B., and Marsh, D. L., "Development of Procedures for Rapid Computation of Dynamic Structural Response," Civil Engineering Studies, Structural Research Series No. 112, University of Illinois, July 1955.

3. Newmark, N. M., "Computation of Dynamic Structural Response in the Range Approaching Failure," Proceedings of the Symposium on Earthquake and Blast Effects on Structures, UCLA, June 1952.

4. Newmark, N. M., "An Engineering Approach to Blast Resistant Design," Proceedings, American Society of Civil Engineers, New York, October 1953.

INDEX OF FIGURES

I MAXIMUM RESPONSE (OF MASS-SPRING SYSTEM) TO INITIAL-PEAK TRIANGULAR PULSE WITH INITIAL IMPULSE

FIGURE NUMBER	PARAMETERS	
x_m/x_y vs t_d/T	k_2/k_1	I/q_yT
4a	0	+1.0
4b	0	+0.5
4c	0	+0.1
4d	0	0.0
4e	0	-0.1
4f	0	-0.5
4g	0	-1.0
5a	0.1	+1.0
5b	0.1	+0.5
5c	0.1	+0.1
5d	0.1	0.0
5e	0.1	-0.1
5f	0.1	-0.5
5g	0.1	-1.0
6a	0.02	+1.0
6b	0.02	+0.5
6c	0.02	+0.1
6d	0.02	0.0
6e	0.02	-0.1
6f	0.02	-0.5
6g	0.02	-1.0
7a	-0.02	+1.0
7b	-0.02	+0.5
7c	-0.02	+0.1
7d	-0.02	0.0
7e	-0.02	-0.1
7f	-0.02	-0.5
7g	-0.02	-1.0
8b	-0.04	+0.5
8c	-0.04	+0.1
8d	-0.04	0.0
8e	-0.04	-0.1
8f	-0.04	-0.5
8g	-0.04	-1.0

II TIME OF MAXIMUM RESPONSE TO INITIAL PEAK TRIANGULAR PULSE WITH INITIAL IMPULSE

FIGURE NUMBER	PARAMETERS		
TIME OF MAXIMUM VS PULSE DURATION	TIME OF PEAK	RATIO OF SECOND SLOPE OF RESISTANCE	RATIO OF PEAK PRESSURE TO YIELD RESISTANCE
t_m/T vs t_d/T	t_1/T	k_2/k_1	p_m/q_y
9a	0	0.0	10.0, 5.0, 2.0
9b	0	0.0	1.0, 0.5, 0.0
10a	0	+0.02	10.0, 5.0, 2.0
10b	0	+0.02	1.0, 0.5, 0.0
11a	0	+0.1	10.0, 5.0, 2.0
11b	0	+0.1	1.0, 0.5, 0.0
12a	0	-0.02	10.0, 5.0, 2.0
12b	0	-0.02	1.0, 0.5, 0.0
13a	0	-0.04	10.0, 5.0, 2.0
13b	0	-0.04	1.0, 0.5, 0.0

III TIME OF MAXIMUM RESPONSE TO DELAYED RISE TRIANGULAR PULSE OF FIGURE 3c WITH TWO IMPULSES

FIGURE NUMBER	PARAMETERS		
t_m/T vs t_d/T	t_1/T	k_2/k_1	p_m/q_y
14a	0.5	0.0	5.0, 2.0
14b	0.5	0.0	1.0, 0.5, 0.0
15a	0.5	+0.02	5.0, 2.0
15b	0.5	+0.02	1.0, 0.5, 0.0
16a	0.5	+0.1	10.0, 5.0, 2.0
16b	0.5	+0.1	1.0, 0.5, 0.0
17a	0.5	-0.02	5.0, 2.0
17b	0.5	-0.02	1.0, 0.5, 0.0
18a	0.5	-0.04	5.0, 2.0
18b	0.5	-0.04	1.0, 0.5, 0.0
19a	1.0	0.0	5.0, 2.0, 1.0
19b	1.0	0.0	0.5, 0.0
20a	1.0	+0.02	5.0, 2.0
20b	1.0	+0.02	1.0, 0.5, 0.0
21a	1.0	+0.1	10.0, 5.0, 2.0
21b	1.0	+0.1	1.0, 0.5, 0.0
22a	1.0	-0.02	2.0, 1.0
22b	1.0	-0.02	0.5, 0.0
23a	1.0	-0.04	2.0, 1.0
23b	1.0	-0.04	0.5, 0.0

III CONTINUED

FIGURE NUMBER	PARAMETERS		
t_m/T vs t_d/T	t_1/T	k_2/k_1	p_m/q_y
24a	1.5	0.0	2.0, 1.0
24b	1.5	0.0	0.5, 0.0
25a	1.5	+0.02	5.0, 2.0
25b	1.5	+0.02	1.0, 0.5, 0.0
26a	1.5	+0.1	5.0, 2.0
26b	1.5	+0.1	1.0, 0.5, 0.0
27a	1.5	-0.02	2.0, 1.0
27b	1.5	-0.02	0.5, 0.0
28a	1.5	-0.04	2.0, 1.0
28b	1.5	-0.04	0.5, 0.0
29a	2.0	0.0	2.0, 1.0
29b	2.0	0.0	0.5, 0.0
30a	2.0	+0.02	2.0
30b	2.0	+0.02	1.0, 0.5, 0.0
31a	2.0	+0.1	5.0, 2.0
31b	2.0	+0.1	1.0, 0.5, 0.0
32a	2.0	-0.02	2.0, 1.0
32b	2.0	-0.02	0.5, 0.0
33a	2.0	-0.04	2.0, 1.0
33b	2.0	-0.04	0.5, 0.0

IV MAXIMUM RESPONSE VERSUS RISE TIME

FIGURE NUMBER	PARAMETERS	
x_m/x_y vs t_1/T	$t_2/T = t_d/T$	k_2/k_1
34	2.0	0
35	5.0	0
36	10.0	0
37	100.0	0
38	1000.0	0
39	10	0
40	10	+0.1
41	10	+0.02
42	10	0.0
43	10	-0.02
44	10	-0.04
45	100	+0.1
46	100	+0.02
47	100	0.0
48	100	-0.02
49	100	-0.04

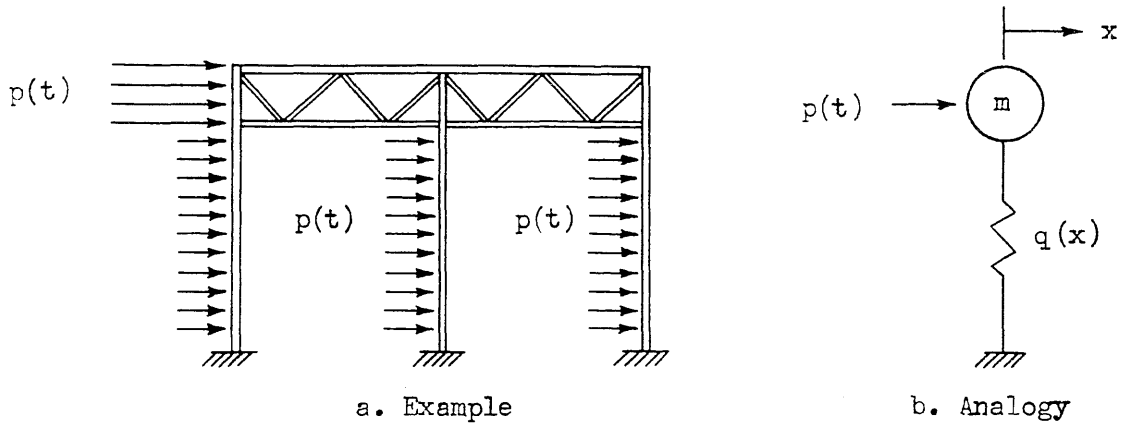

Fig. 1 Single-Degree-of-Freedom System

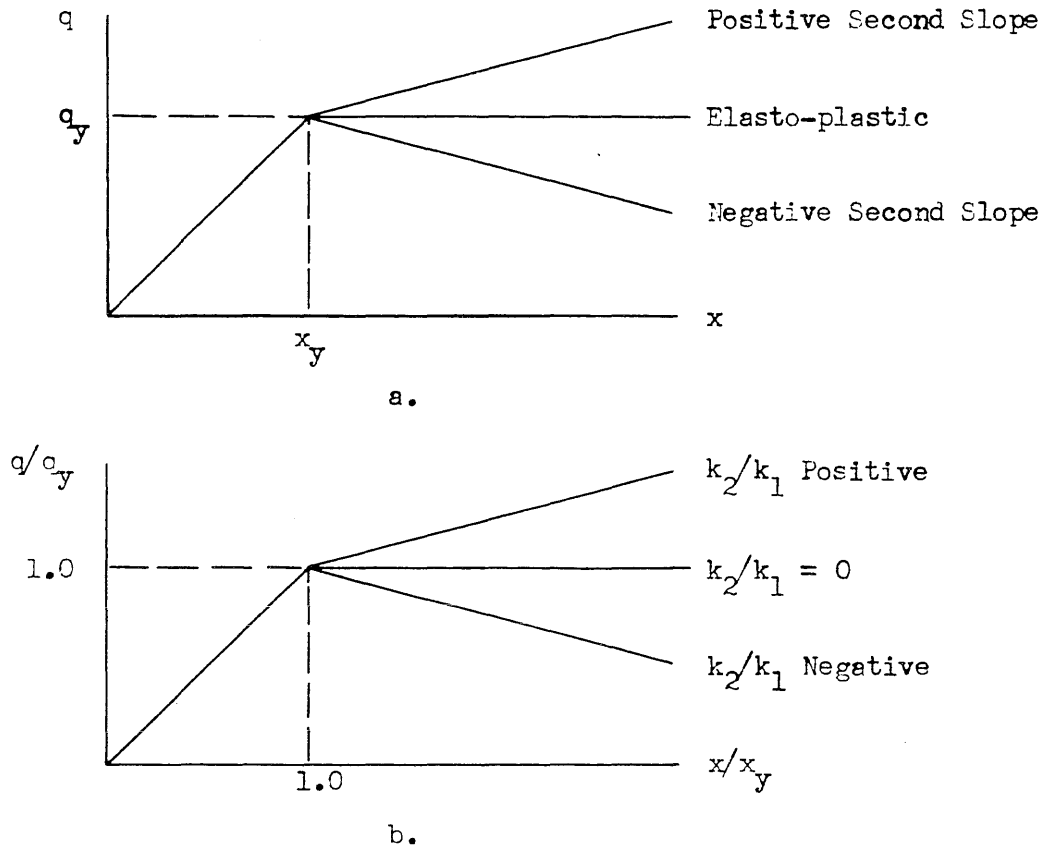

Fig. 2 Bilinear Resistance

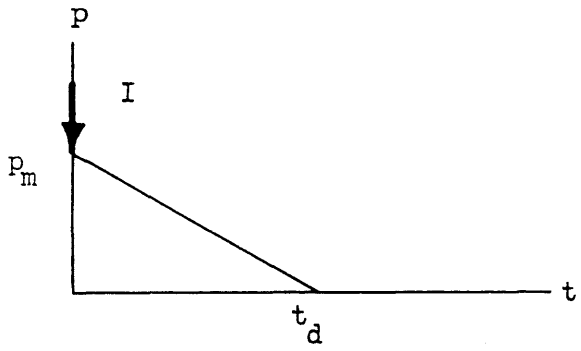

a. Initial Peak Triangular Pulse with Initial Impulse

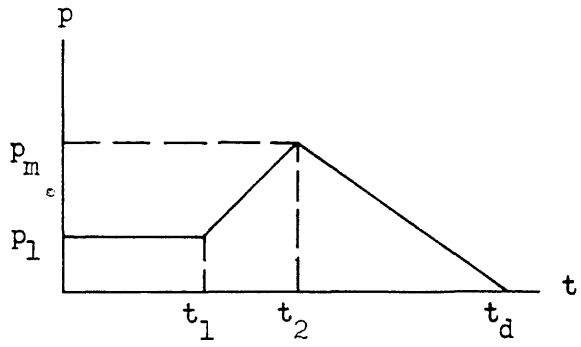

b. Polygonal Pulse

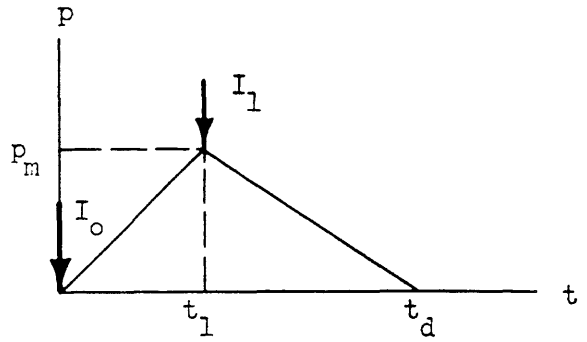

c.

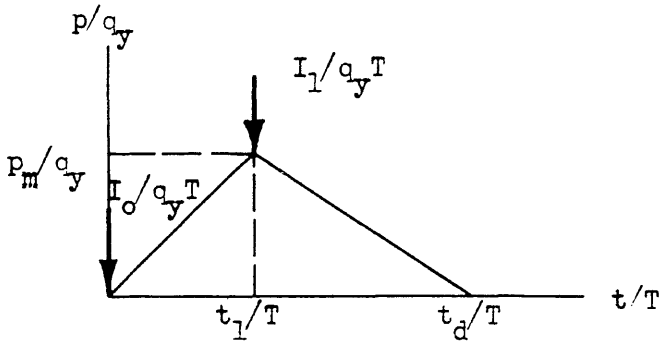

d.

Delayed Rise Triangular Force Pulse with Two Equal Impulses

Fig. 3 Applied Force Functions

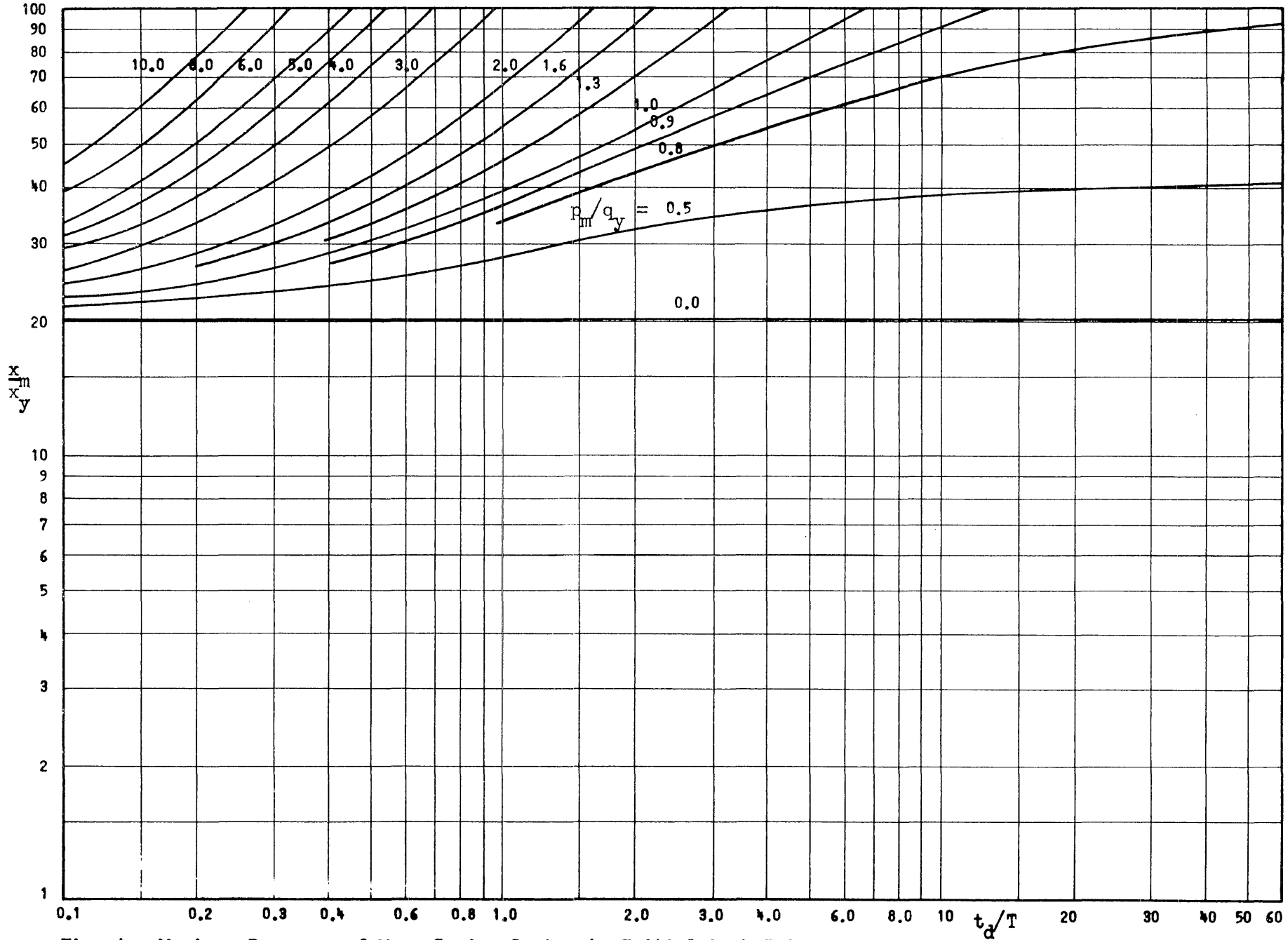

Fig. 4a Maximum Response of Mass-Spring System to Initial-Peak Triangular Pulse with Initial Impulse $k_2/k_1=0$, $I/q_yT=+1.0$, $t_1/T=0$

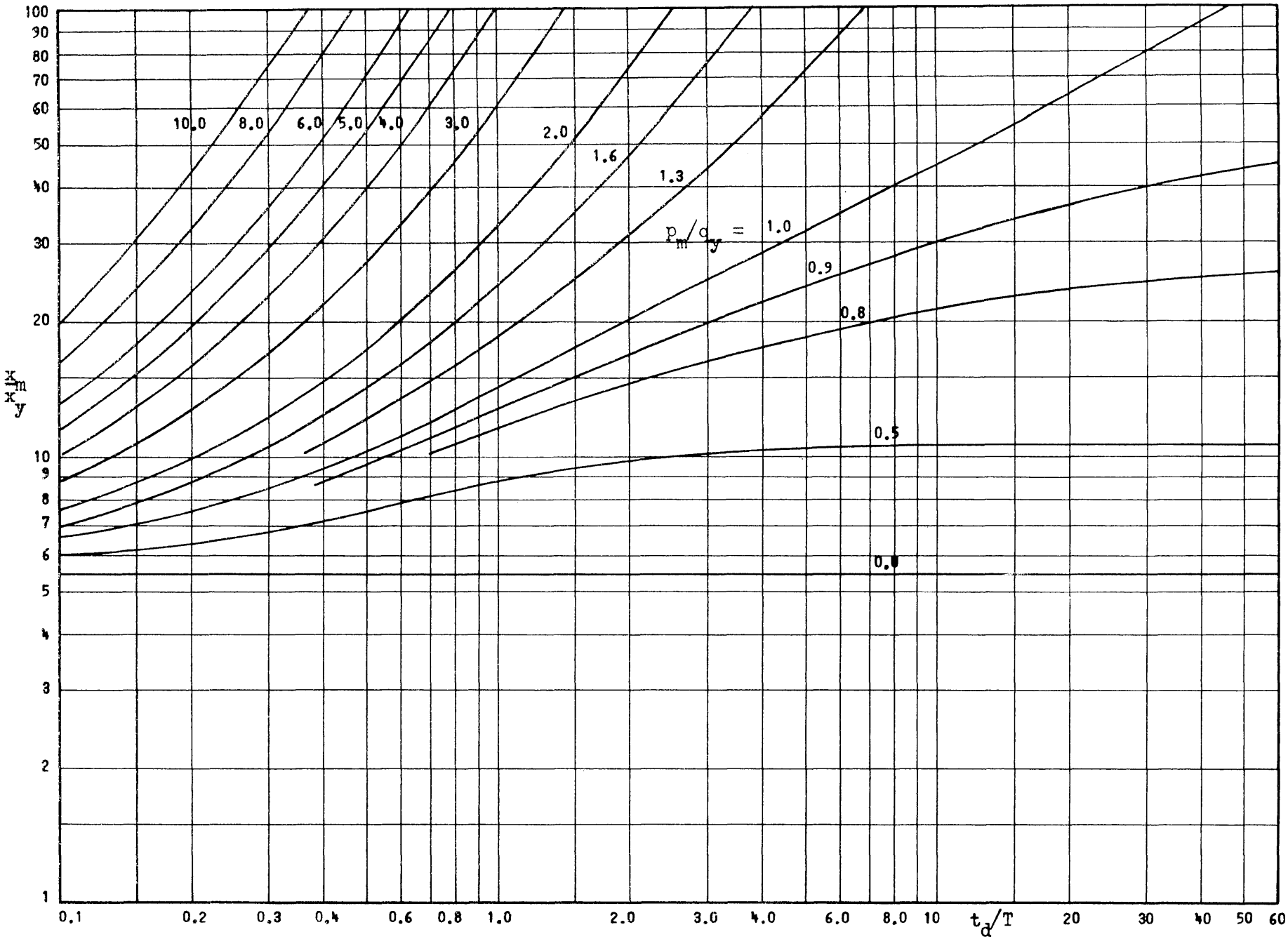

Fig. 4b Maximum Response of Mass-Spring System to Initial-Peak Triangular Pulse with Initial Impulse

$k_2/k_1=0$, $I/q_yT=+0.5$, $t_1/T=0$

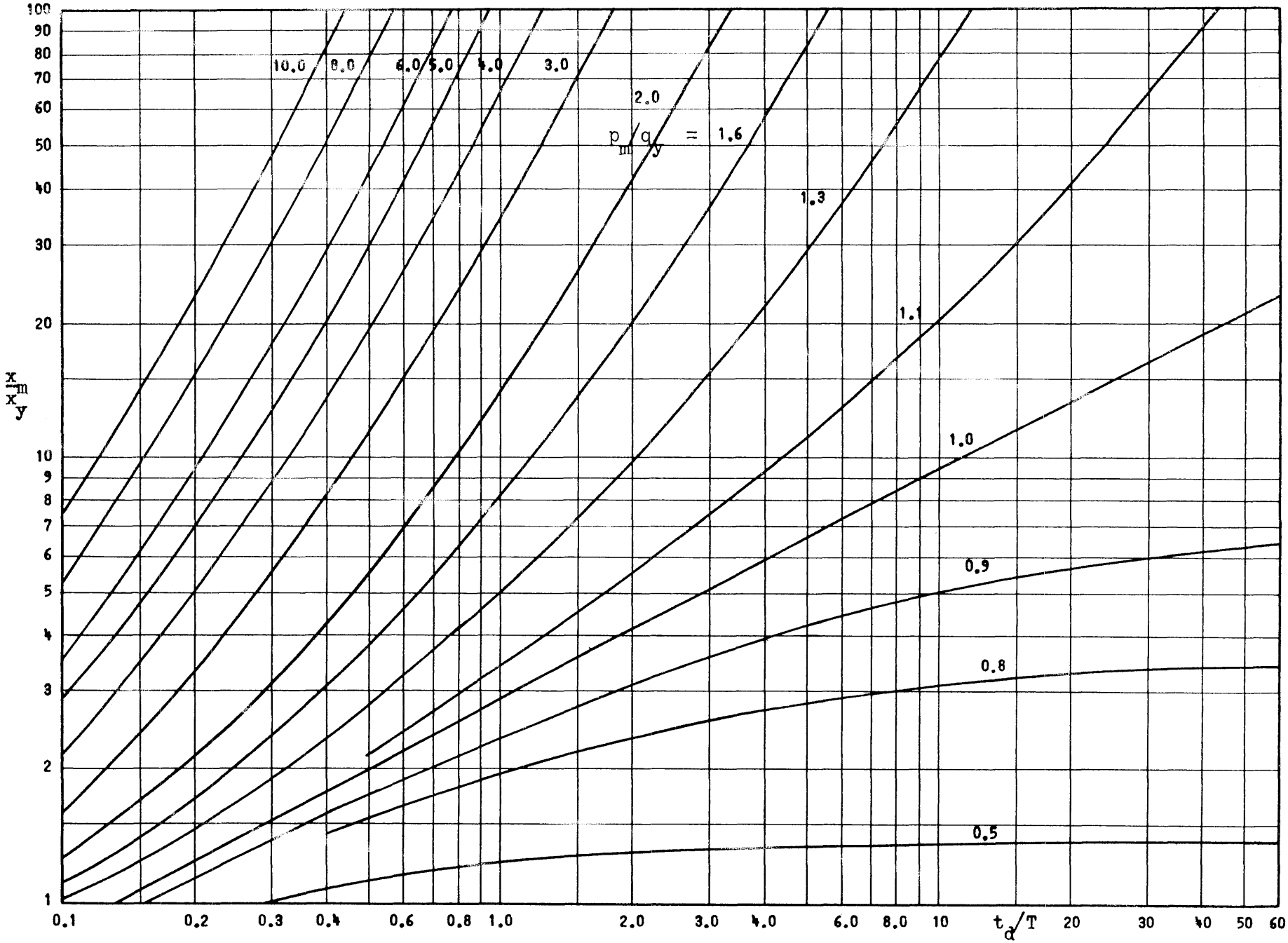

Fig. 4c Maximum Response of Mass-Spring System to Initial-Peak Triangular Pulse with Initial Impulse

$k_2/k_1=0$, $I/q_yT=+0.1$, $t_1/T=0$

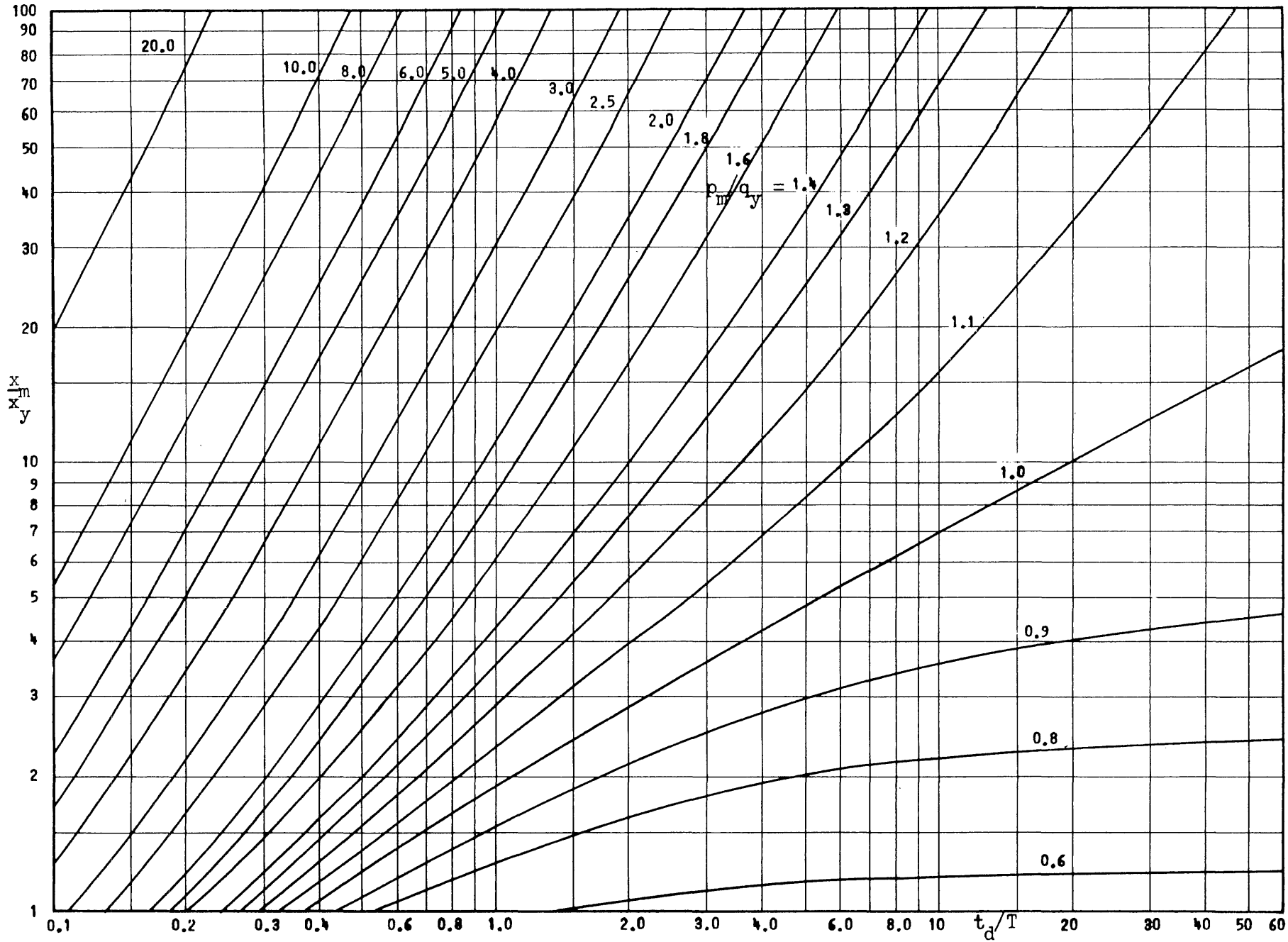

Fig. 4d Maximum Response of Mass-Spring System to Initial-Peak Triangular Pulse

$k_2/k_1 = 0$, $I/q_yT = 0.0$, $t_1/T = 0$

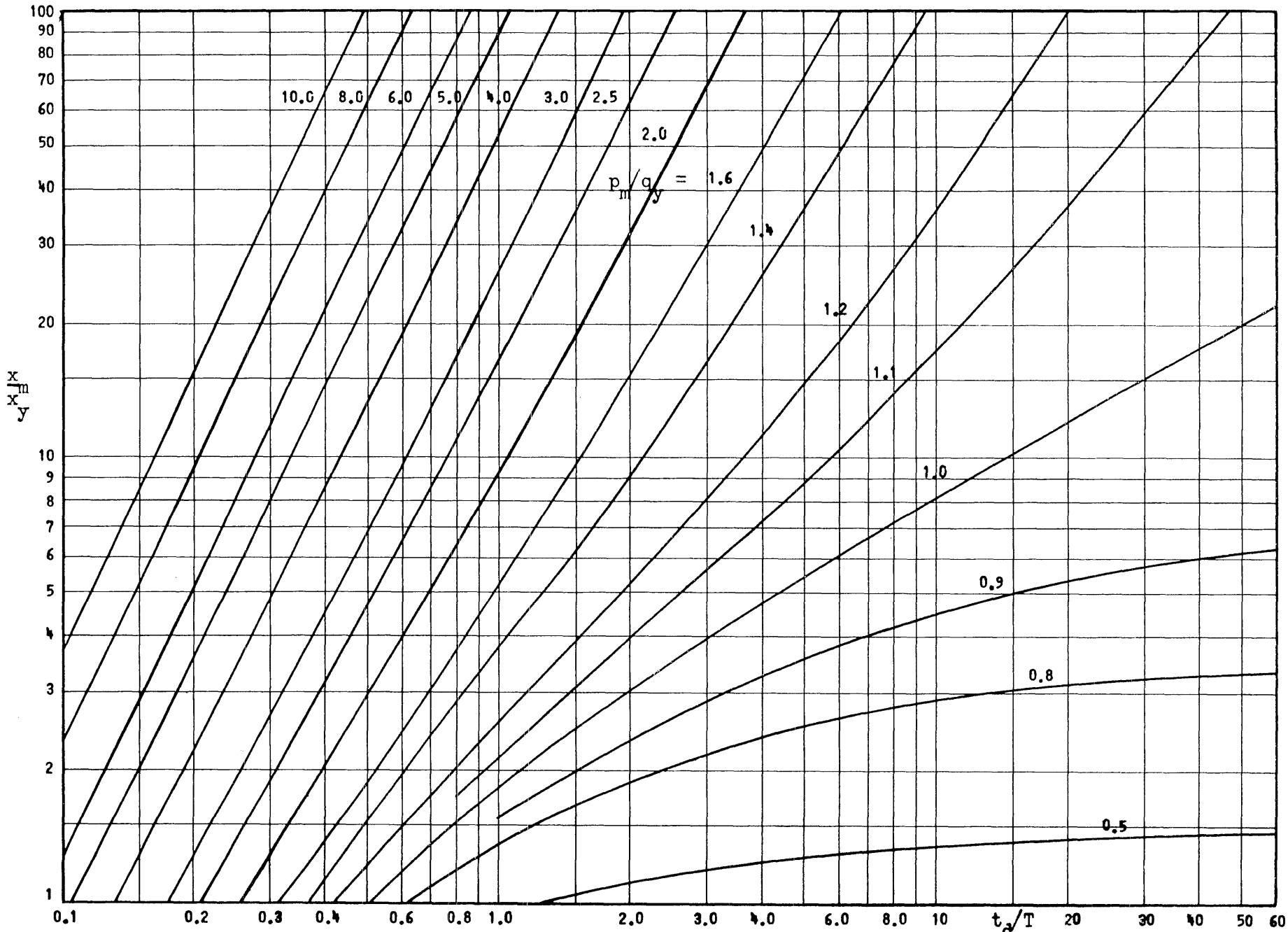

Fig. 4e Maximum Response of Mass-Spring System to Initial-Peak Triangular Pulse with Initial Impulse

$k_2/k_1=0$, $I/q_y T=0.1$, $t_1/T=0$

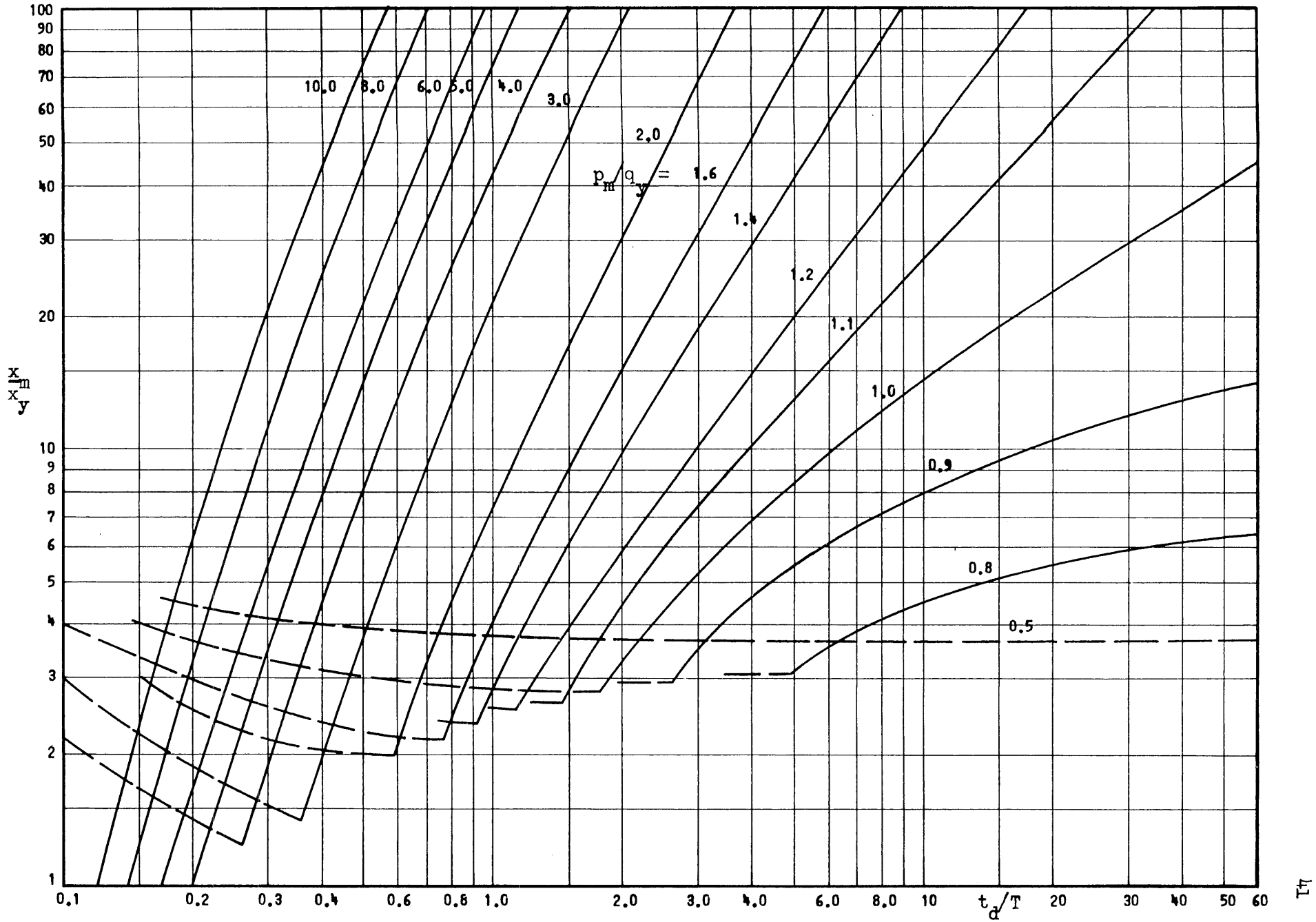

Fig. 4f Maximum Response of Mass-Spring System to Initial-Peak Triangular Pulse with Initial Impulse $k_2/k_1=0$, $I/q_yT=-0.5$, $t_1/T=0$

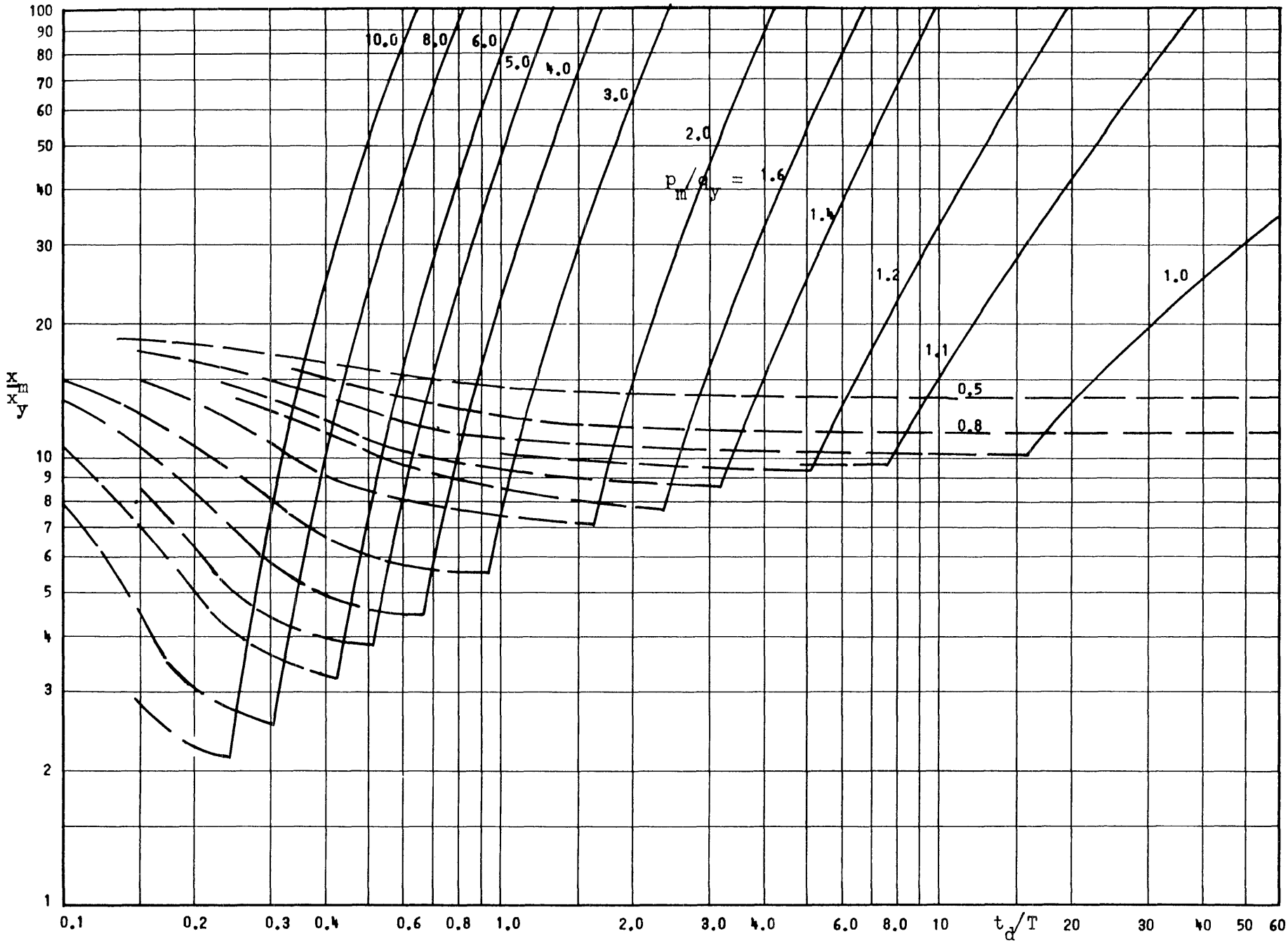

Fig. 4g Maximum Response of Mass-Spring System to Initial-Peak Triangular Pulse with Initial Impulse $k_2/k_1=0$, $I/q_yT=-1.0$, $t_1/T=0$

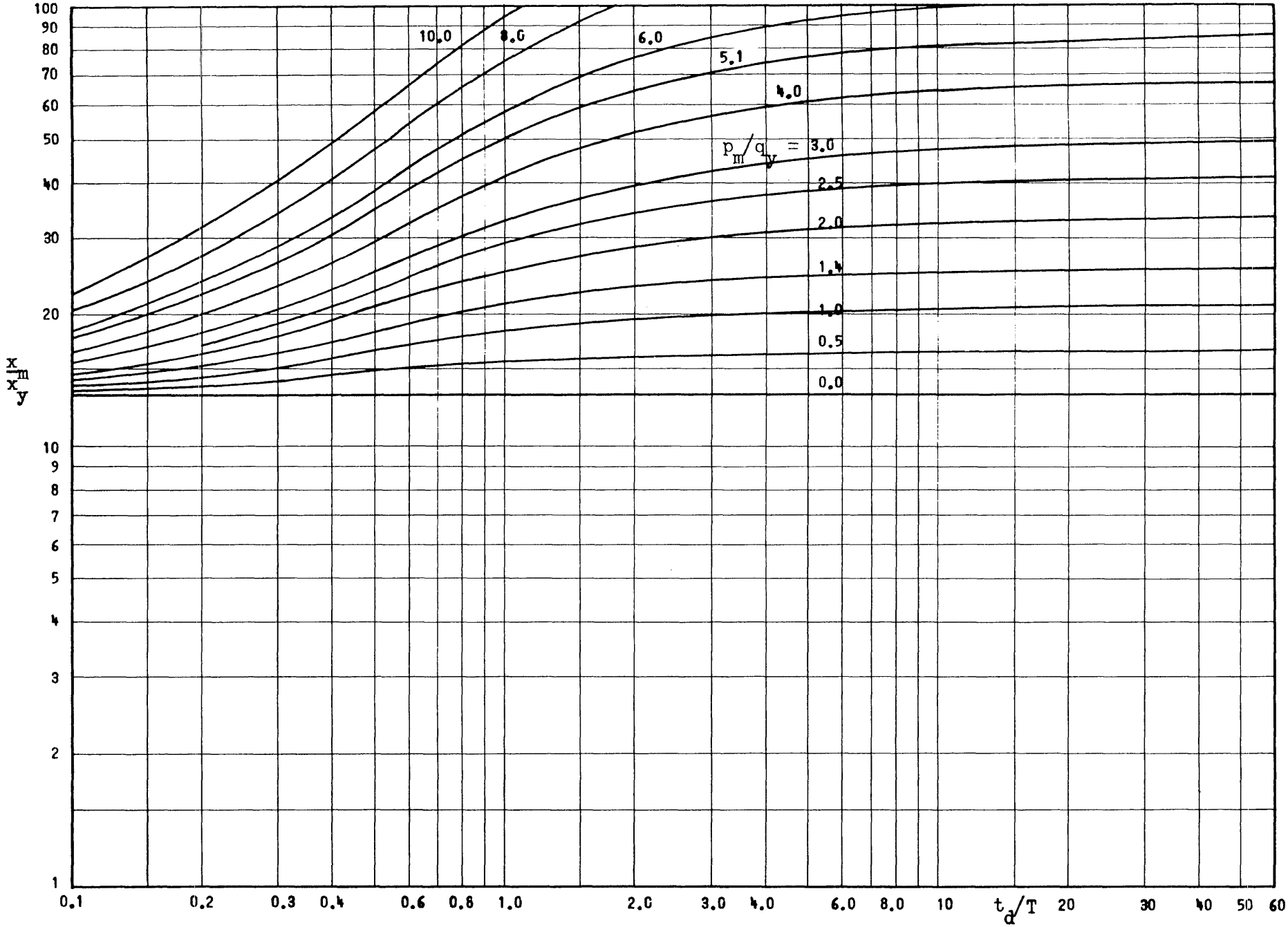

Fig. 5a Maximum Response of Mass-Spring System to Initial-Peak Triangular Pulse with Initial Impulse $k_2/k_1=0.1$, $I/q_yT=+1.0$, $t_1/T=0$

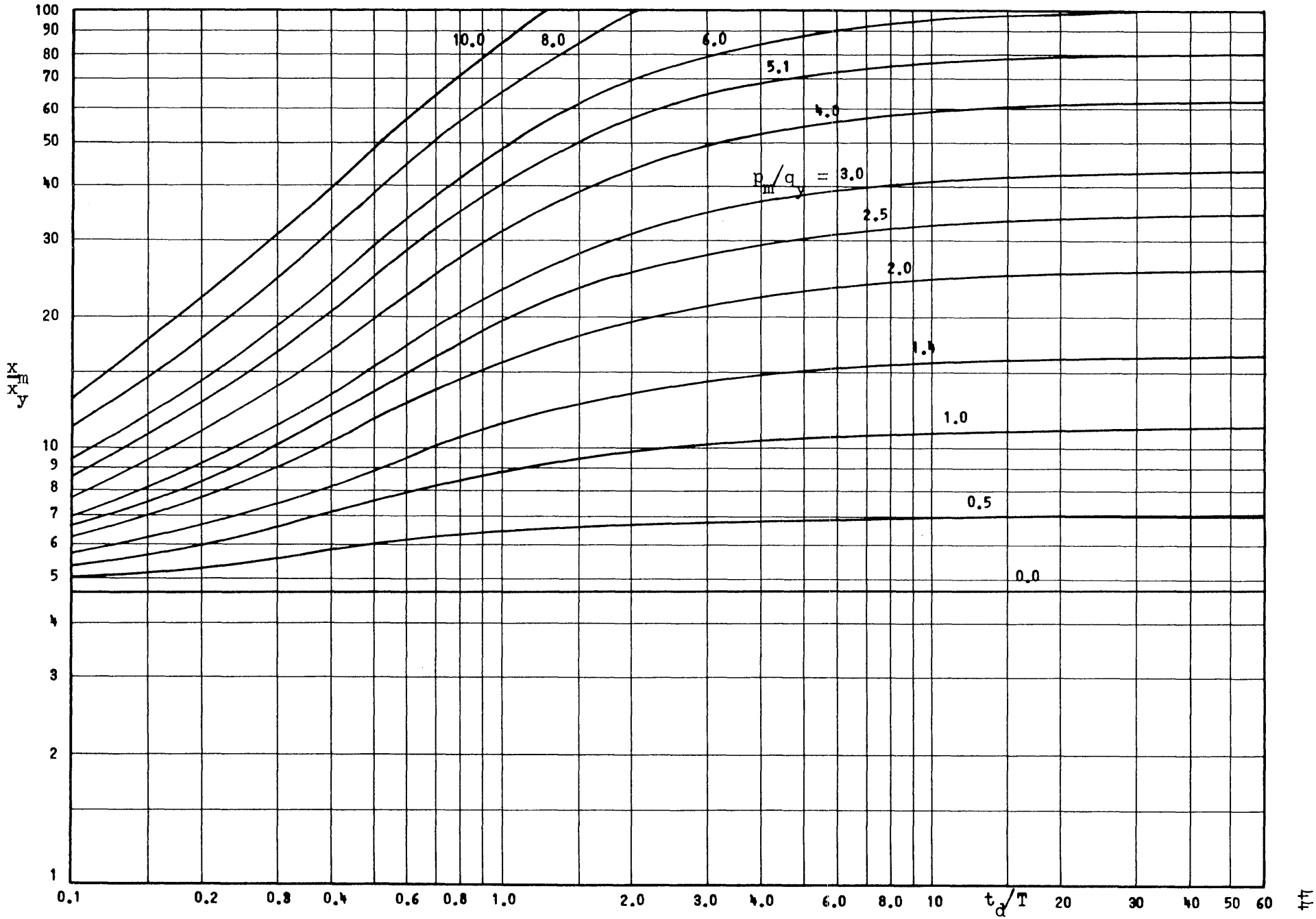

Fig. 5b Maximum Response of Mass-Spring System to Initial-Peak Triangular Pulse with Initial Impulse $k_2/k_1=0.1$, $I/q_yT=+0.5$, $t_1/T=0$

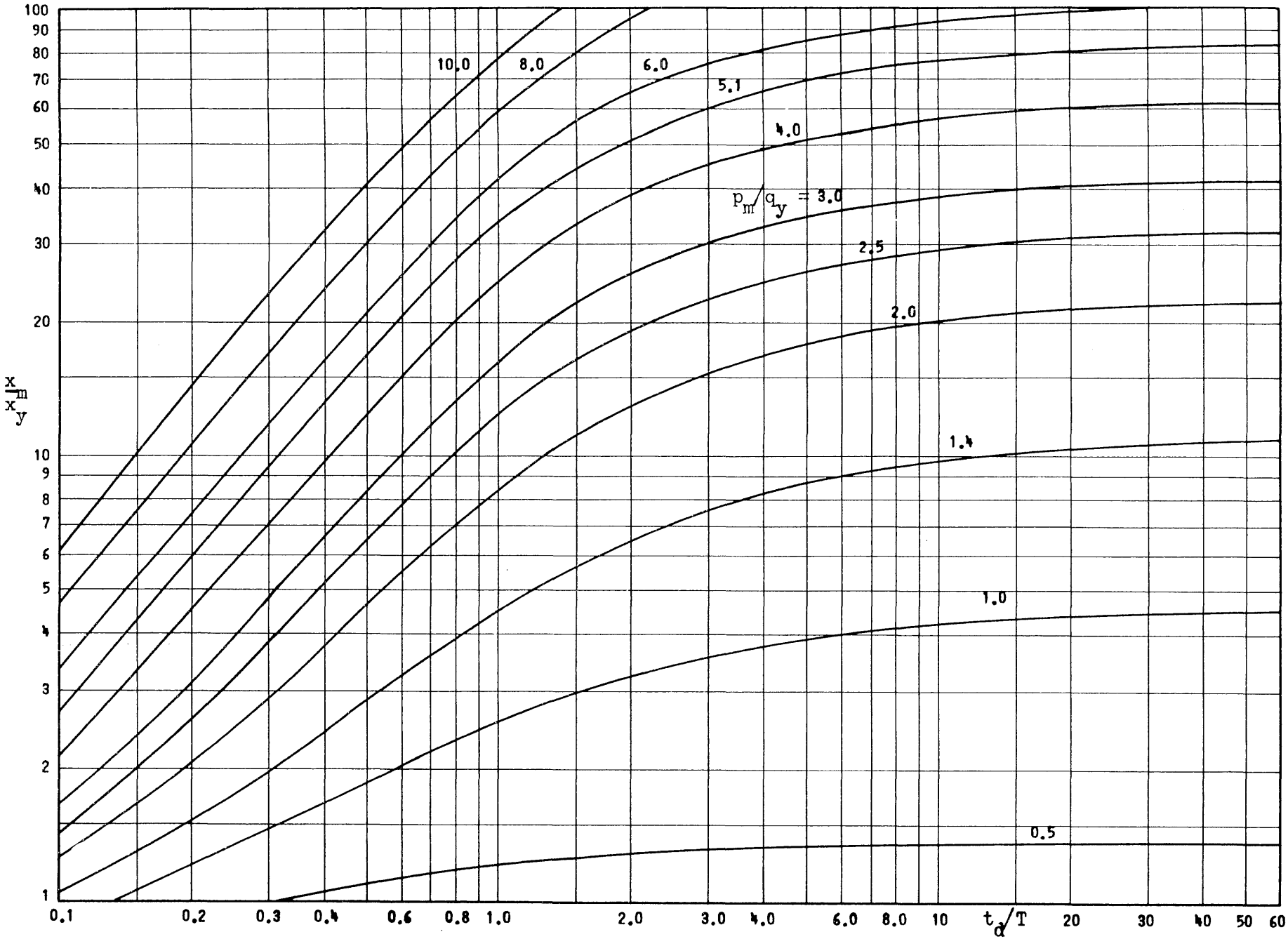

Fig. 5c Maximum Response of Mass-Spring System to Initial-Peak Triangular Pulse with Initial Impulse

$k_2/k_1=0.1$, $I/q_yT=+0.1$, $t_1/T=0$

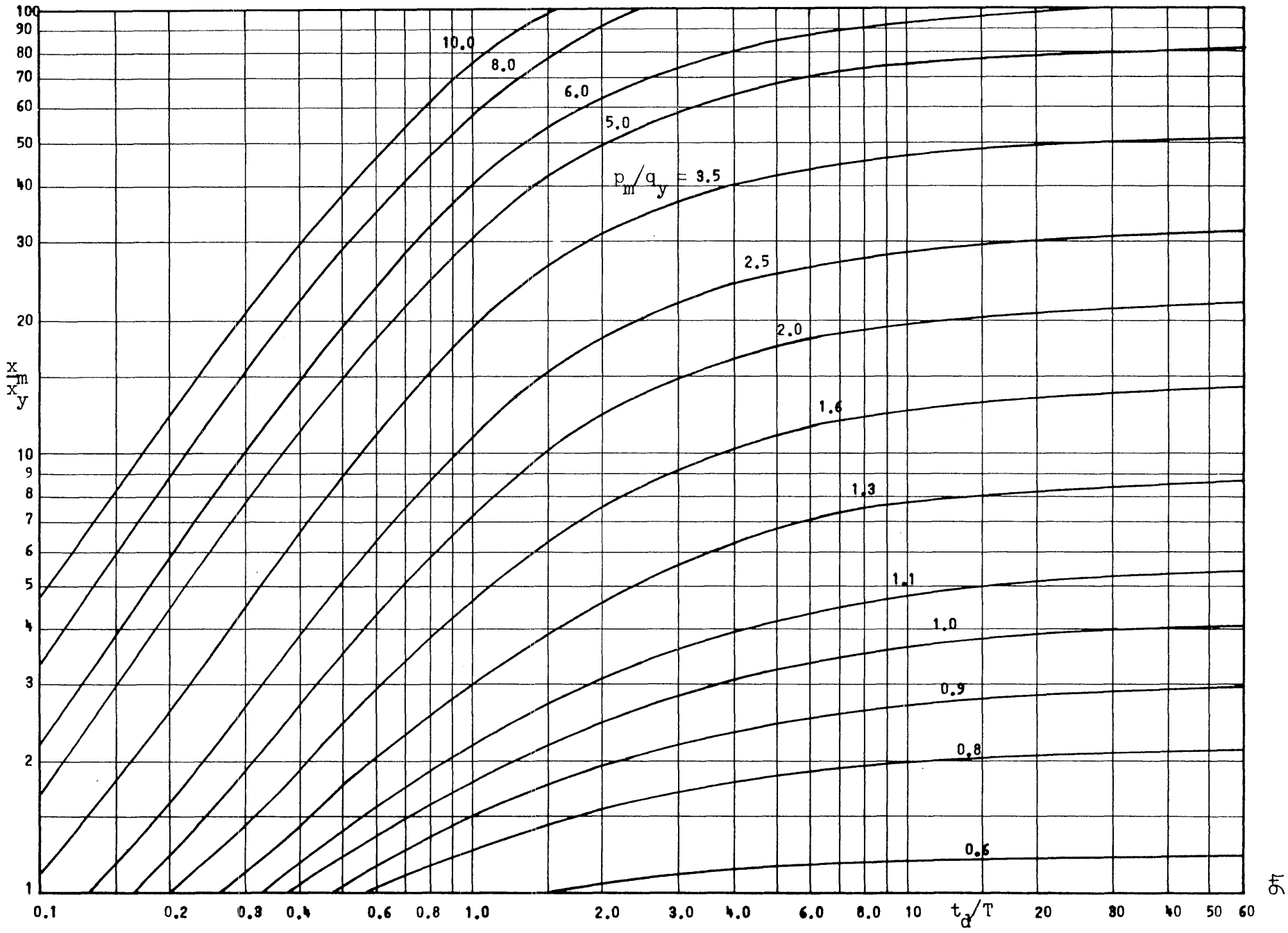

Fig. 5d Maximum Response of Mass-Spring System to Initial-Peak Triangular Pulse
$k_2/k_1 = +0.1$, $I/q_yT = 0.0$, $t_1/T = 0$

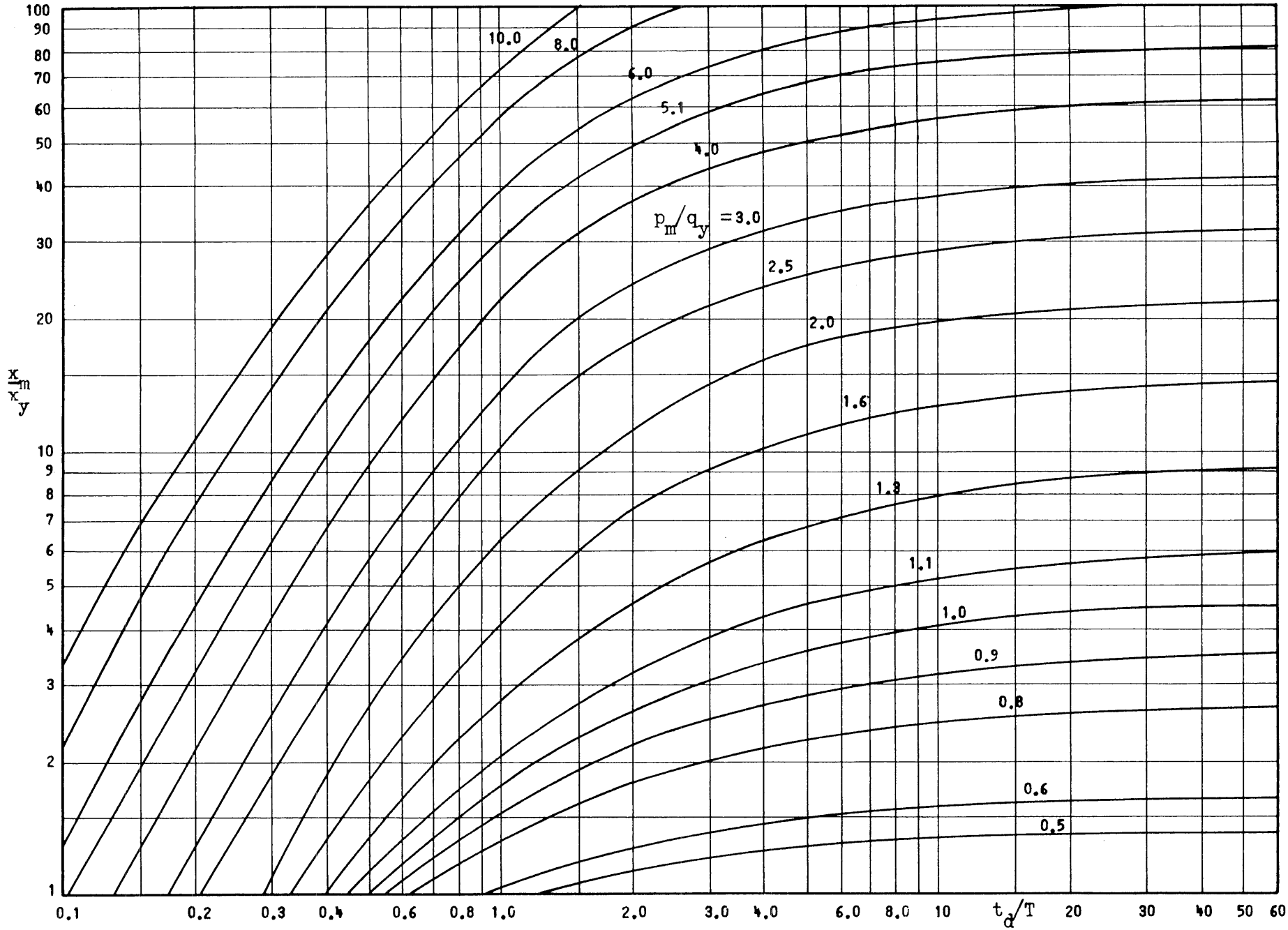

Fig. 5e Maximum Response of Mass-Spring System to Initial-Peak Triangular Pulse with Initial Impulse

k_2/k_1=0.1, I/q_yT=-0.1, t_1/T=0

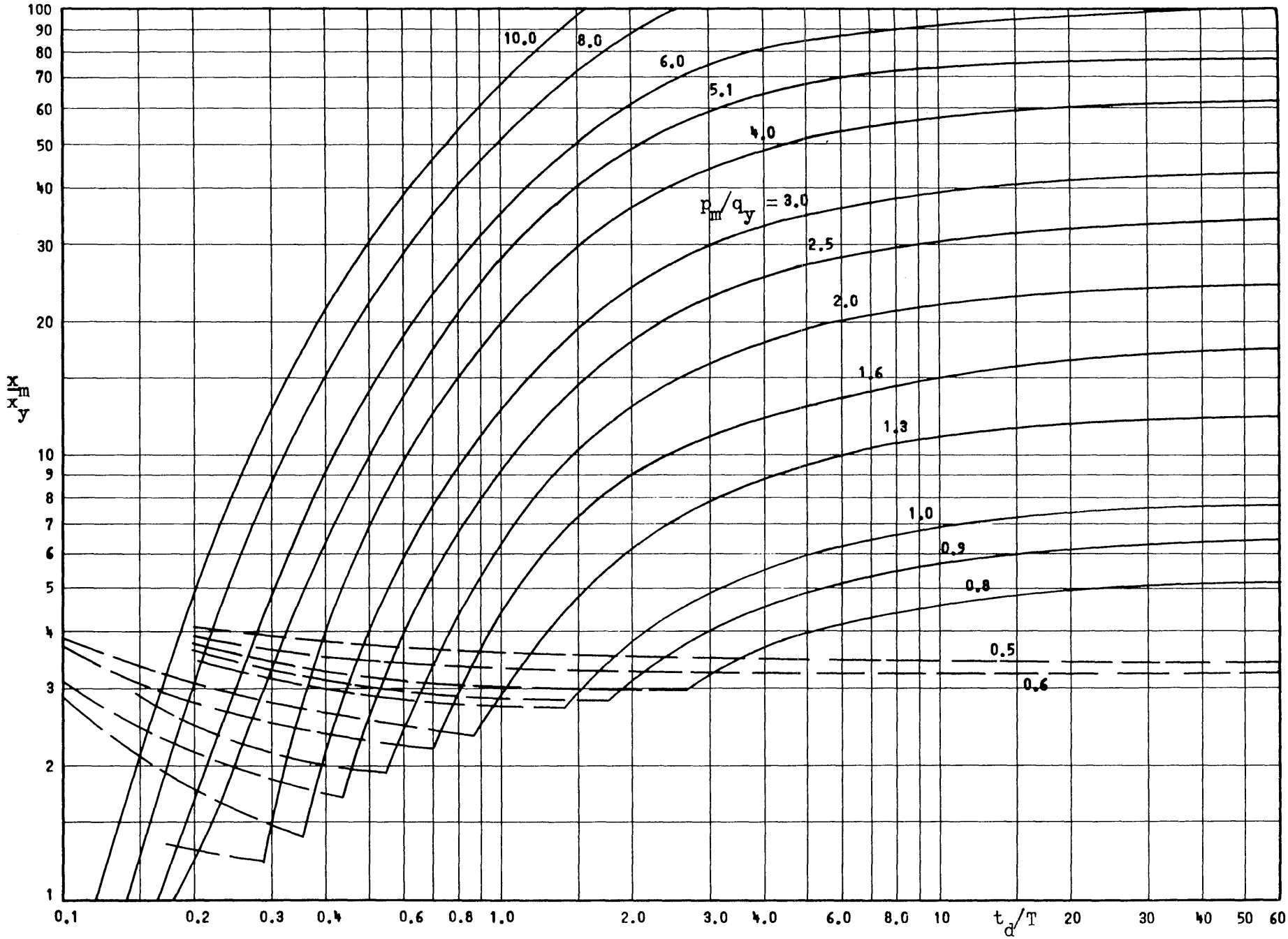

Fig. 5f Maximum Response of Mass-Spring System to Initial-Peak Triangular Pulse with Initial Impulse $k_2/k_1=0.1$, $I/q_yT=-0.5$, $t_1/T=0$

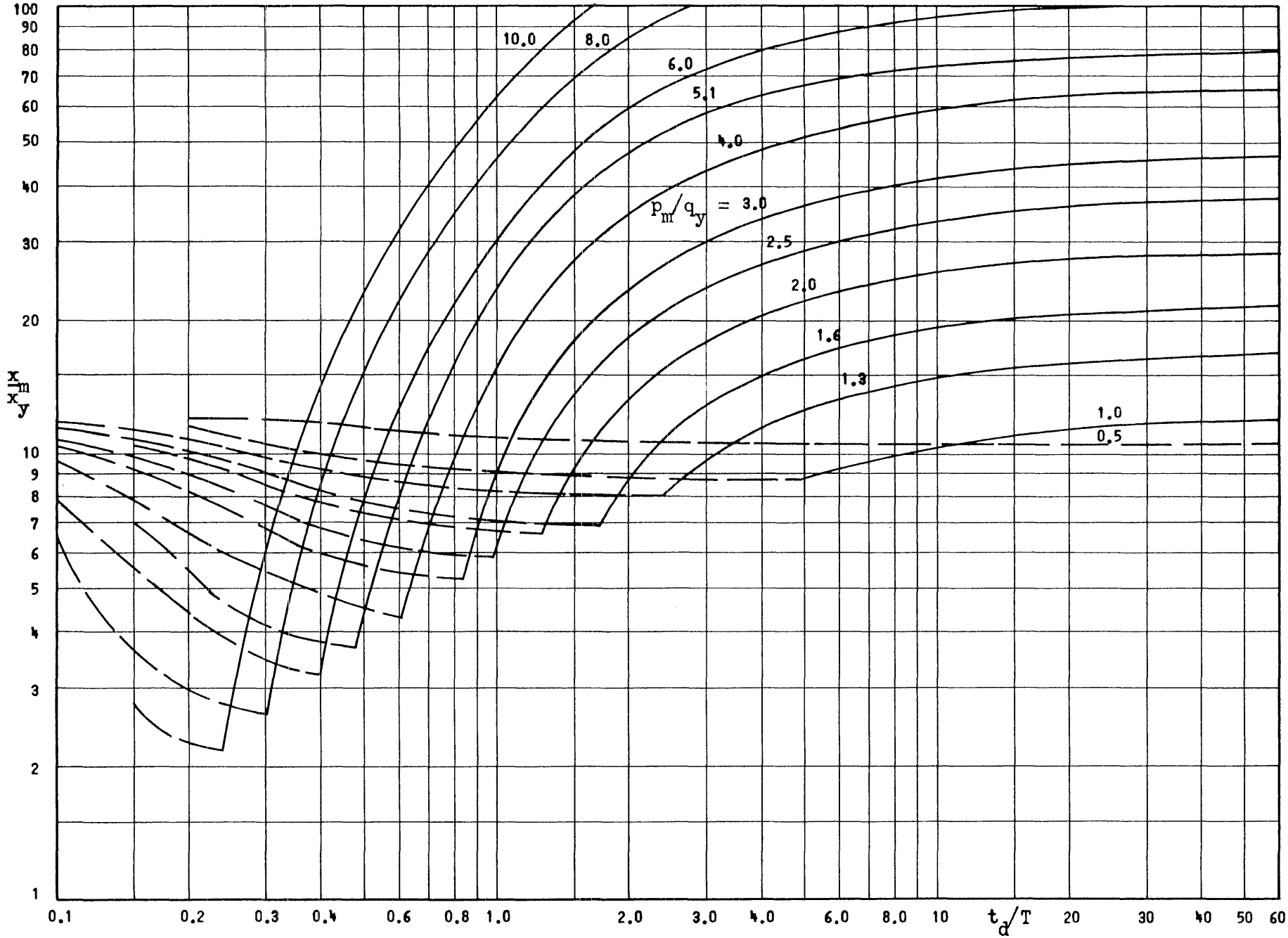

Fig. 5g Maximum Response of Mass-Spring System to Initial-Peak Triangular Pulse with Initial Impulse $k_2/k_1=0.1$, $I/q_yT=-1.0$, $t_1/T=0$

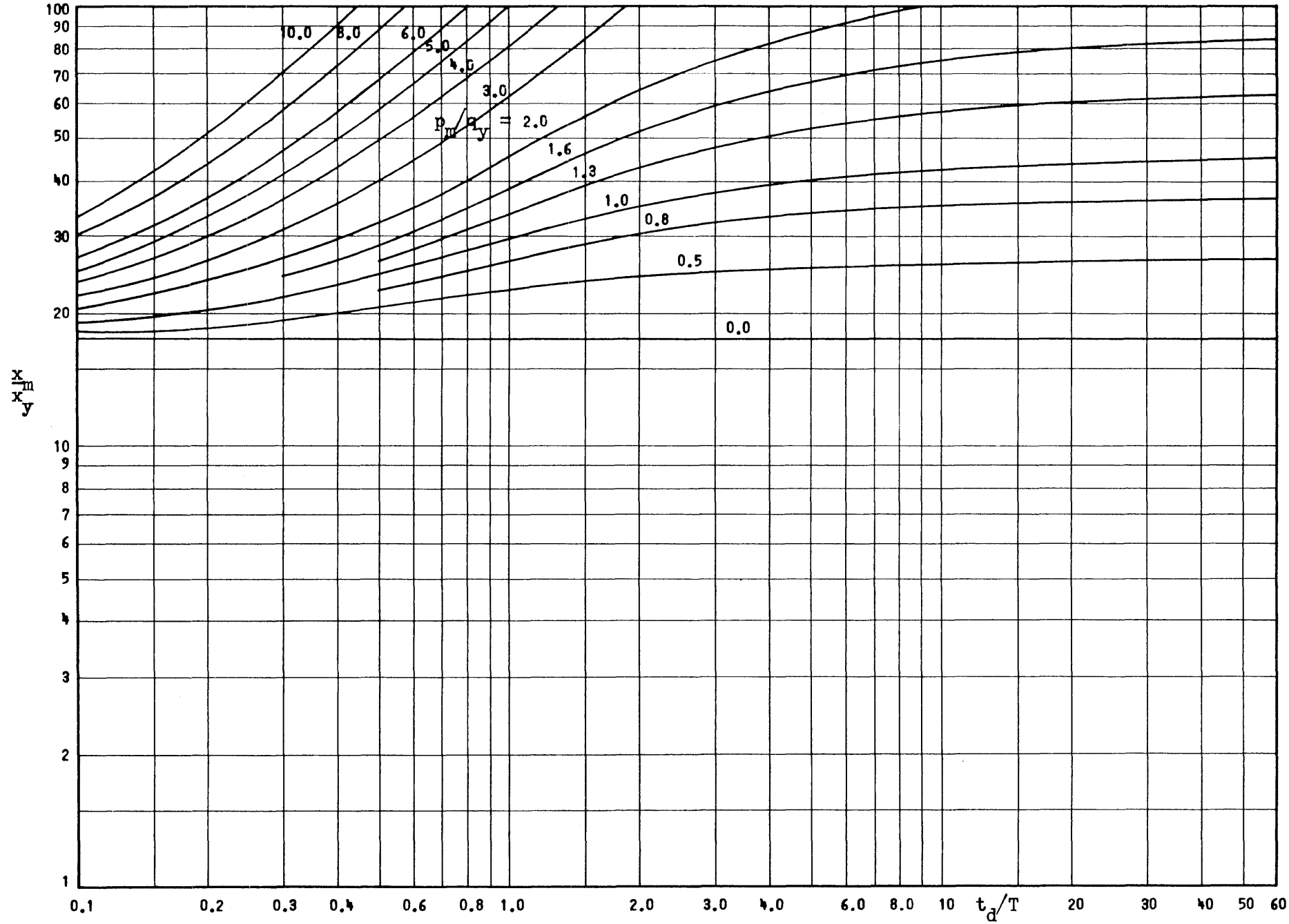

Fig. 6a Maximum Response of Mass-Spring System to Initial-Peak Triangular Pulse with Initial Impulse $k_2/k_1=0.02$, $I/q_yT=+1.0$, $t_1/T=0$

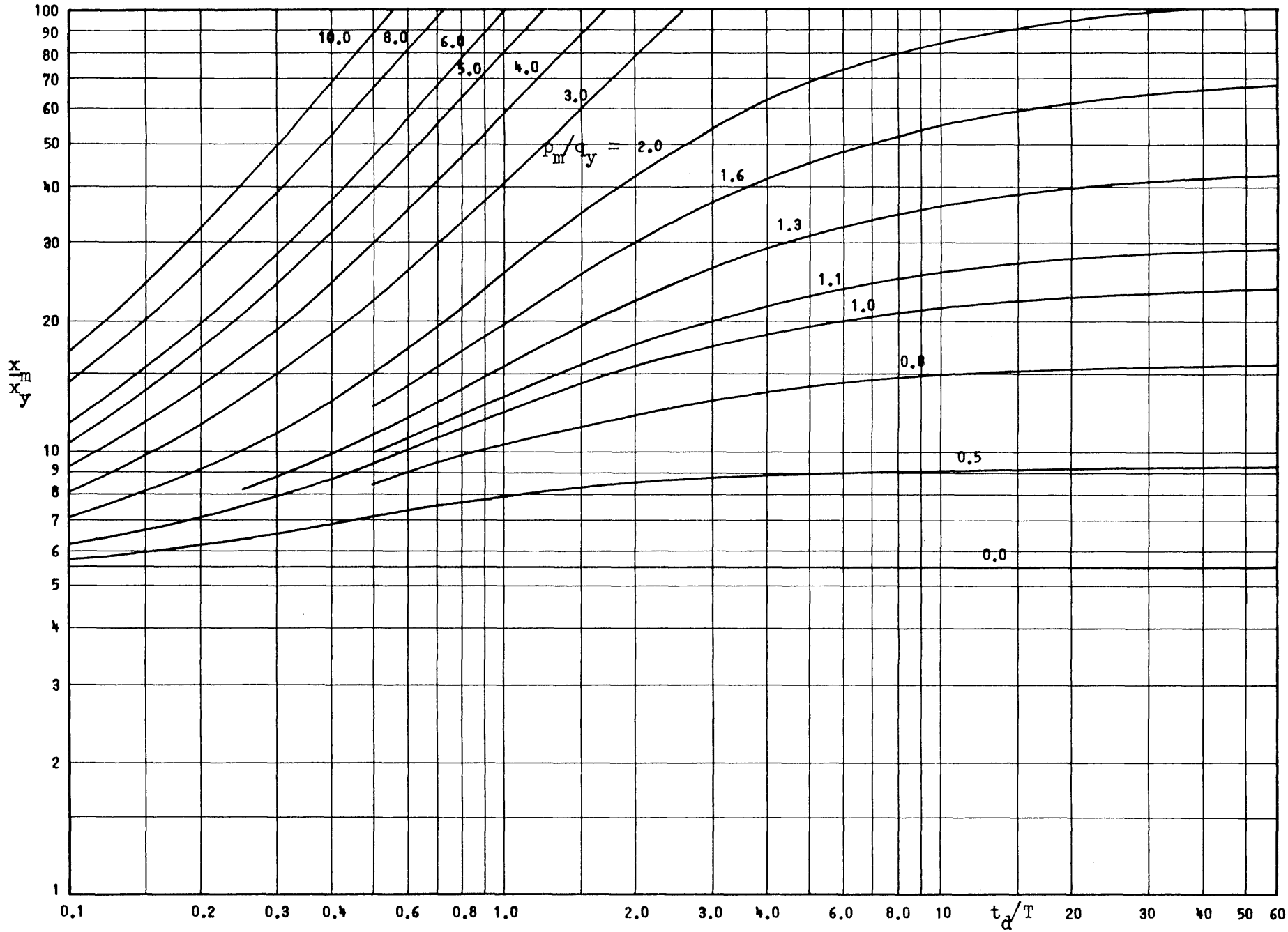

Fig. 6b Maximum Response of Mass-Spring System to Initial-Peak Triangular Pulse with Initial Impulse k_2/k_1=0.02, I/q_yT=+0.5, t_1/T=0

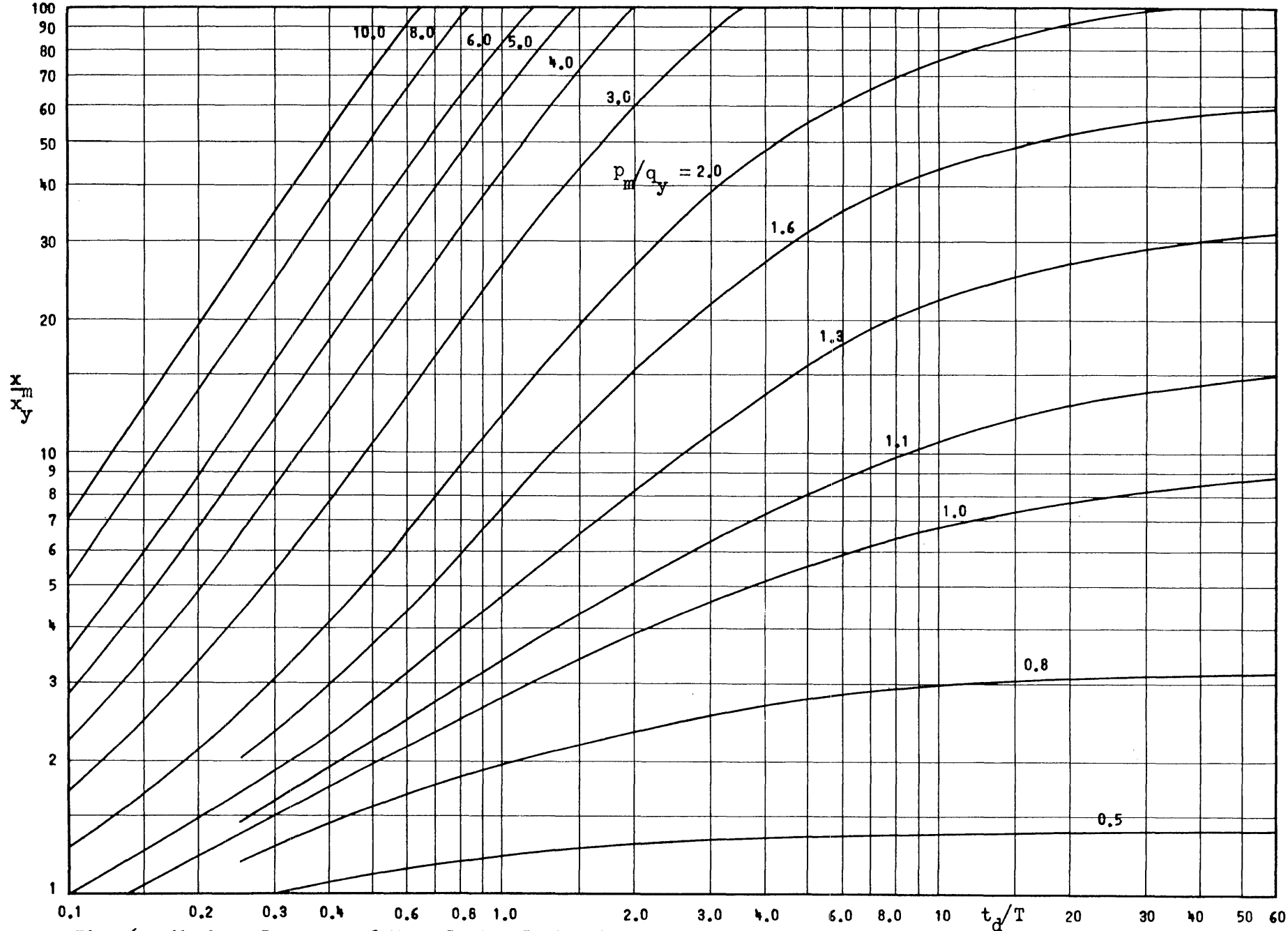

Fig. 6c Maximum Response of Mass-Spring System to Initial-Peak Triangular Pulse with Initial Impulse

$k_2/k_1=0.02$, $I/q_yT=+0.1$, $t_1/T=0$

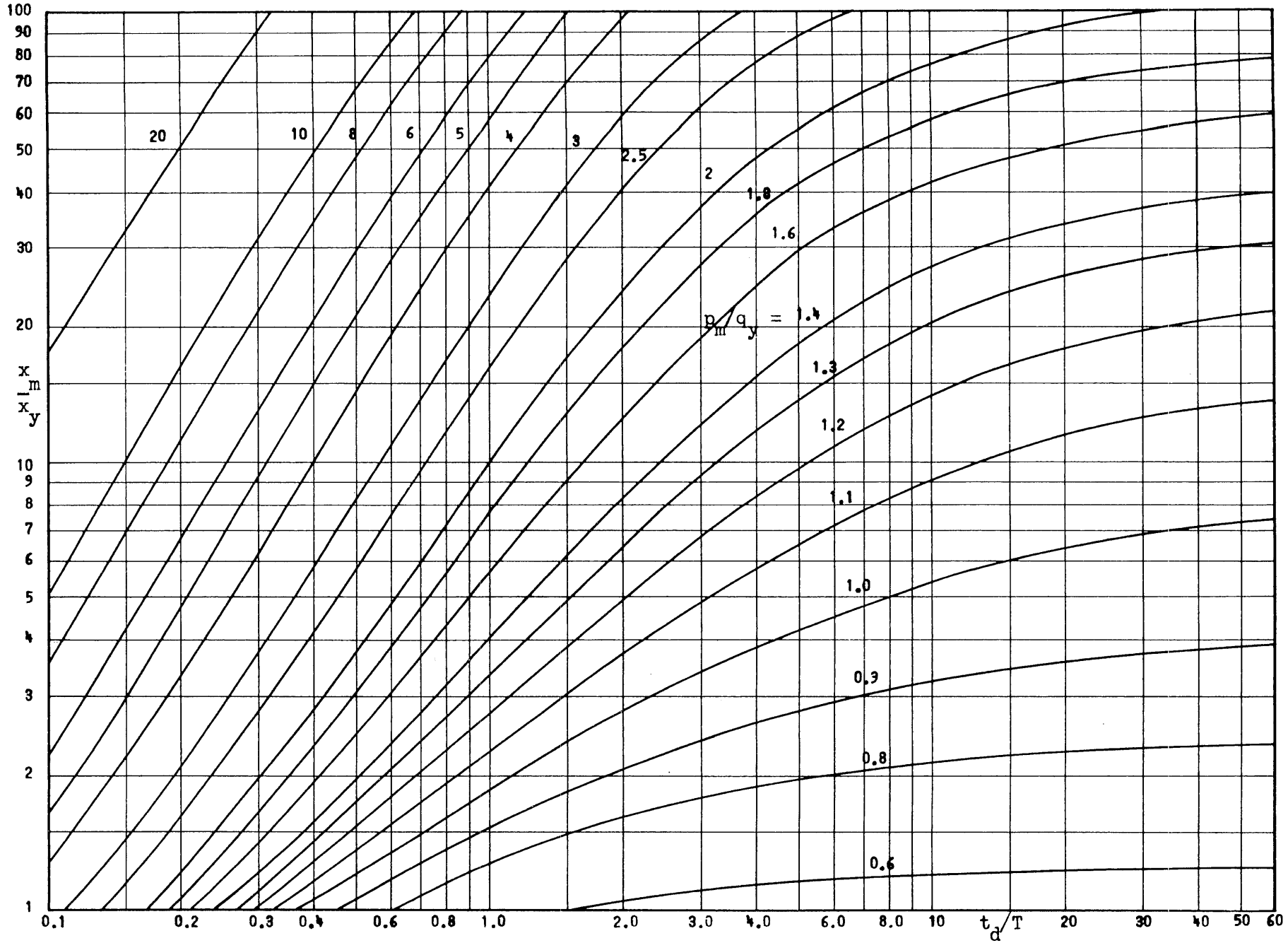

Fig. 6d Maximum Response of Mass-Spring System to Initial-Peak Triangular Pulse with Initial Impulse $K_2/K_1 = 0.02$, $I/q_yT = 0$, $t_1/T = 0$

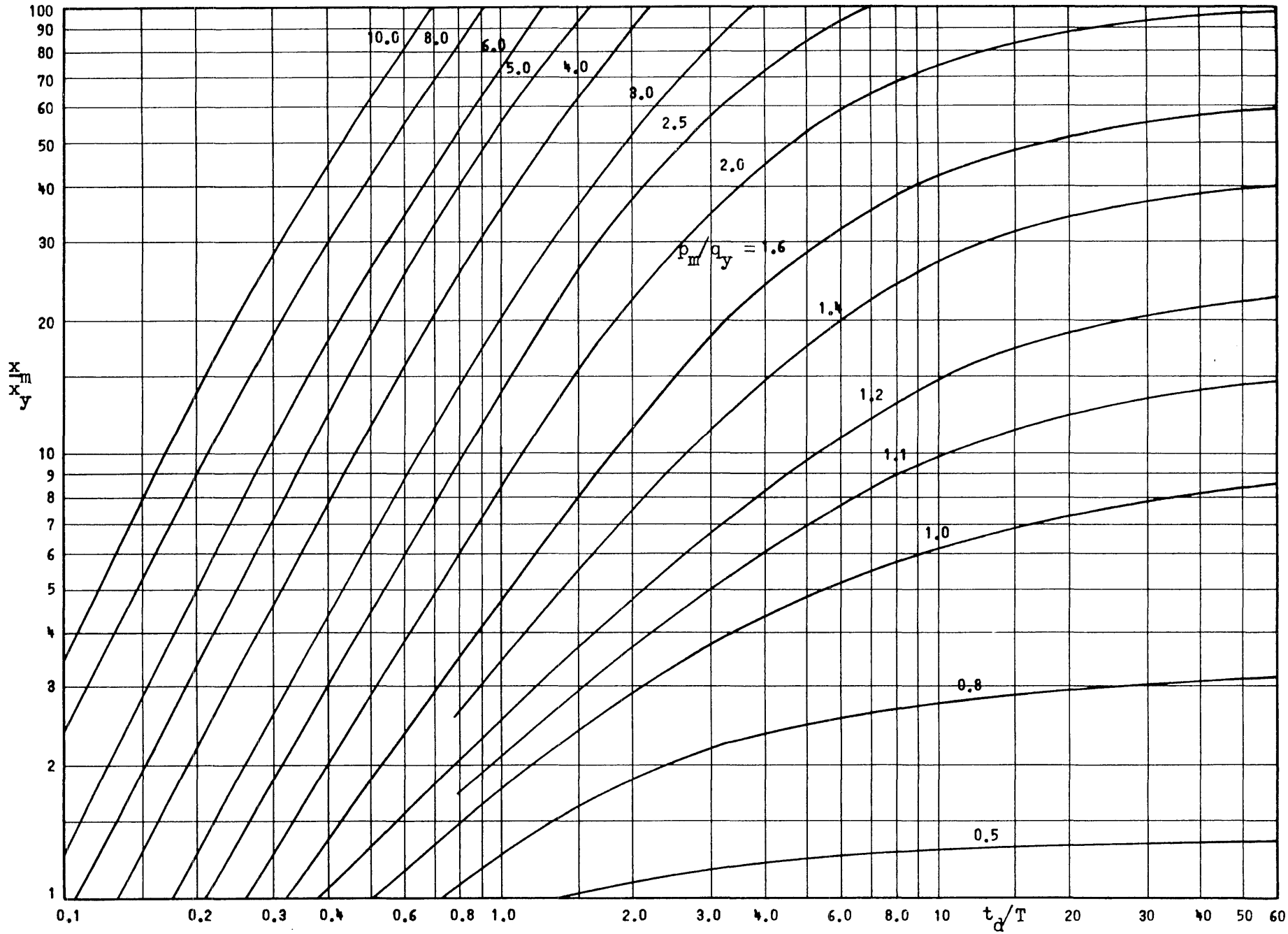

Fig. 6e Maximum Response of Mass-Spring System to Initial-Peak Triangular Pulse with Initial Impulse

k_2/k_1=0.02, I/q_yT=-0.1, t_1/T=0

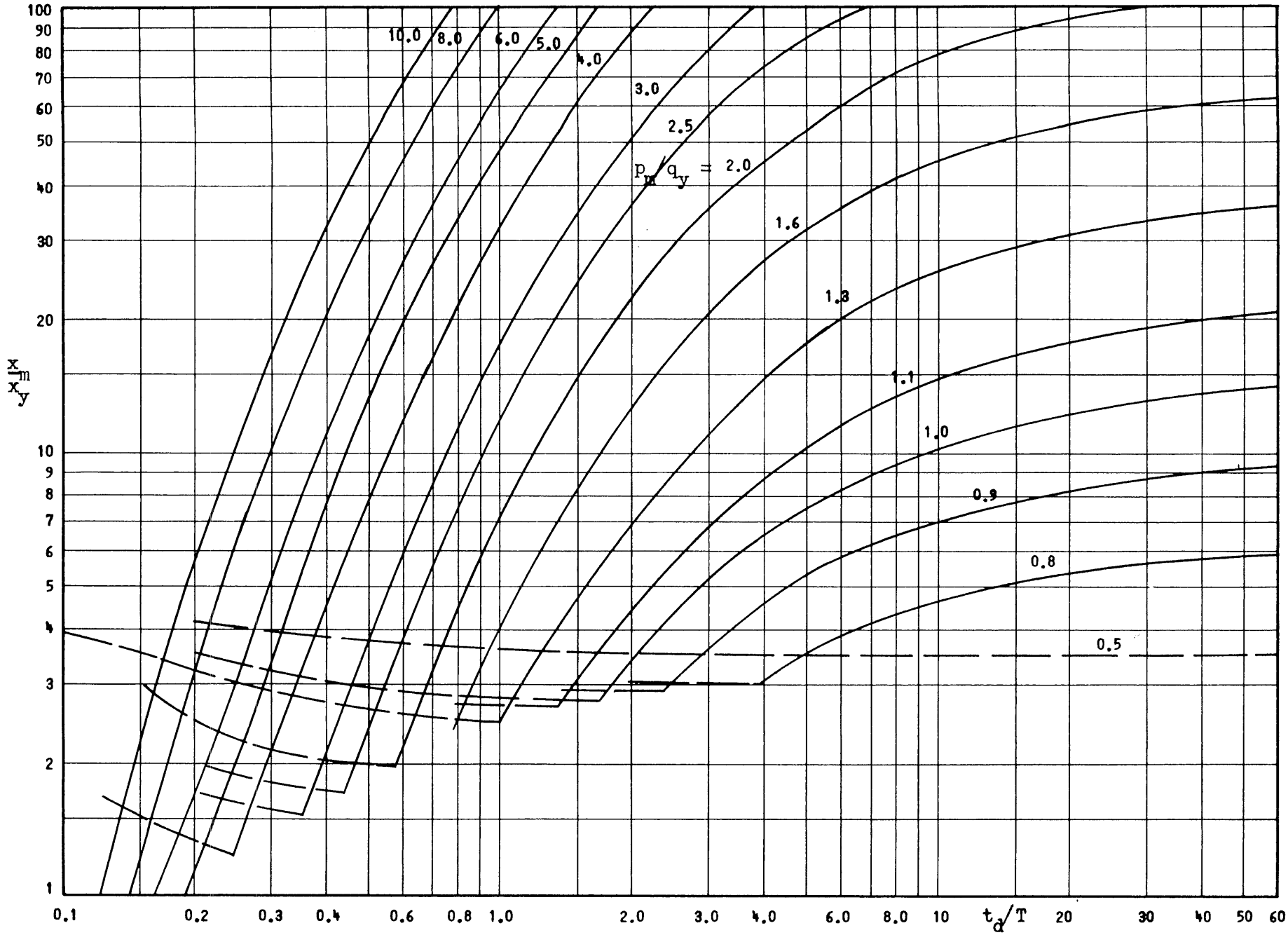

Fig. 6f Maximum Response of Mass-Spring System to Initial-Peak Triangular Pulse with Initial Impulse
$k_2/k_1=0.02$, $I/q_yT=-0.5$, $t_1/T=0$

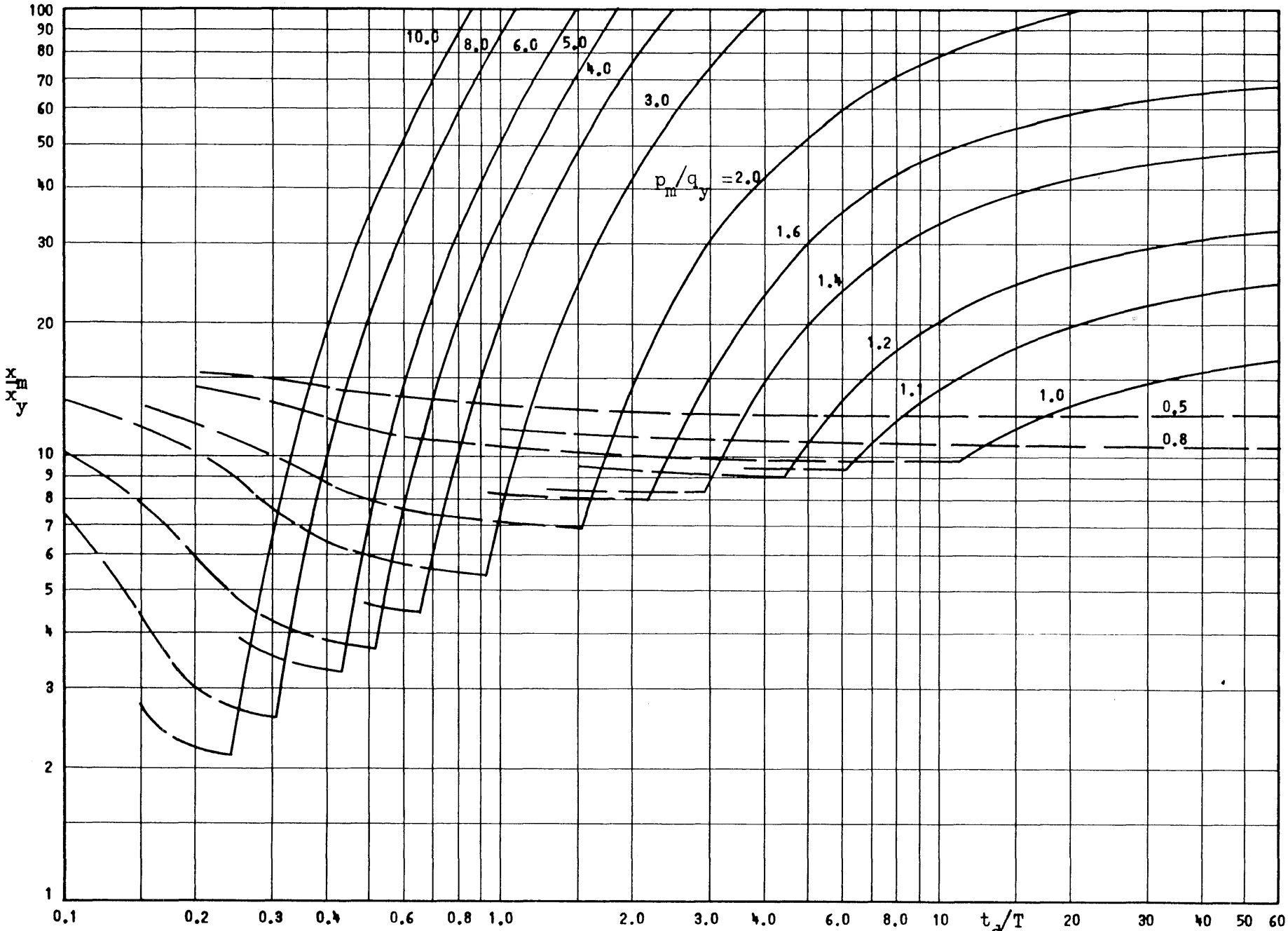

Fig. 6g Maximum Response of Mass-Spring System to Initial-Peak Triangular Pulse with Initial Impulse

$k_2/k_1=0.02$, $I/q_yT=-1.0$, $t_1/T=0$

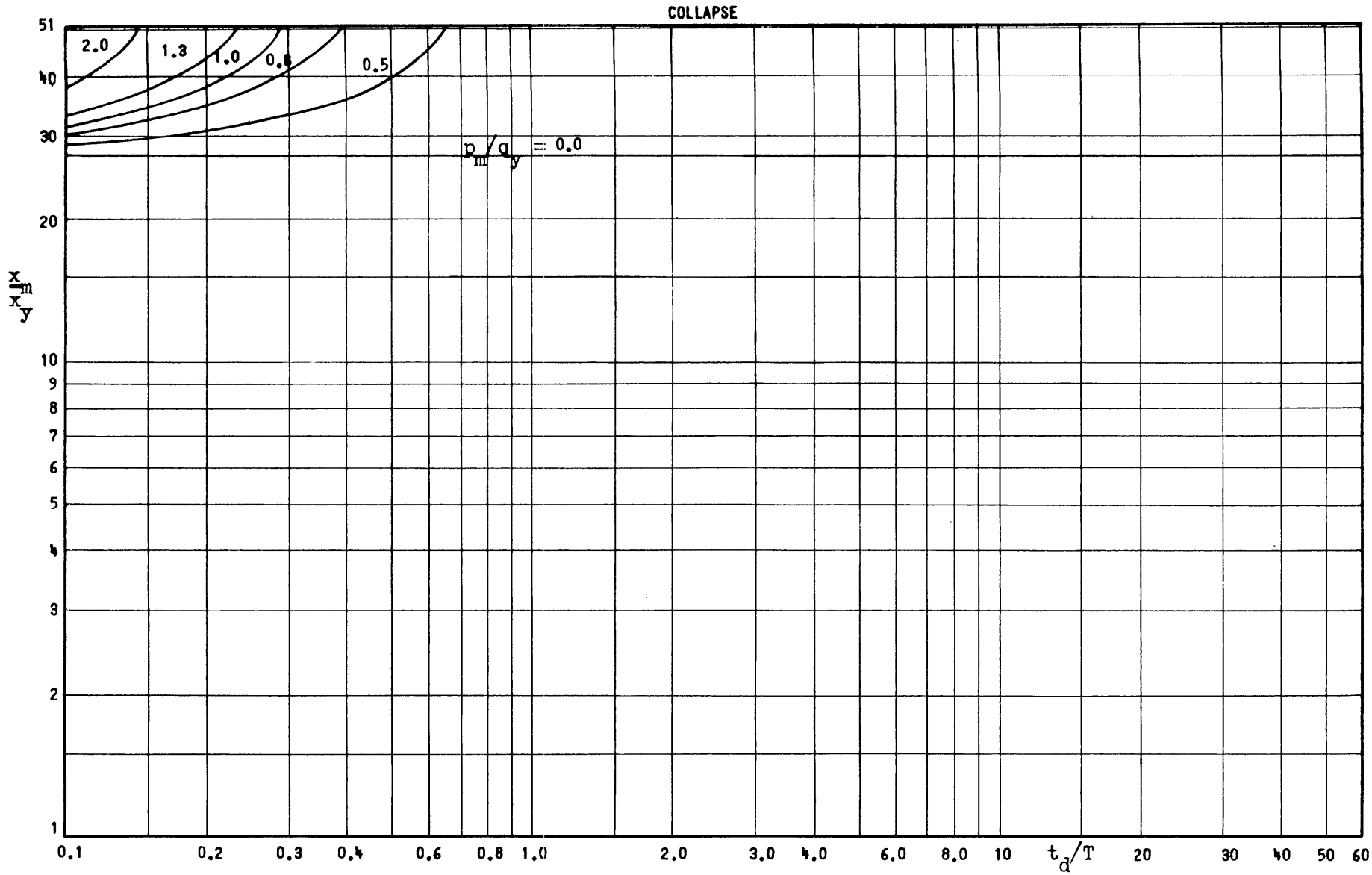

Fig. 7a Maximum Response of Mass-Spring System to Initial-Peak Triangular Pulse with Initial Impulse $k_2/k_1=-0.02$, $I/q_yT=+1.0$, $t_1/T=0$

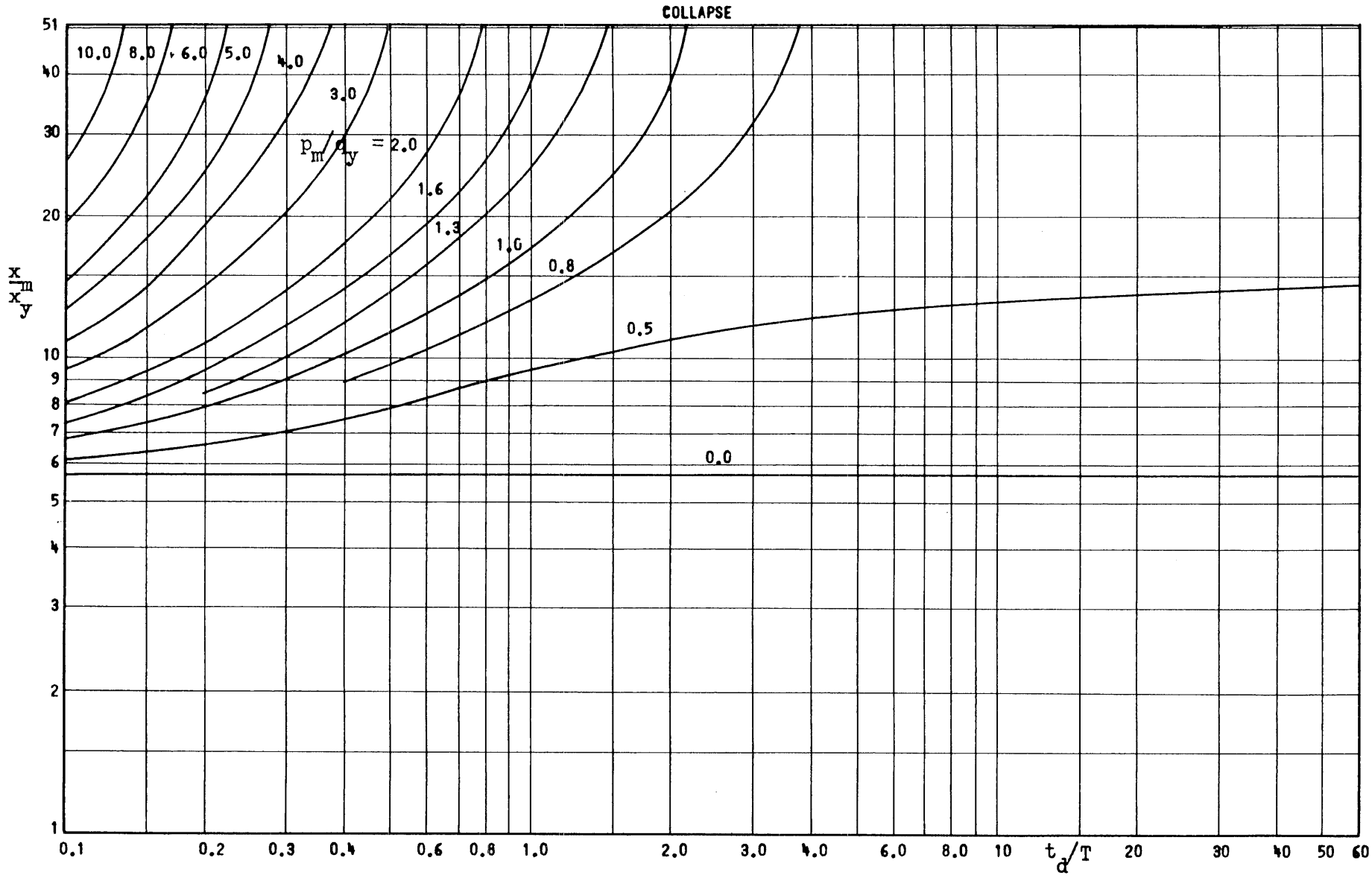

Fig. 7b Maximum Response of Mass-Spring System to Initial-Peak Triangular Pulse with Initial Impulse $k_2/k_1=-0.02$, $I/q_yT=+0.5$, $t_1/T=0$

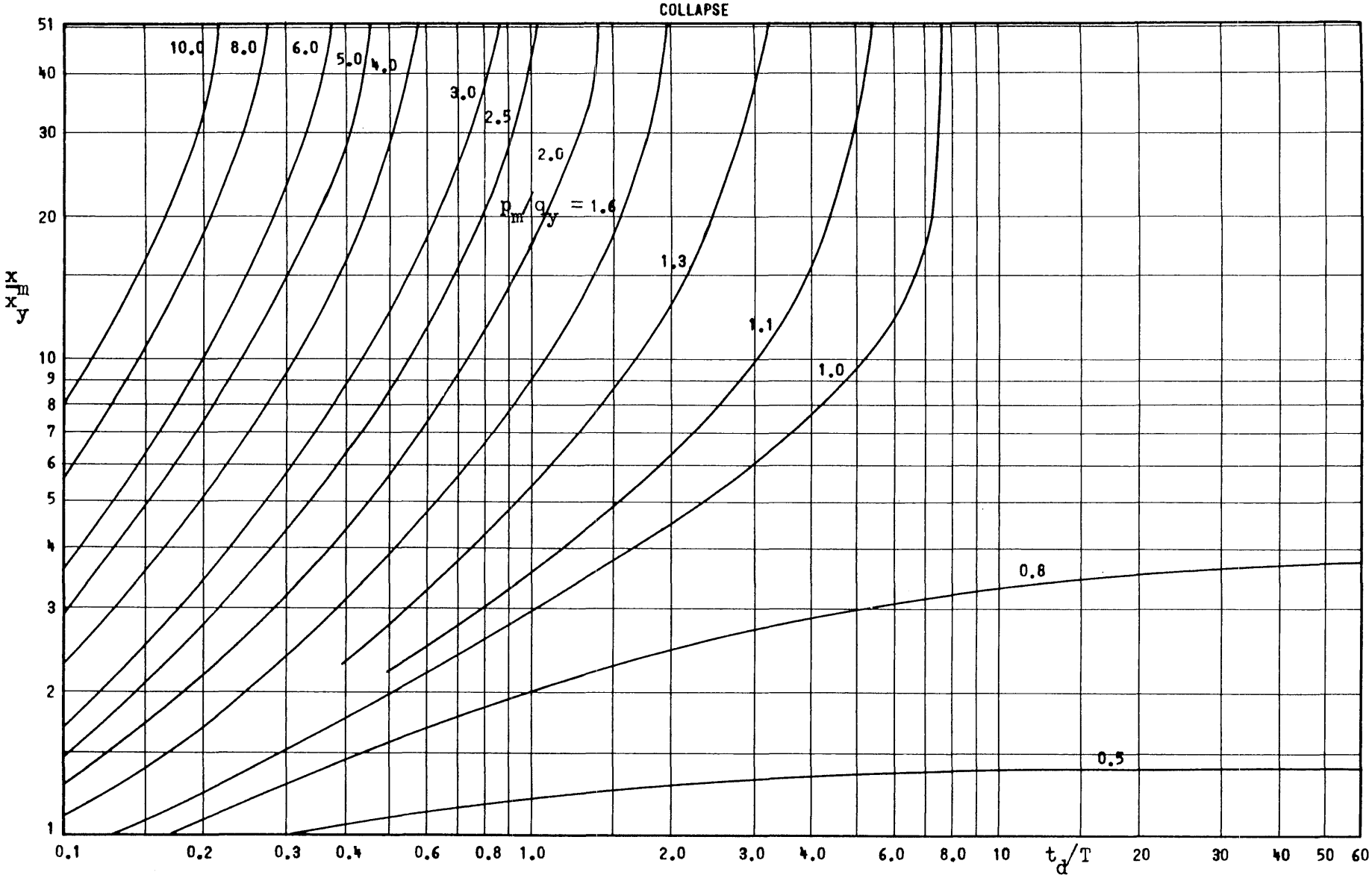

Fig. 7c Maximum Response of Mass-Spring System to Initial-Peak Triangular Pulse with Initial Impulse $k_2/k_1=-0.02$, $I/q_yT=+0.1$, $t_1/T=0$

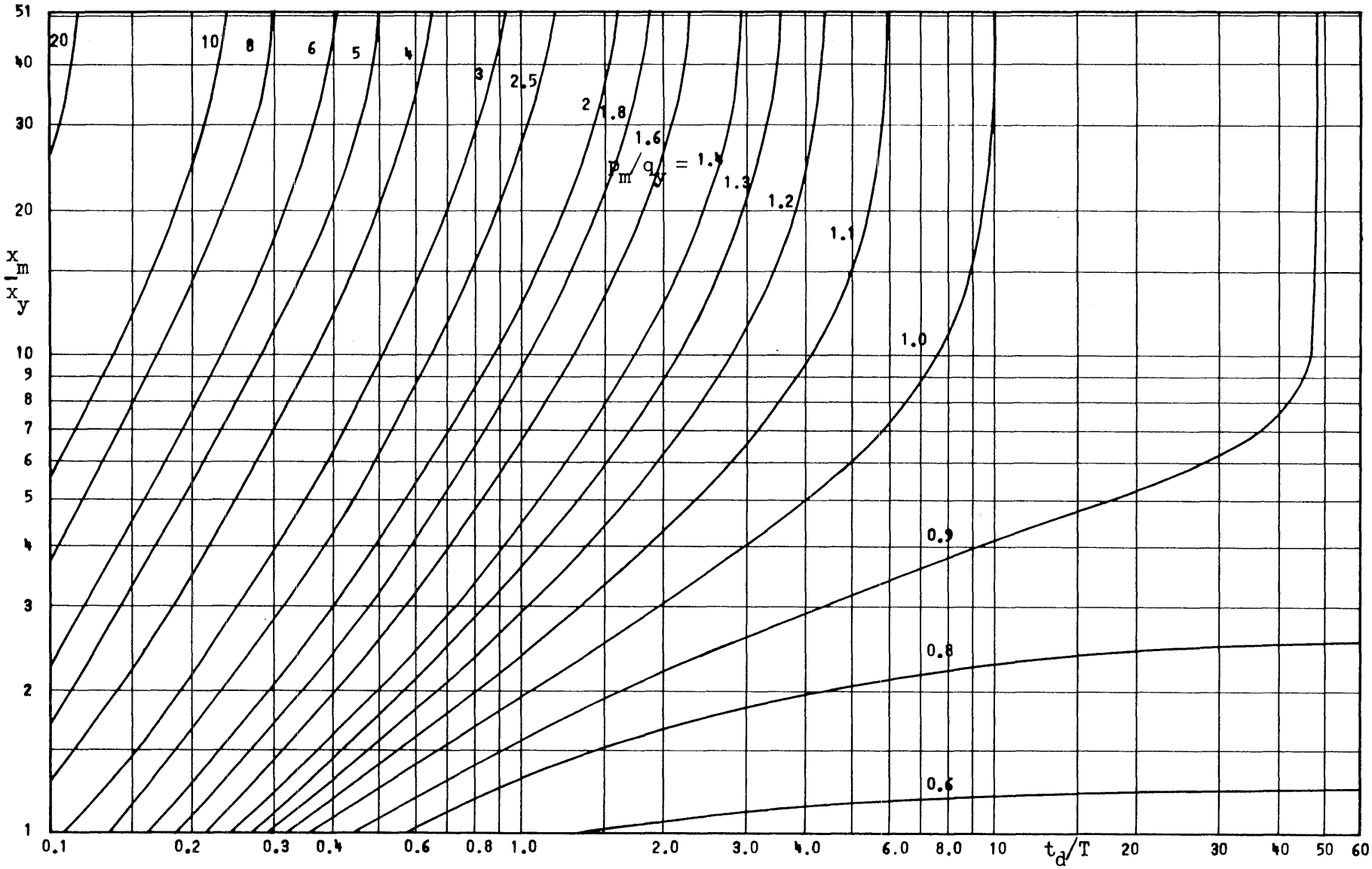

Fig. 7d Maximum Response of Mass-Spring System to Initial-Peak Triangular Pulse with Initial Impulse $K_2/K_1 = -0.02$, $I/q_yT = 0$, $t_1/T = 0$

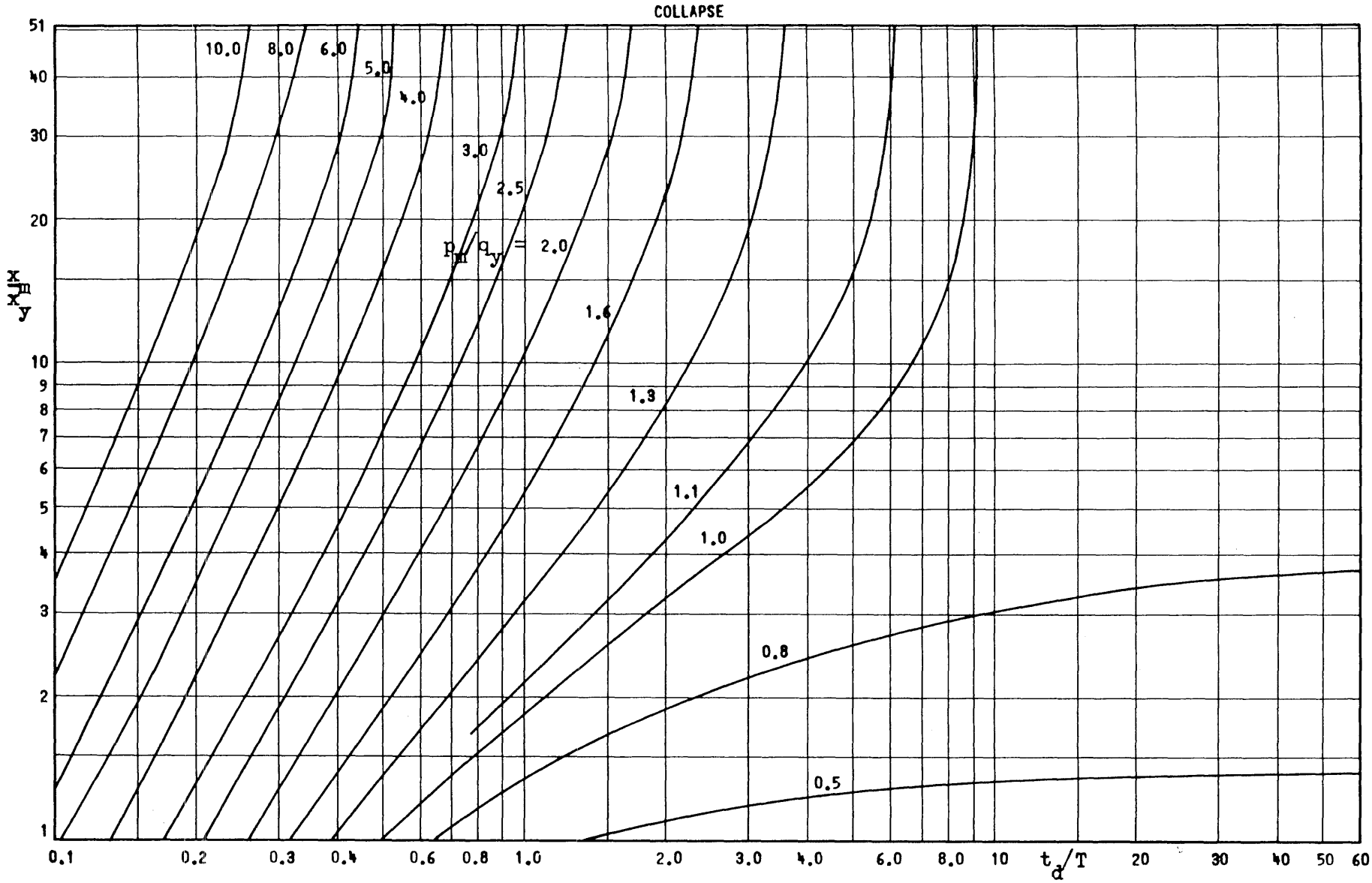

Fig. 7e Maximum Response of Mass-Spring System to Initial-Peak Triangular Pulse with Initial Impulse $k_2/k_1=-0.02$, $I/q_yT=-0.1$, $t_1/T=0$

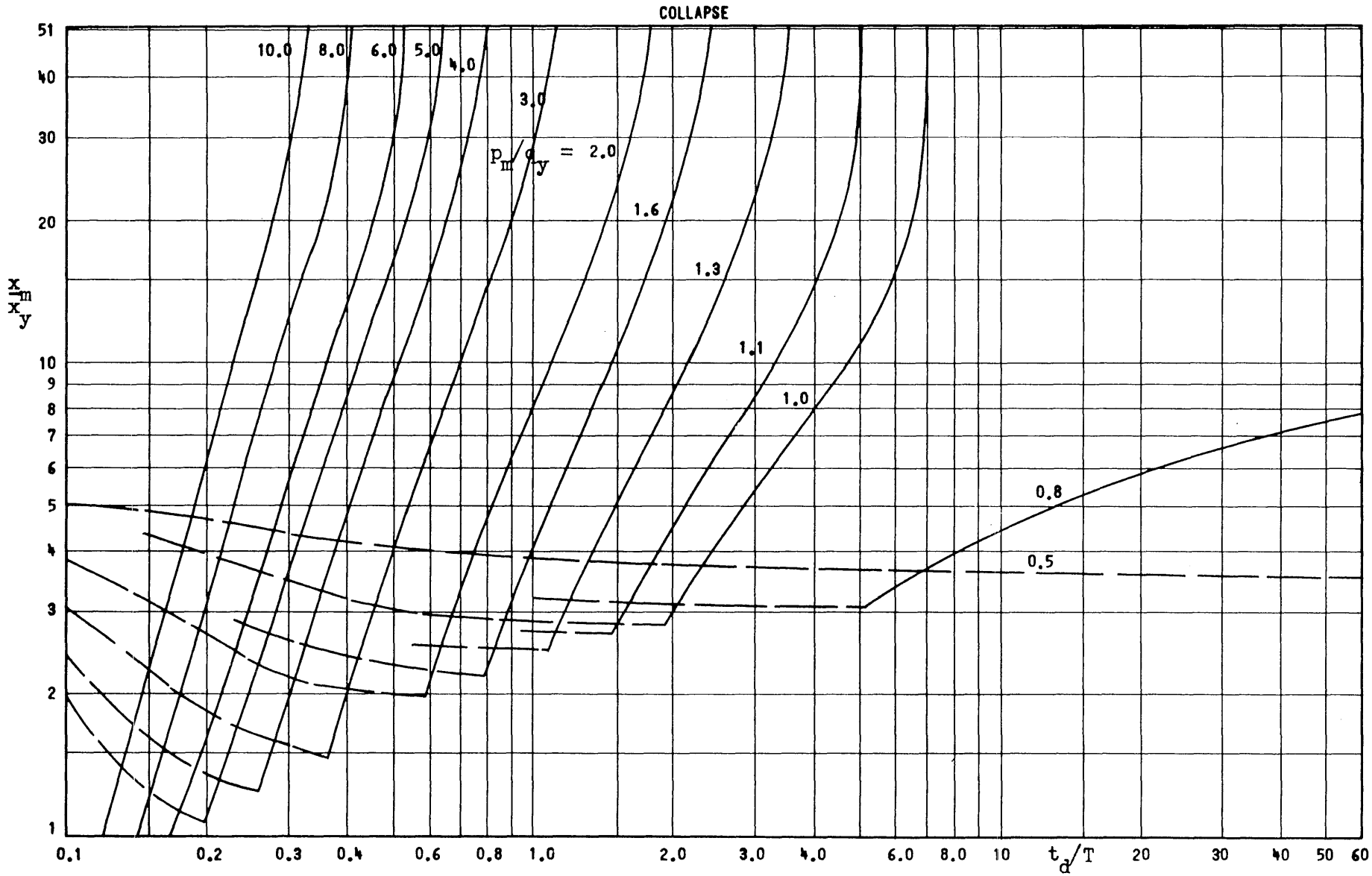

Fig. 7f Maximum Response of Mass-Spring System to Initial-Peak Triangular Pulse with Initial Impulse

$k_2/k_1=-0.02$, $I/q_yT=-0.5$, $t_1/T=0$

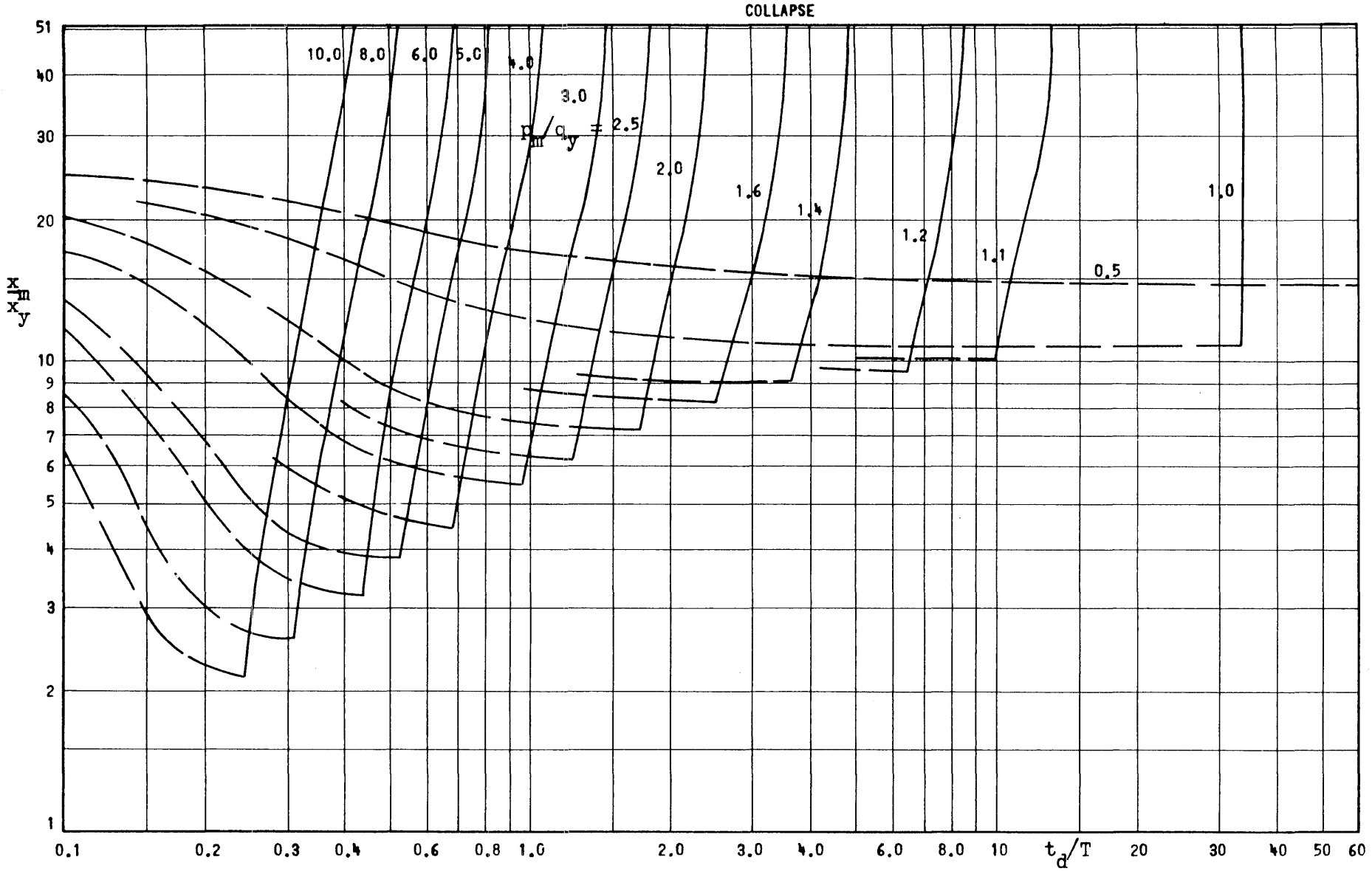

Fig. 7g Maximum Response of Mass-Spring System to Initial-Peak Triangular Pulse with Initial Impulse $k_2/k_1=-0.02$, $I/q_yT=-1.0$, $t_1/T=0$

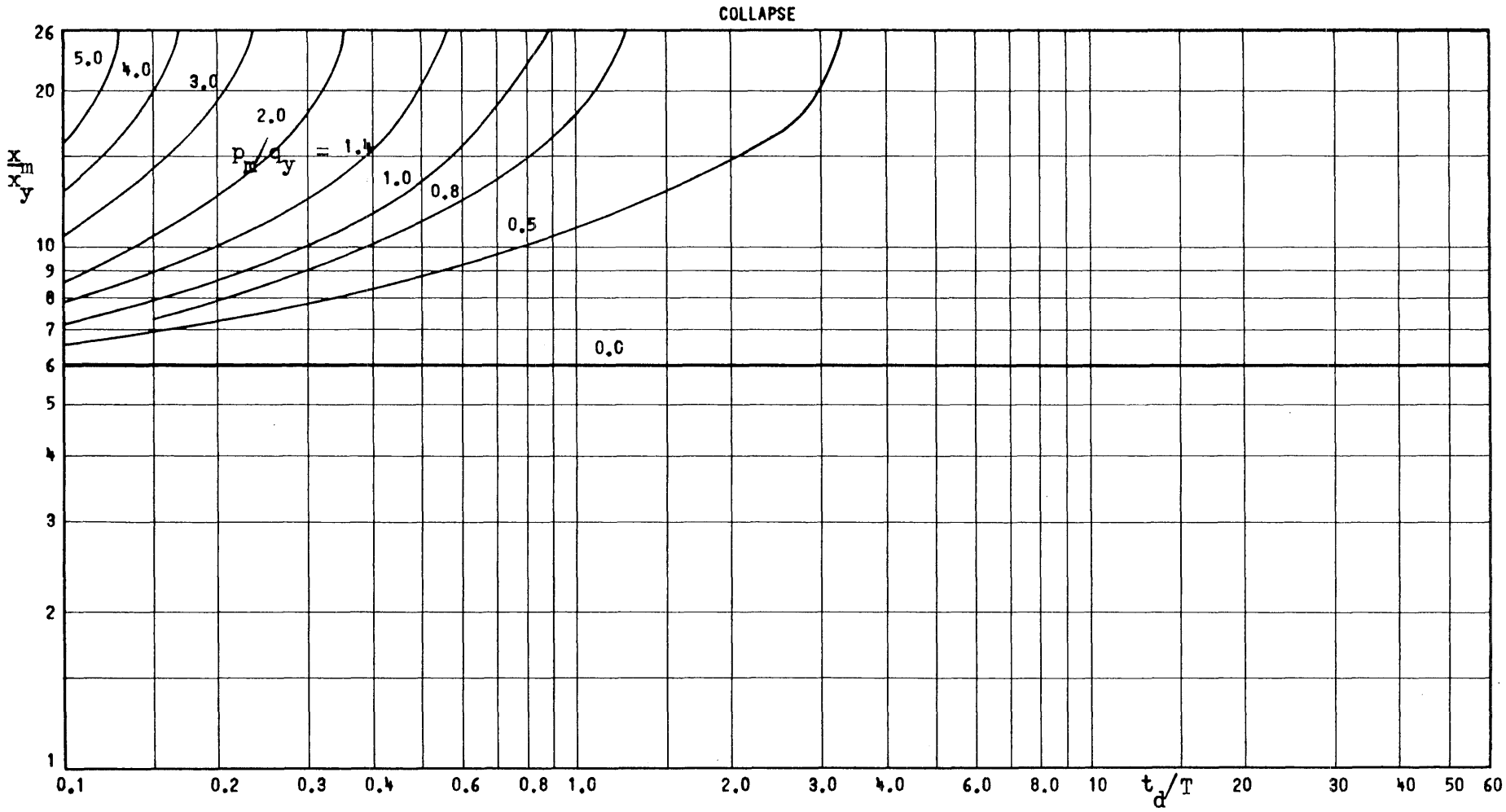

Fig. 8b Maximum Response of Mass-Spring System to Initial-Peak Triangular Pulse with Initial Impulse $k_2/k_1=-0.04$, $I/q_yT=+0.5$, $t_1/T=0$

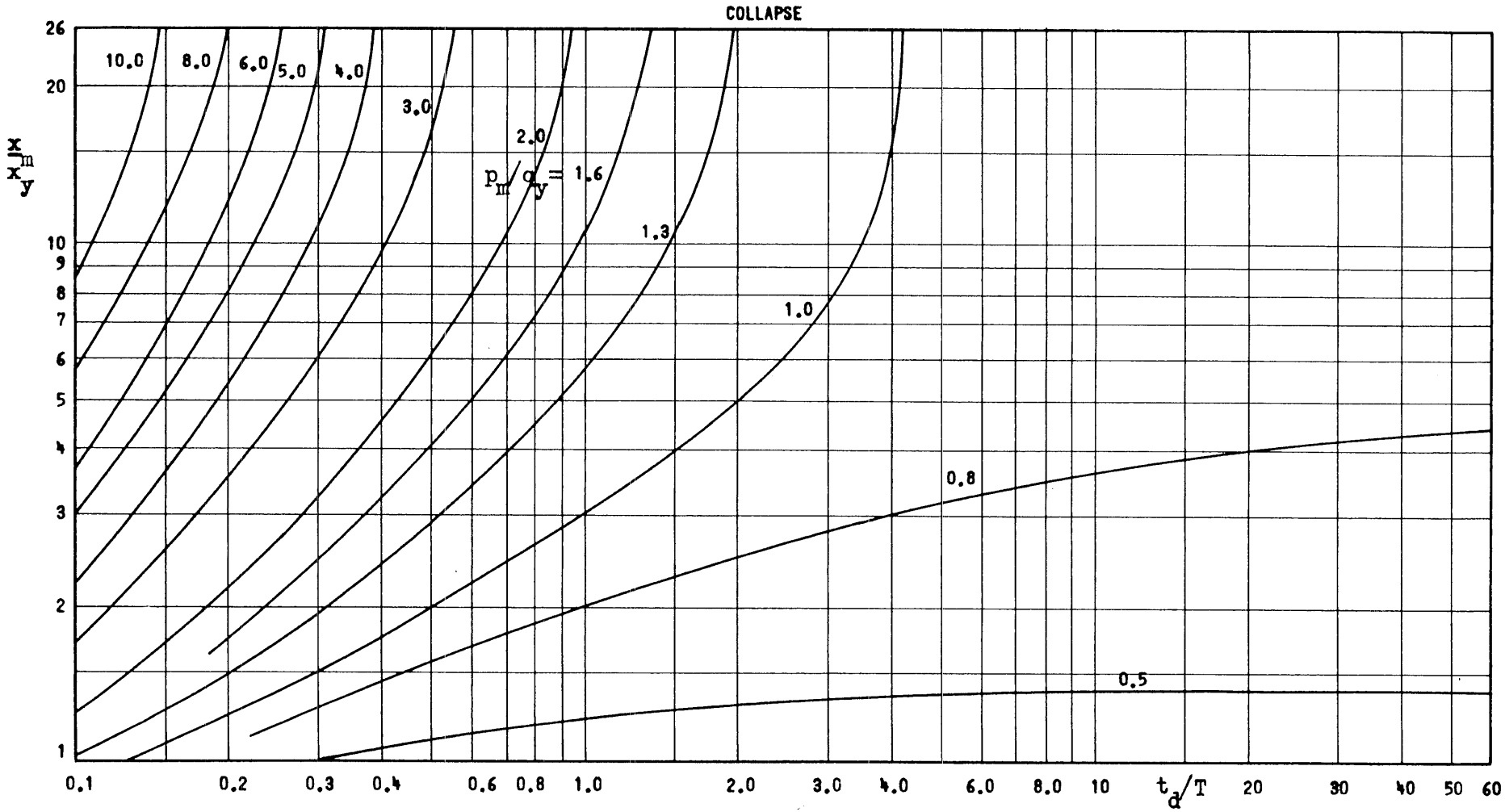

Fig. 8c Maximum Response of Mass-Spring System to Initial-Peak Triangular Pulse with Initial Impulse $k_2/k_1=-0.04$, $I/q_yT=+0.1$, $t_1/T=0$

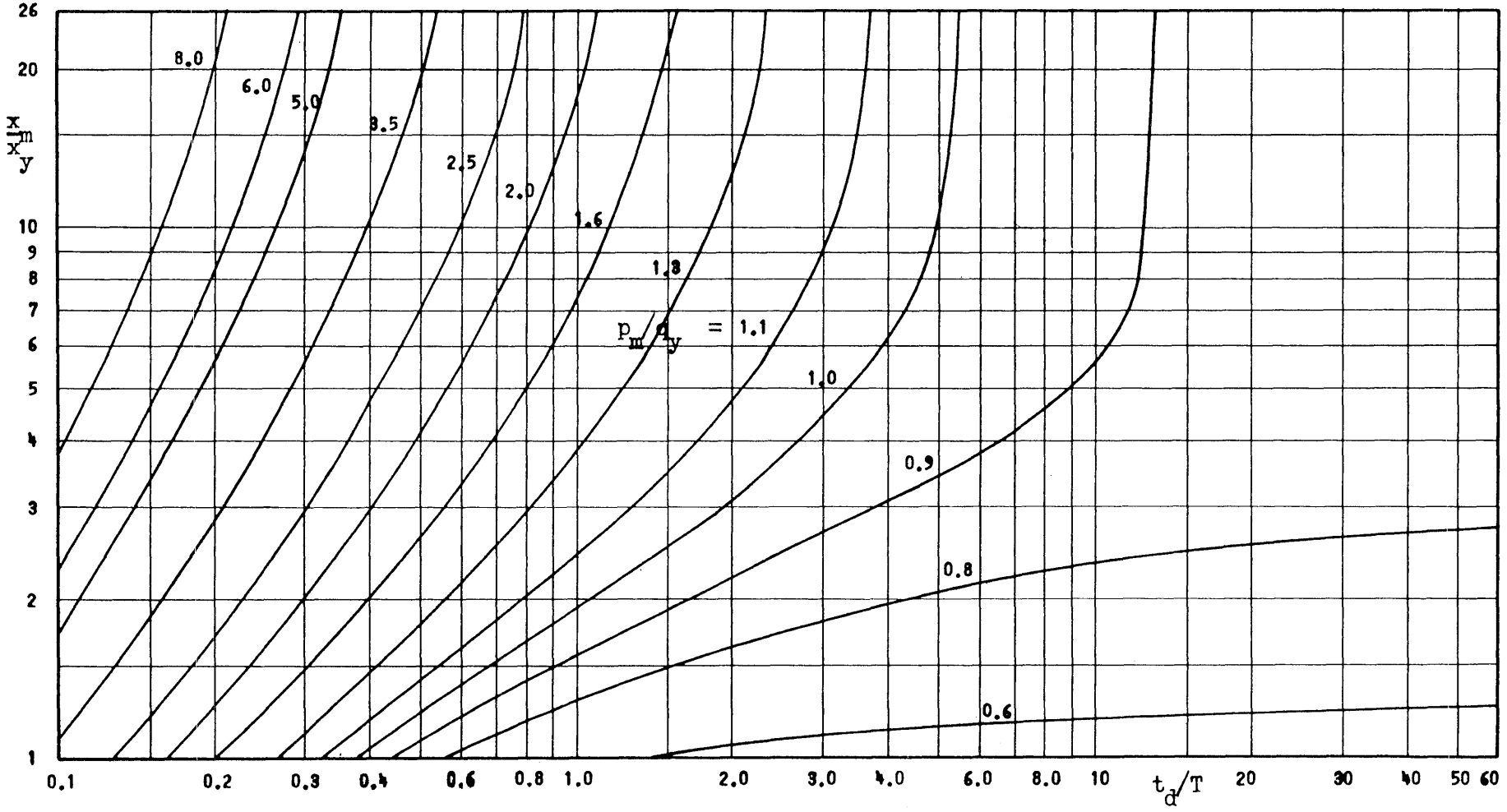

Fig. 8d Maximum Response of Mass-Spring System to Initial-Peak Triangular Pulse

$k_2/k_1 = -0.04$, $I/q_yT = 0.0$, $t_1/T = 0$

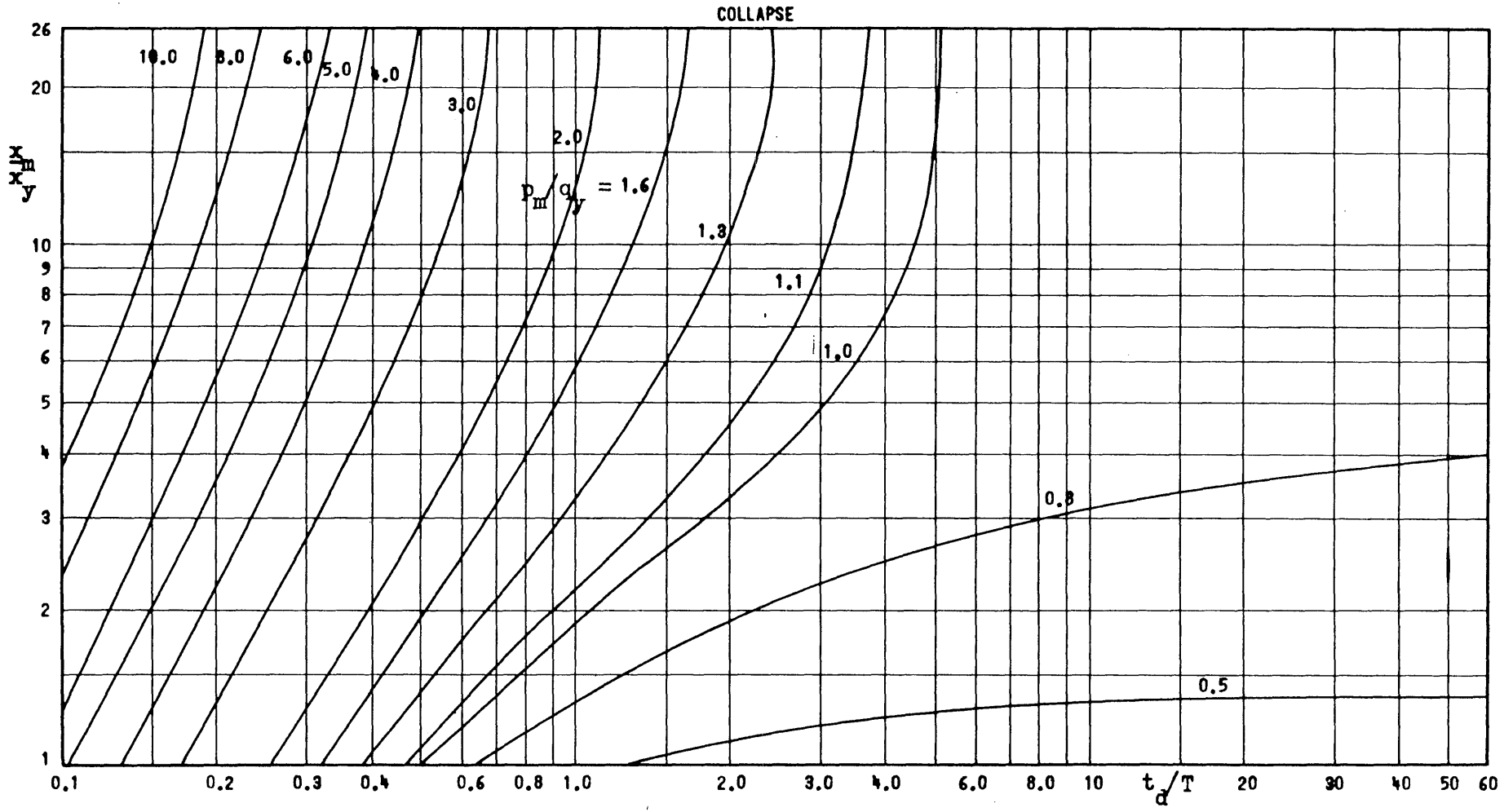

Fig. 8e Maximum Response of Mass-Spring System to Initial-Peak Triangular Pulse with Initial Impulse $k_2/k_1=-0.04$, $I/q_yT=-0.1$, $t_1/T=0$

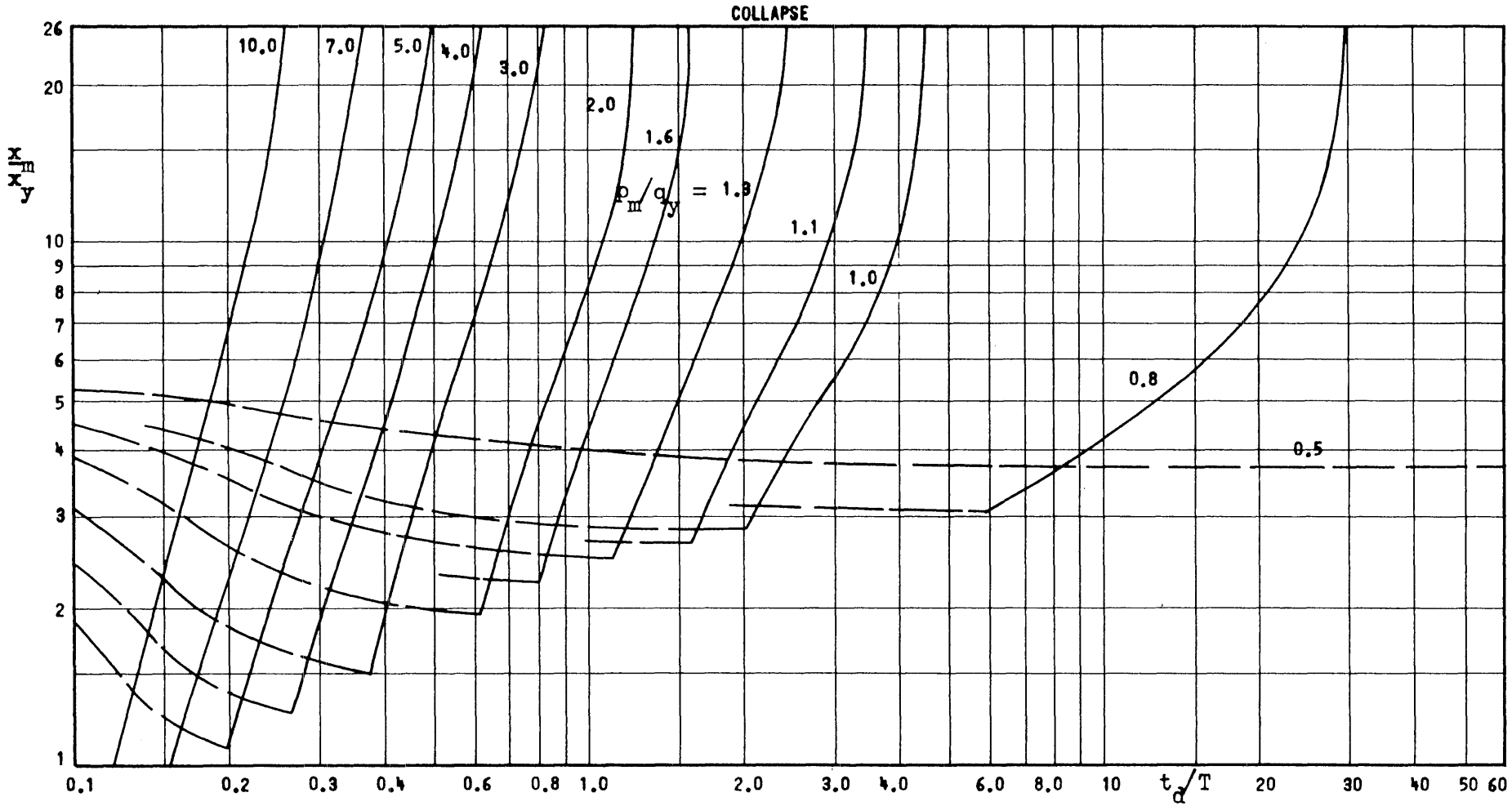

Fig. 8f Maximum Response of Mass-Spring System to Initial-Peak Triangular Pulse with Initial Impulse

k_2/k_1=-0.04, I/q_yT=-0.5, t_1/T=0

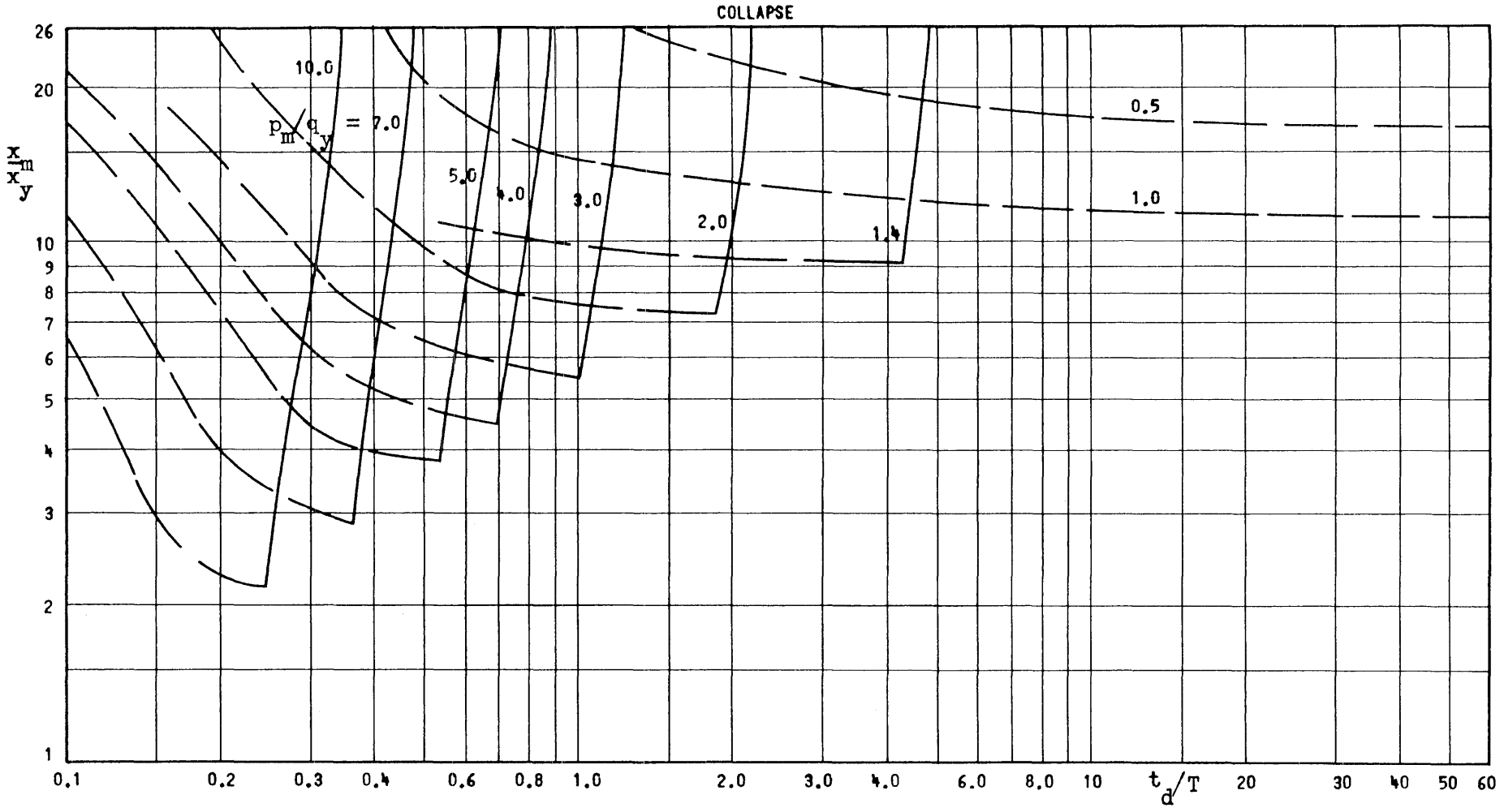

Fig. 8g Maximum Response of Mass-Spring System to Initial-Peak Triangular Pulse with Initial Impulse k_2/k_1=-0.04, I/q_yT=-1.0, t_1/T=0

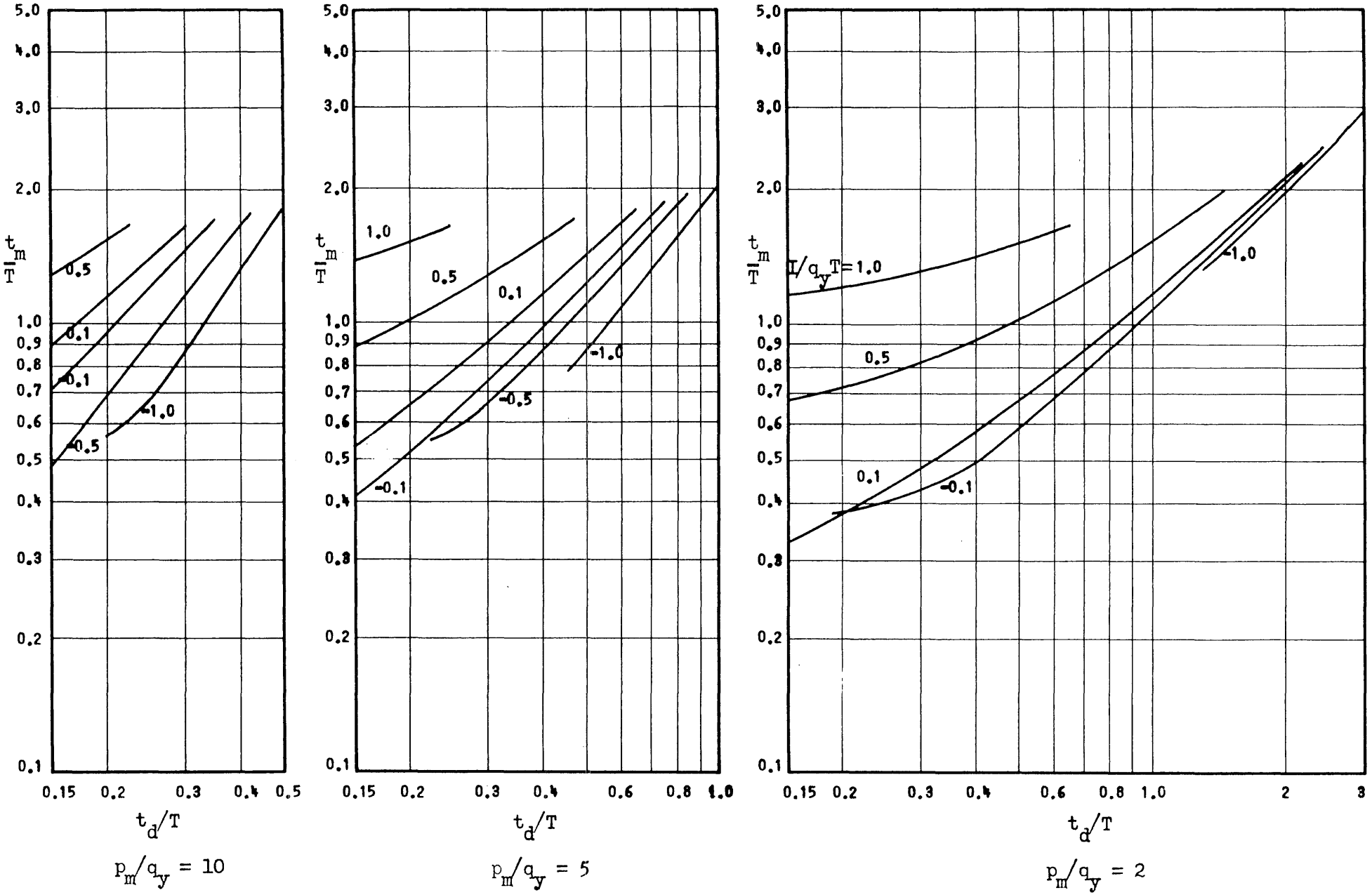

Fig. 9a Time of Maximum Response to Initial Peak Triangular Pulse with Initial Impulse
$k_2/k_1 = 0$

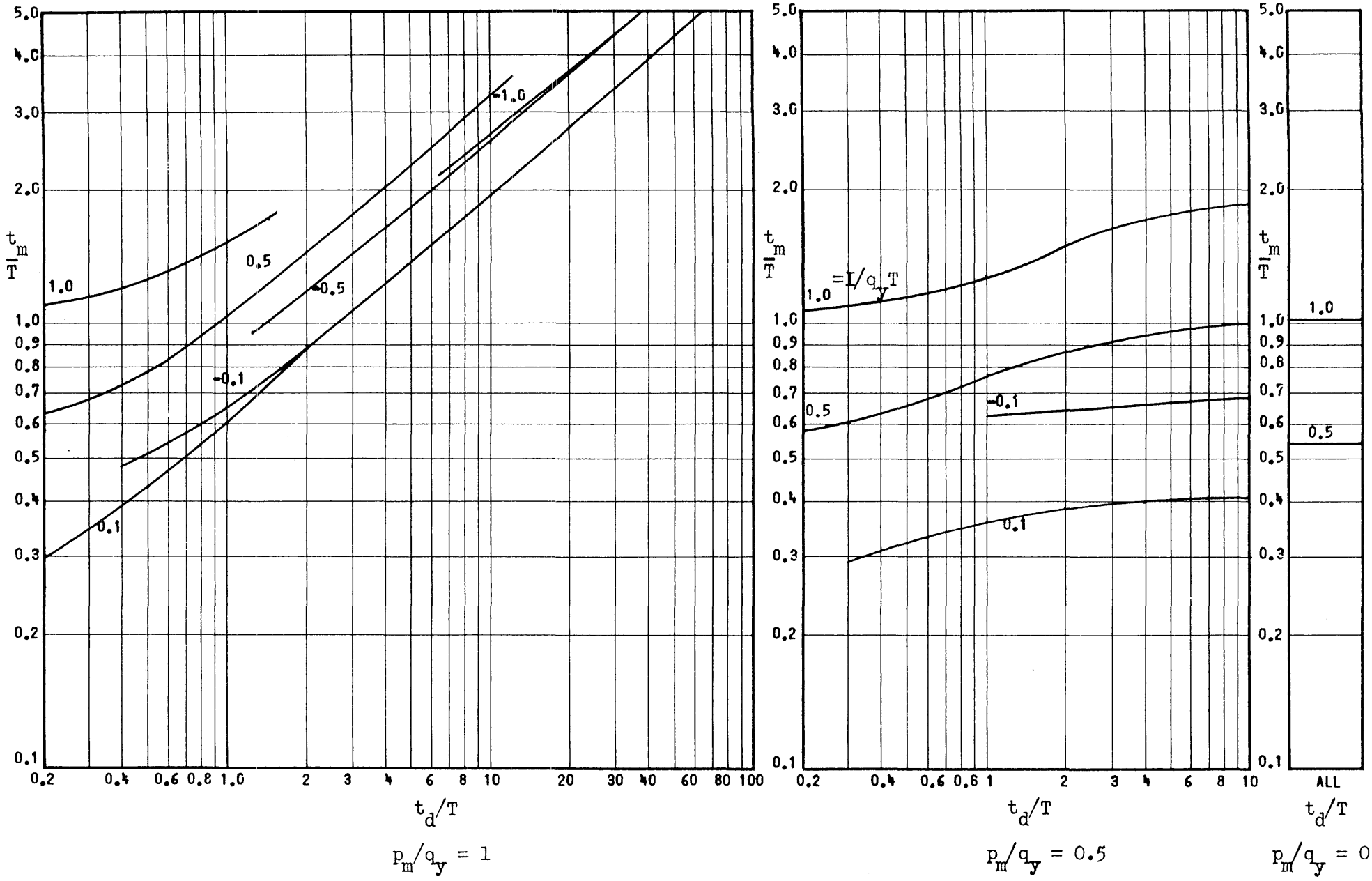

Fig. 9b Time of Maximum Response to Initial Peak Triangular Pulse with Initial Impulse
$k_2/k_1 = 0$

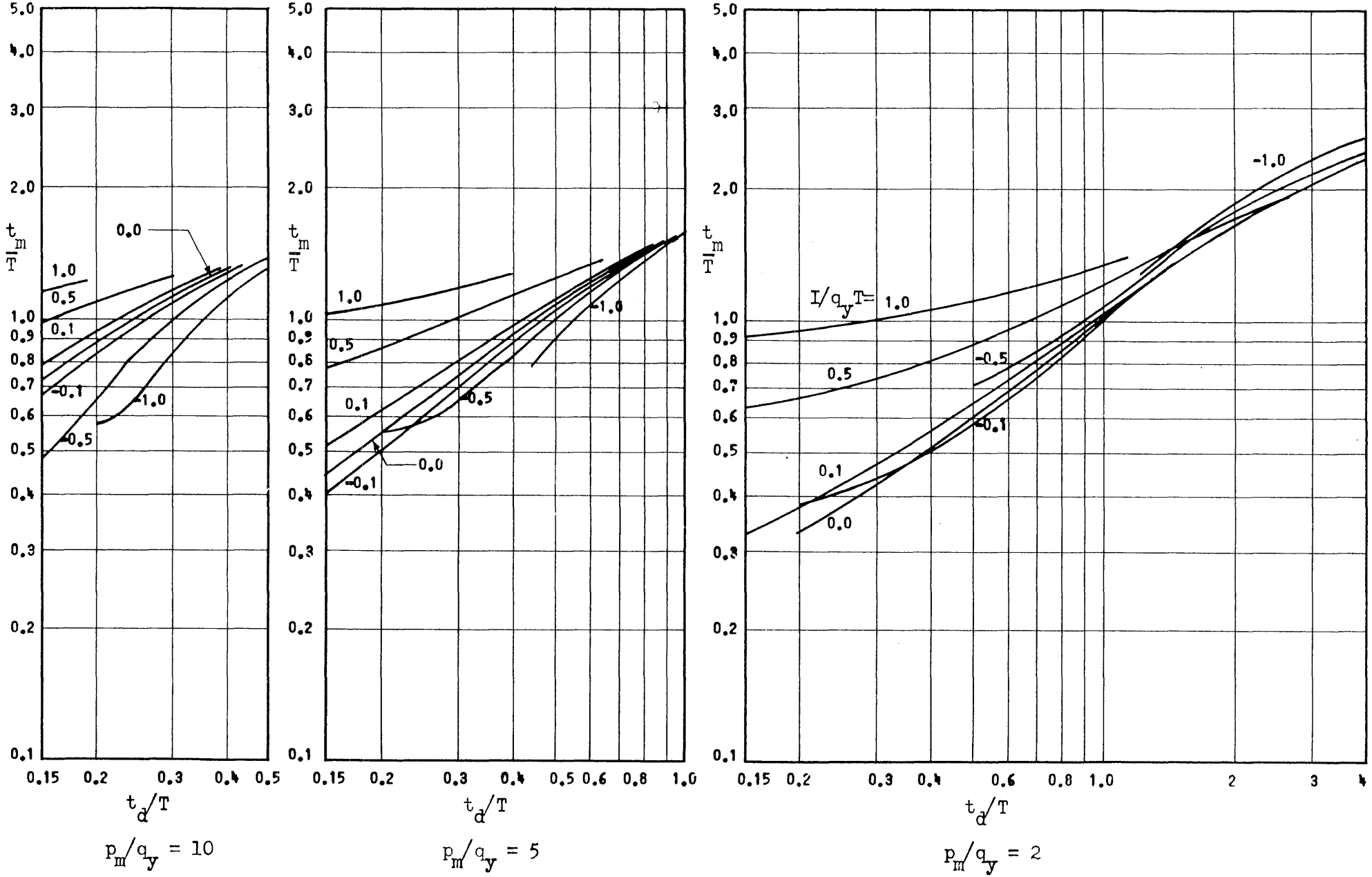

Fig. 10a Time of Maximum Response to Initial Peak Triangular Pulse with Initial Impulse

$k_2/k_1 = +0.02$

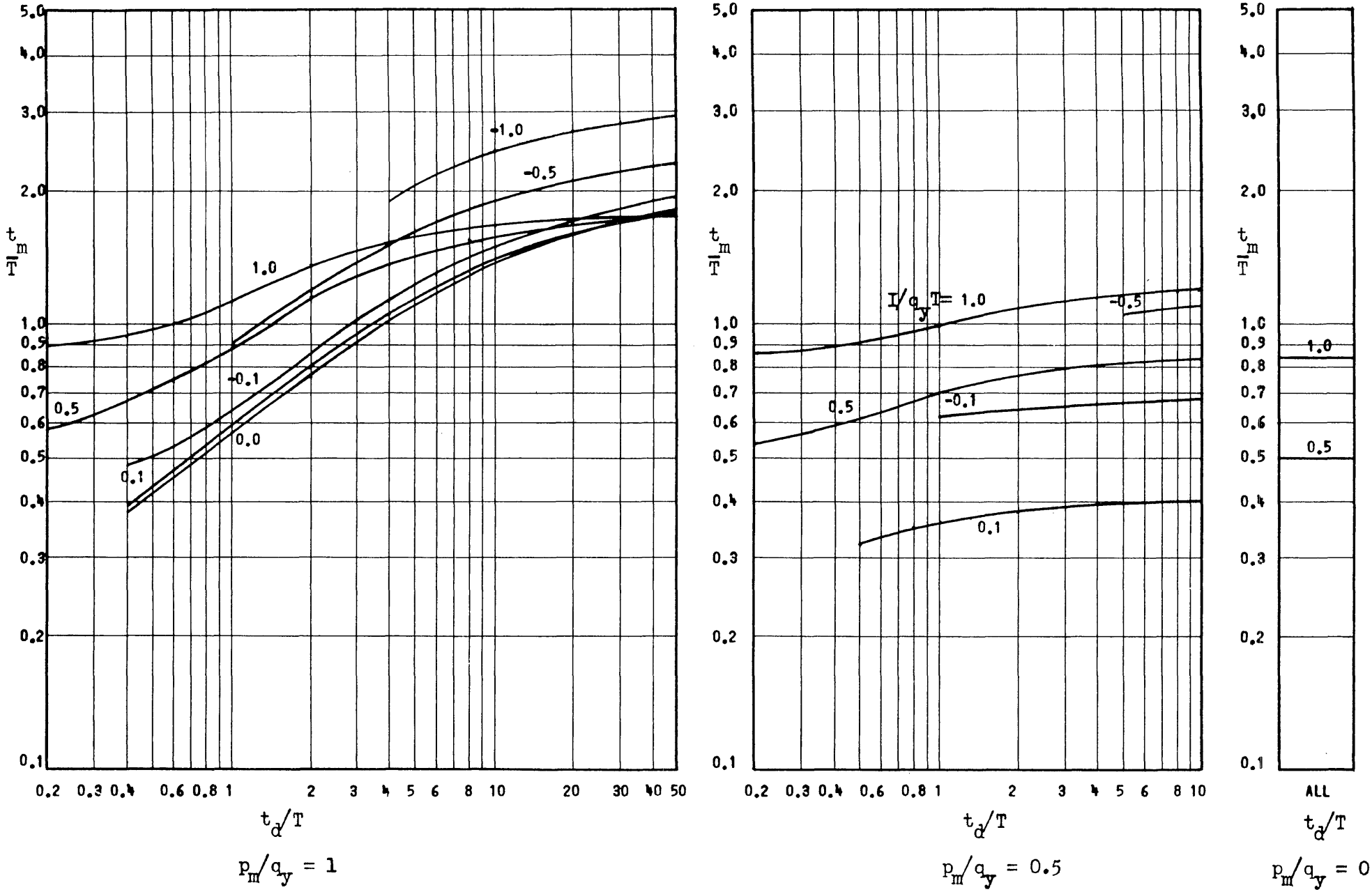

Fig. 10b Time of Maximum Response to Initial Peak Triangular Pulse with Initial Impulse

$k_2/k_1 = +0.02$

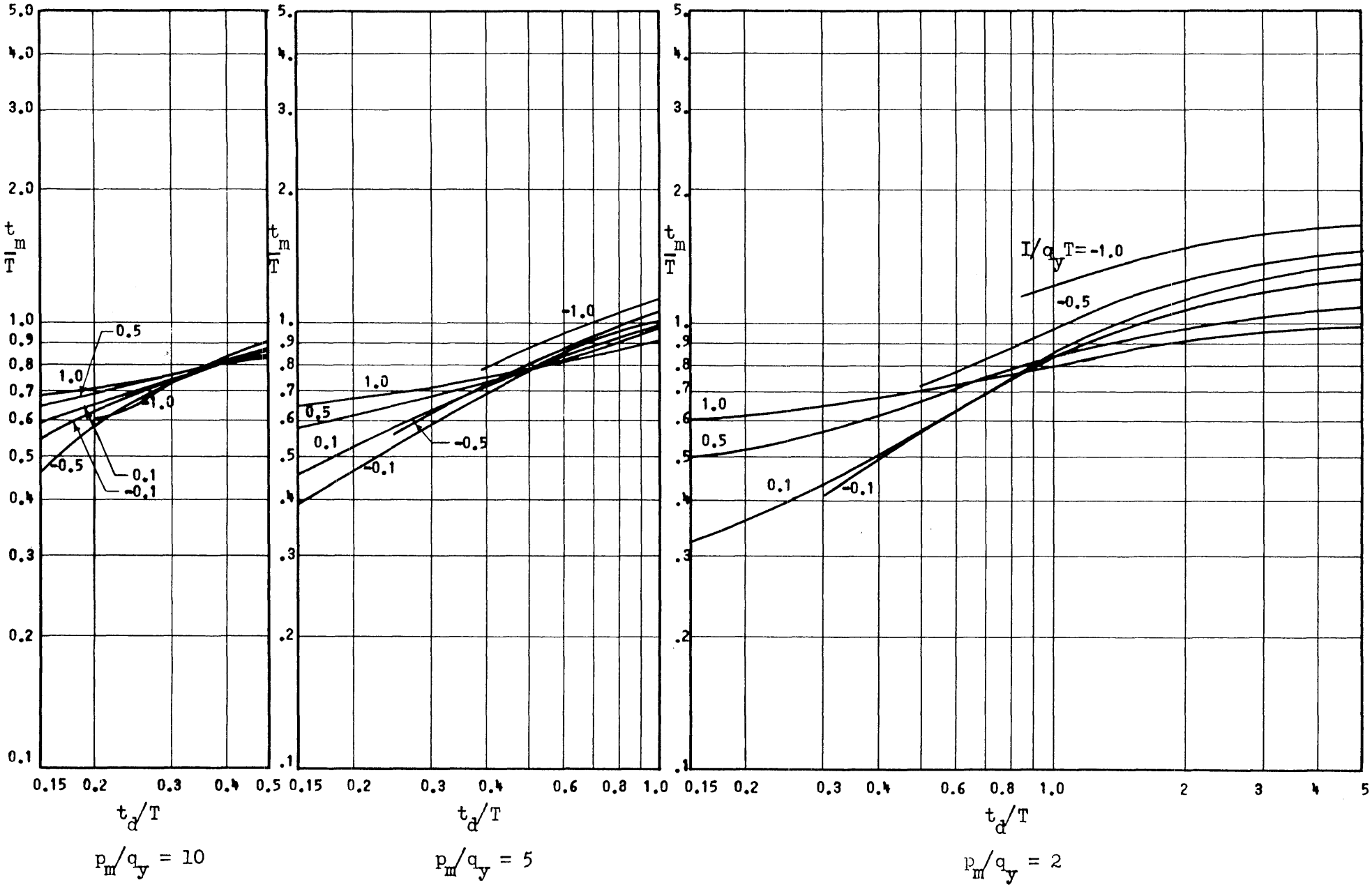

Fig. 11a Time of Maximum Response to Initial Peak Triangular Pulse with Initial Impulse

$k_2/k_1 = +0.1$

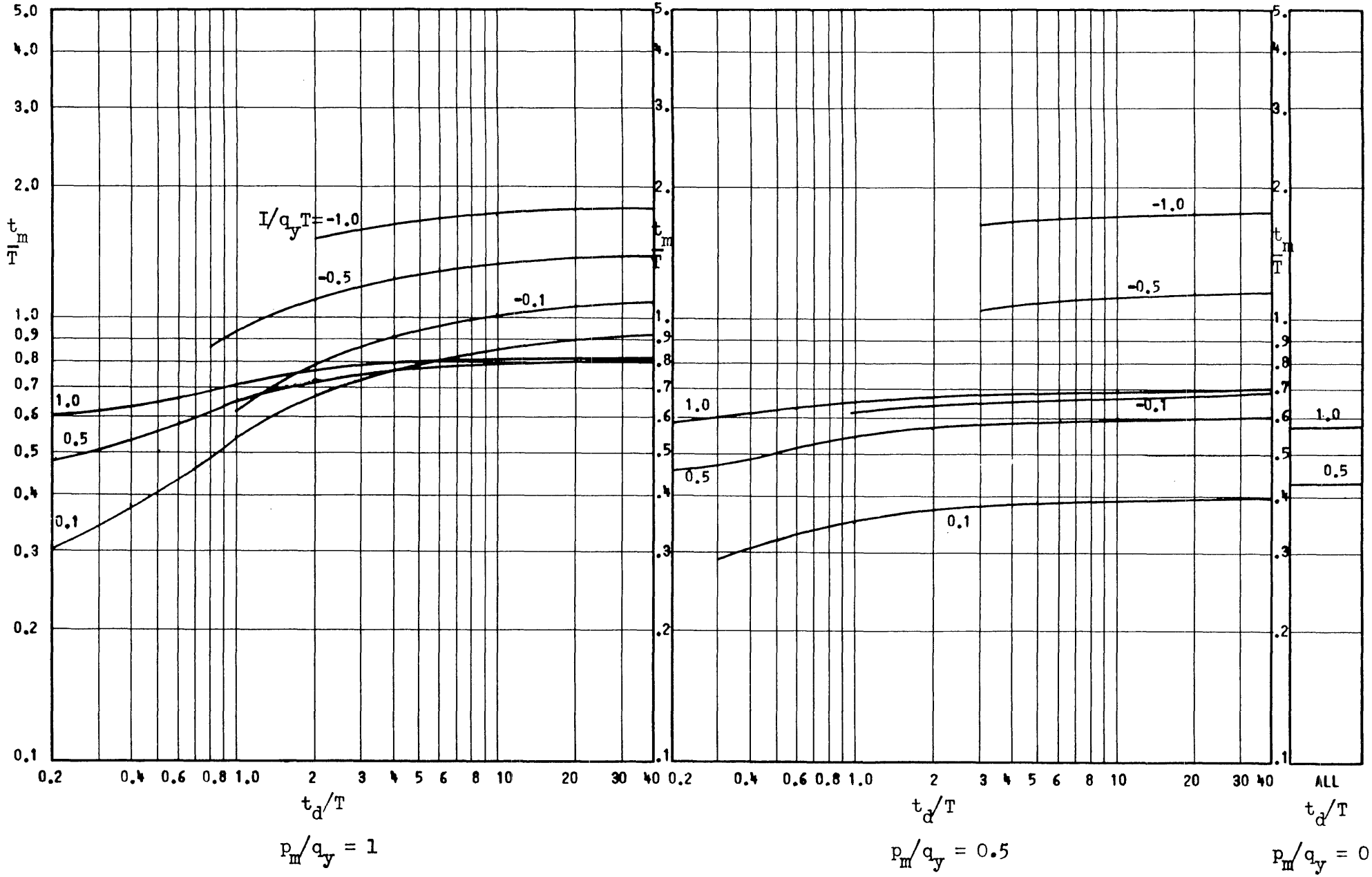

Fig. 11b Time of Maximum Response to Initial Peak Triangular Pulse with Initial Impulse

$k_2/k_1 = +0.1$

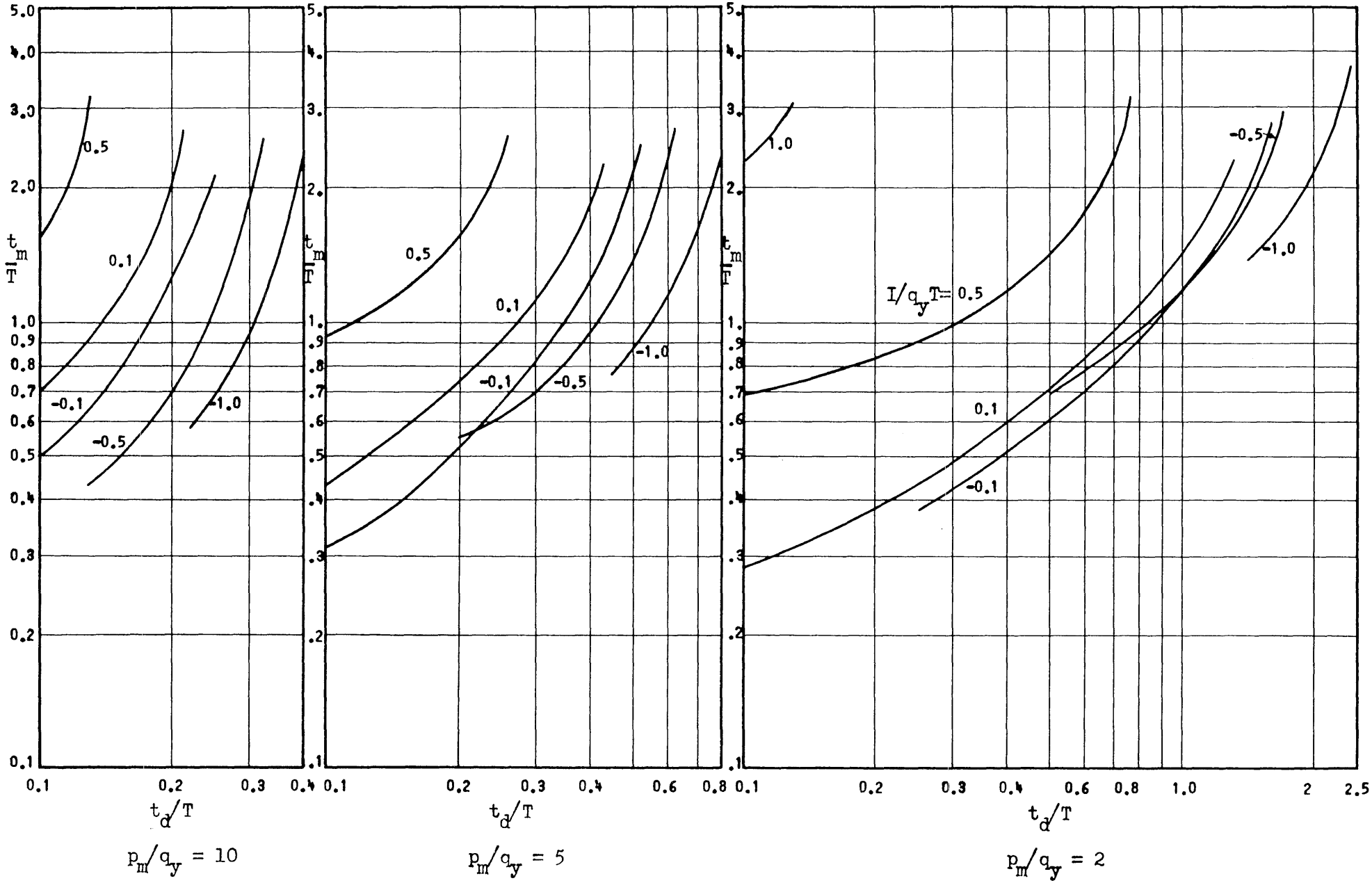

Fig. 12a Time of Maximum Response to Initial Peak Triangular Pulse with Initial Impulse

$k_2/k_1 = -0.02$

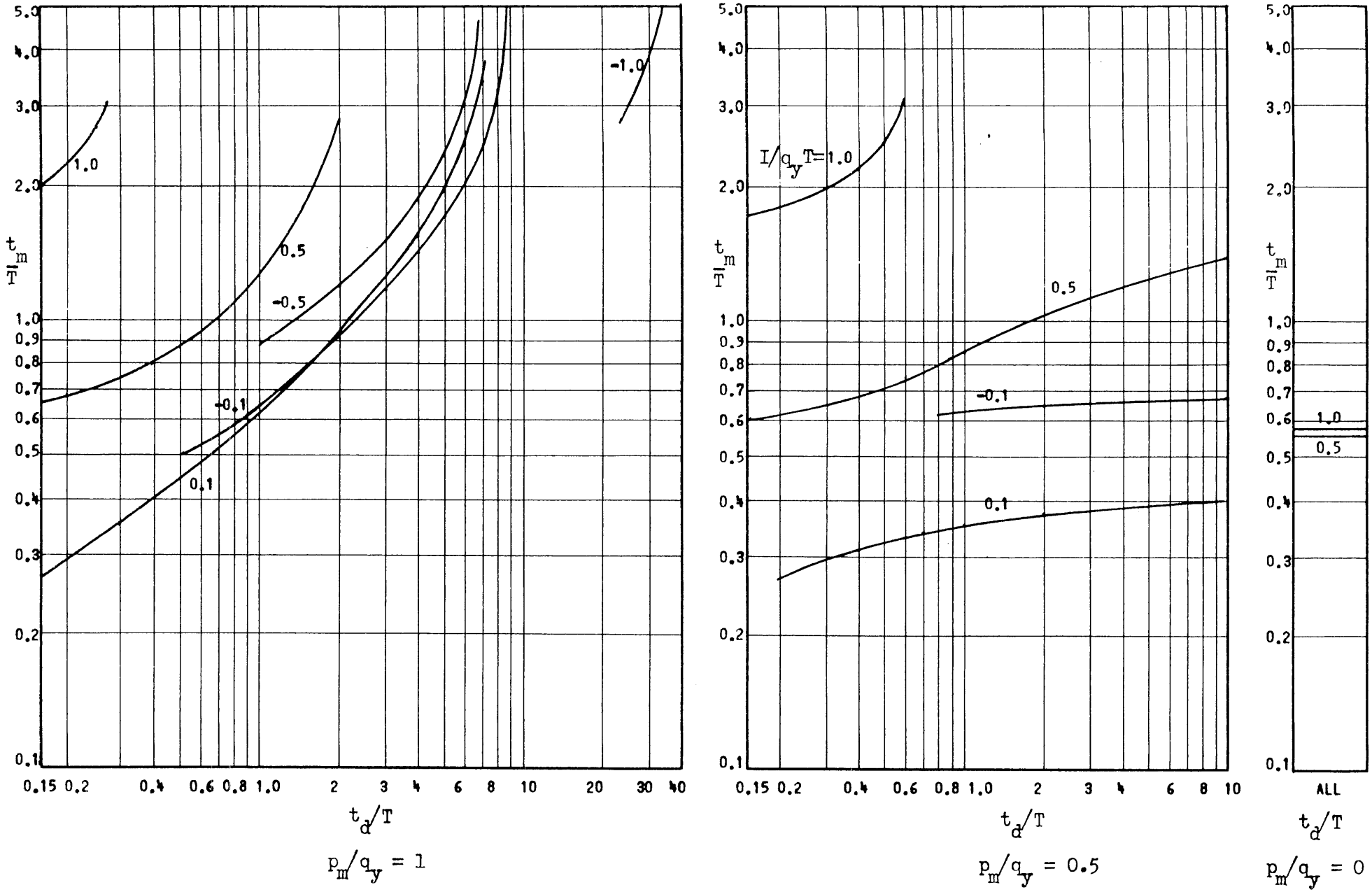

Fig. 12b Time of Maximum Response to Initial Peak Triangular Pulse with Initial Impulse

$k_2/k_1 = -0.02$

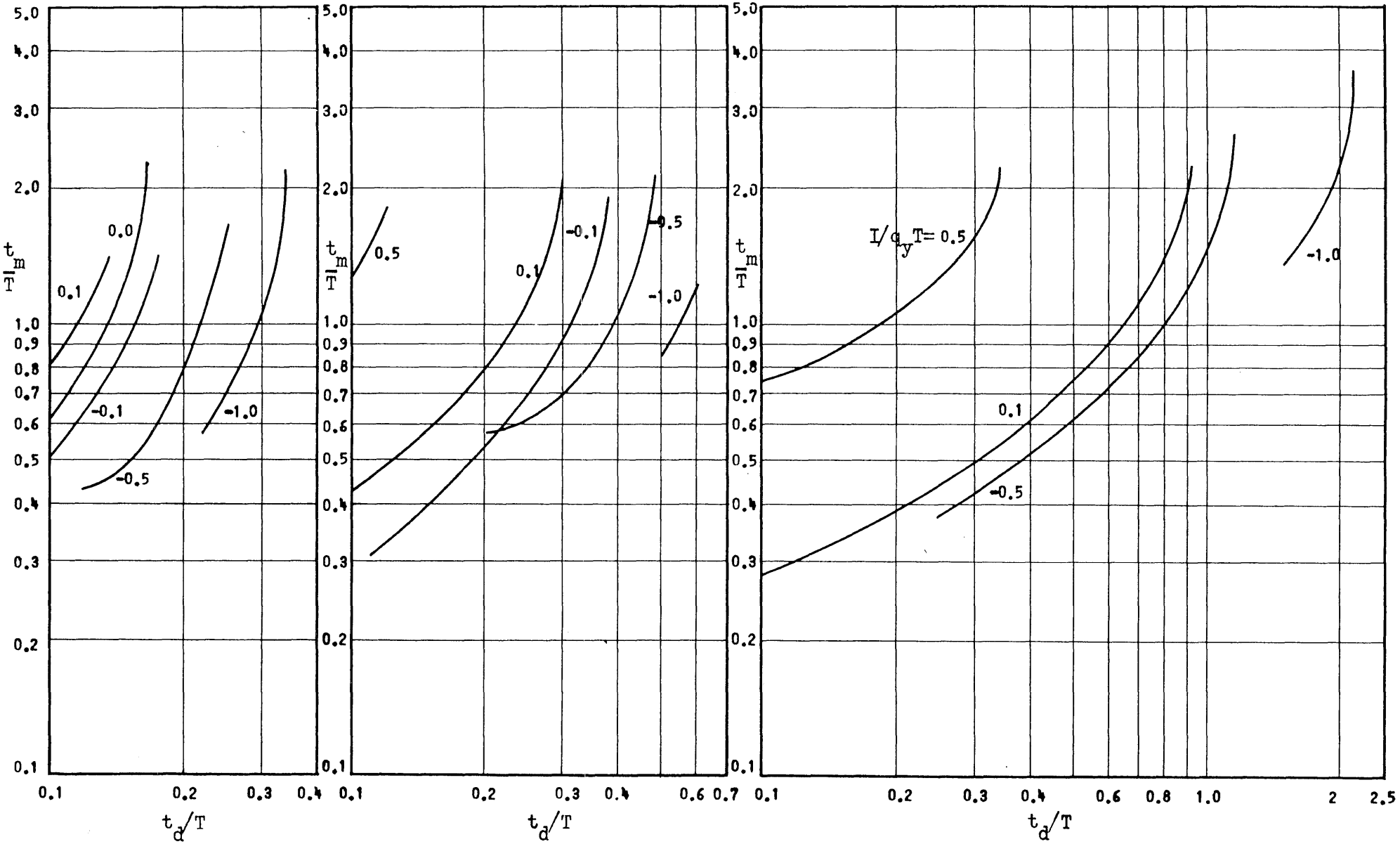

Fig. 13a Time of Maximum Response to Initial Peak Triangular Pulse with Initial Impulse

$k_2/k_1 = -0.04$

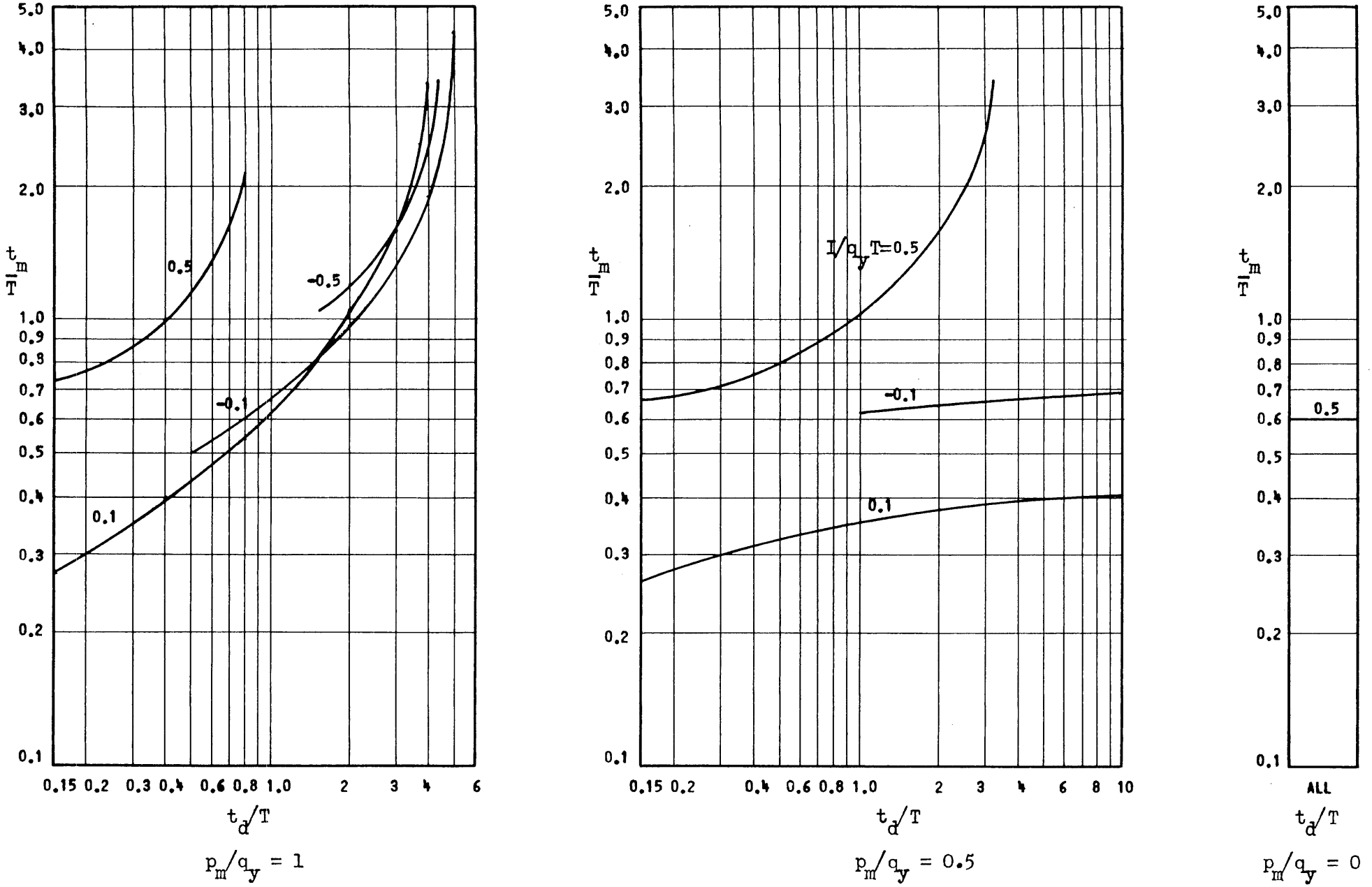

Fig. 13b Time of Maximum Response to Initial Peak Triangular Pulse with Initial Impulse

$k_2/k_1 = -0.04$

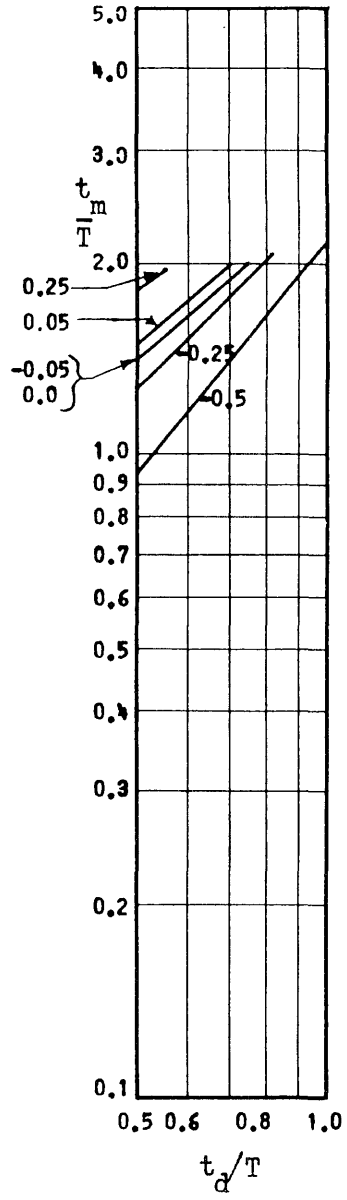

$p_m/q_y = 5$

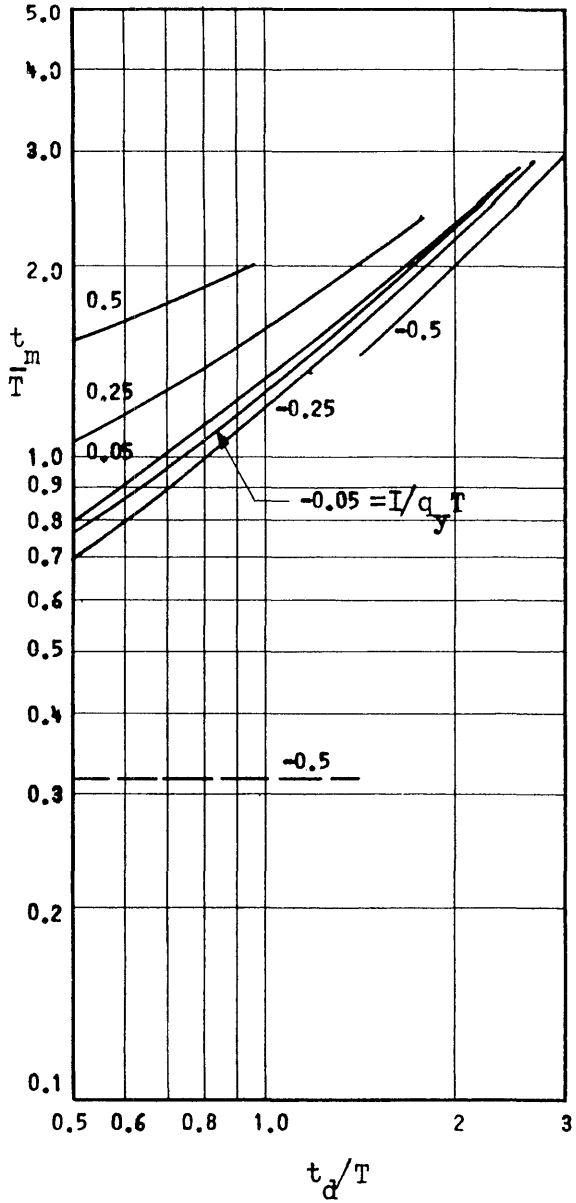

$p_m/q_y = 2$

Fig. 14a Time of Maximum Response to Delayed Rise Triangular Pulse of Fig. 3c with Two Impulses $I_o = I_1$, $t_1/T = 0.5$, $k_2/k_1 = 0$

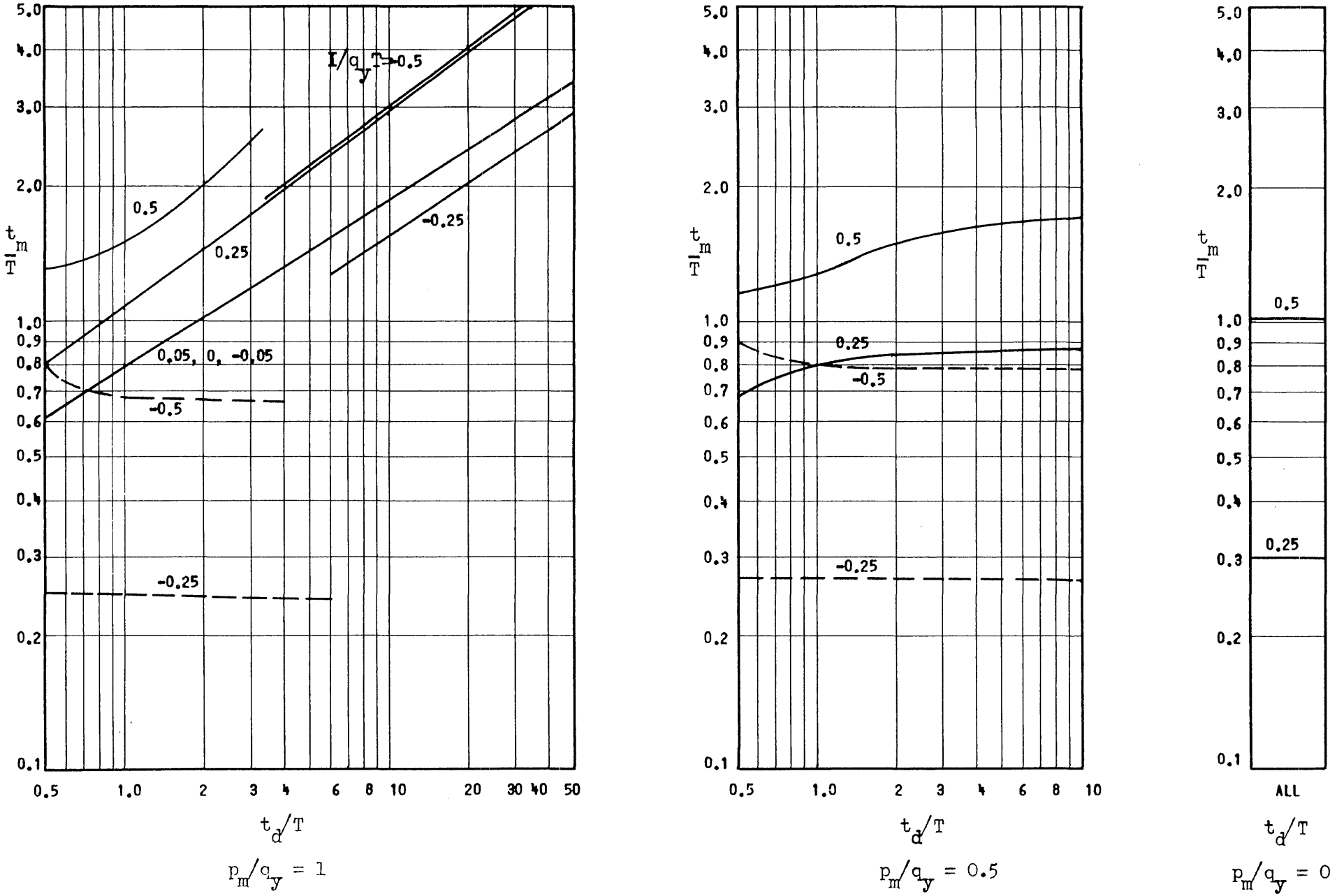

Fig. 14b Time of Maximum Response to Delayed Rise Triangular Pulse of Fig. 3c with Two Impulses

$I_o = I_1$, $t_1/T = 0.5$, $k_2/k_1 = 0$

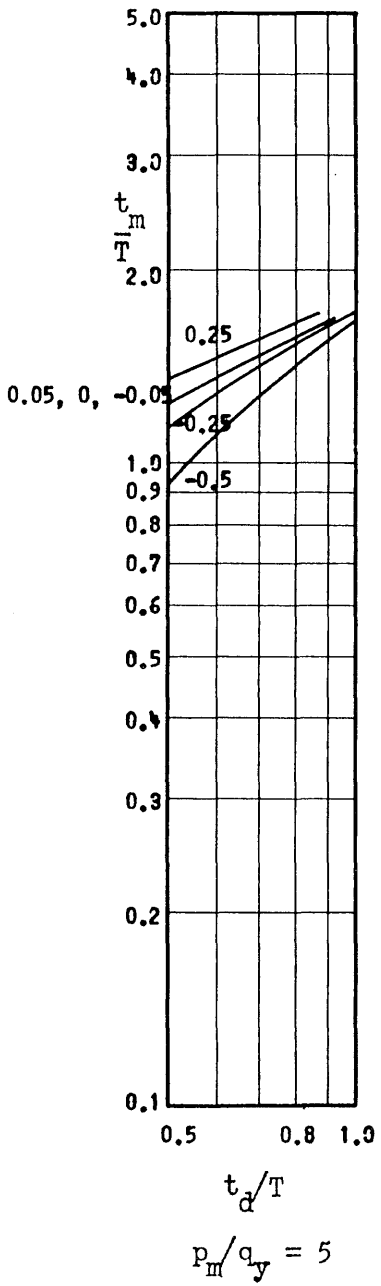

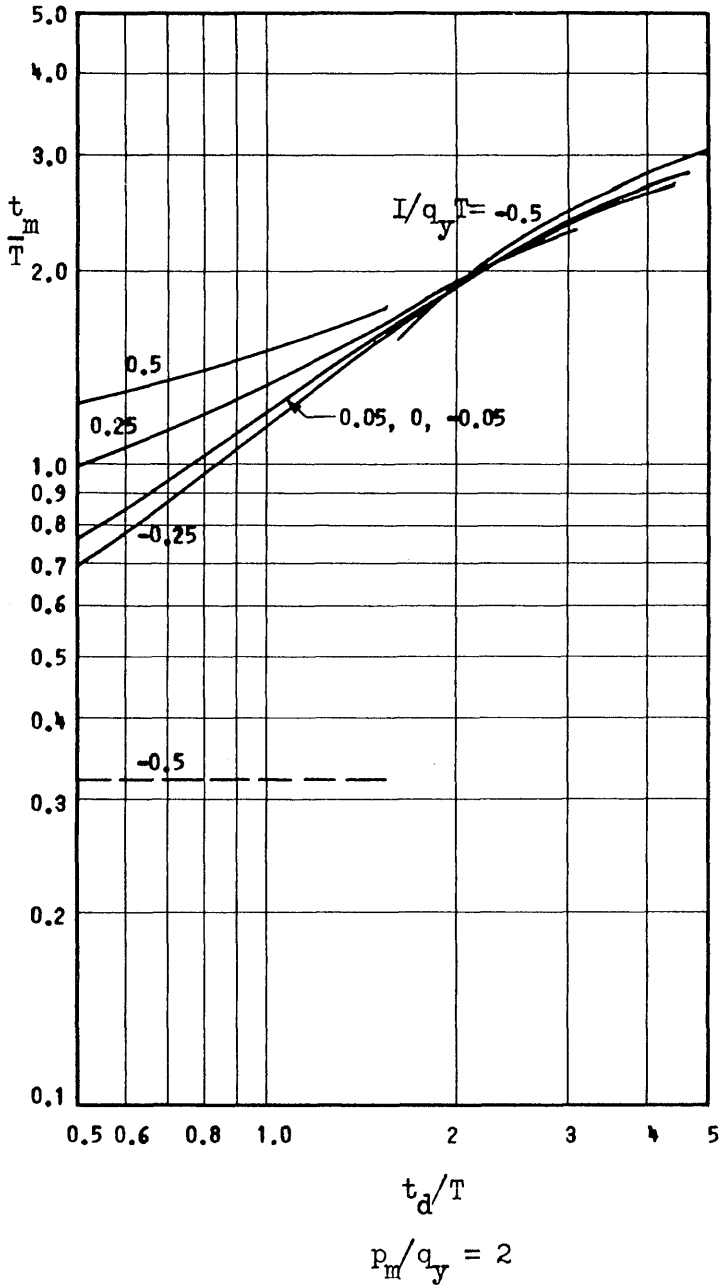

Fig. 15a Time of Maximum Response to Delayed Rise Triangular Pulse of Fig. 3c with Two Impulses

$I_o = I_1$, $t_1/T = 0.5$, $k_2/k_1 = +0.02$

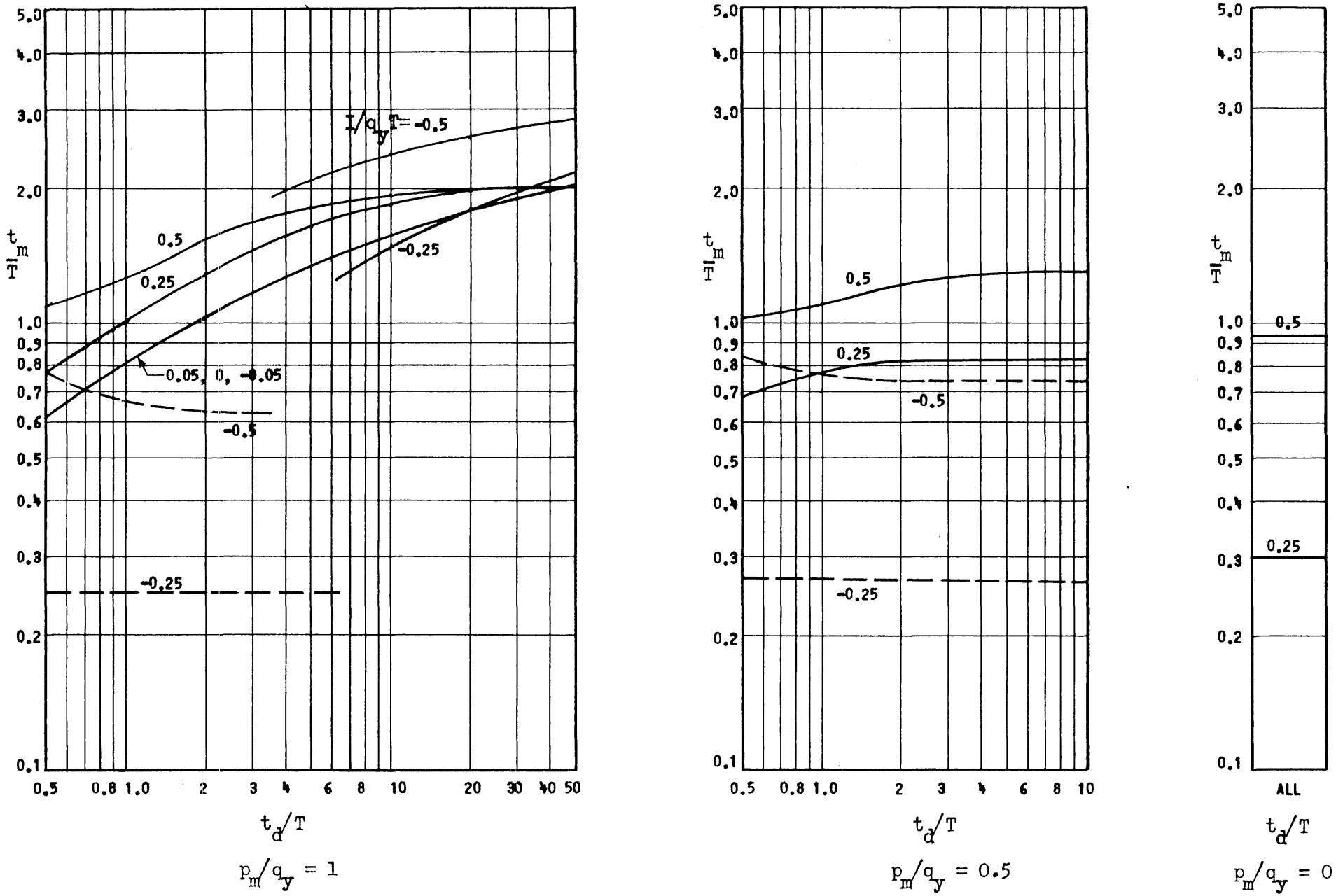

Fig. 15b Time of Maximum Response to Delayed Rise Triangular Pulse of Fig. 3c with Two Impulses

$I_o = I_1$, $t_1/T = 0.5$, $k_2/k_1 = +0.02$

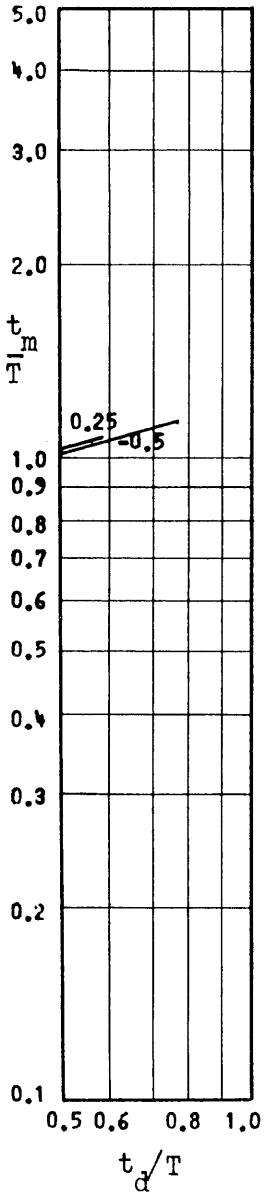

$p_m/q_y = 10$

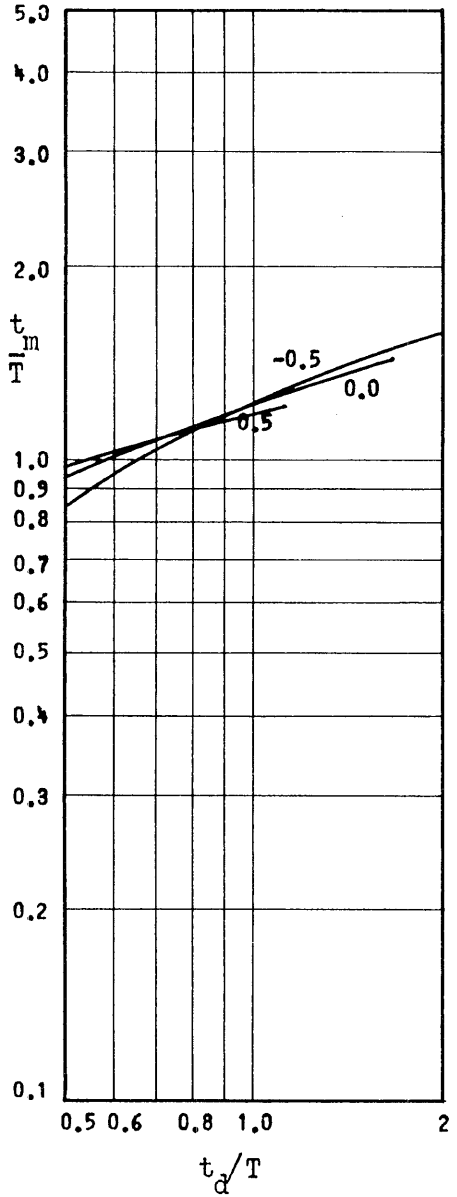

$p_m/q_y = 5$

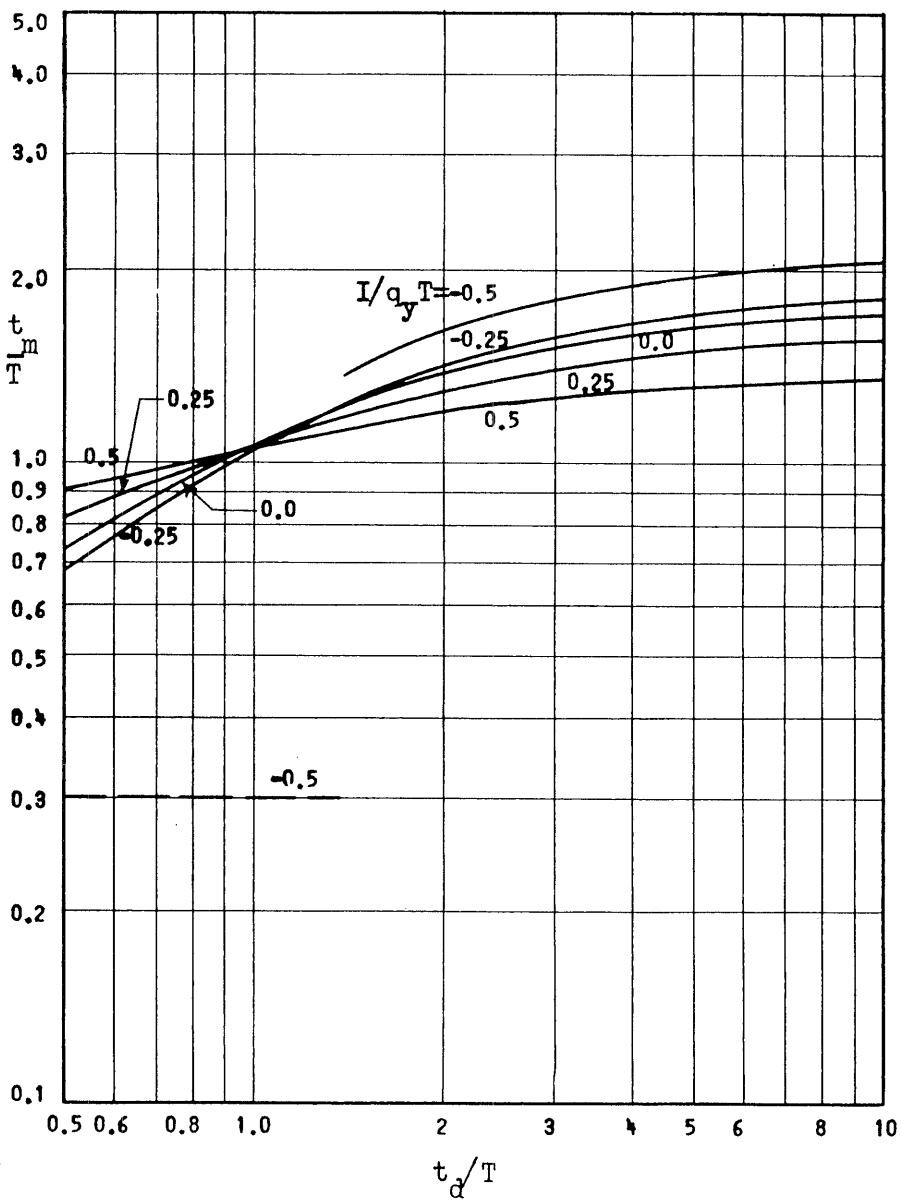

$p_m/q_y = 2$

Fig. 16a Time of Maximum Response to Delayed Rise Triangular Pulse of Fig. 3c with Two Impulses

$I_o = I_1$, $t_1/T = 0.5$, $k_2/k_1 = +0.1$

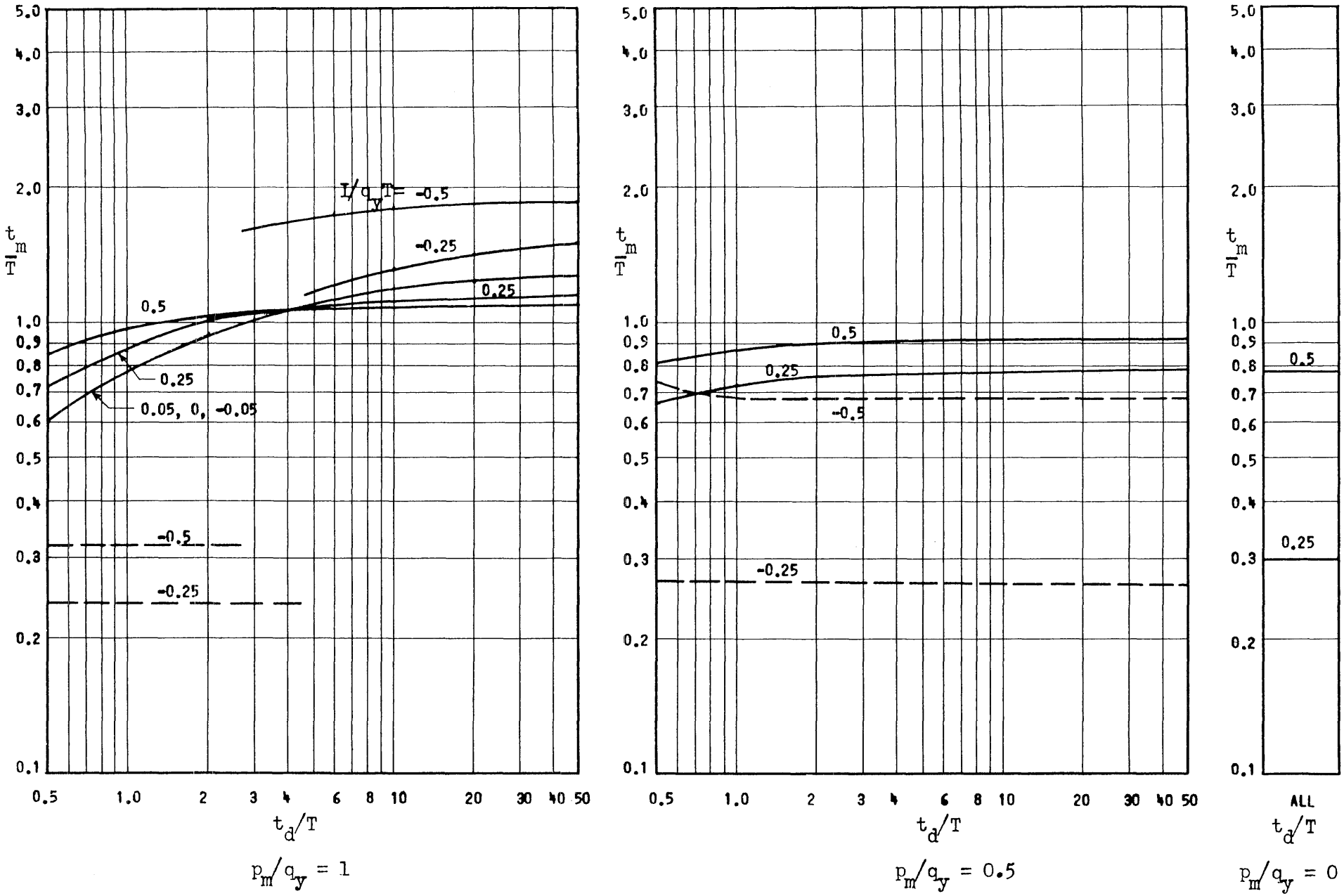

Fig. 16b Time of Maximum Response to Delayed Rise Triangular Pulse of Fig. 3c with Two Impulses

$I_o = I_1$, $t_1/T = 0.5$, $k_2/k_1 = +0.1$

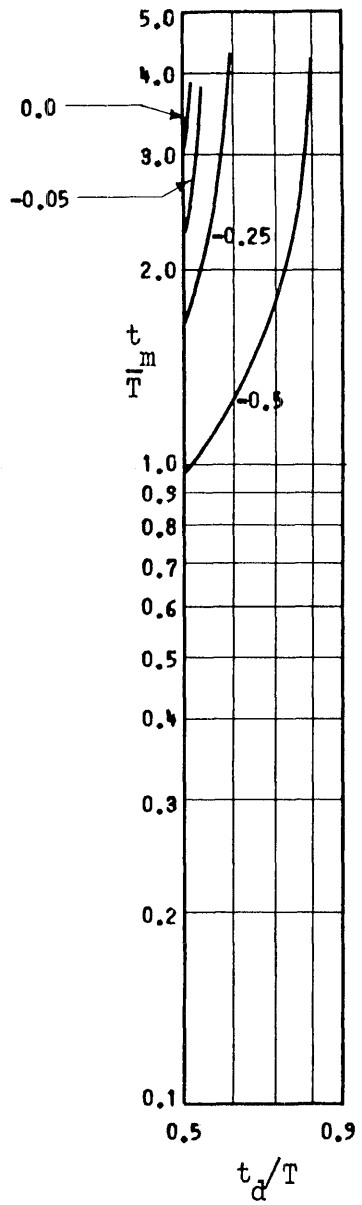

$p_m/q_y = 5$

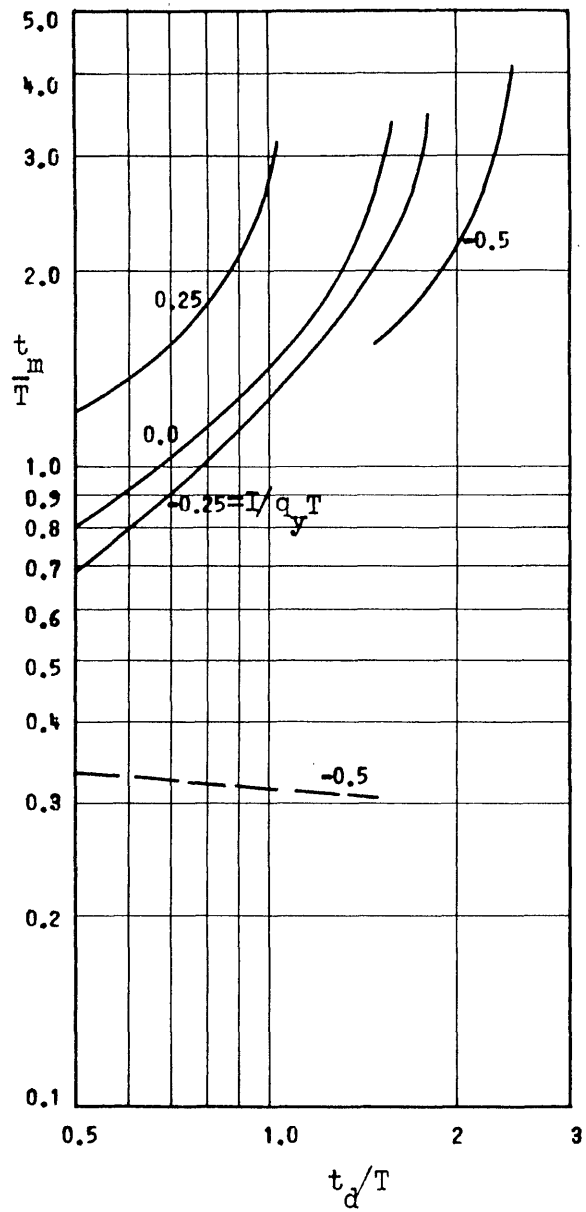

$p_m/q_y = 2$

Fig. 17a Time of Maximum Response to Delayed Rise Triangular Pulse of Fig. 3c with Two Impulses

$I_o = I_1$, $t_1/T = 0.5$, $k_2/k_1 = -0.02$

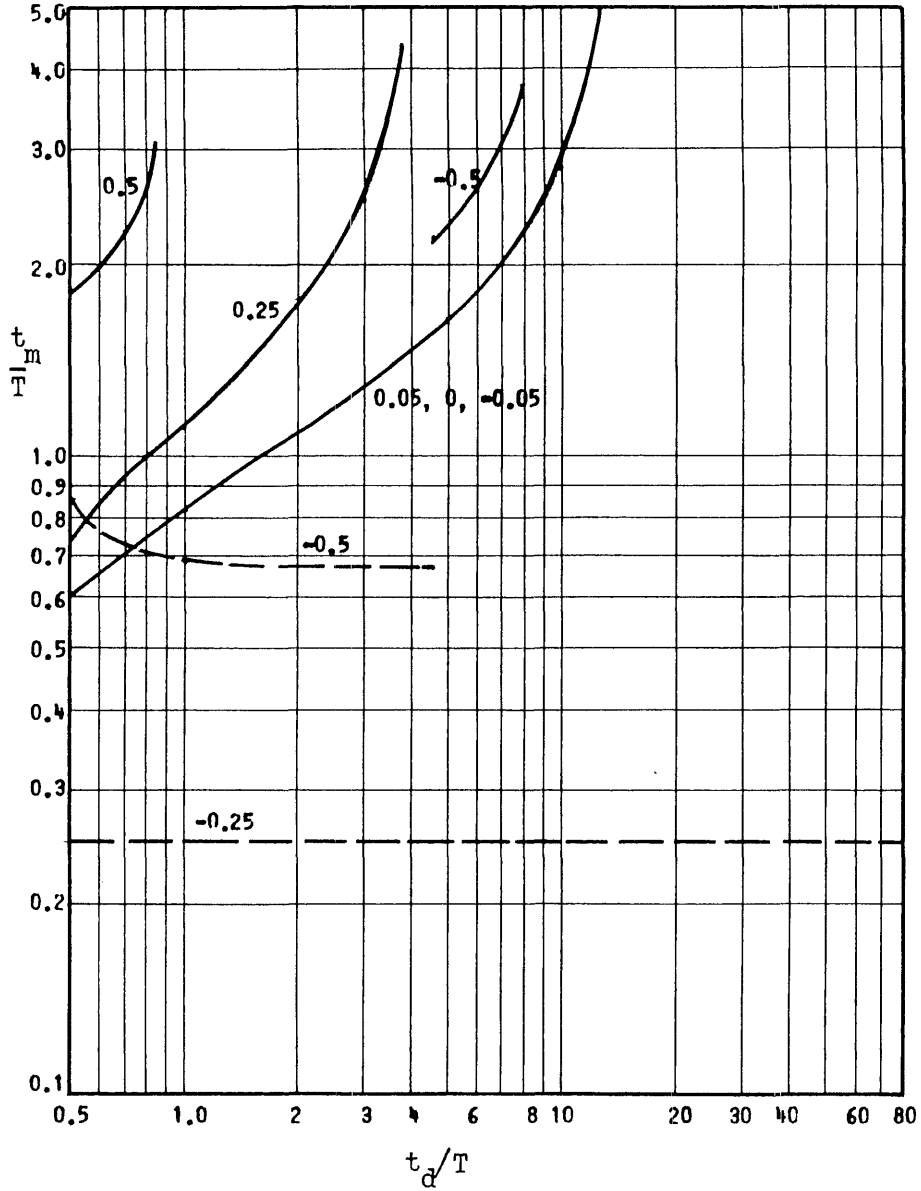

$p_m/q_y = 1$

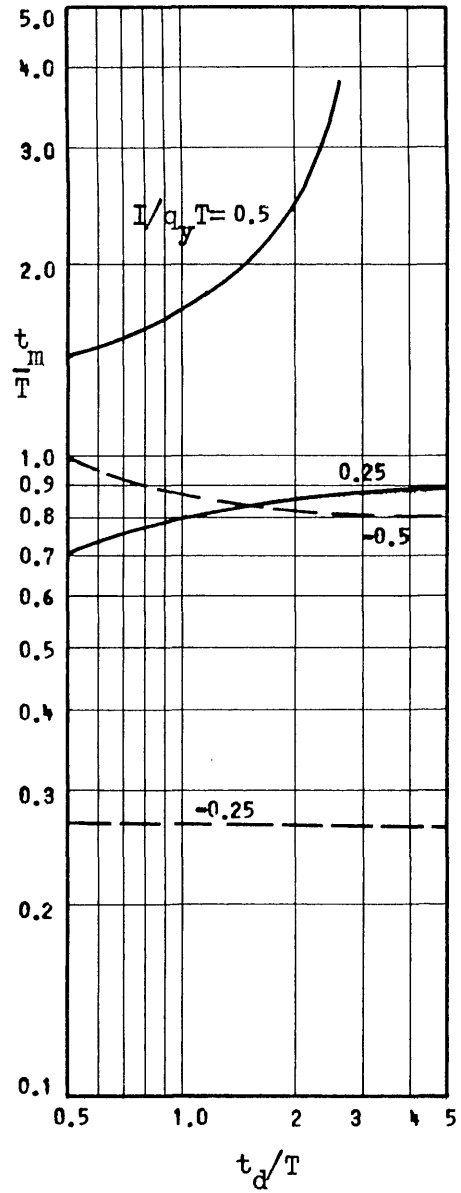

$p_m/q_y = 0.5$

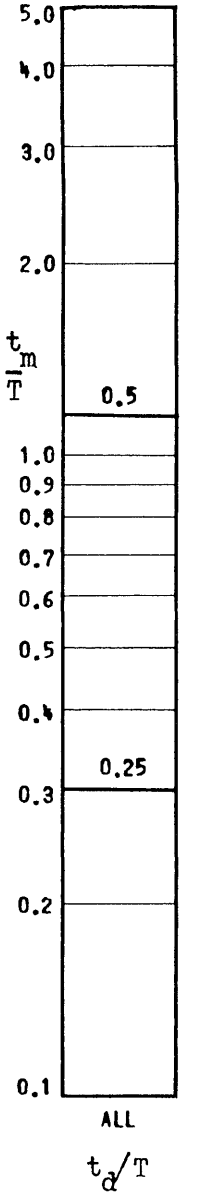

$p_m/q_y = 0$

Fig. 17b Time of Maximum Response to Delayed Rise Triangular Pulse of Fig. 3c with Two Impulses

$I_o = I_1$, $t_1/T = 0.5$, $k_2/k_1 = -0.02$

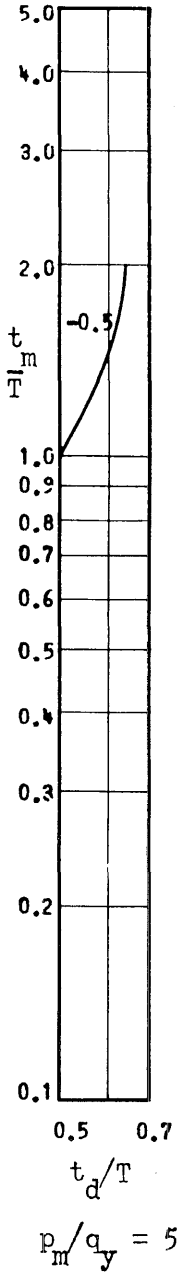

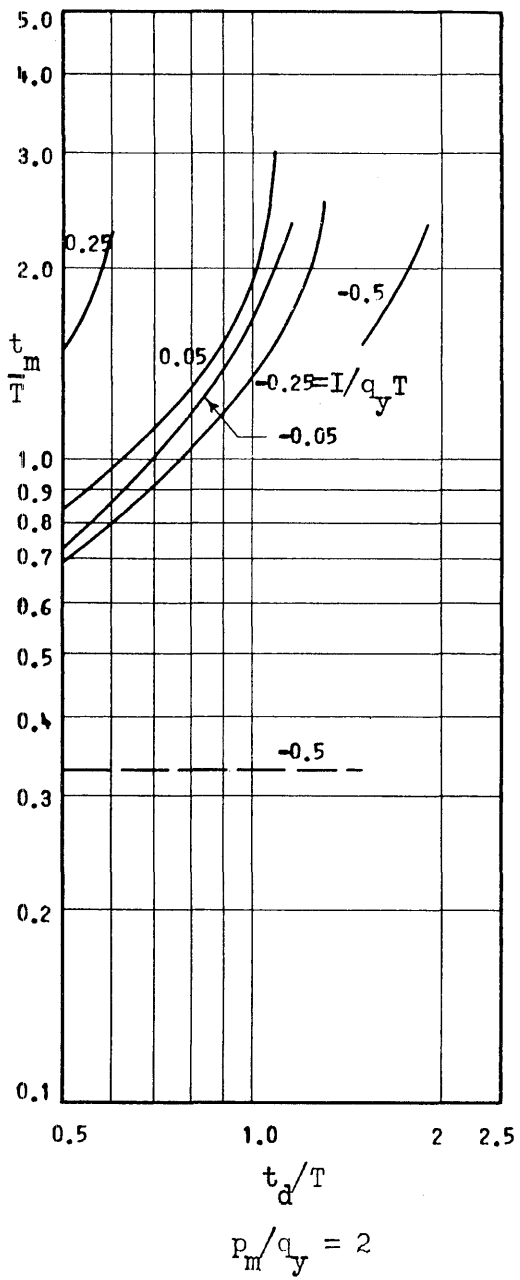

Fig. 18a Time of Maximum Response to Delayed Rise Triangular Pulse of Fig. 3c with Two Impulses $I_o = I_1$, $t_1/T = 0.5$, $k_2/k_1 = -0.04$

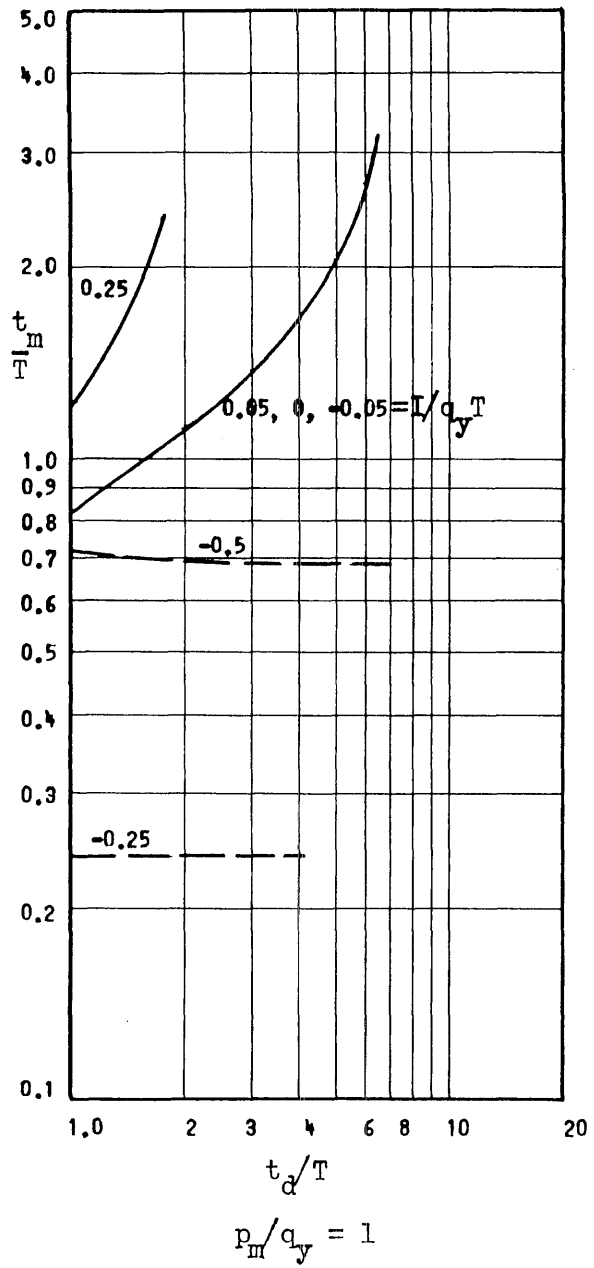

$p_m/q_y = 1$

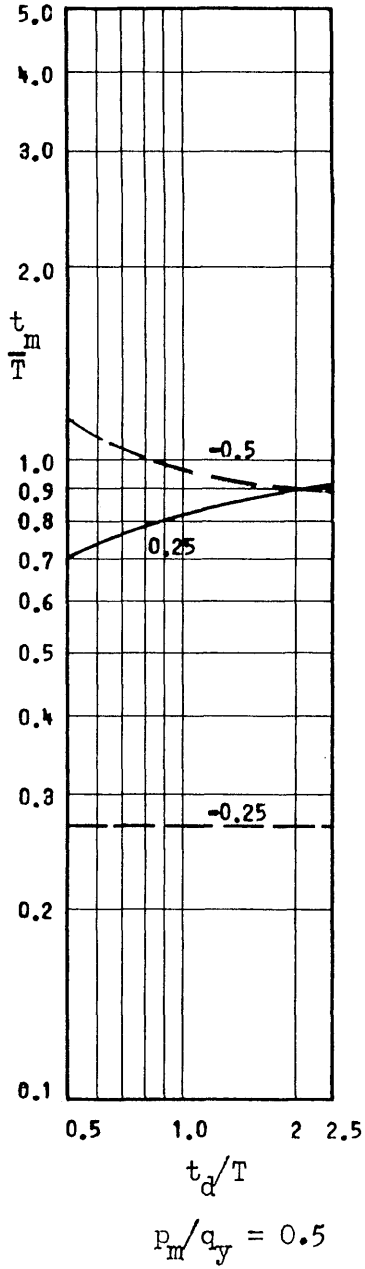

$p_m/q_y = 0.5$

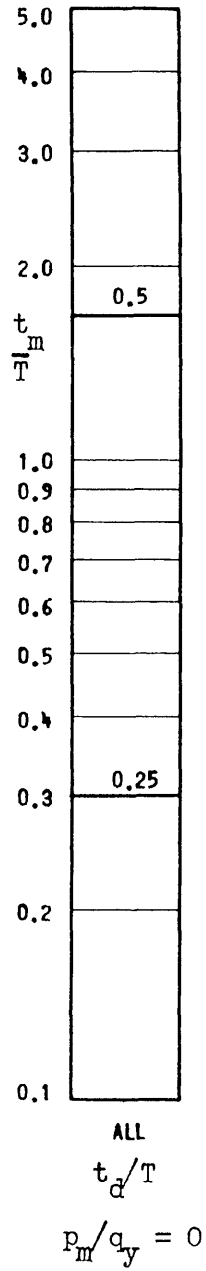

$p_m/q_y = 0$

Fig. 18b Time of Maximum Response to Delayed Rise Triangular Pulse of Fig. 3c with Two Impulses

$I_o = I_1$, $t_1/T = 0.5$, $k_2/k_1 = -0.04$

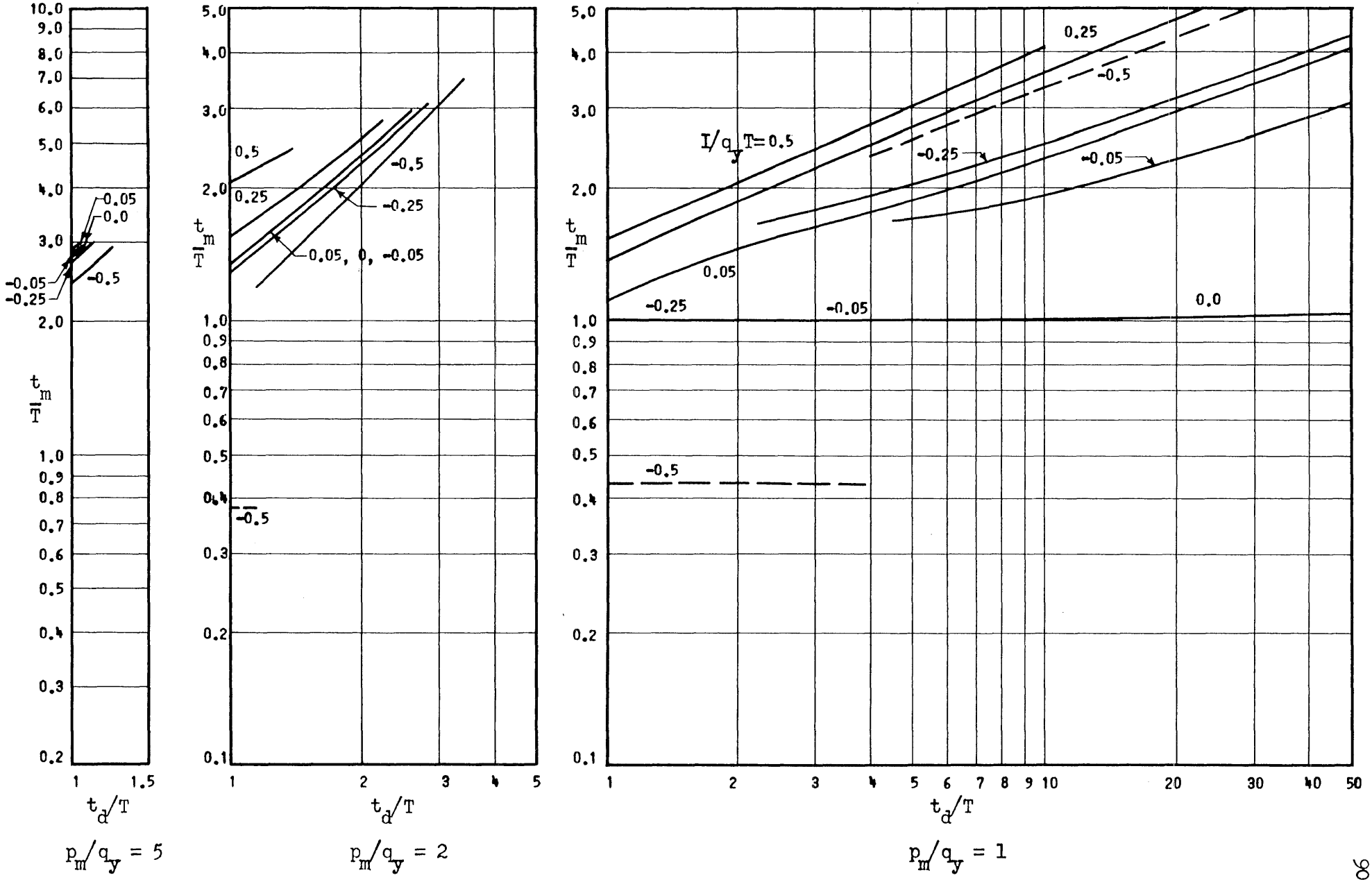

Fig. 19a Time of Maximum Response to Delayed Rise Triangular Pulse of Fig. 3c with Two Impulses

$I_o = I_1$, $t_1/T = 1.0$, $k_2/k_1 = 0$

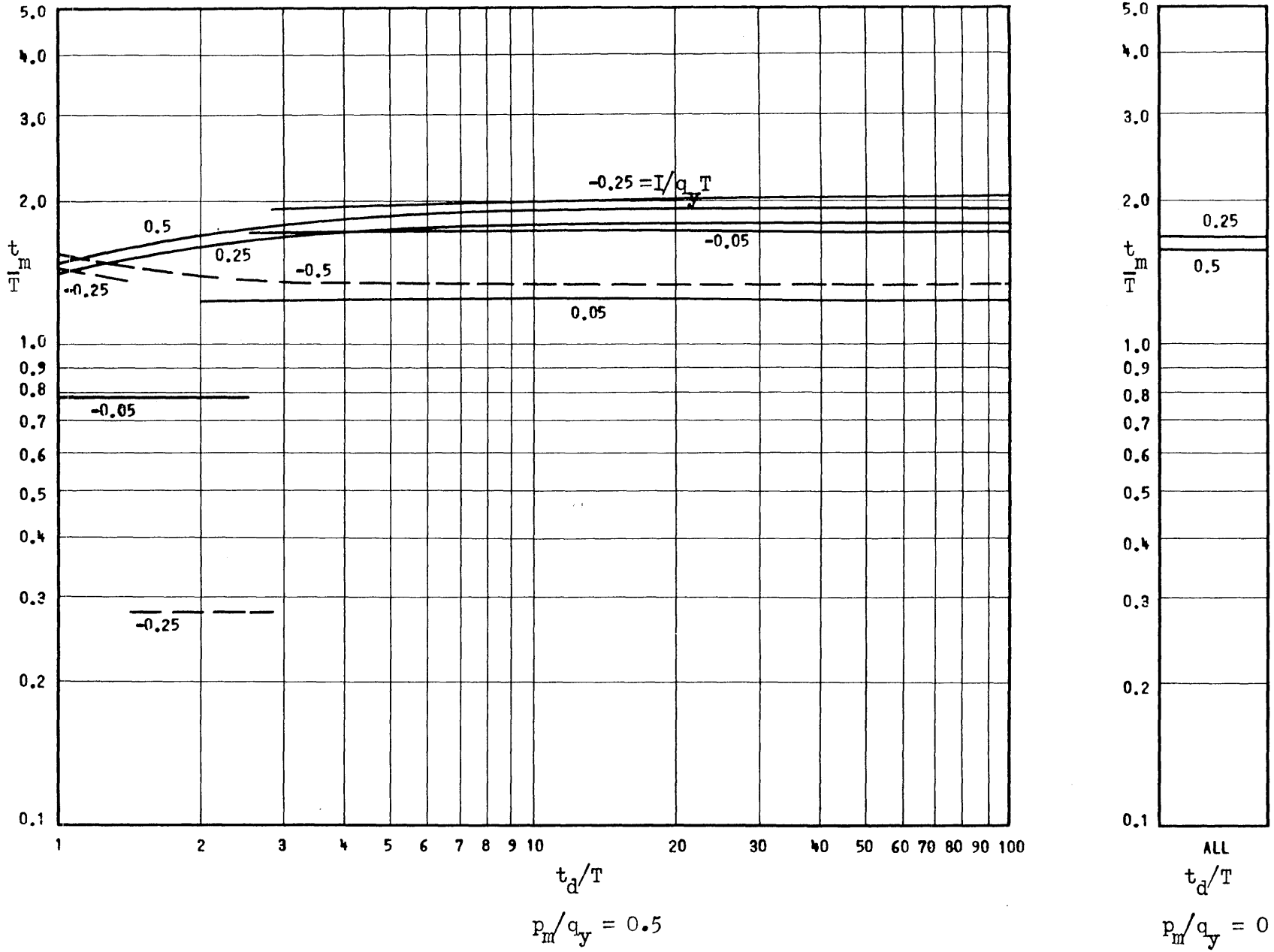

Fig. 19b Time of Maximum Response to Delayed Rise Triangular Pulse of Fig. 3c with Two Impulses

$I_o = I_1$, $t_1/T = 1.0$, $k_2/k_1 = 0$

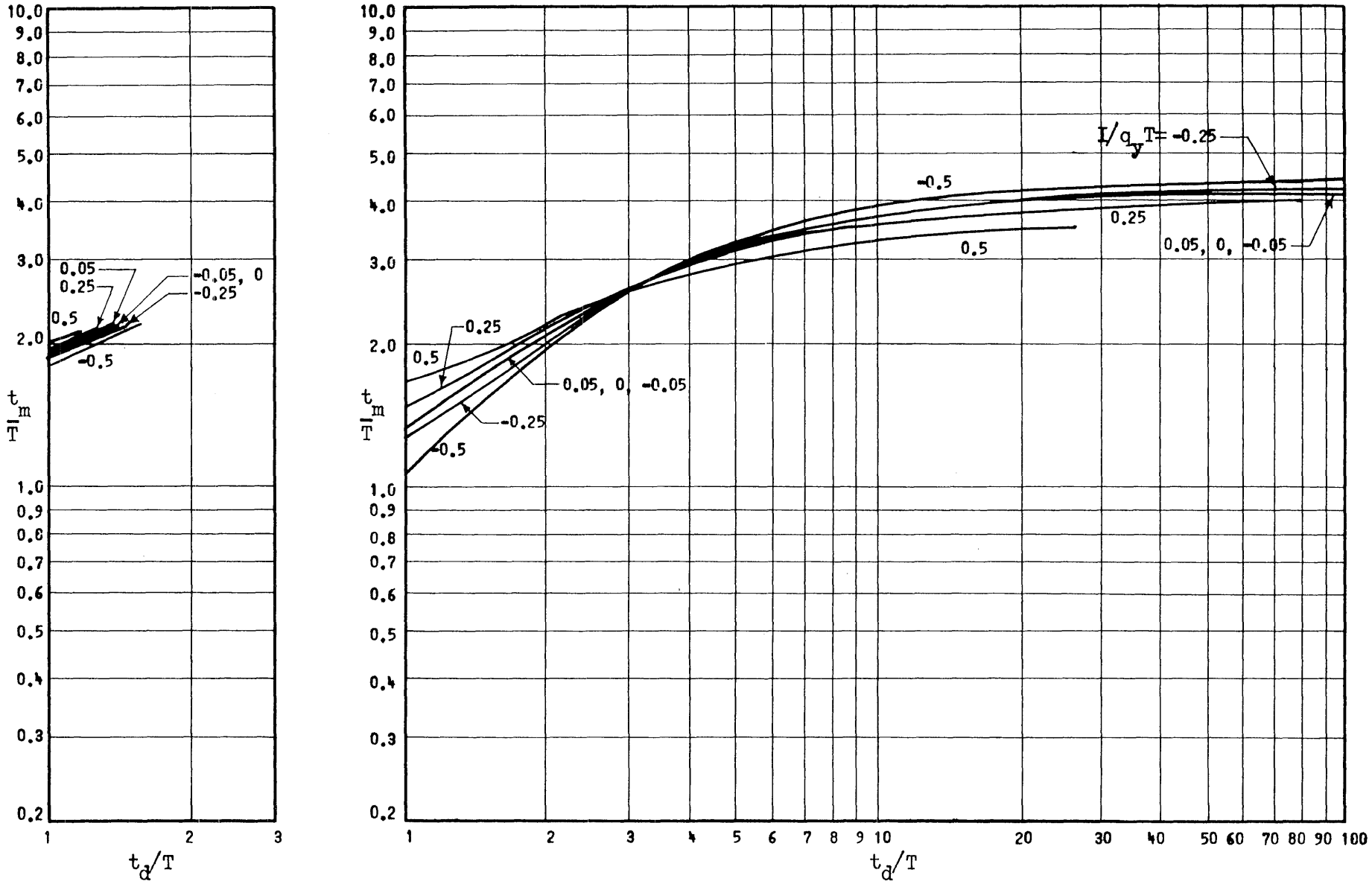

Fig. 20a Time of Maximum Response to Delayed Rise Triangular Pulse of Fig. 3c with Two Impulses

$I_o = I_1$, $t_1/T = 1.0$, $k_2/k_1 = +0.02$

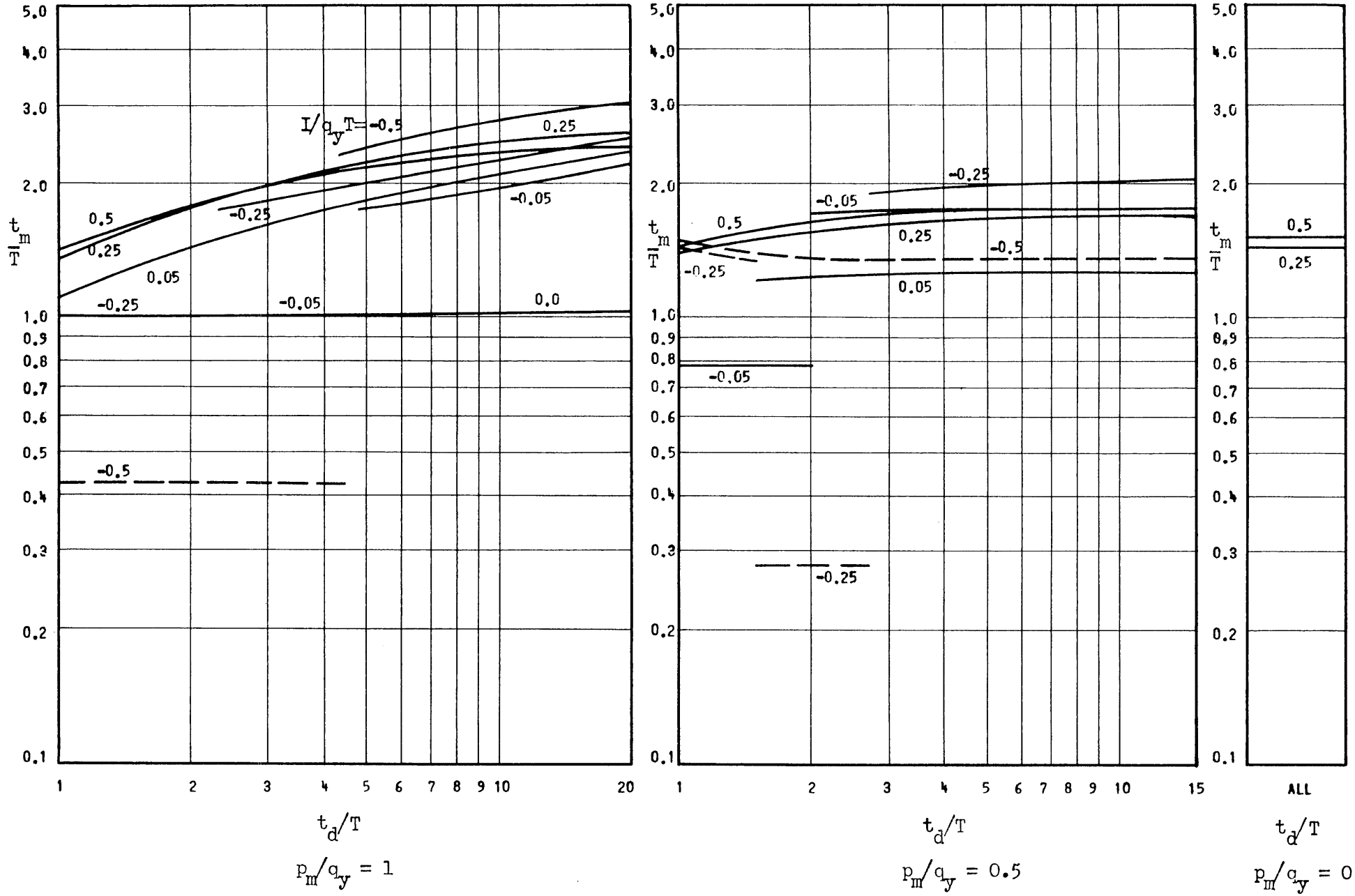

Fig. 20b Time of Maximum Response to Delayed Rise Triangular Pulse of Fig. 3c with Two Impulses

$I_o = I_1$, $t_1/T = 1.0$, $k_2/k_1 = +0.02$

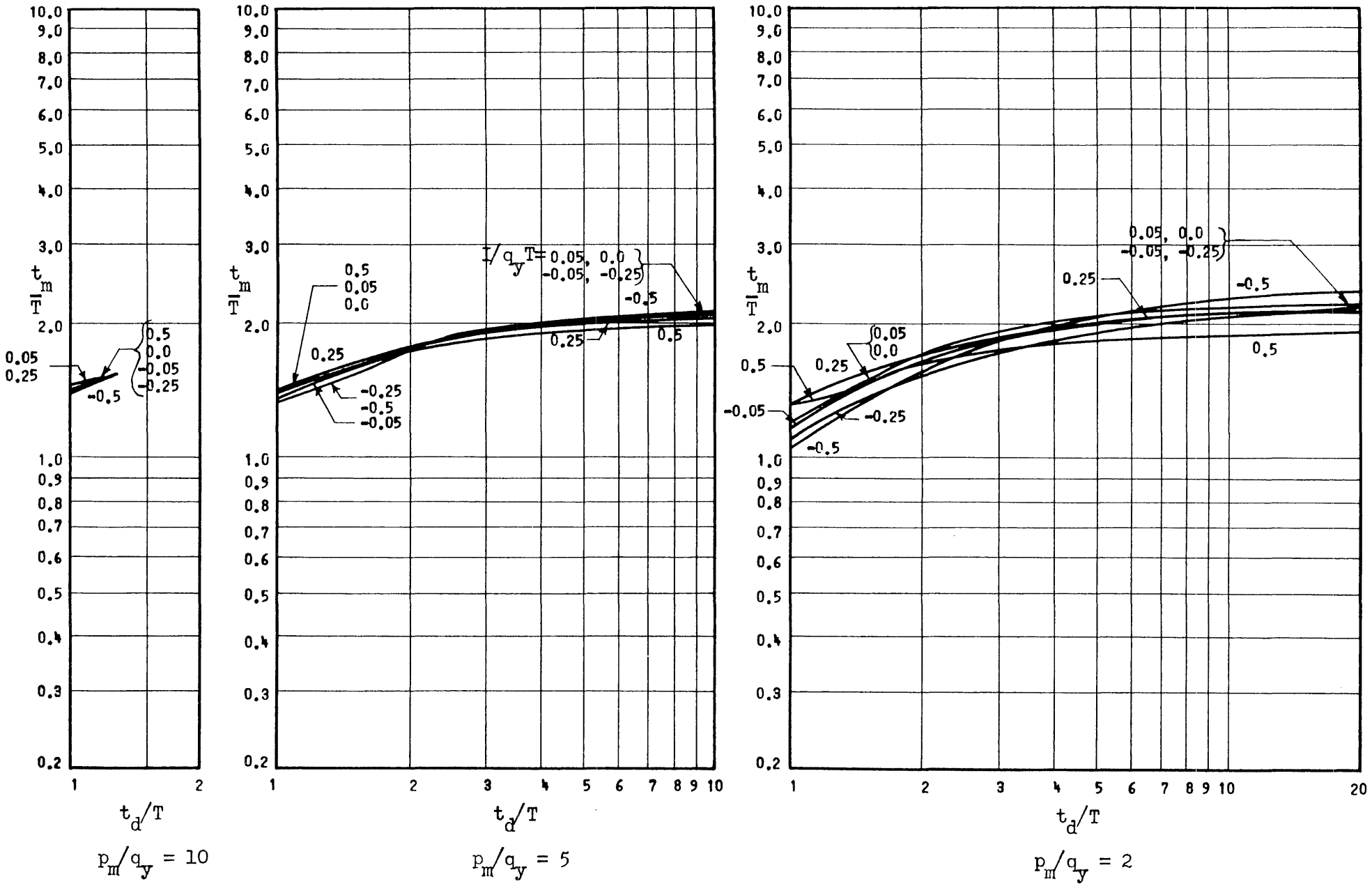

Fig. 21a Time of Maximum Response to Delayed Rise Triangular Pulse of Fig. 3c with Two Impulses

$I_o = I_1$, $t_1/T = 1.0$, $k_2/k_1 = +0.1$

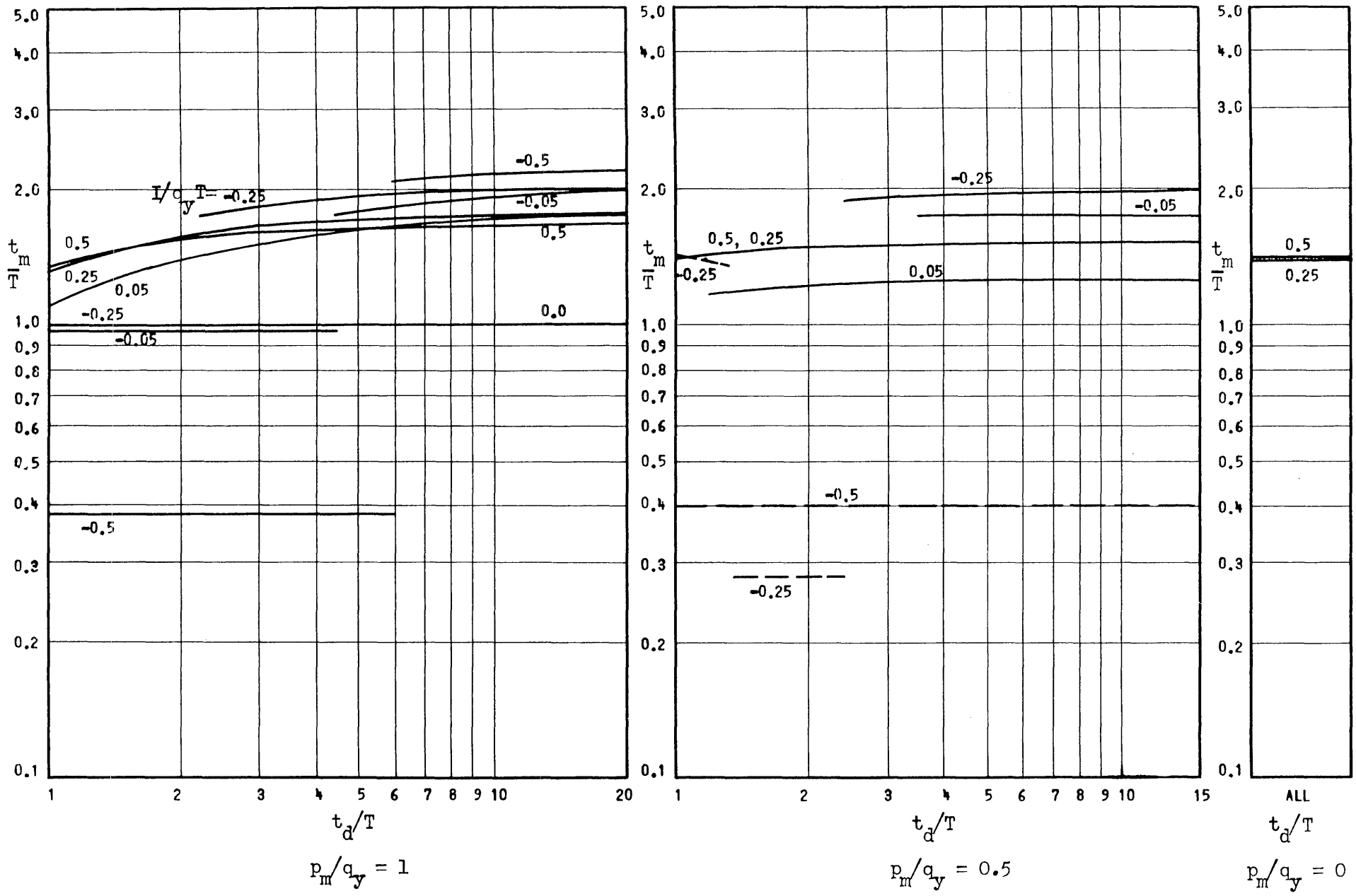

Fig. 21b Time of Maximum Response to Delayed Rise Triangular Pulse of Fig. 3c with Two Impulses

$I_o = I_1$, $t_1/T = 1.0$, $k_2/k_1 = +0.1$

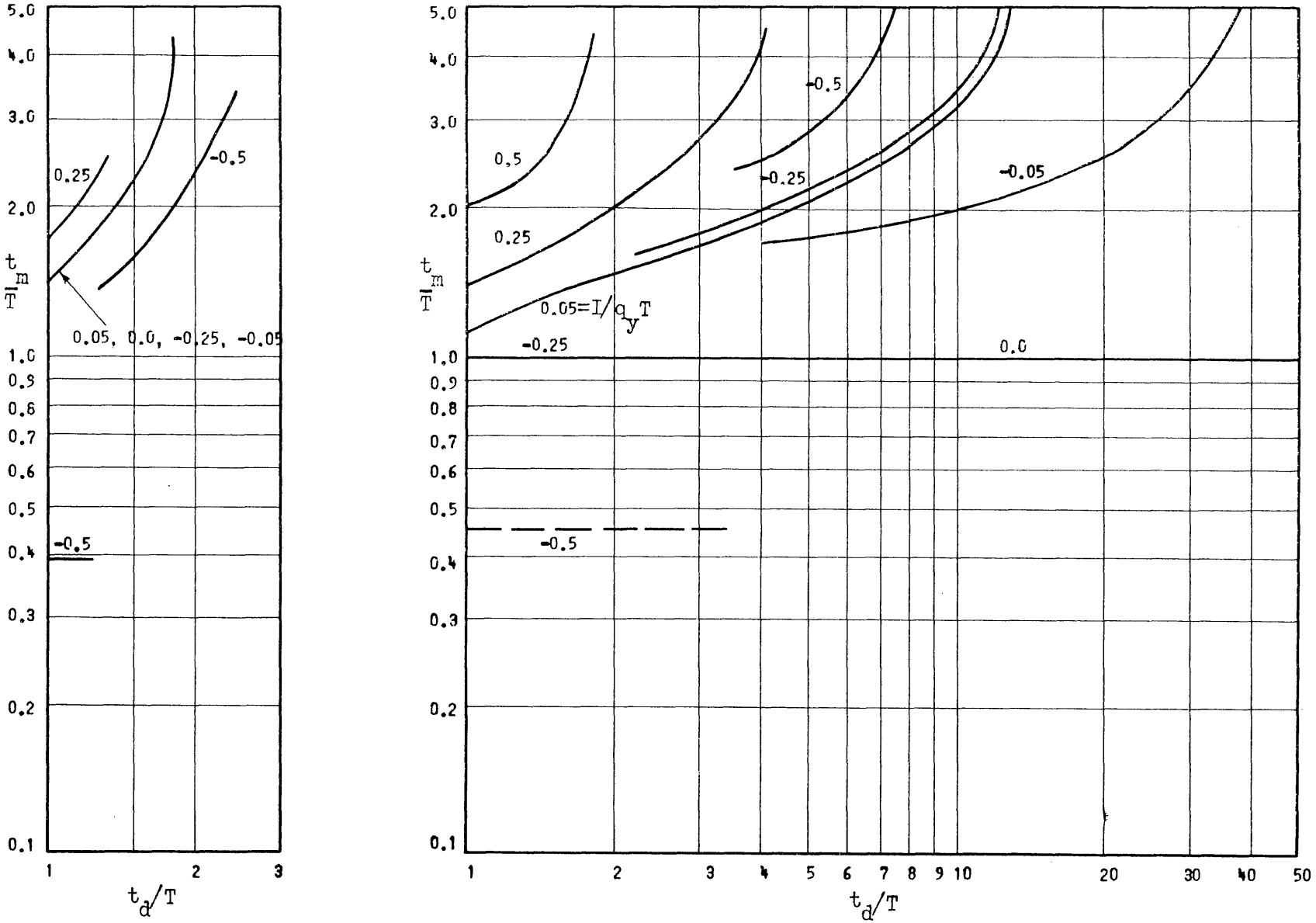

Fig. 22a Time of Maximum Response to Delayed Rise Triangular Pulse of Fig. 3c with Two Impulses

$I_o = I_1$, $t_1/T = 1.0$, $k_2/k_1 = -0.02$

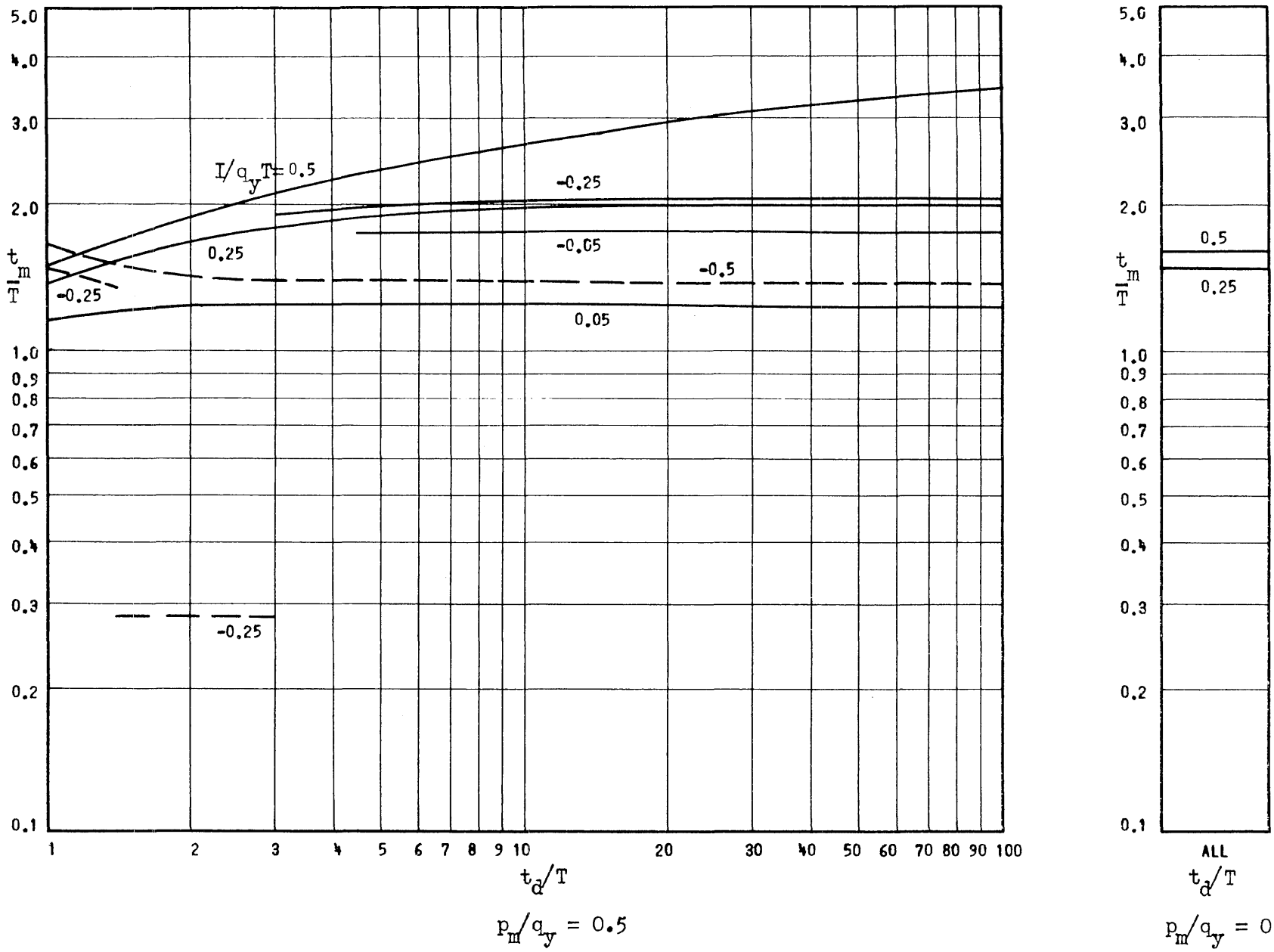

Fig. 22b Time of Maximum Response to Delayed Rise Triangular Pulse of Fig. 3c with Two Impulses

$I_o = I_1$, $t_1/T = 1.0$, $k_2/k_1 = -0.02$

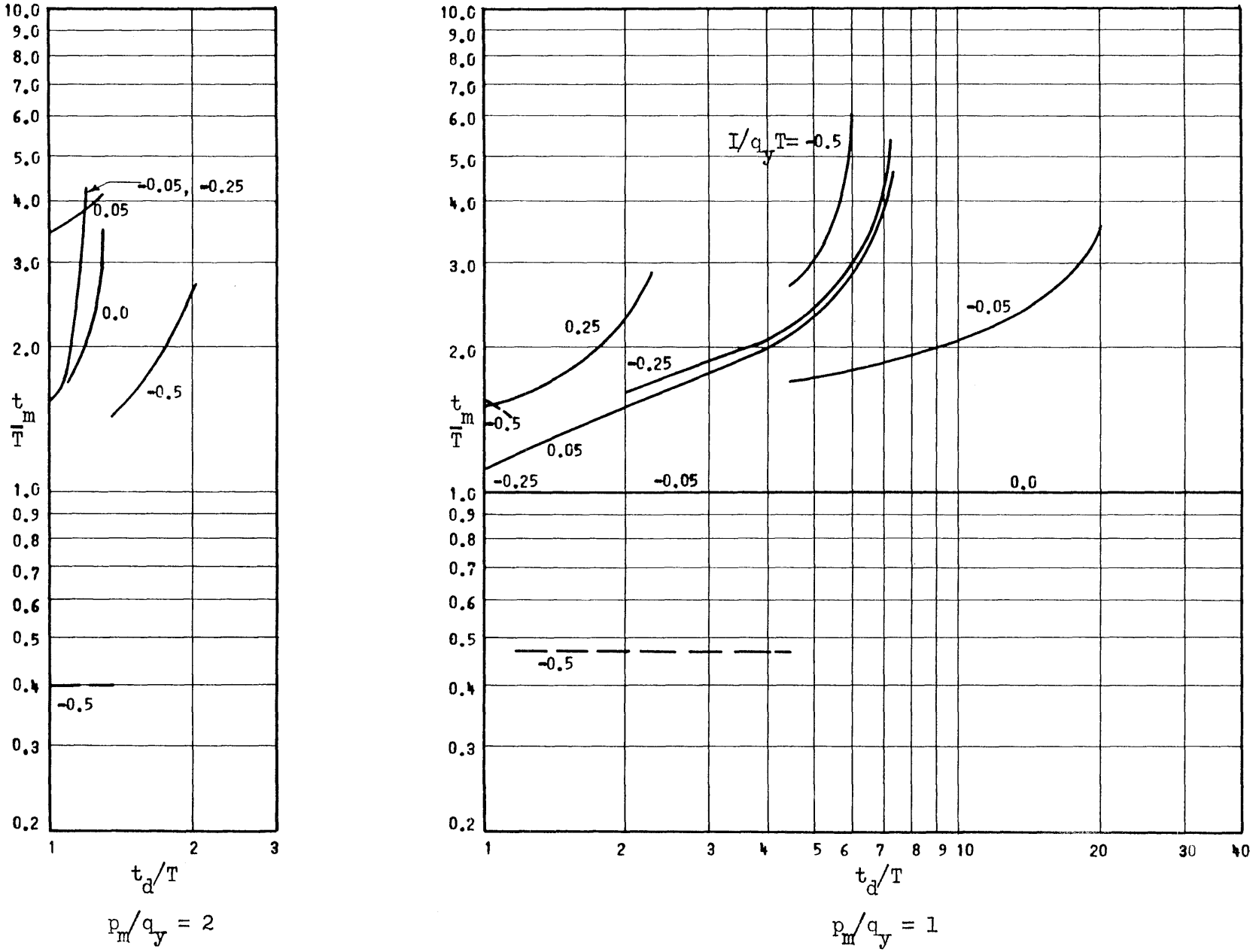

Fig. 23a Time of Maximum Response to Delayed Rise Triangular Pulse of Fig. 3c with Two Impulses

$I_o = I_1$, $t_1/T = 1.0$, $k_2/k_1 = -0.04$

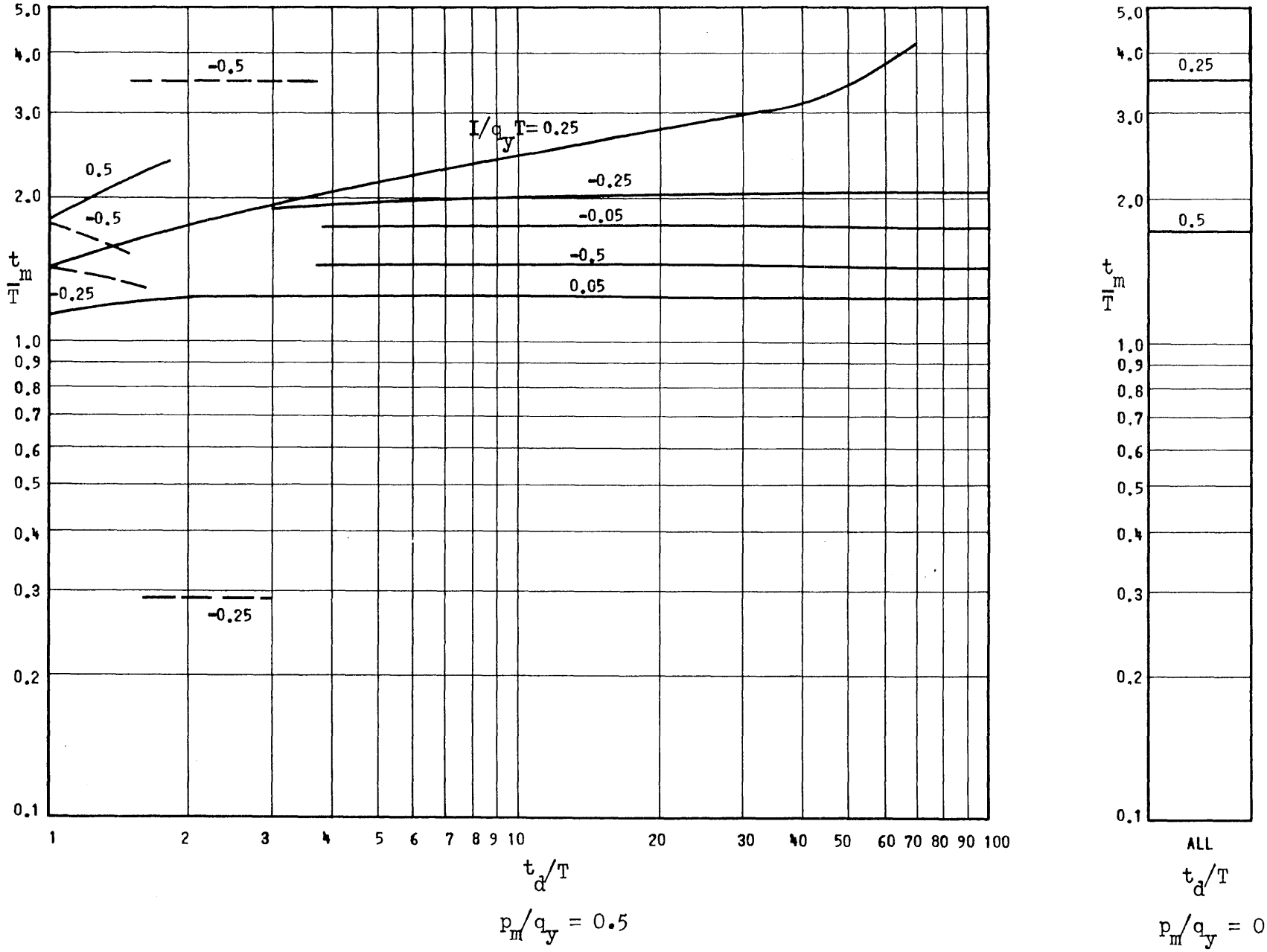

Fig. 23b Time of Maximum Response to Delayed Rise Triangular Pulse of Fig. 3c with Two Impulses

$I_o = I_1$, $t_1/T = 1.0$, $k_2/k_1 = -0.04$

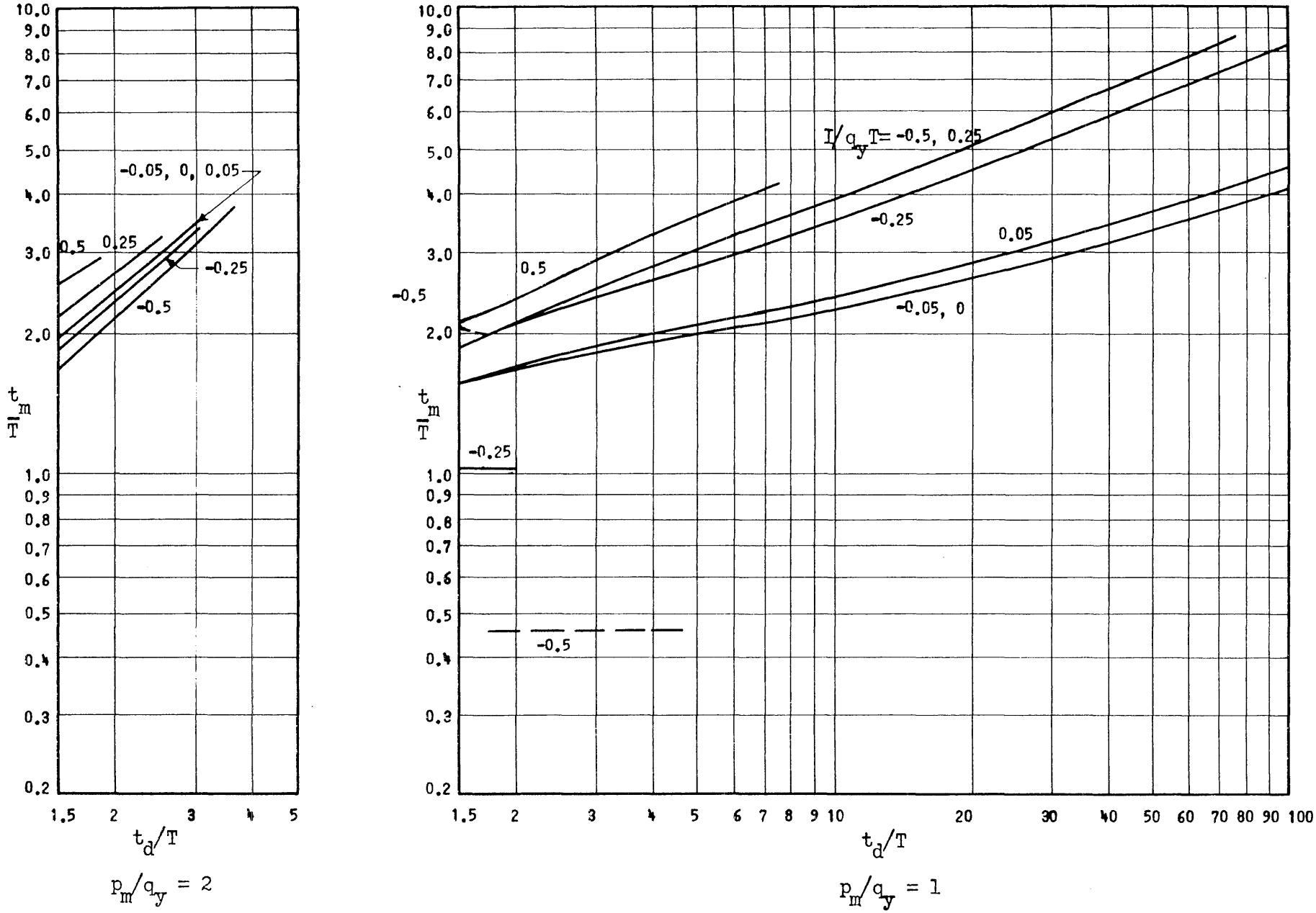

Fig. 24a Time of Maximum Response to Delayed Rise Triangular Pulse of Fig. 3c with Two Impulses

$I_o = I_1$, $t_1/T = 1.5$, $k_2/k_1 = 0$

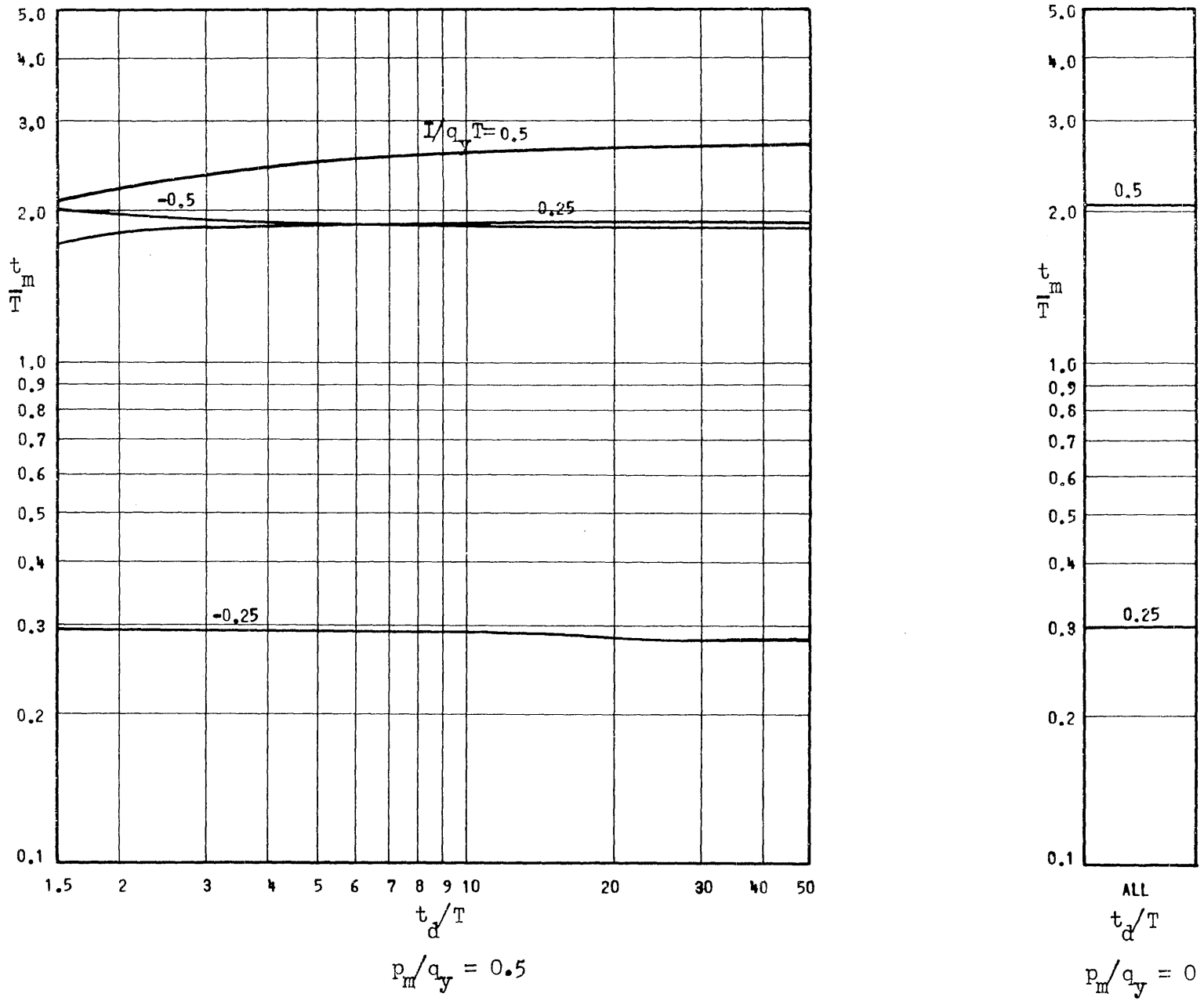

Fig. 24b Time of Maximum Response to Delayed Rise Triangular Pulse of Fig. 3c with Two Impulses

$I_o = I_1$, $t_1/T = 1.5$, $k_2/k_1 = 0$

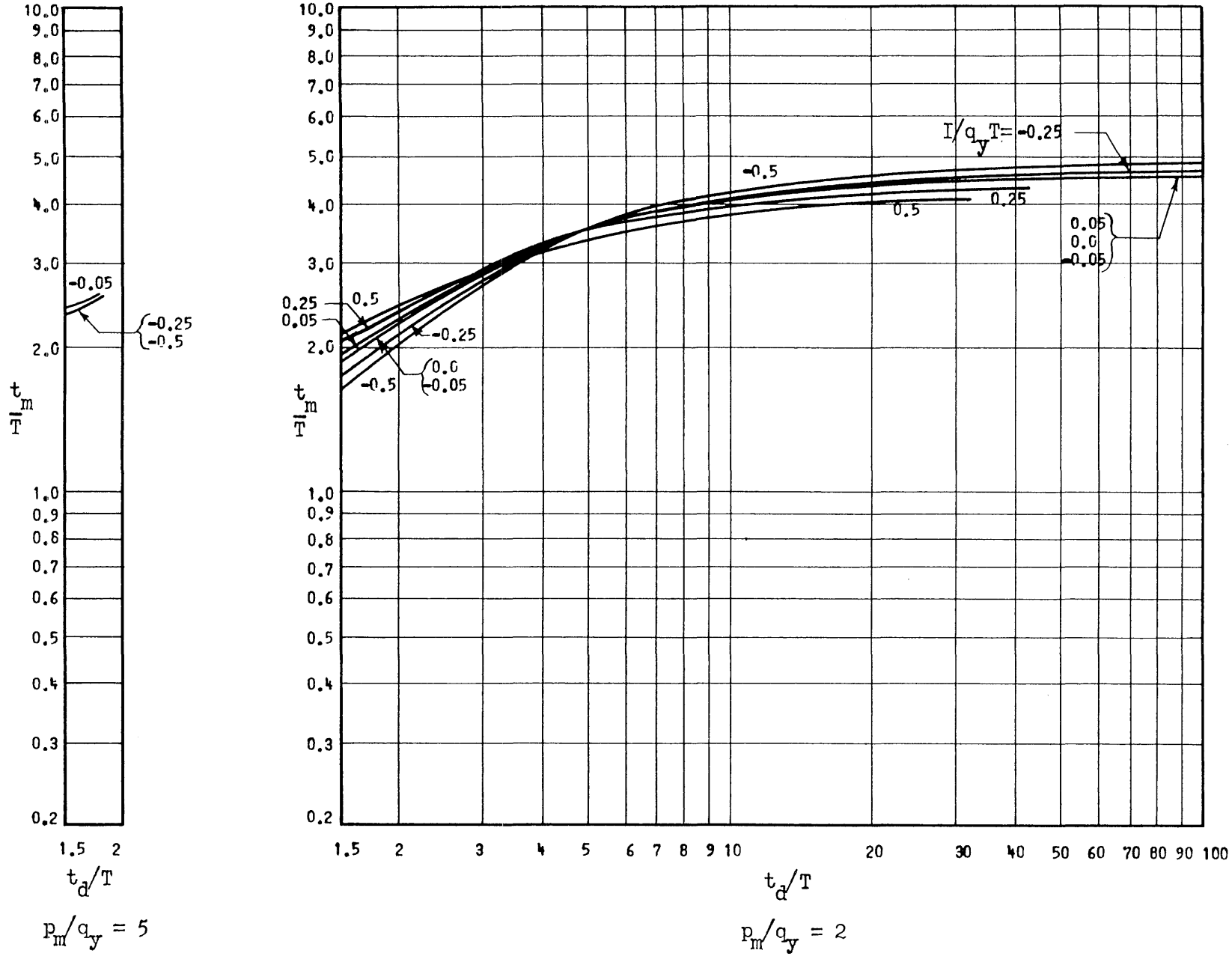

Fig. 25a Time of Maximum Response to Delayed Rise Triangular Pulse of Fig. 3c with Two Impulses

$I_o = I_1$, $t_1/T = 1.5$, $k_2/k_1 = +0.02$

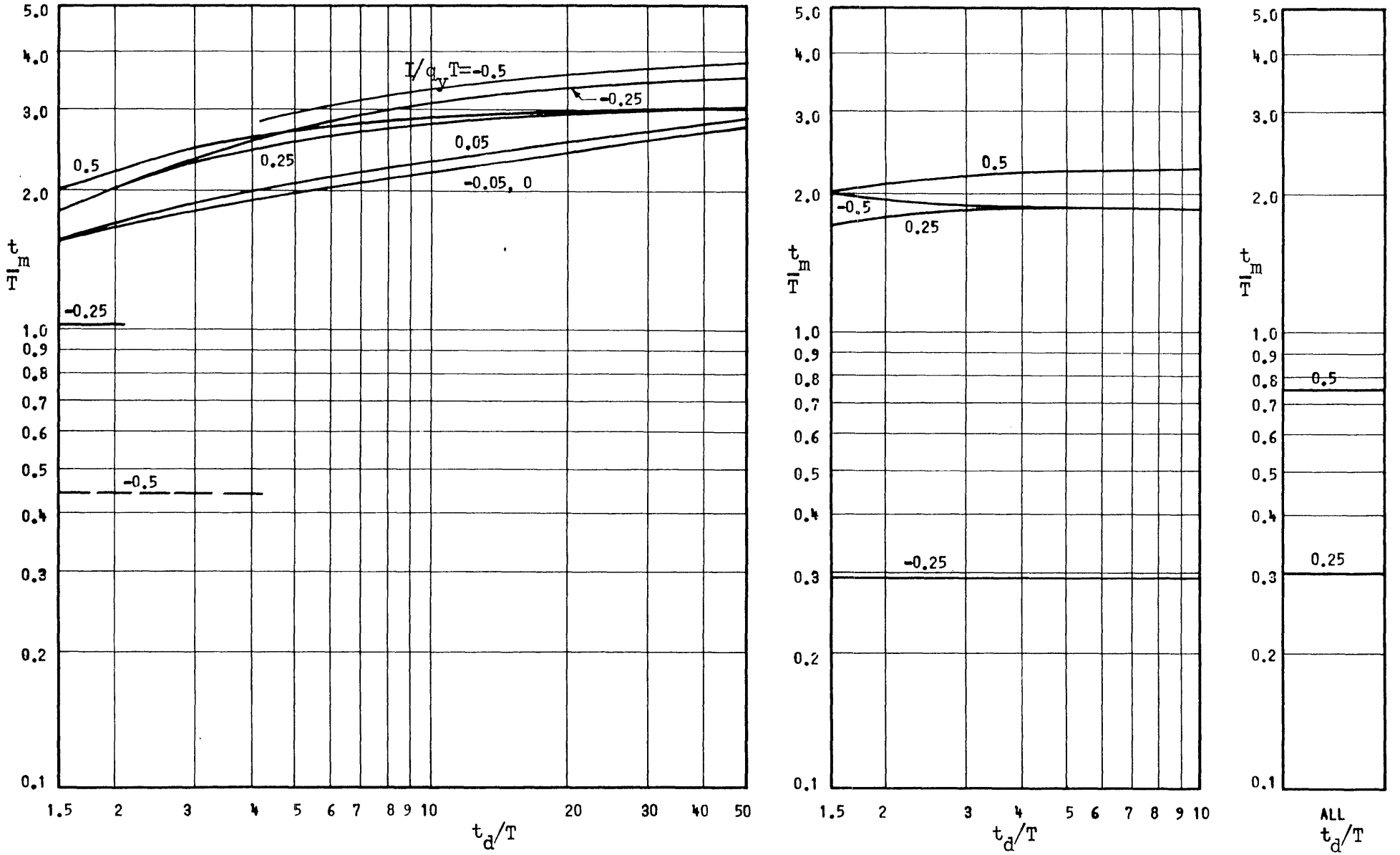

Fig. 25b Time of Maximum Response to Delayed Rise Triangular Pulse of Fig. 3c with Two Impulses

$I_o = I_1$, $t_1/T = 1.5$, $k_2/k_1 = +0.02$

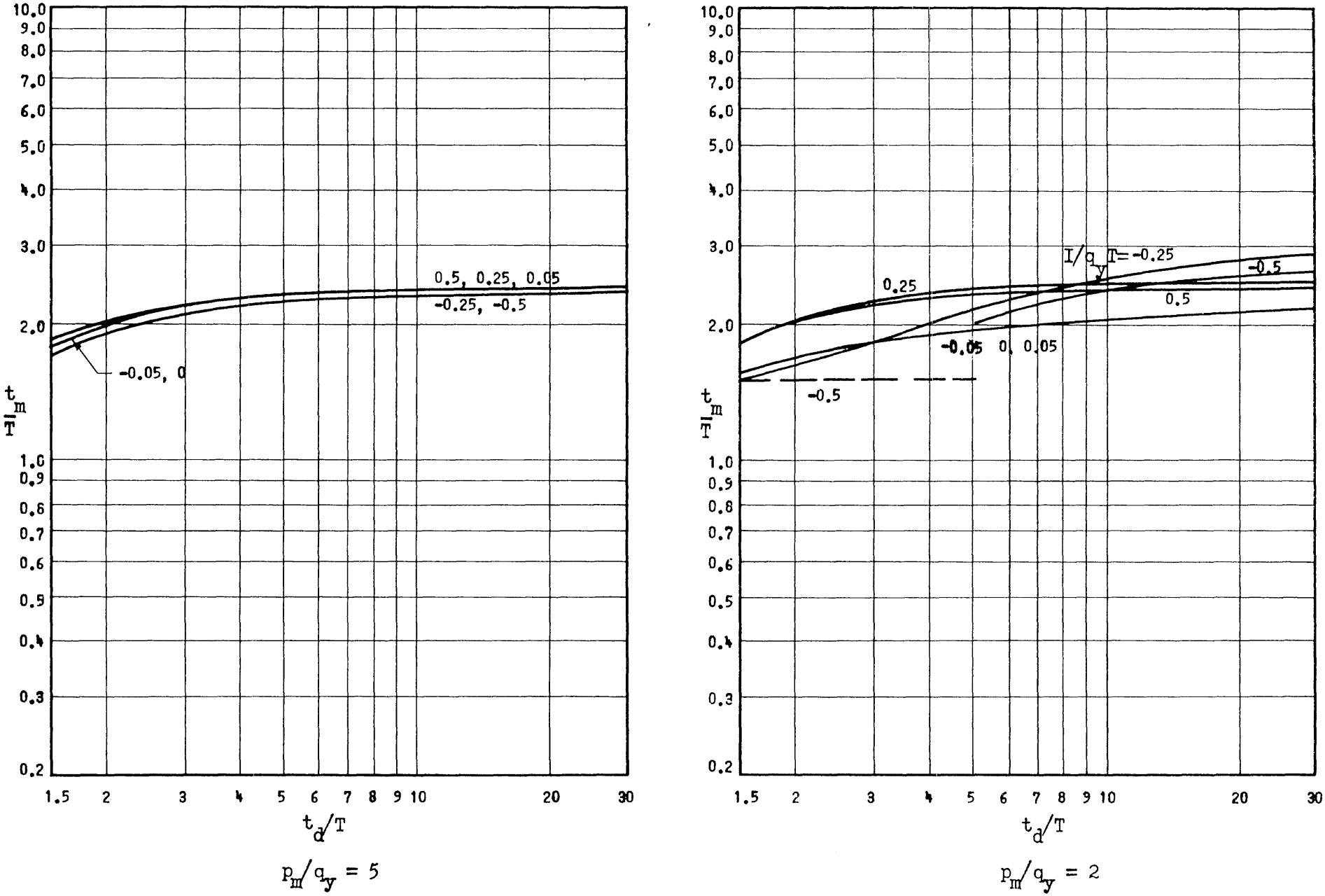

Fig. 26a Time of Maximum Response to Delayed Rise Triangular Pulse of Fig. 3c with Two Impulses

$I_o = I_1$, $t_1/T = 1.5$, $k_2/k_1 = +0.1$

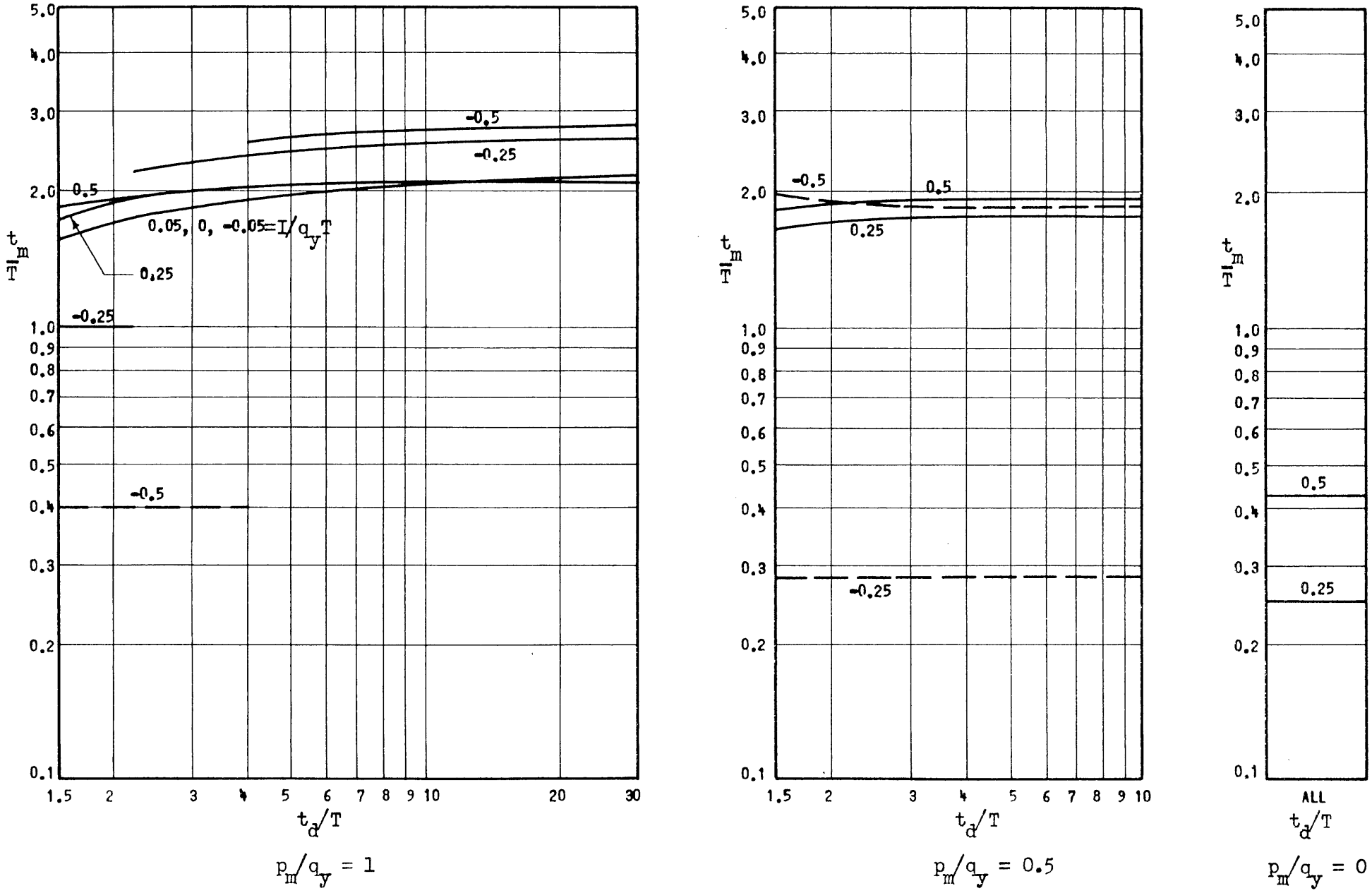

Fig. 26b Time of Maximum Response to Delayed Rise Triangular Pulse of Fig. 3c with Two Impulses

$I_o = I_1$, $t_1/T = 1.5$, $k_2/k_1 = +0.1$

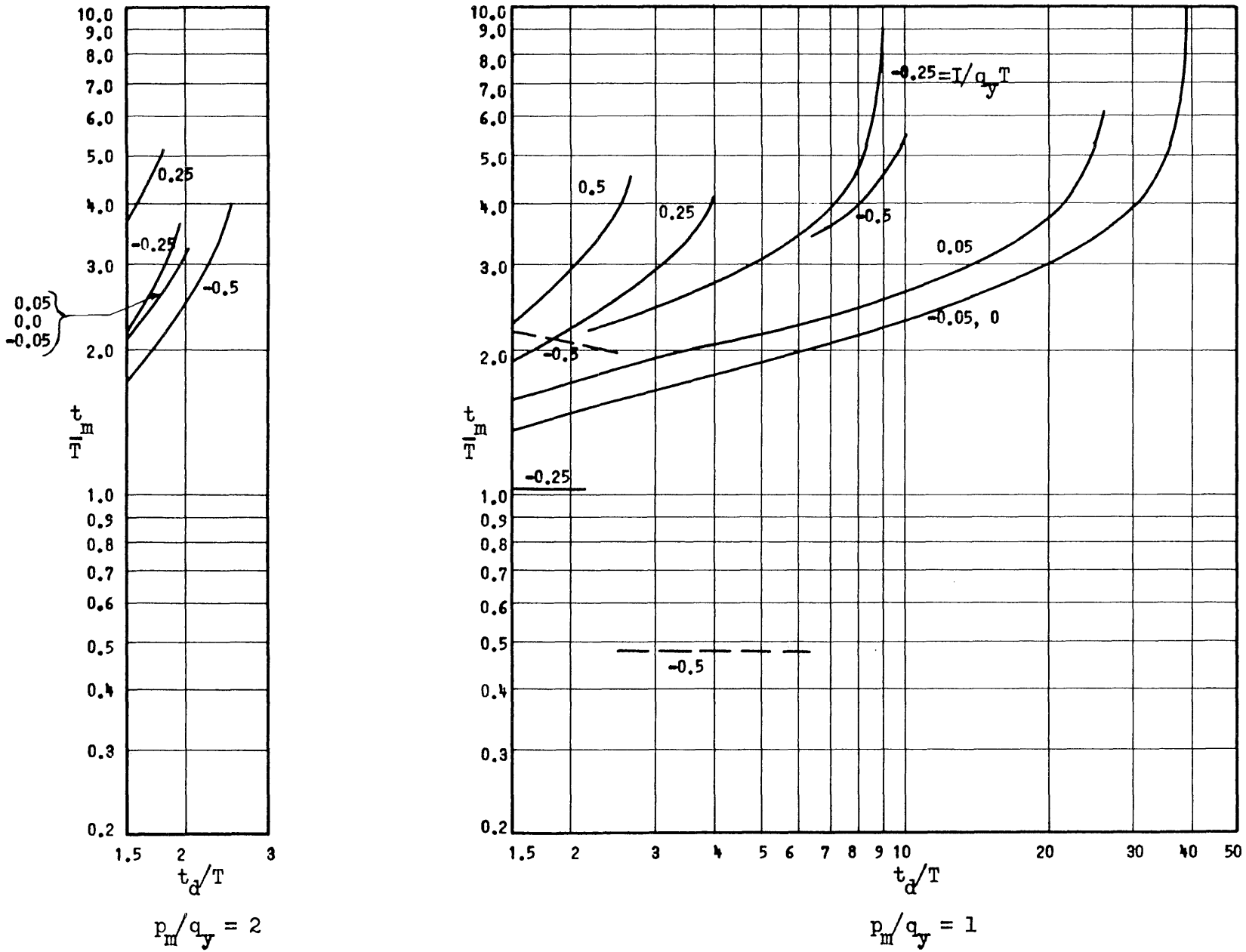

Fig. 27a Time of Maximum Response to Delayed Rise Triangular Pulse of Fig. 3c with Two Impulses

$I_o = I_1$, $t_1/T = 1.5$, $k_2/k_1 = -0.02$

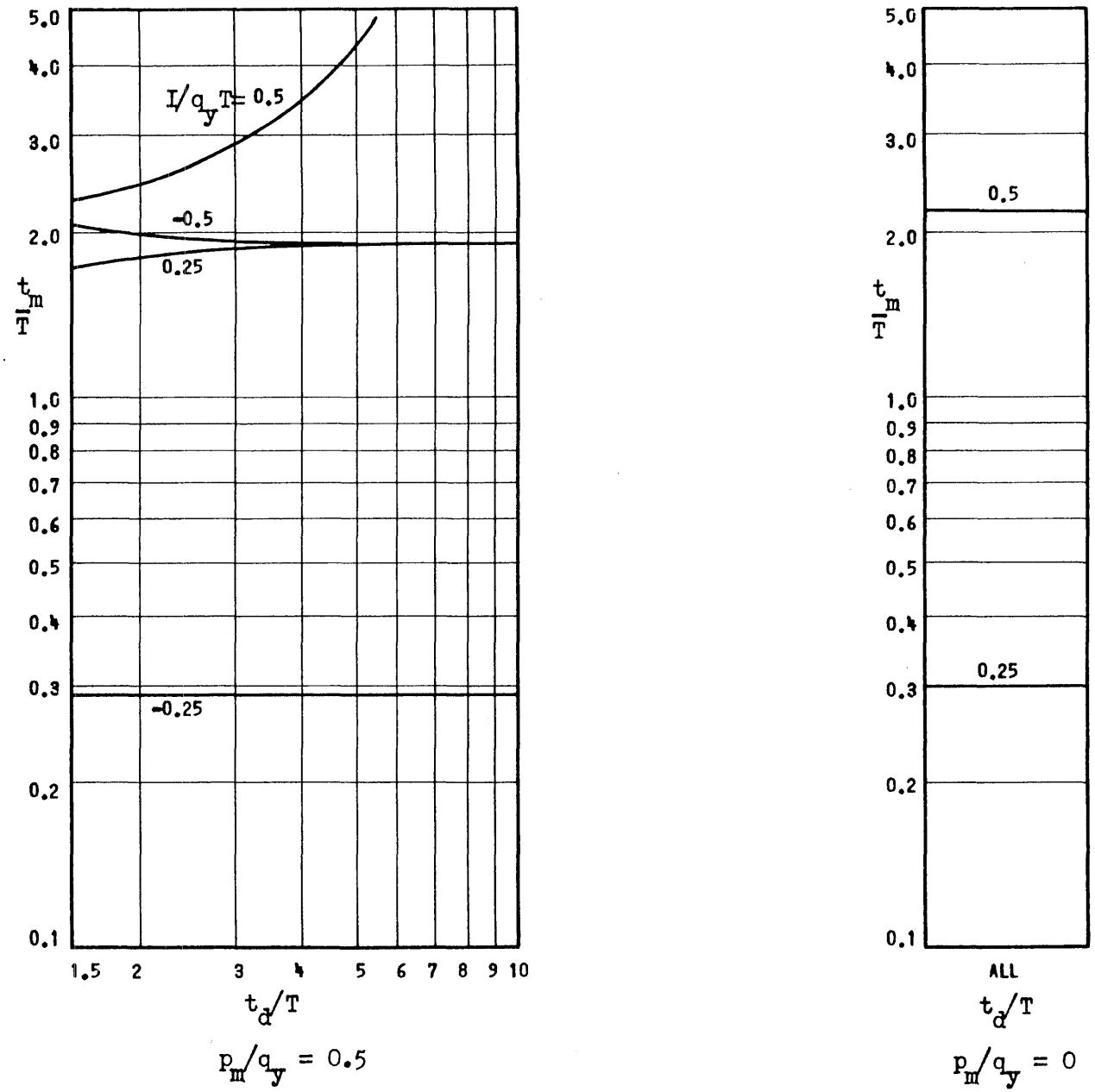

Fig. 27b Time of Maximum Response to Delayed Rise Triangular Pulse of Fig. 3c with Two Impulses

$I_o = I_1$, $t_1/T = 1.5$, $k_2/k_1 = -0.02$

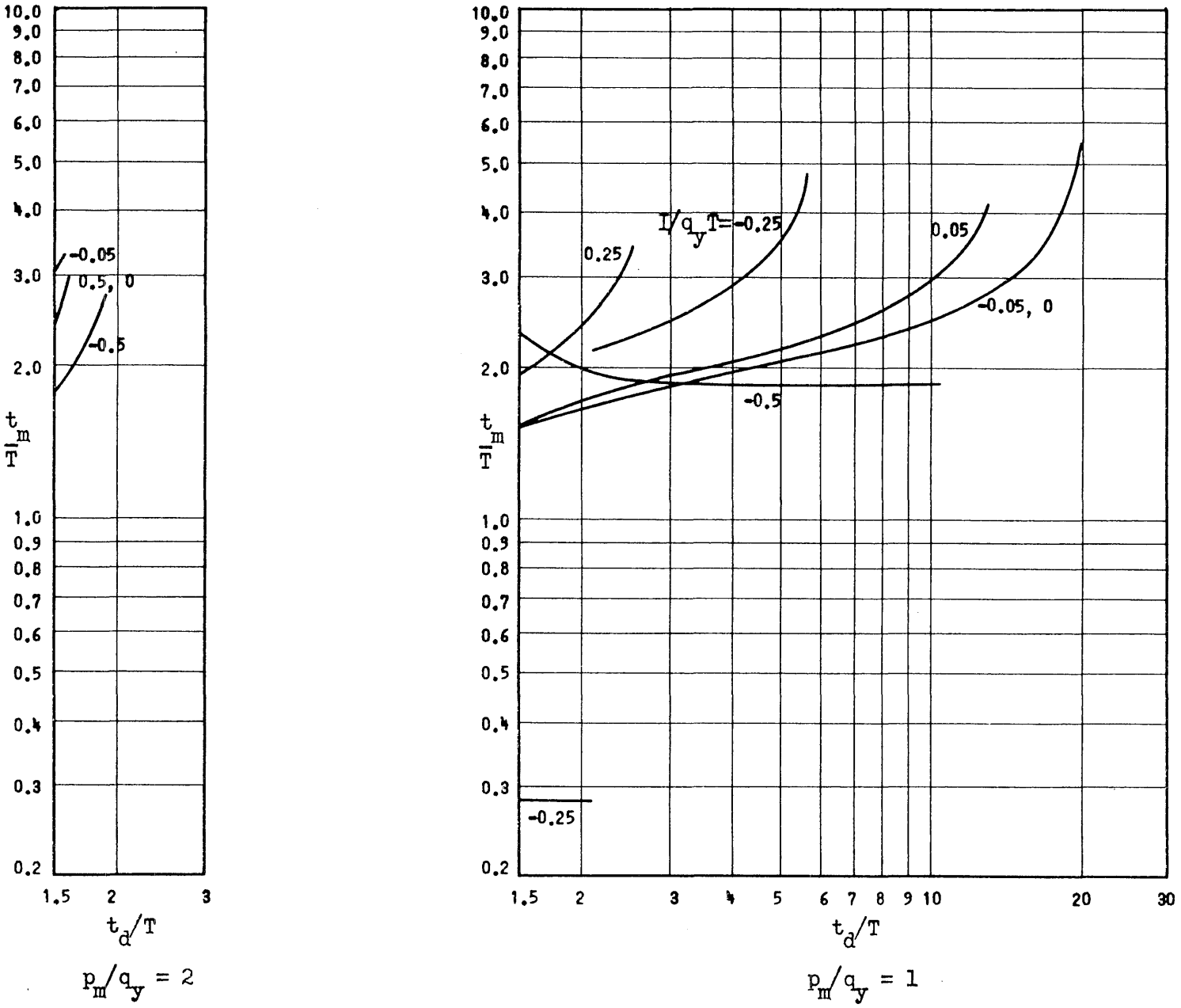

Fig. 28a Time of Maximum Response to Delayed Rise Triangular Pulse of Fig. 3c with Two Impulses

$I_o = I_1$, $t_1/T = 1.5$, $k_2/k_1 = -0.04$

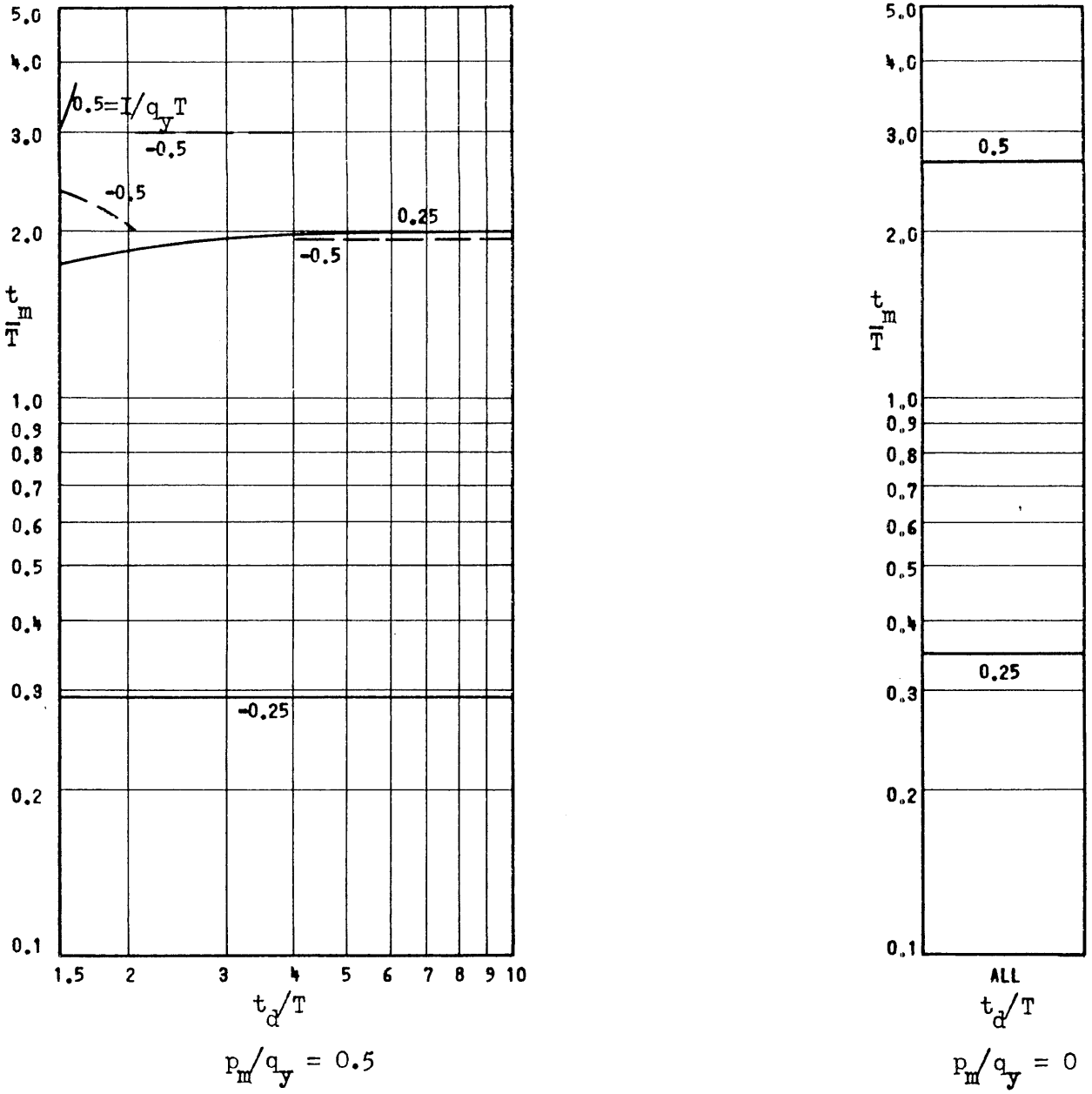

Fig. 28b Time of Maximum Response to Delayed Rise Triangular Pulse of Fig. 3c with Two Impulses $I_o = I_1$, $t_1/T = 1.5$, $k_2/k_1 = -0.04$

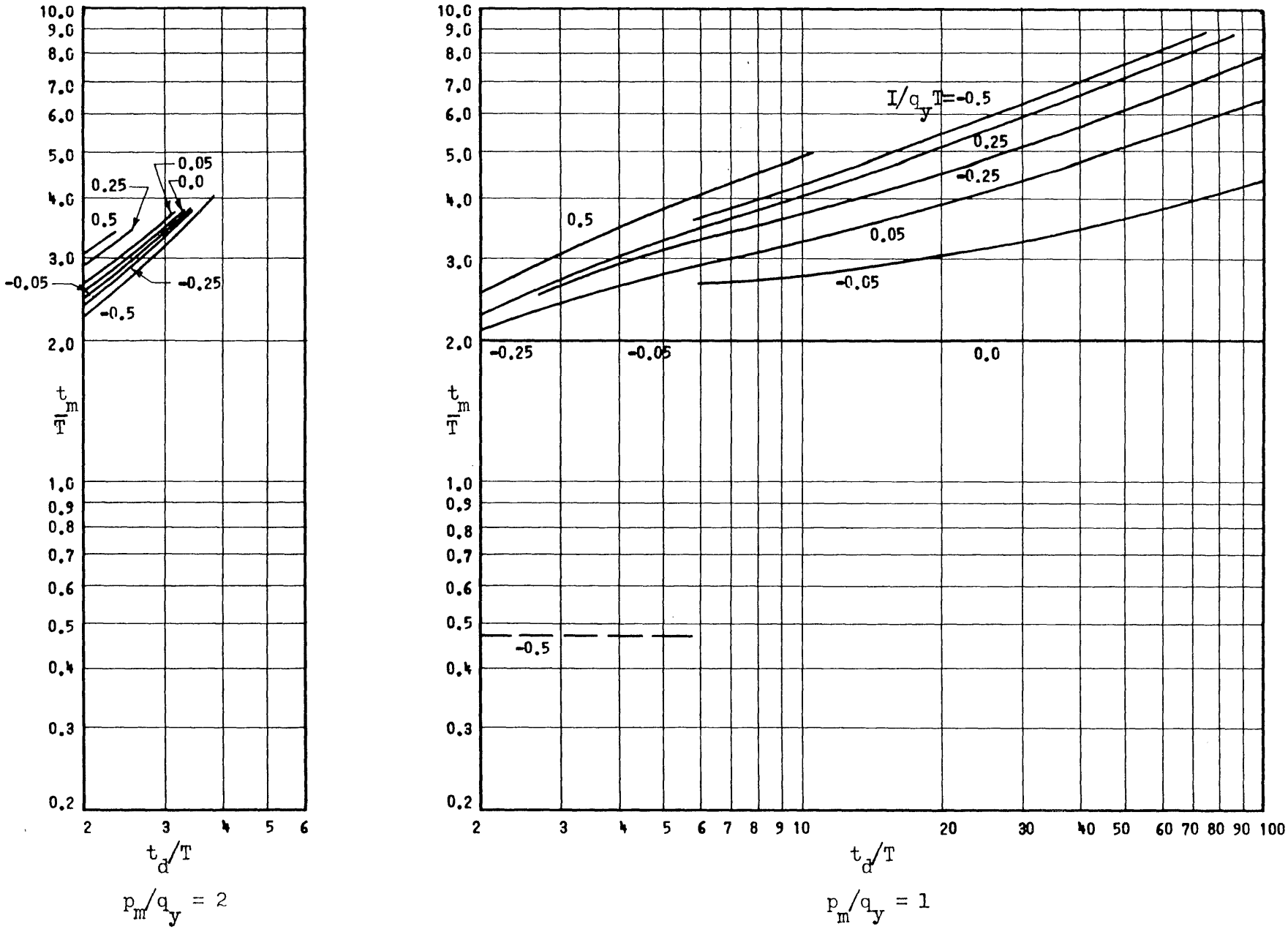

Fig. 29a Time of Maximum Response to Delayed Rise Triangular Pulse of Fig. 3c with Two Impulses

$I_o = I_1$, $t_1/T = 2.0$, $k_2/k_1 = 0$

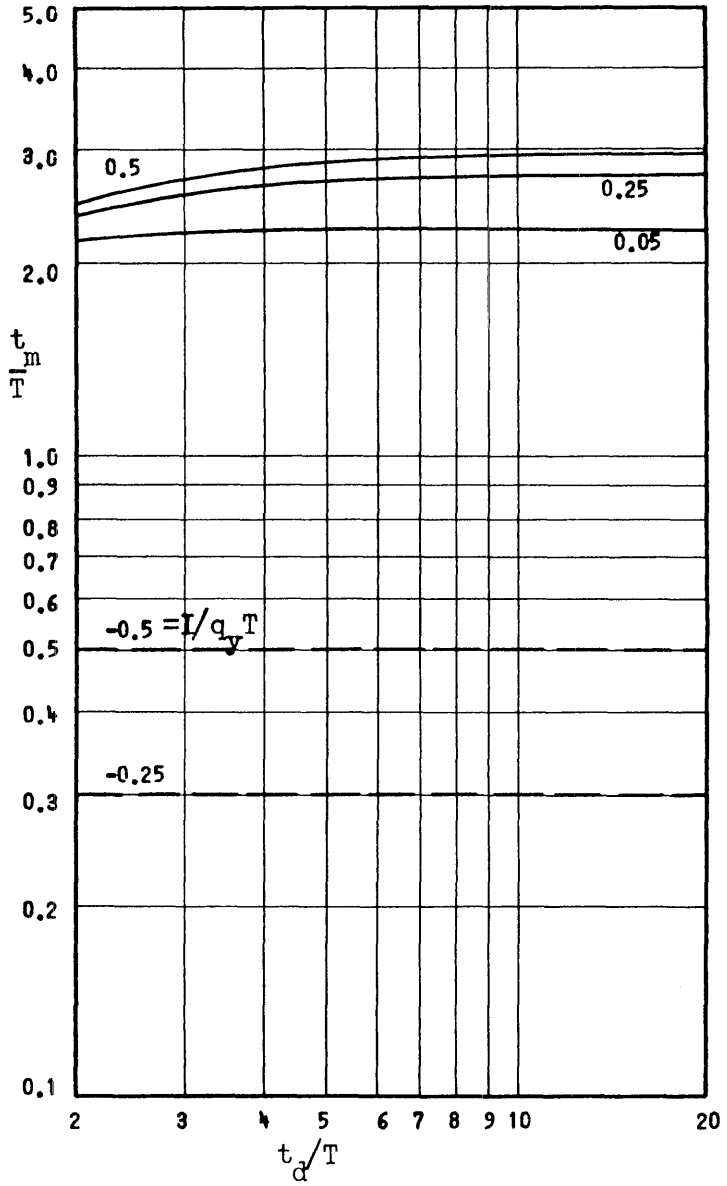

$p_m/q_y = 0.5$

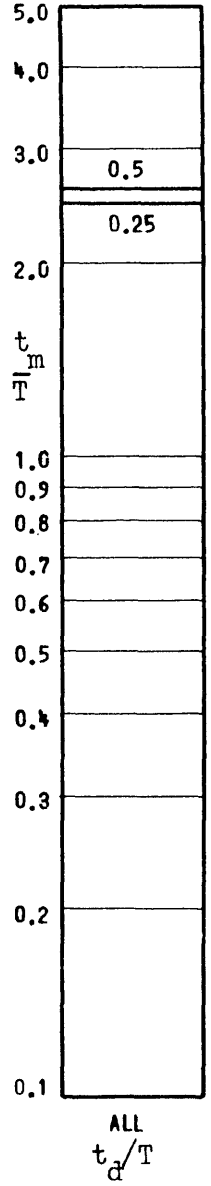

$p_m/q_y = 0$

Fig. 29b Time of Maximum Response to Delayed Rise Triangular Pulse of Fig. 3c with Two Impulses

$I_o = I_1$, $t_1/T = 2$, $k_2/k_1 = 0$

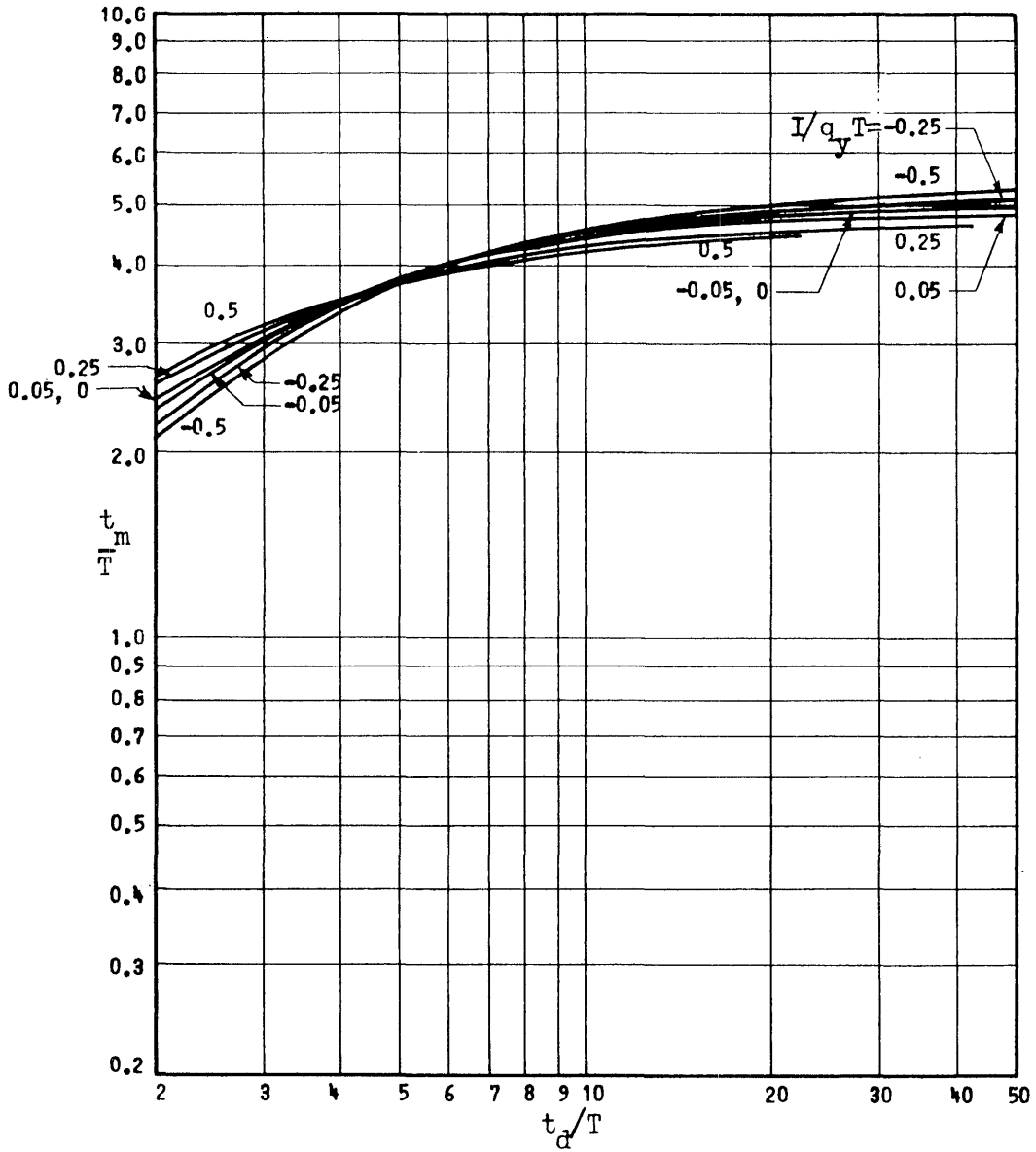

$p_m/q_y = 2$

Fig. 30a Time of Maximum Response to Delayed Rise Triangular Pulse of Fig. 3c with Two Impulses

$I_o = I_1$, $t_1/T = 2$, $k_2/k_1 = +0.02$

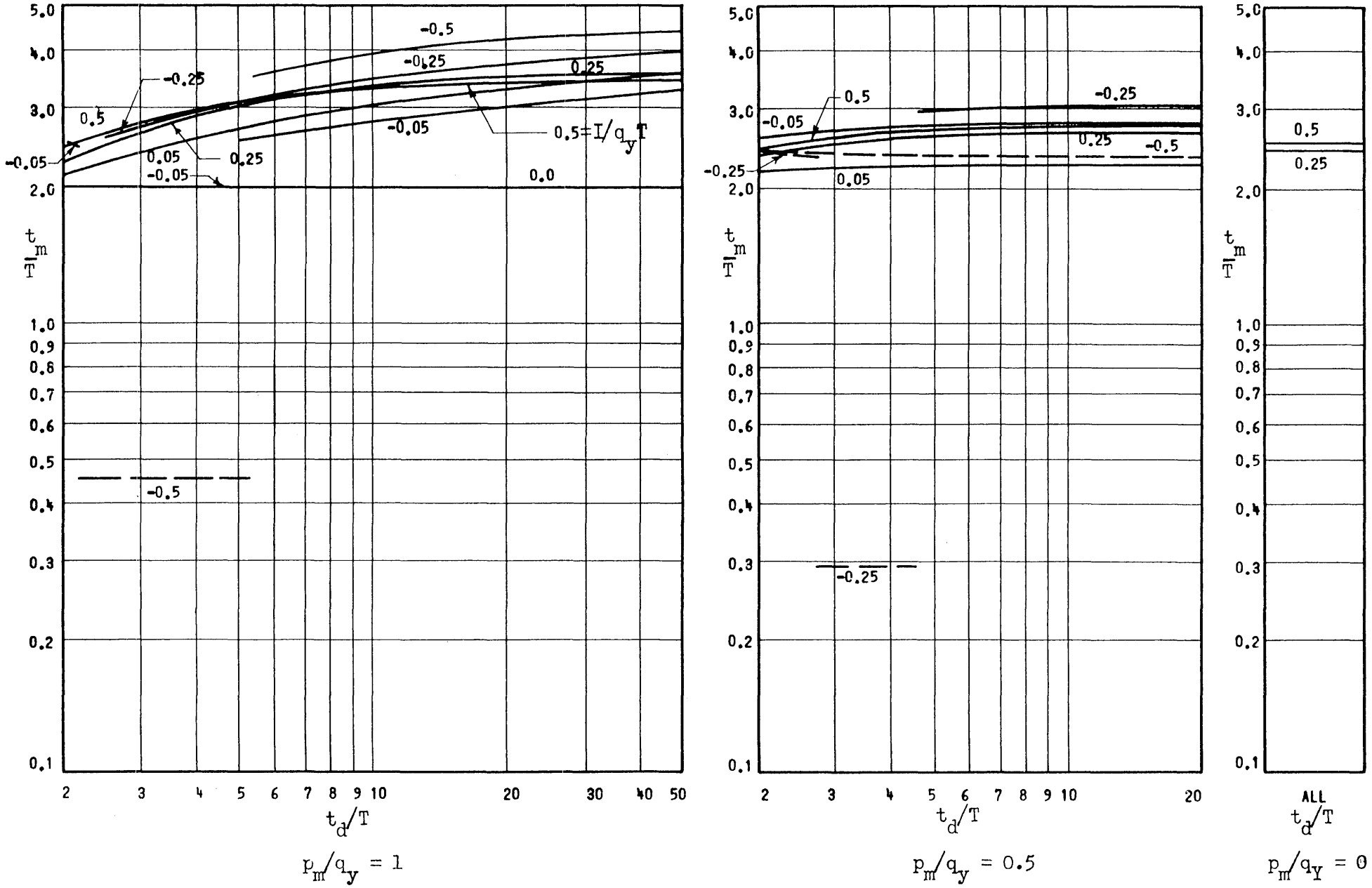

Fig. 30b Time of Maximum Response to Delayed Rise Triangular Pulse of Fig. 3c with Two Impulses

$I_o = I_1$, $t_1/T = 2$, $k_2/k_1 = +0.02$

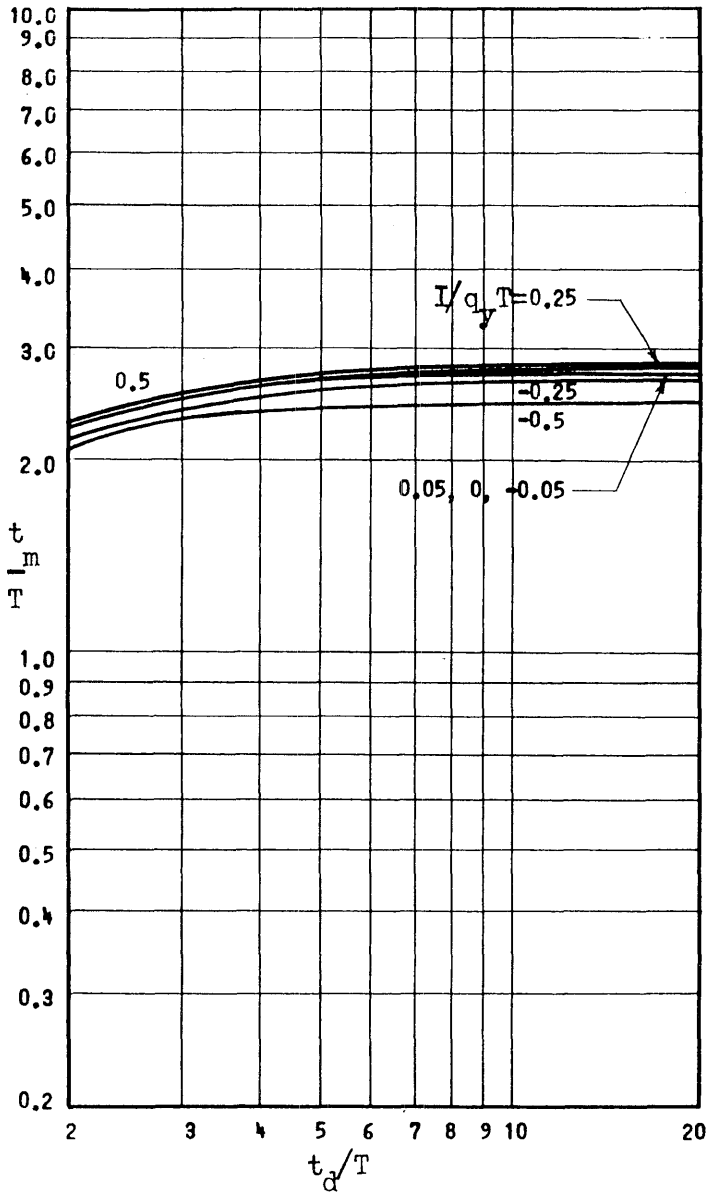

$p_m/q_y = 5$

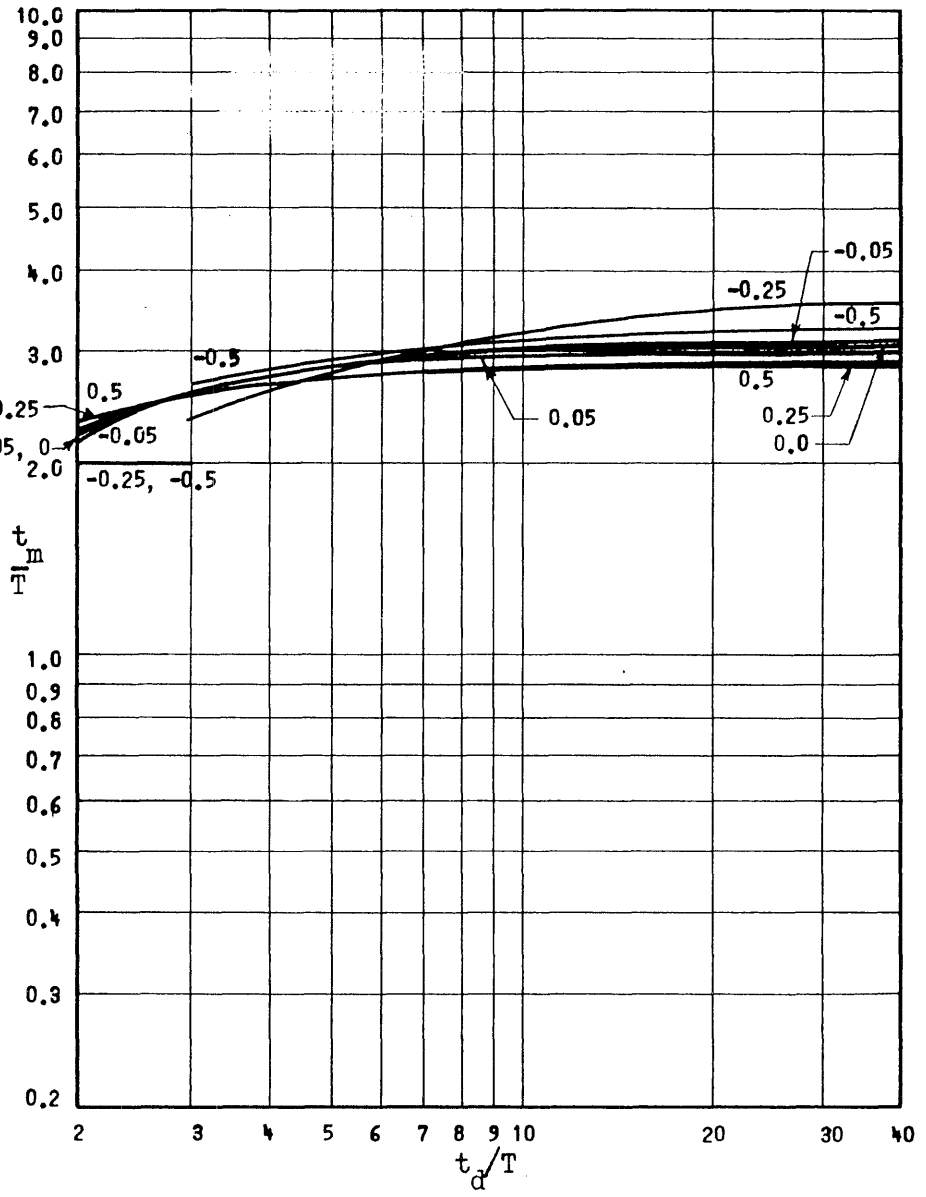

$p_m/q_y = 2$

Fig. 31a Time of Maximum Response to Delayed Rise Triangular Pulse of Fig. 3c with Two Impulses

$I_o = I_1$, $t_1/T = 2$, $k_2 k_1 = +0.1$

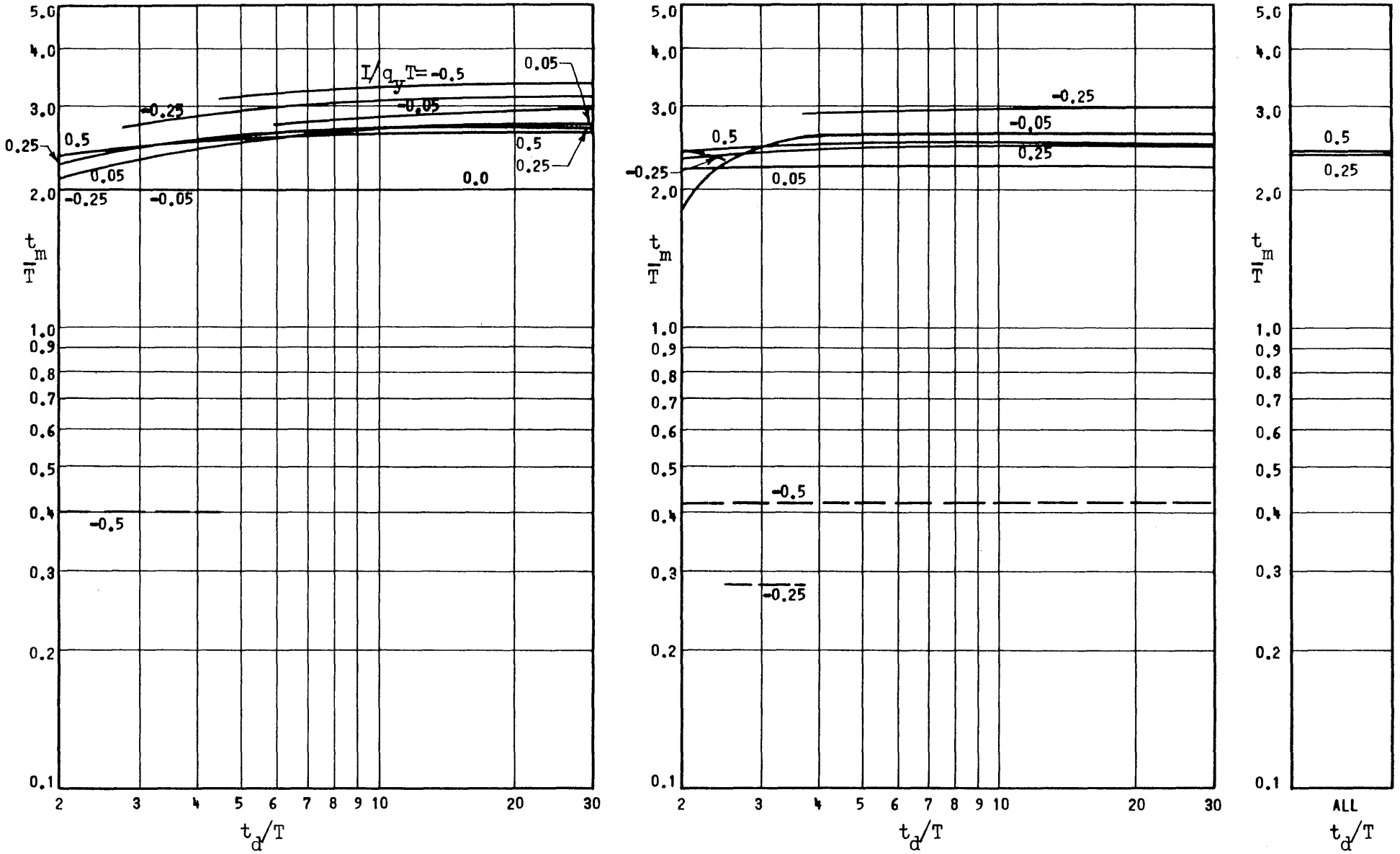

Fig. 31b Time of Maximum Response to Delayed Rise Triangular Pulse of Fig. 3c with Two Impulses

$I_o = I_1$, $t_1/T = 2$, $k_2/k_1 = +0.1$

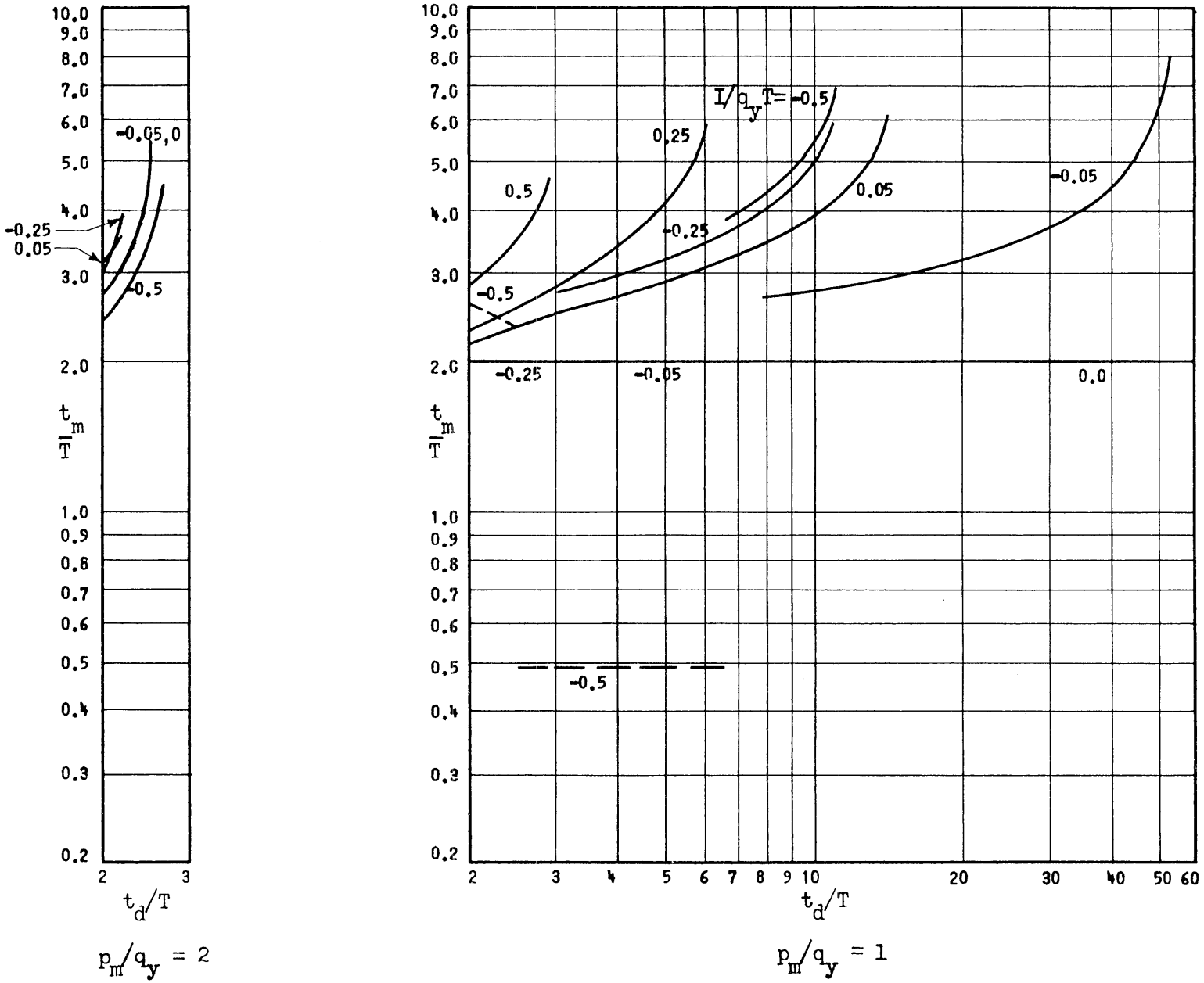

Fig. 32a Time of Maximum Response to Delayed Rise Triangular Pulse of Fig. 3c with Two Impulses

$I_o = I_1$, $t_1/T = 2$, $k_2/k_1 = -0.02$

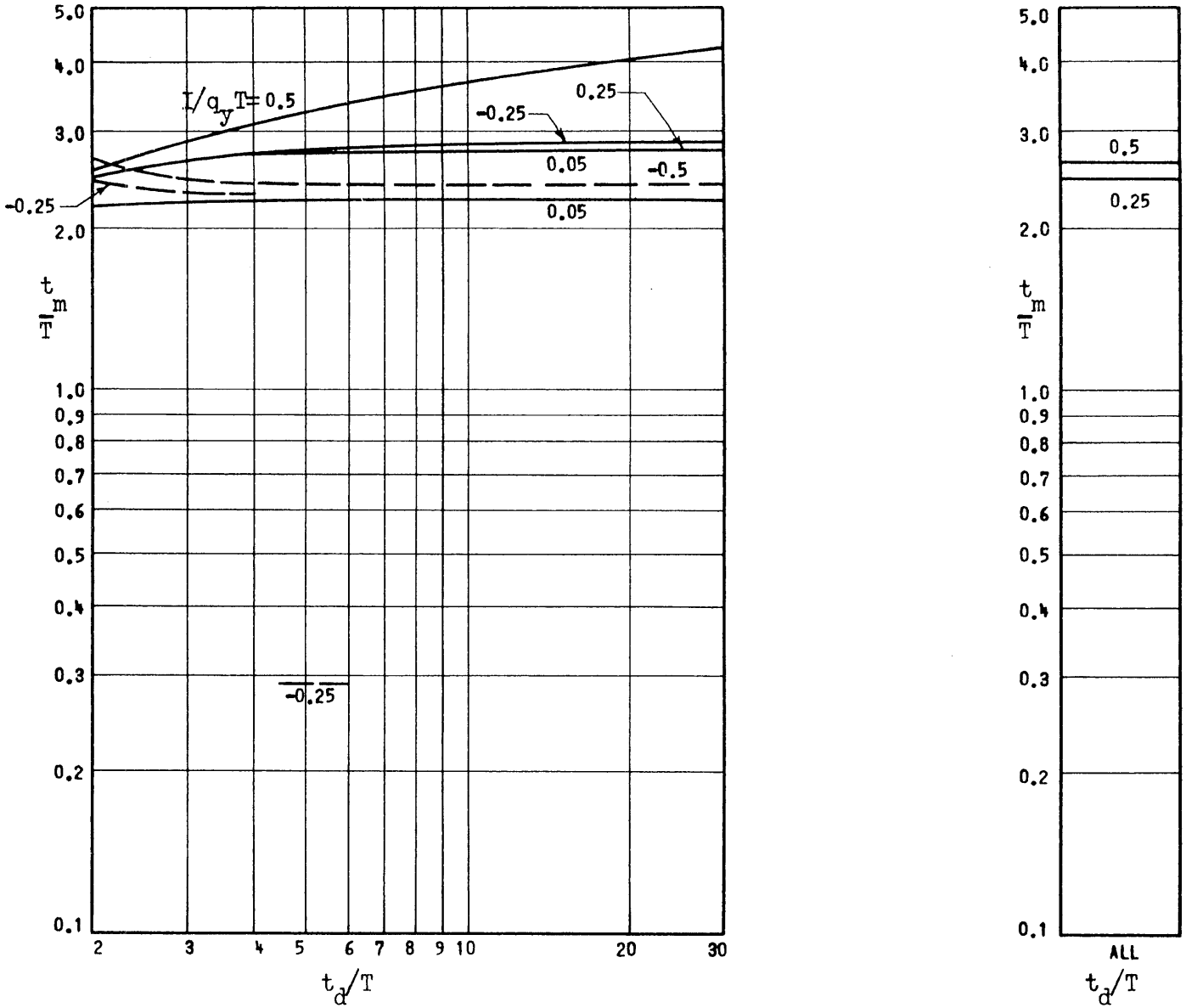

Fig. 32b Time of Maximum Response to Delayed Rise Triangular Pulse of Fig. 3c with Two Impulses

$I_o = I_1$, $t_1/T = 2$, $k_2/k_1 = -0.02$

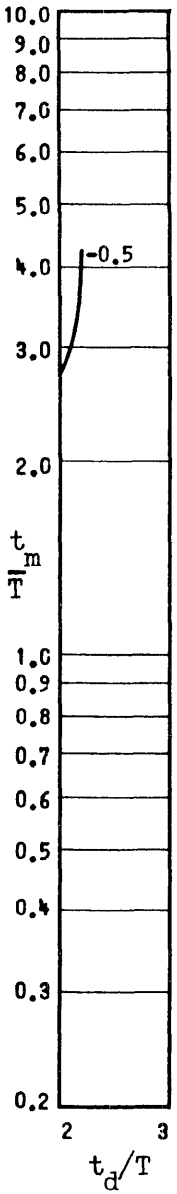

$p_m/q_y = 2$

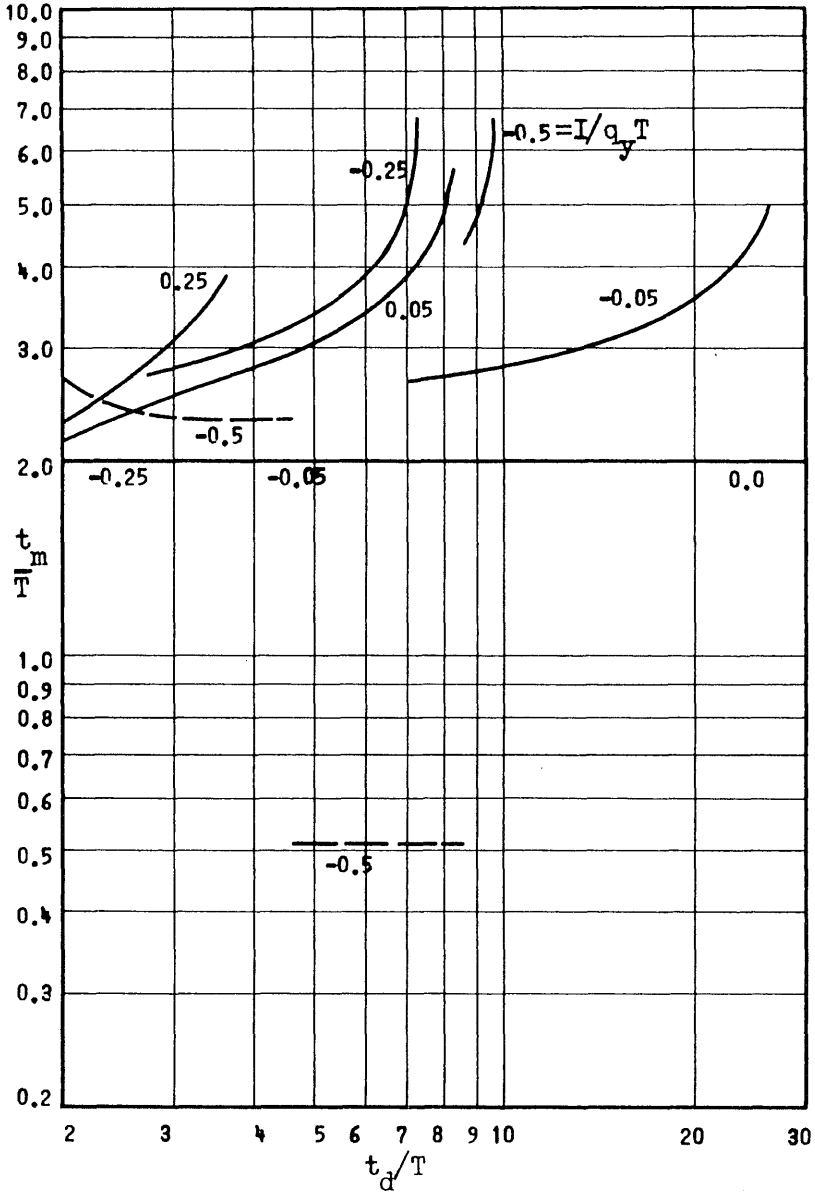

$p_m/q_y = 1$

Fig. 33a Time of Maximum Response to Delayed Rise Triangular Pulse of Fig. 3c with Two Impulses

$I_o = I_1$, $t_1/T = 2$, $k_2/k_1 = -0.04$

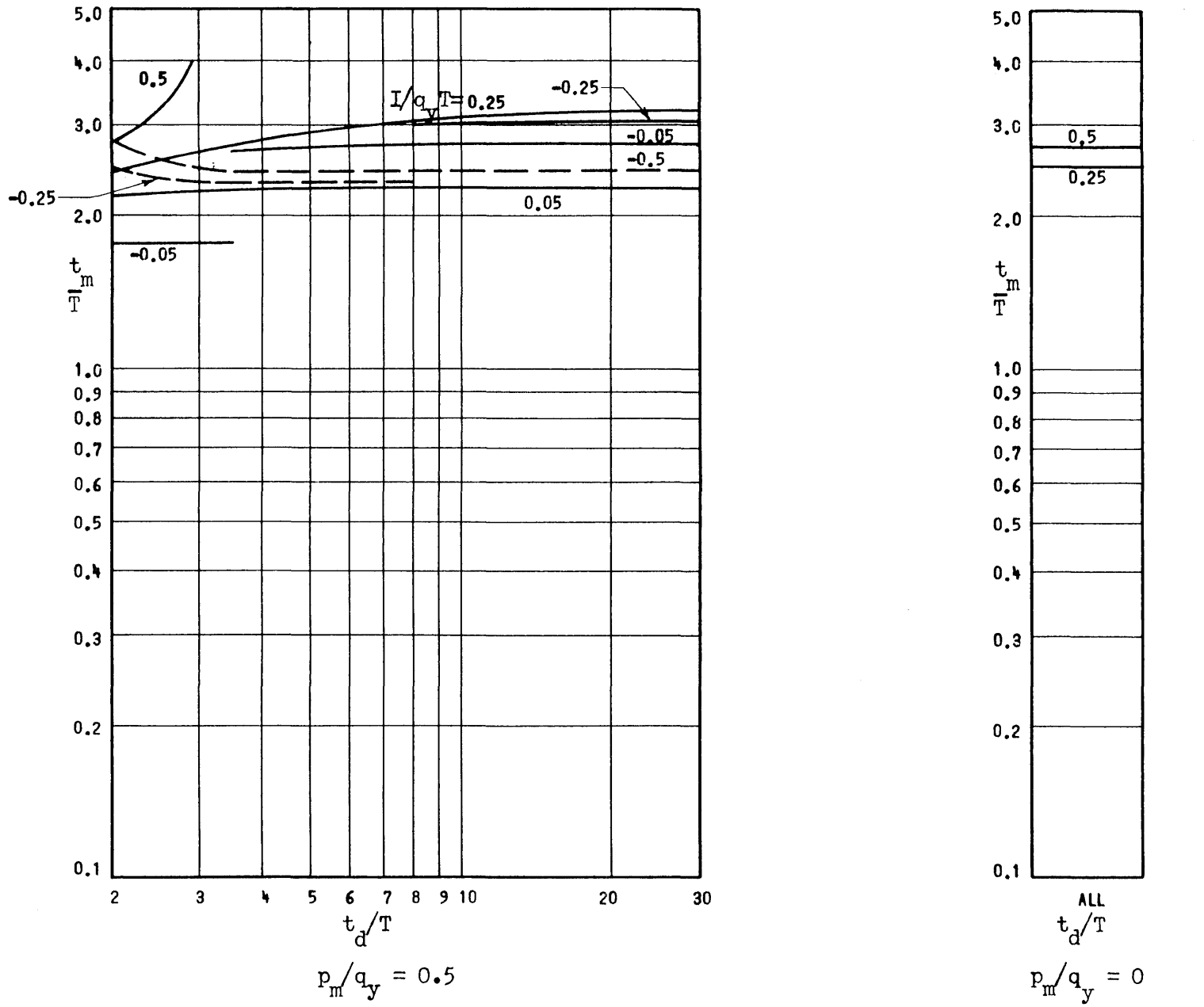

Fig. 33b Time of Maximum Response to Delayed Rise Triangular Pulse of Fig. 3c with Two Impulses

$I_o = I_1$, $t_1/T = 2$, $k_2/k_1 = -0.04$

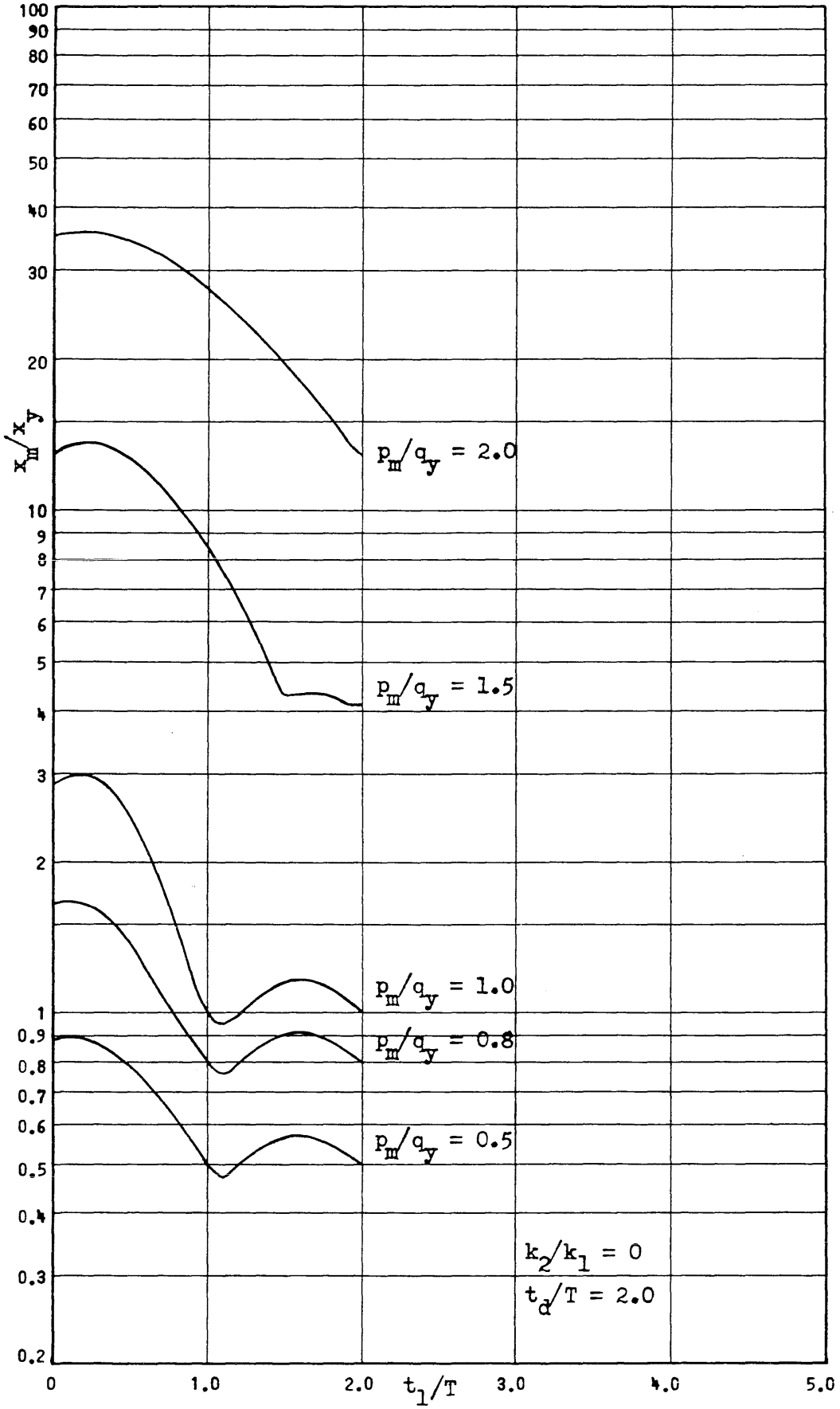

Fig. 34 Maximum Response Versus Rise Time for Delayed Rise Triangular Force Pulse with Elasto-Plastic Resistance

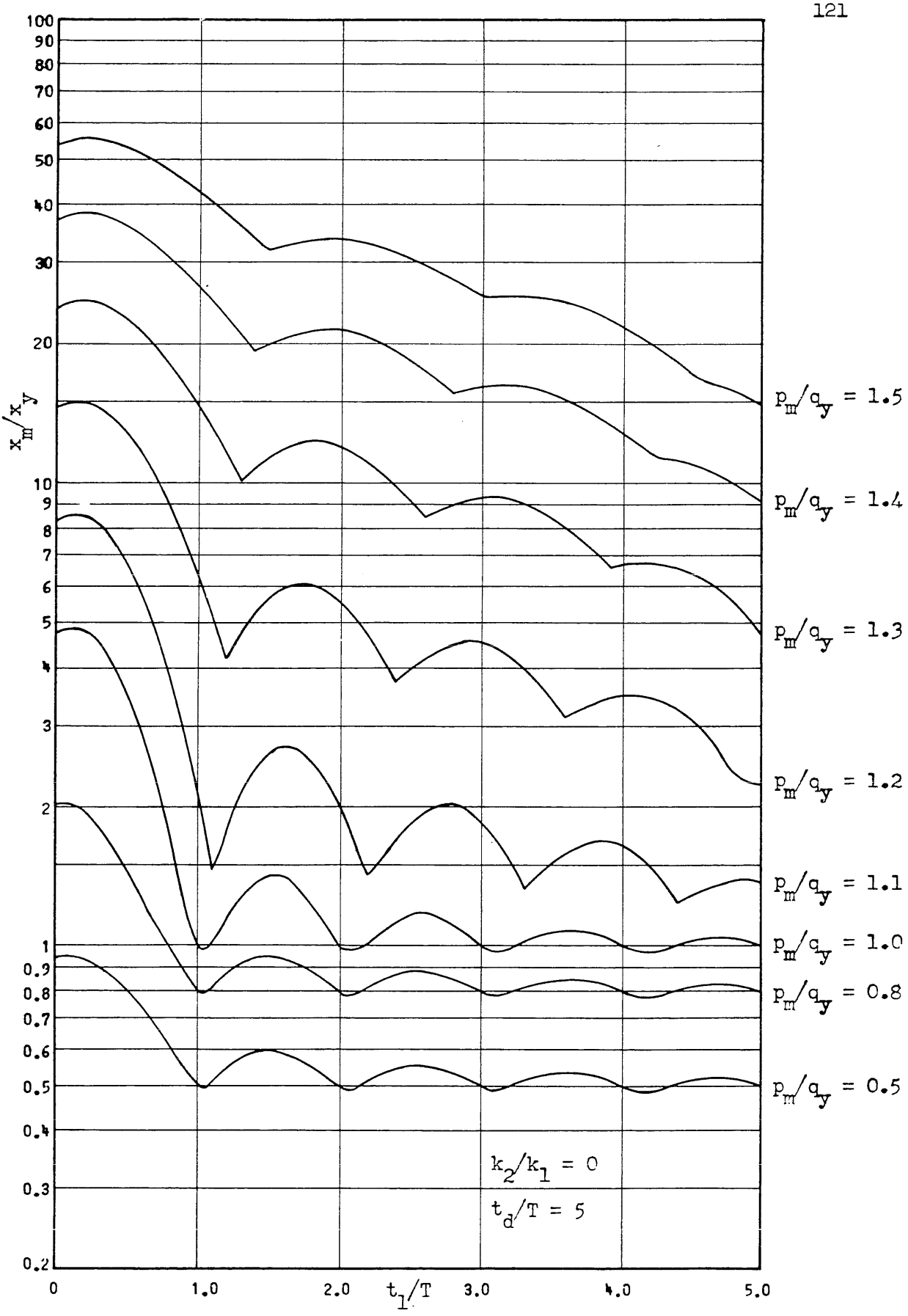

Fig. 35 Maximum Response Versus Rise Time for Delayed Rise Triangular Force Pulse with Elasto-Plastic Resistance

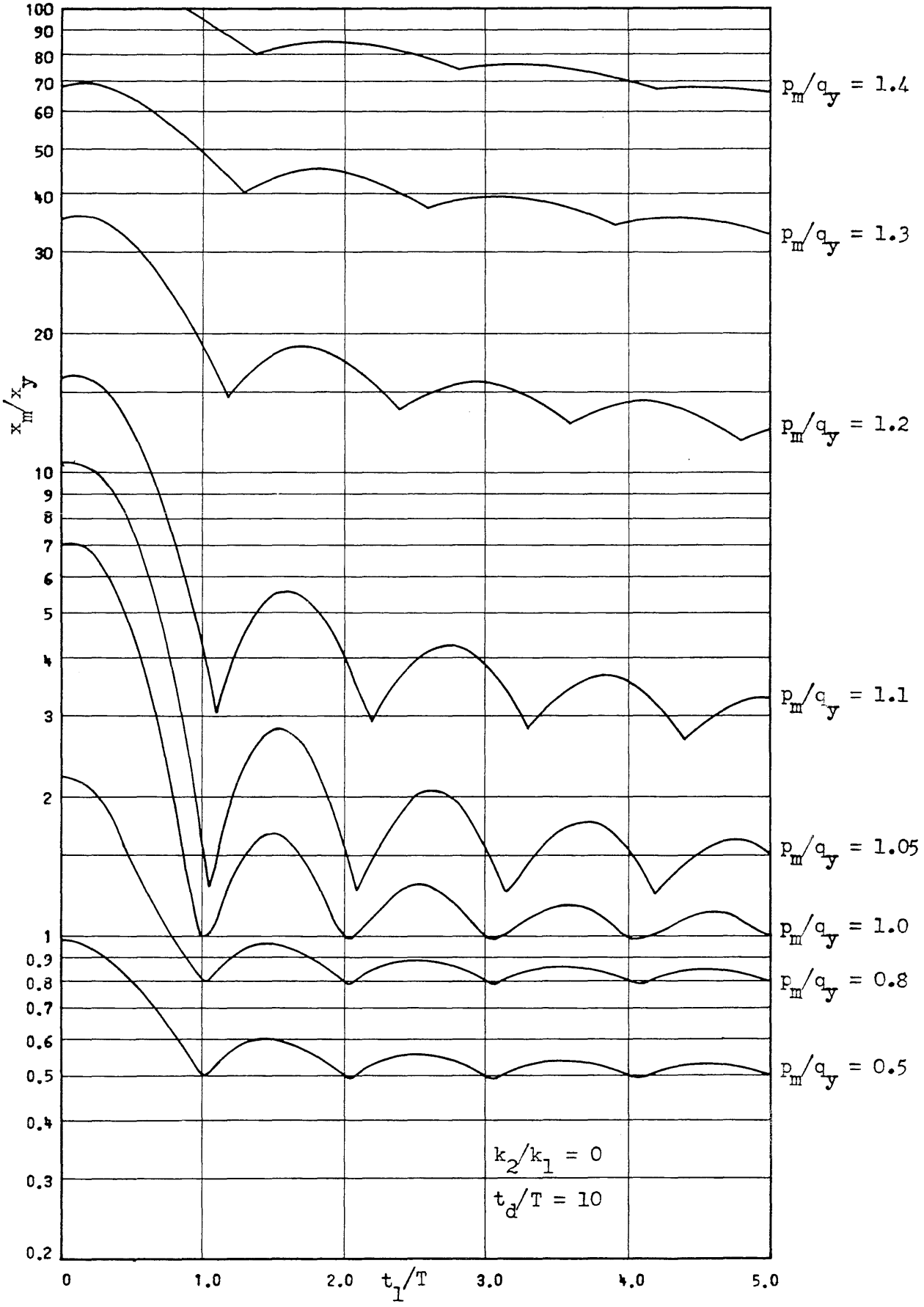

Fig. 36 Maximum Response Versus Rise Time for Delayed Rise Triangular Force Pulse with Elasto-Plastic Resistance

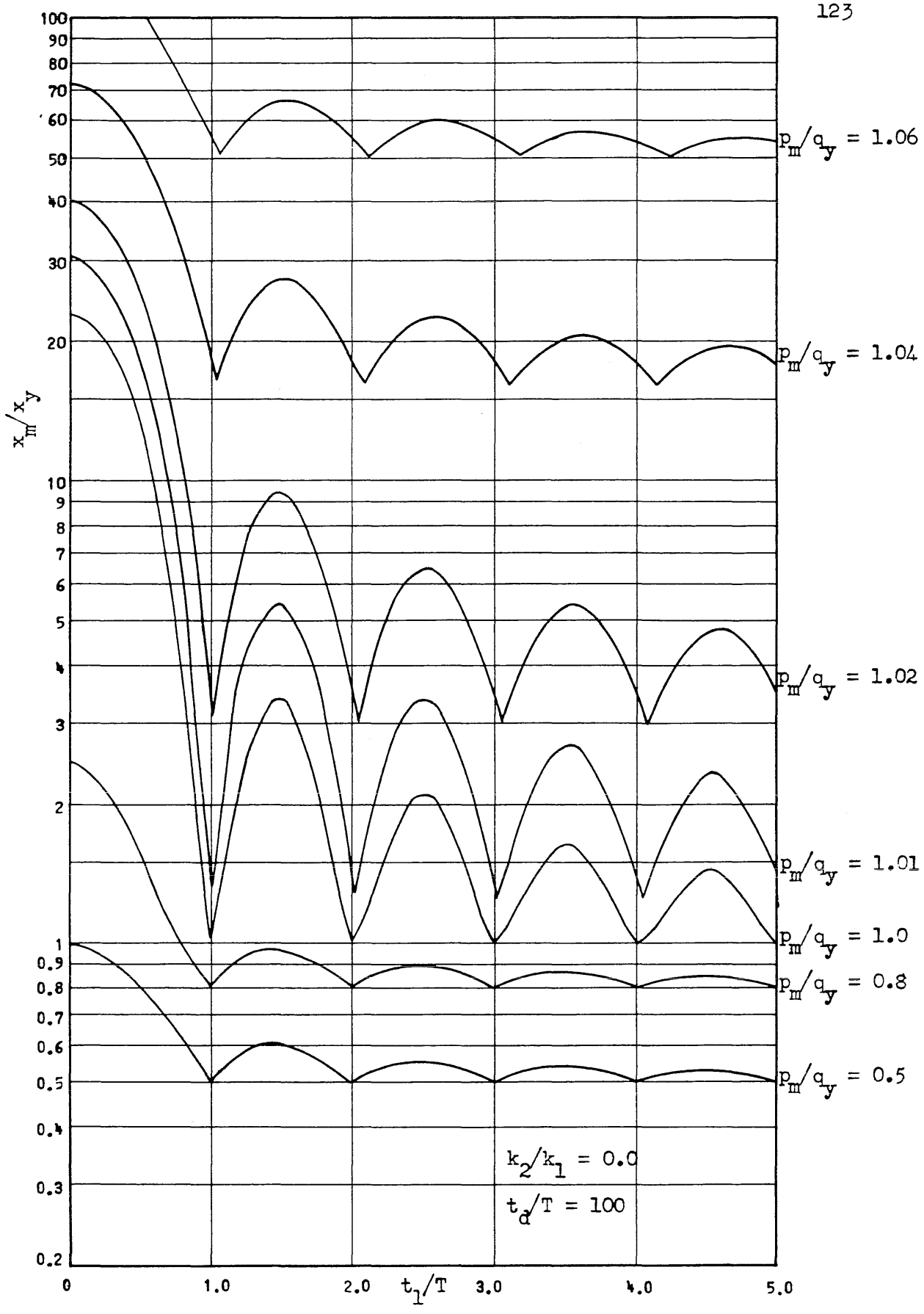

Fig. 37 Maximum Response Versus Rise Time for Delayed Rise Triangular Force Pulse with Elasto-Plastic Resistance

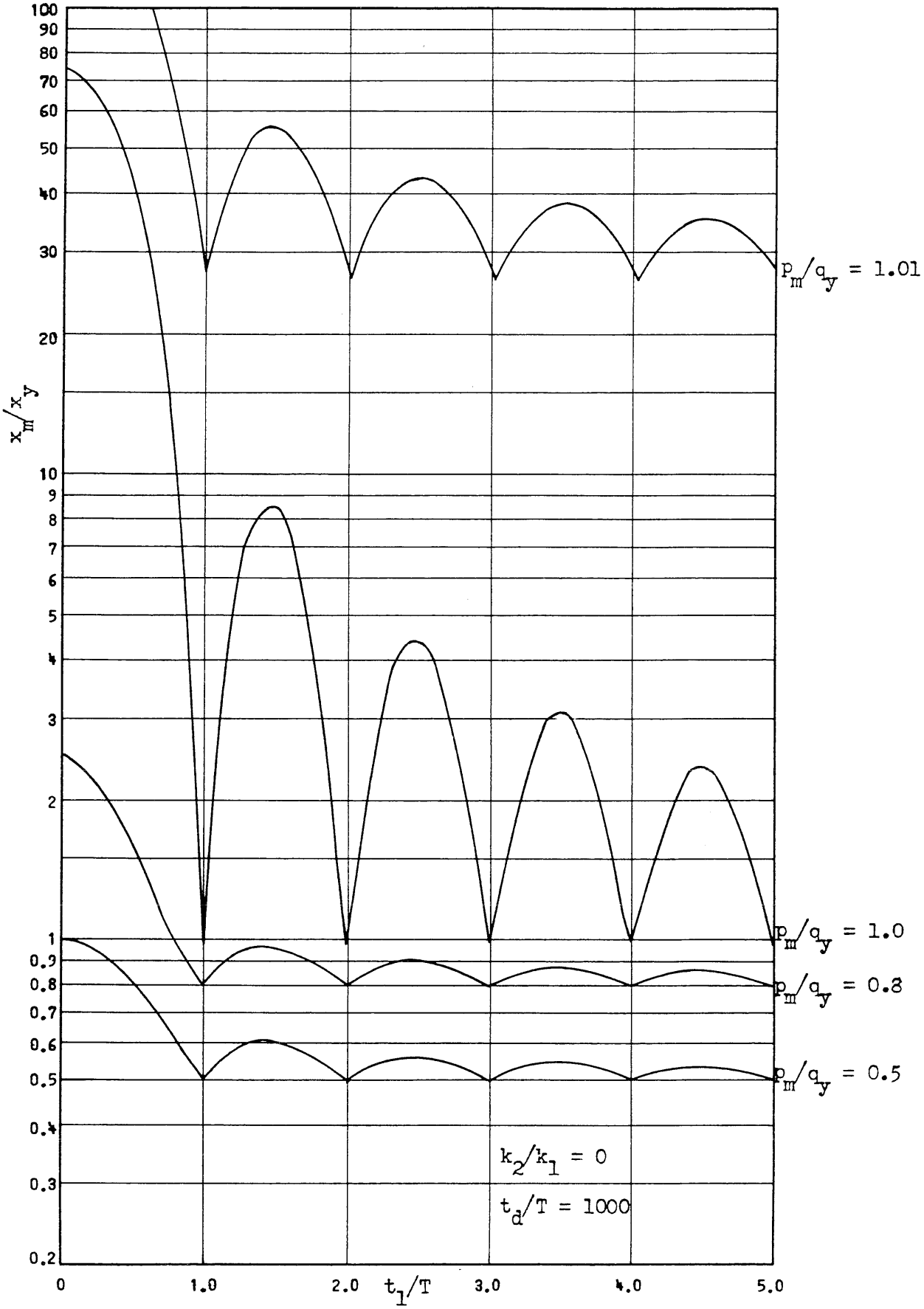

Fig. 38 Maximum Response Versus Rise Time for Delayed Rise Triangular Force Pulse with Elasto-Plastic Resistance

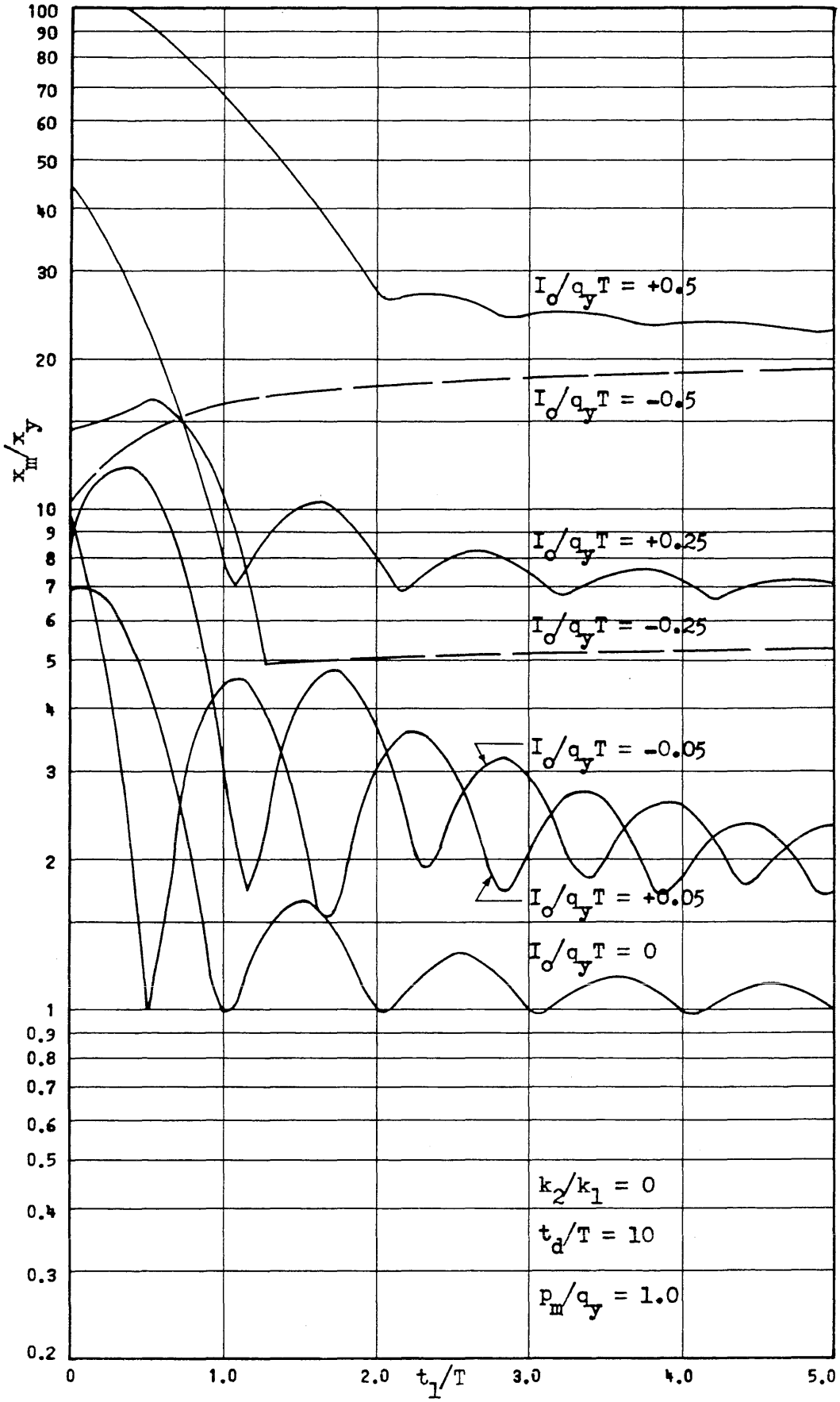

Fig. 39 Maximum Response Versus Rise Time for Delayed Rise Triangular Force Pulse with Impulses

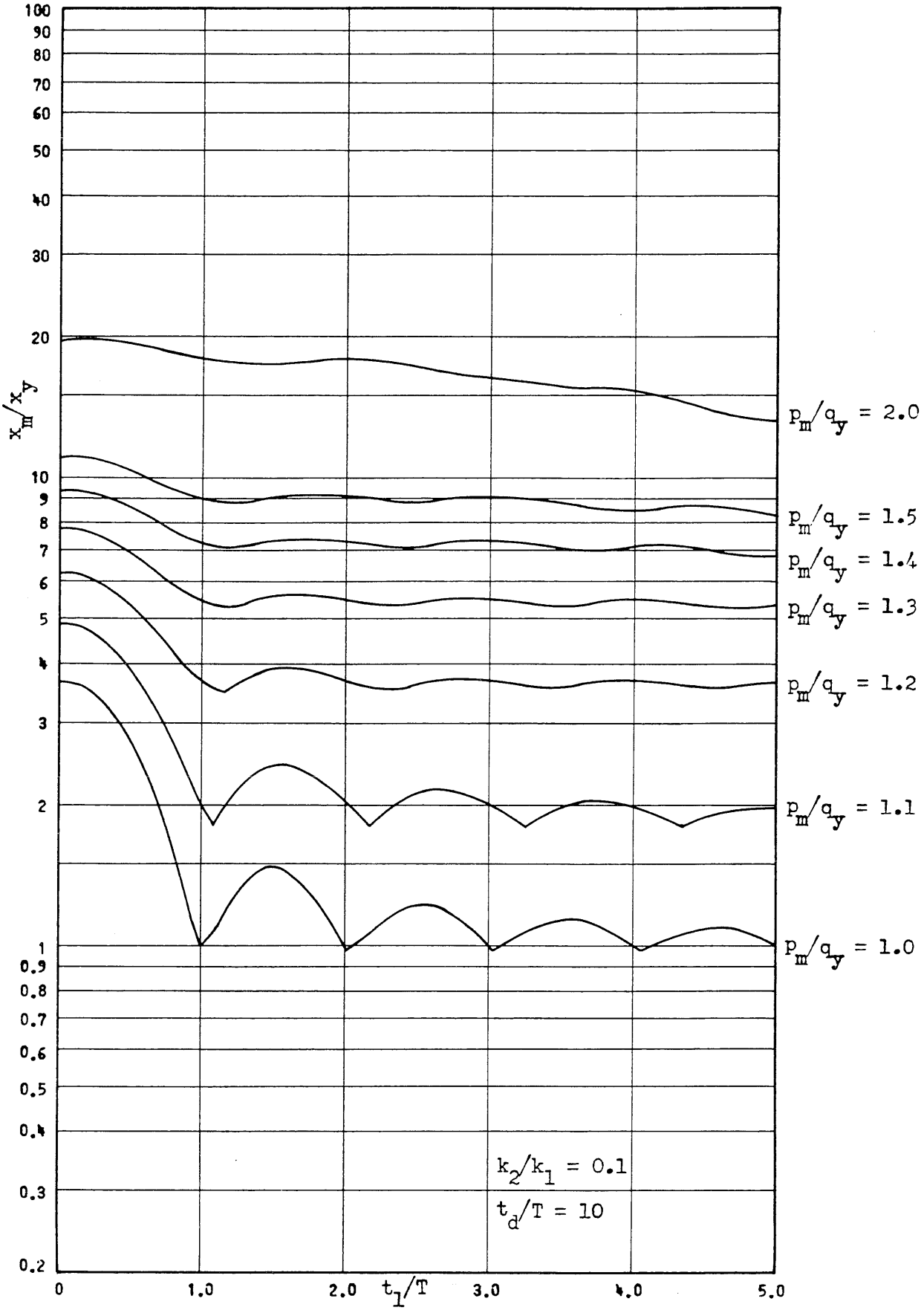

Fig. 40 Maximum Response Versus Rise Time for Delayed Rise Triangular Force Pulse with Various Bilinear Resistances

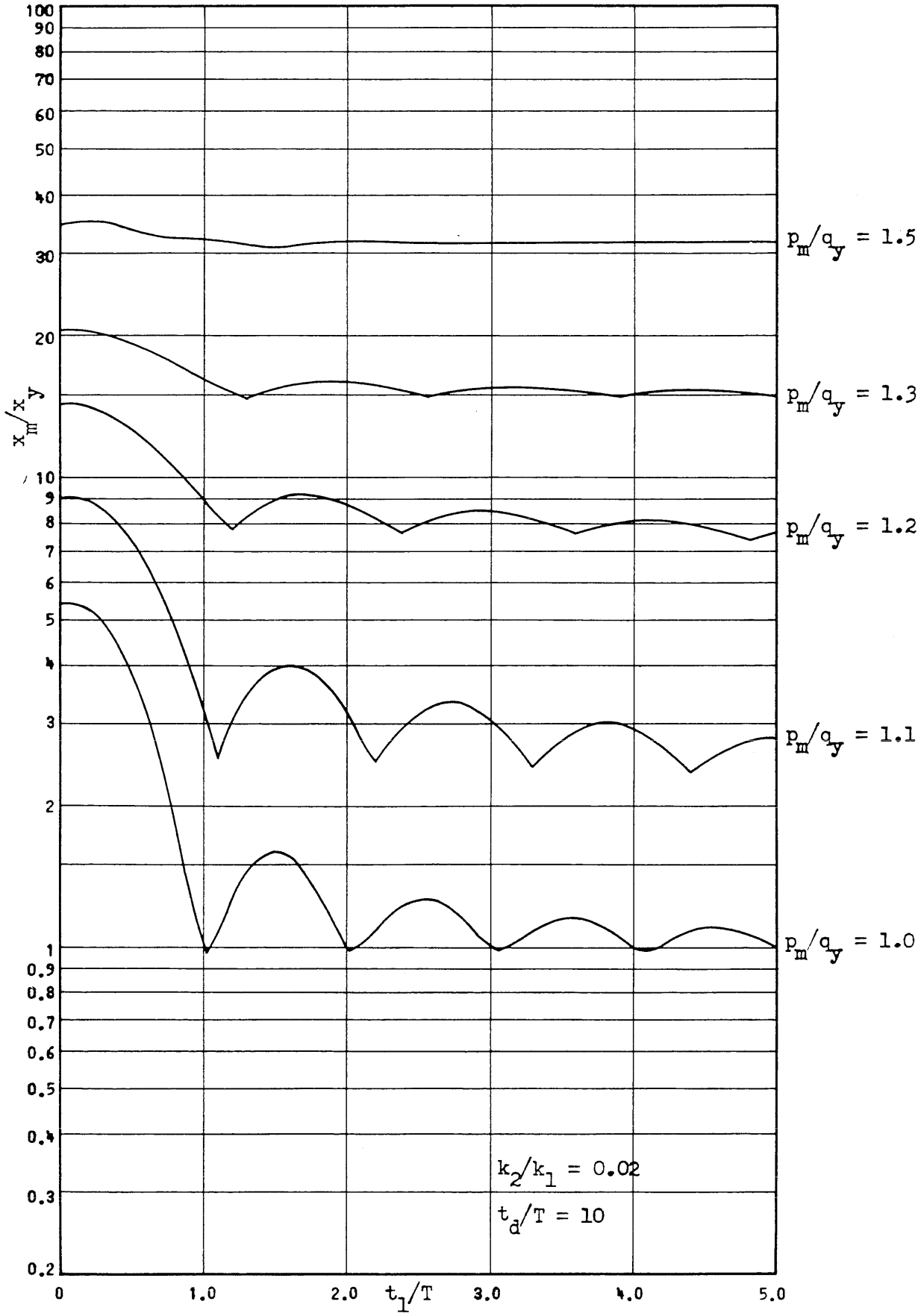

Fig. 41 Maximum Response Versus Rise Time for Delayed Rise Triangular Force Pulse with Various Bilinear Resistances

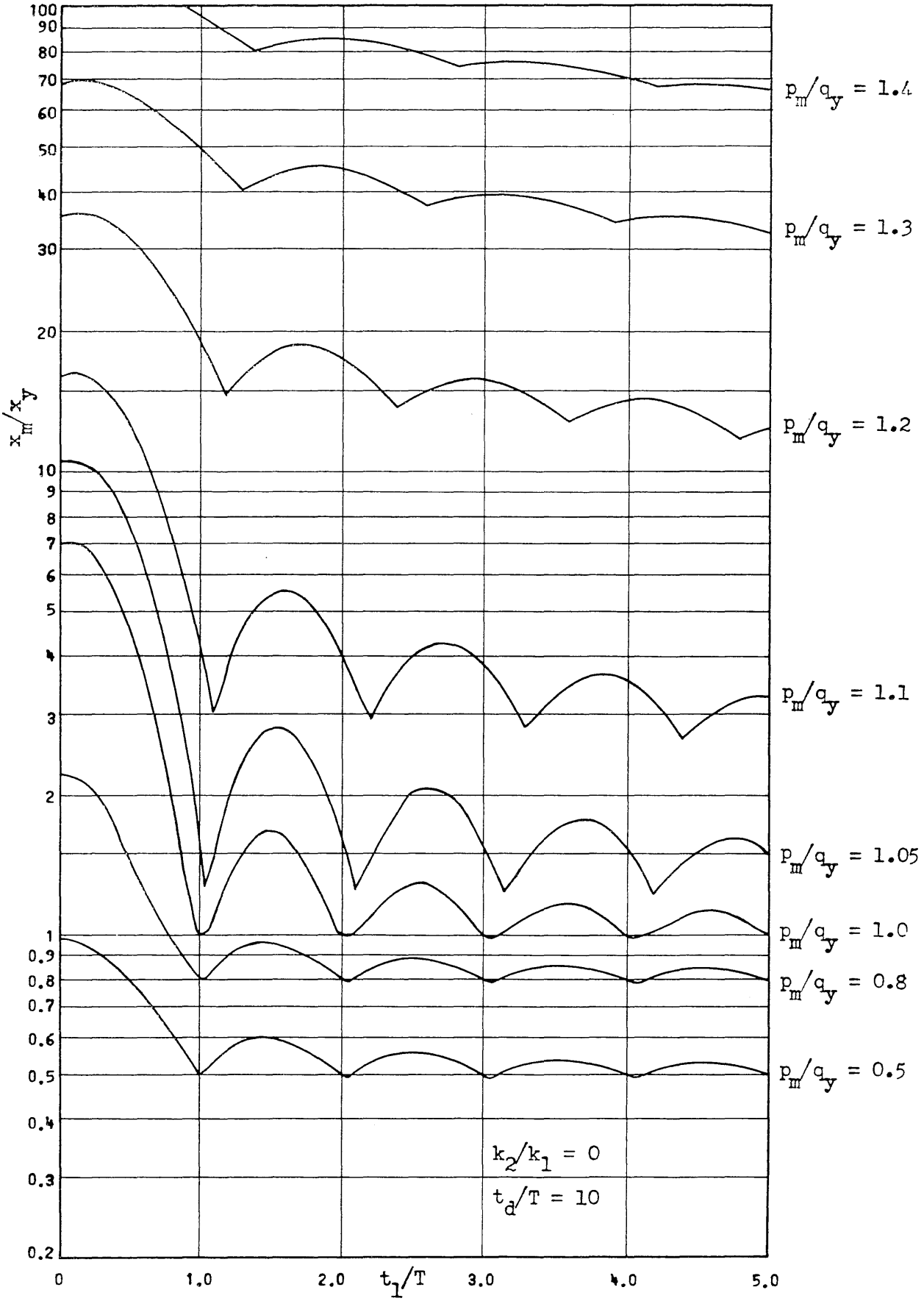

Fig. 42 Maximum Response Versus Rise Time for Delayed Rise Triangular Force Pulse with Various Bilinear Resistances

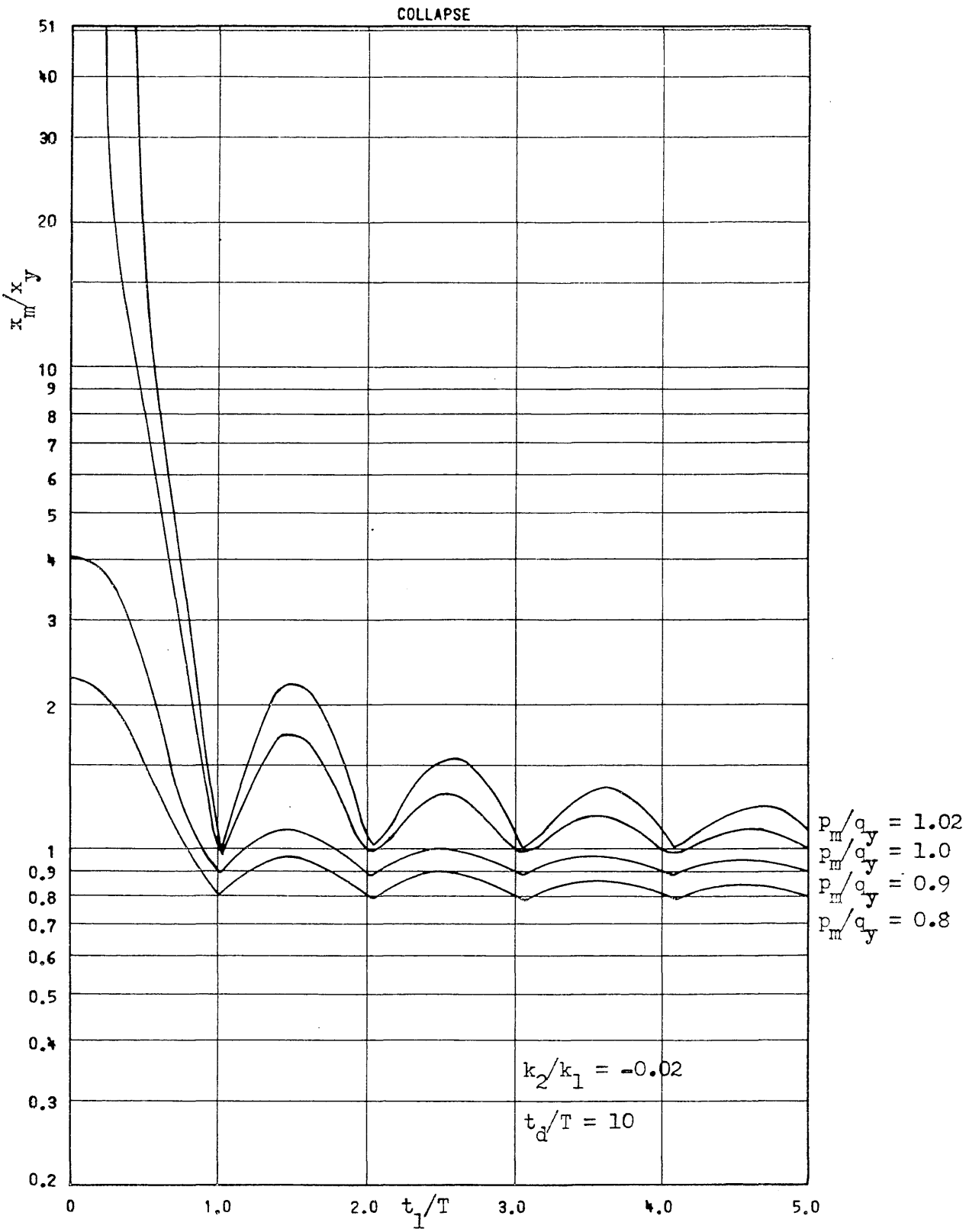

Fig. 43 Maximum Response Versus Rise Time for Delayed Rise Triangular Force Pulse with Various Bilinear Resistances

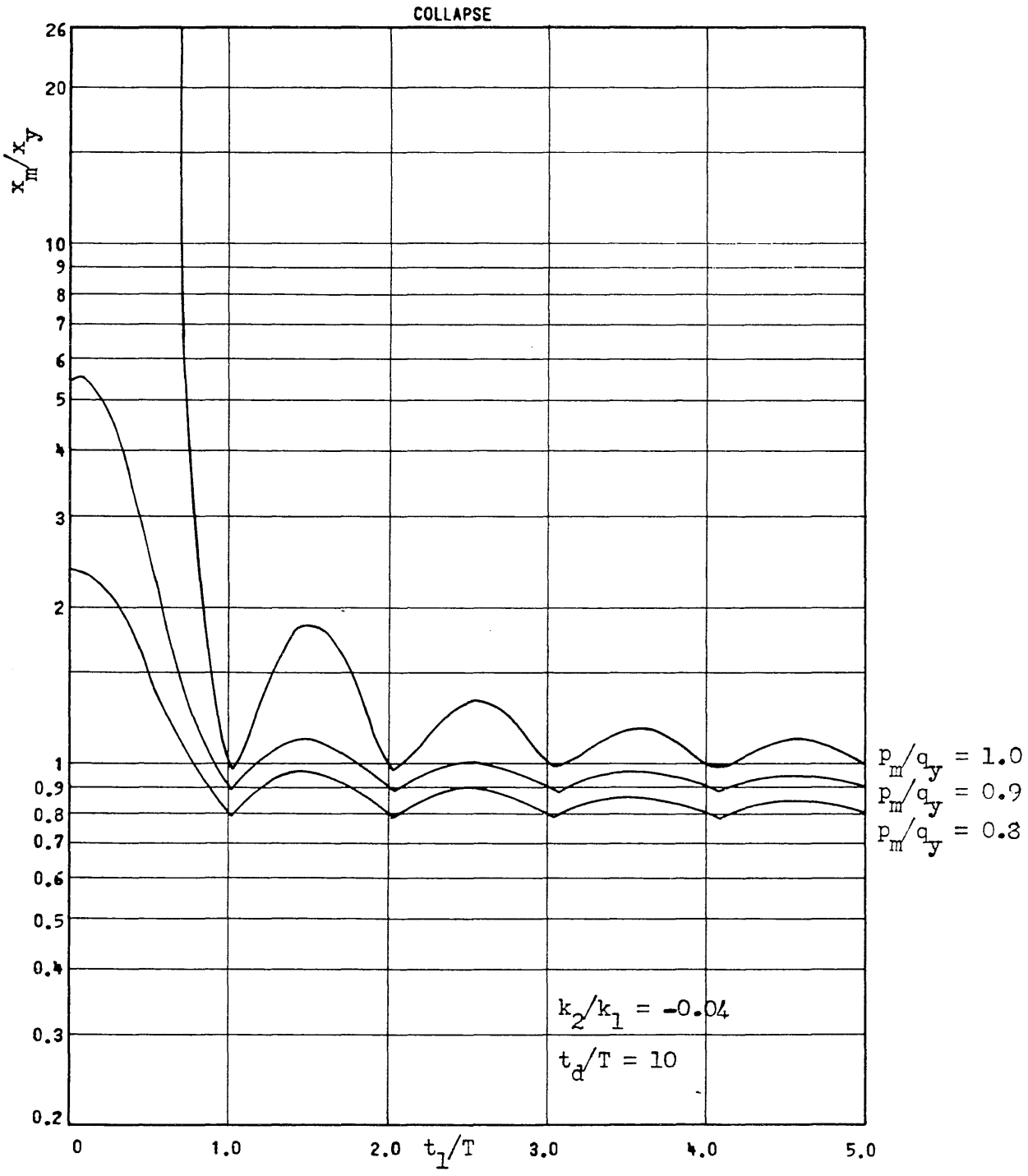

Fig. 44 Maximum Response Versus Rise Time for Delayed Rise Triangular Force Pulse with Various Bilinear Resistances

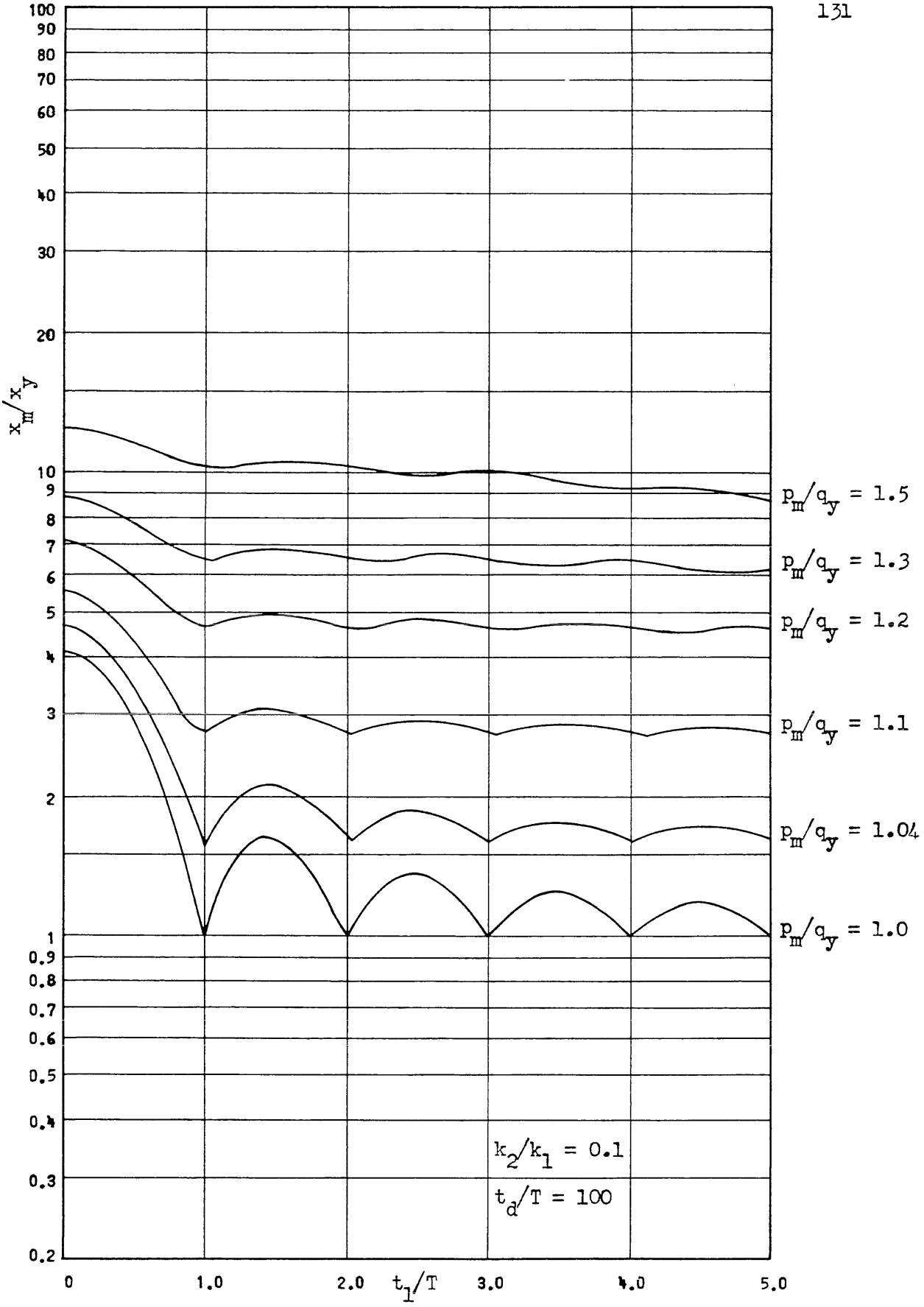

Fig. 45 Maximum Response Versus Rise Time for Delayed Rise Triangular Force Pulse with Various Bilinear Resistances

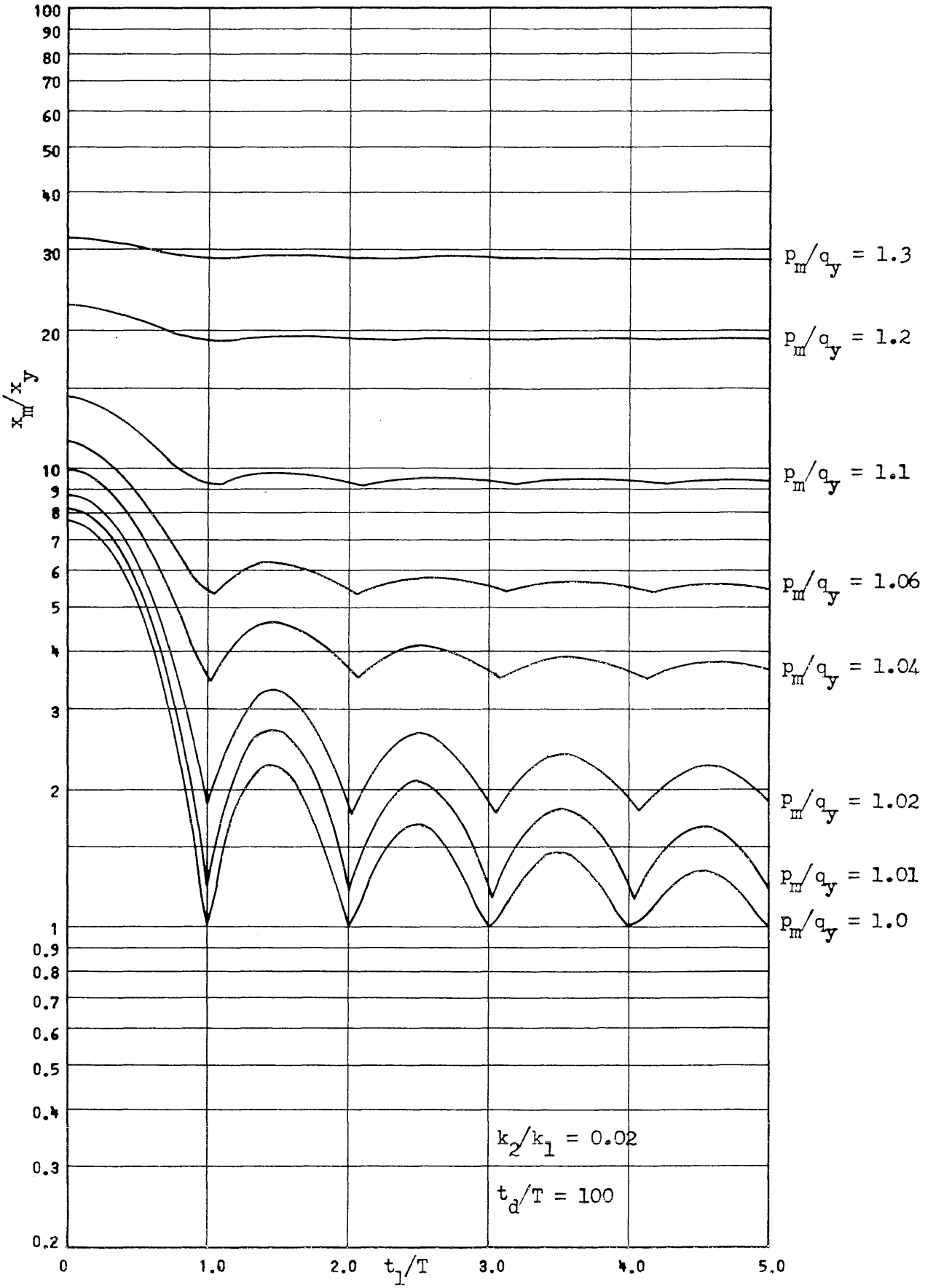

Fig. 46 Maximum Response Versus Rise Time for Delayed Rise Triangular Force Pulse with Various Bilinear Resistances

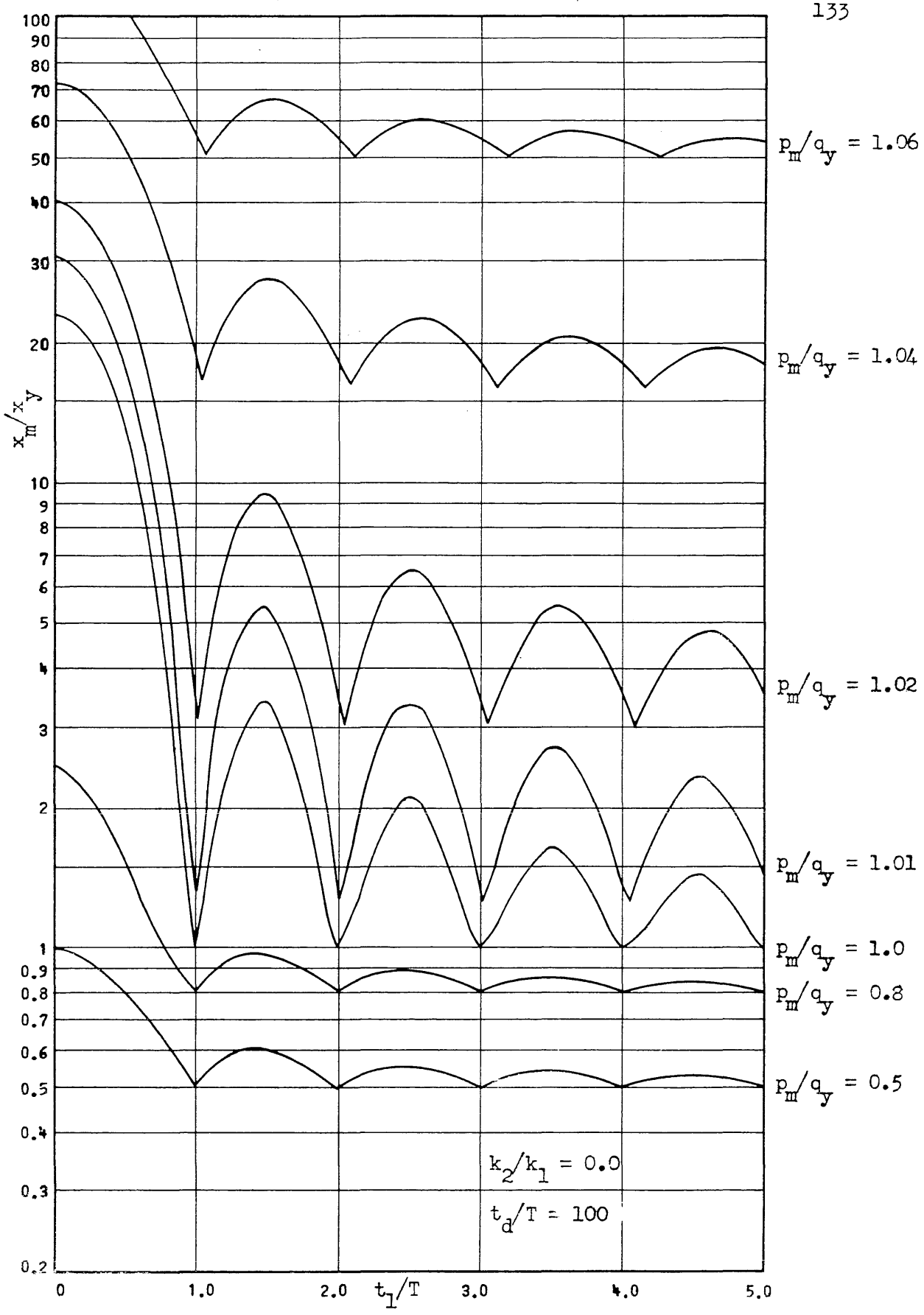

Fig. 47 Maximum Response Versus Rise Time for Delayed Rise Triangular Force Pulse with Various Bilinear Resistances

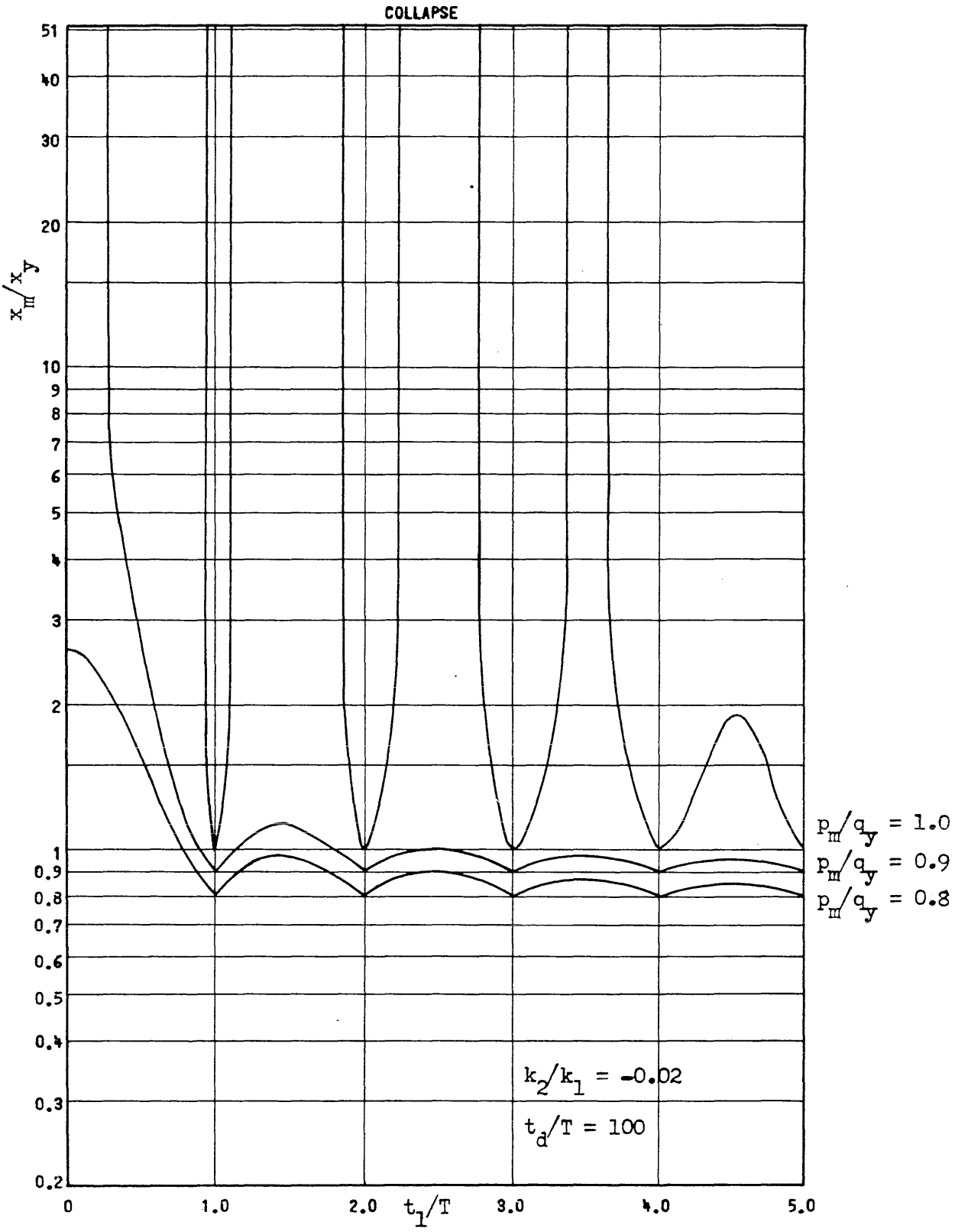

Fig. 48 Maximum Response Versus Rise Time for Delayed Rise Triangular Force Pulse with Various Bilinear Resistances

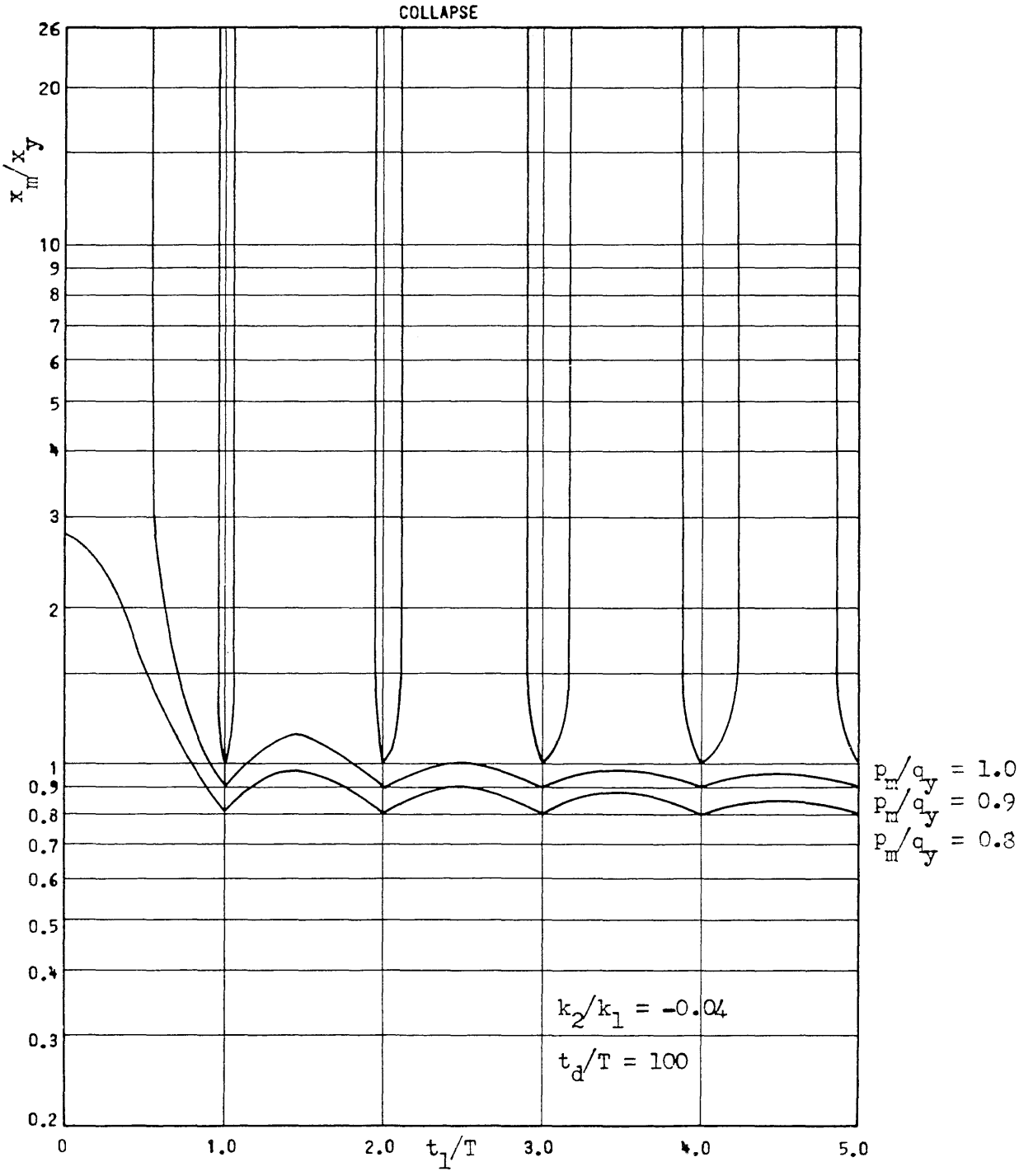

Fig. 49 Maximum Response Versus Rise Time for Delayed Rise Triangular Force Pulse with Various Bilinear Resistances

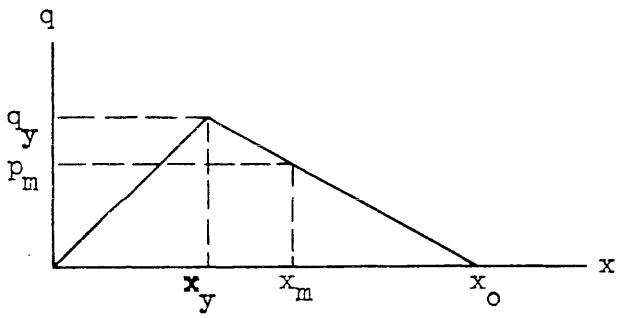

Fig. 50a Unstable Bilinear Resistance

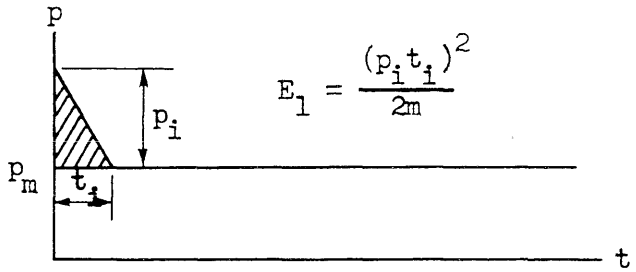

50b Force Pulse

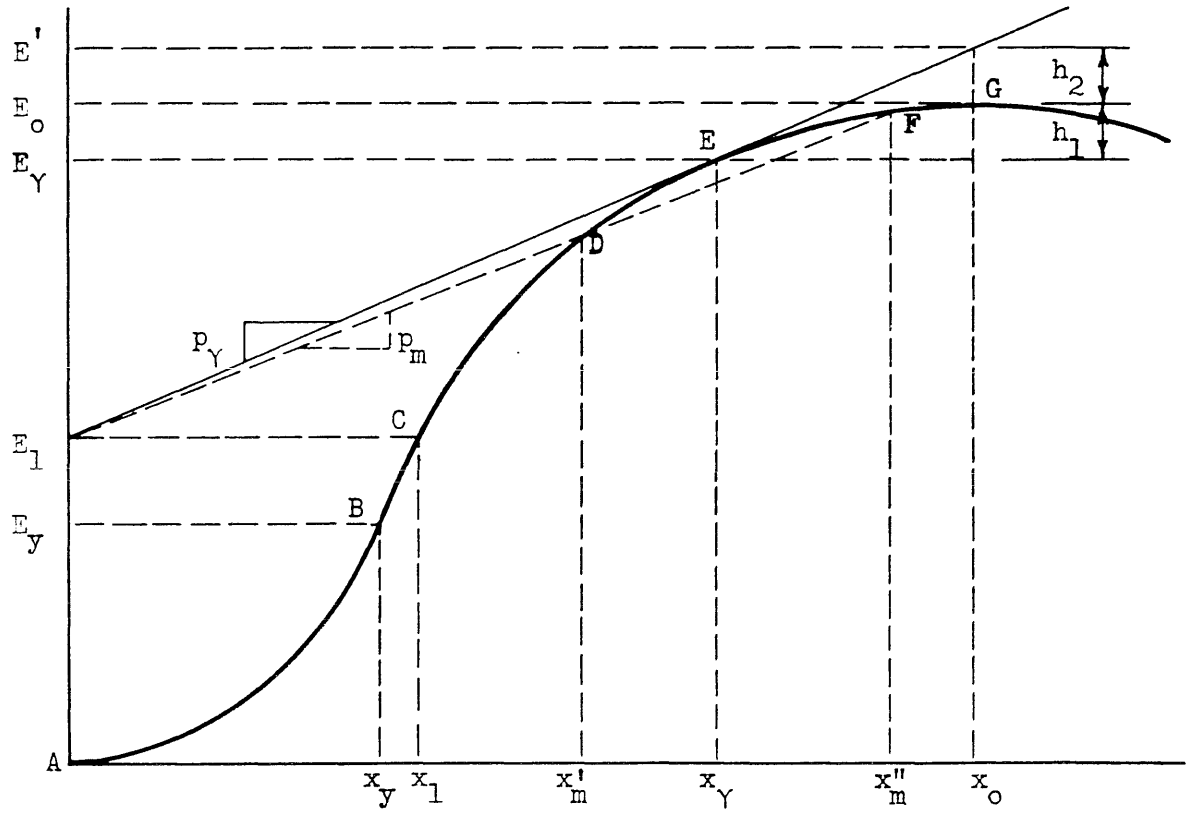

Fig. 51 Energy Level Versus Response

DISTRIBUTION

Copy No.	Recipient
	AIR FORCE
1-9 (With Master Copy)	Director of Intelligence Headquarters, USAF ATTN: Deputy Director for Targets Physical Vulnerability Division, AFOIN-3B Washington 25, D. C.
10, 11	Commander Air Research and Development Command P. O. Box 1395 ATTN: Office of Deputy for Development Baltimore 3, Maryland
12	Commander Tactical Air Command Langley Air Force Base, Virginia
13	Commander Strategic Air Command Offutt Air Force Base ATTN: Director of Intelligence Omaha, Nebraska
14	Commander Strategic Air Command Offutt Air Force Base ATTN: Operations Analysis Office Omaha, Nebraska
15	Commanding General Air University Maxwell Air Force Base ATTN: Air University Library Montgomery, Alabama
16	Deputy Chief of Staff, Operations Operations Analysis Division Washington 25, D. C.
17	Chief, Structures Division Research Directorate Air Force Special Weapons Center ATTN: SWRS, Eric H. Wang Kirtland Air Force Base, New Mexico

Copy No.	Recipient
	AIR FORCE
18	Deputy Chief of Staff, Development Director of Research and Development Headquarters, USAF Washington 25, D. C.
19	Deputy Chief of Staff, Operations Assistant for Atomic Energy Headquarters, USAF Washington 25, D. C.
20	Deputy Chief of Staff, Material Director of Industrial Resources Headquarters, USAF Washington 25, D. C.
21	Commander Air Force Cambridge Research Center 230 Albany Street ATTN: ERHS-1, Geographical Res. Library Cambridge 39, Massachusetts
22	Commander Air Force Special Weapons Center Kirtland Air Force Base Albuquerque, New Mexico
	ARMY
23	Department of the Army Office, Chief of Engineers Engineering Division Protective Construction Branch Washington 25, D. C.
24	Department of the Army Ballistic Research Laboratories ATTN: Dr. Lampson Aberdeen Proving Ground, Maryland
25	Department of the Army Office of the Secretary of the Army ATTN: Director, Army Library Washington 25, D. C.

Copy No.	Recipient
	ARMY
26	Commanding Officer Engineering Research and Development Laboratory Ft. Belvoir, Virginia
27	Department of the Army Office of Asst. Chief of Staff, G-3 ATTN: ORO Liaison Officer Washington 25, D. C.
	NAVY
28	Naval Ordnance Laboratory ATTN: Dr. G. K. Hartmann White Oak, Maryland
29	Chief of Naval Operations Office of Naval Intelligence ATTN: OP922V1B Washington 25, D. C.
30	Bureau of Yards and Docks Department of the Navy Washington 25, D. C.
31	Office of Naval Research Department of the Navy ATTN: Mathematical Sciences Division Washington 25, D. C.
	JOINT MILITARY GROUPS
32, 33	Document Service Center Armed Services Technical Information Agency Knott Building Dayton 2, Ohio
34	Commander Armed Forces Special Weapons Project Sandia Base Post Office Box 5100 ATTN: Research and Development Division Albuquerque, New Mexico

Copy No.	Recipient
JOINT MILITARY GROUPS	
35	Director Weapons Sytems Evaluation Group Office of the Secretary of Defense Room 2E995, the Pentagon Washington 25, D. C.
36	Chief Armed Forces Special Weapons Project Post Office Box 2610 ATTN: Col. D. L. Lay Washington 25, D. C.
37	Assistant Secretary of Defense Research and Development Washington 25, D. C.
OTHER ORGANIZATIONS	
38	Dr. R. J. Hansen Department of Civil and Sanitary Engineering Massachusetts Institute of Technology Cambridge 39, Massachusetts
39, 40	Armour Research Foundation Illinois Institute of Technology Technology Center 35 West 33rd Street Chicago 16, Illinois
41	The Rand Corporation 1700 Main Street ATTN: Mr. Marc Peter Santa Monica, California
42	Chairman U.S. Atomic Energy Commission 1901 Constitution Avenue NW ATTN: Dean H. L. Bowman Civil Defense Liaison Branch Division of Biology and Medicine Washington 25, D. C.
43	Sandia Corporation - 5112 Sandia Base ATTN: Dr. J. D. Shreve Albuquerque, New Mexico

Copy No.	Recipient
	OTHER ORGANIZATIONS
44	American Machine and Foundry Company Mechanics Research Department 1104 South Wabash Avenue Chicago 5, Illinois
45	Security Office Engineering Research Institute University of Michigan ATTN: Professor Bruce G. Johnston Ann Arbor, Michigan
	UNIVERSITY OF ILLINOIS
46, 47	Dr. N. M. Newmark
48	J. W. Melin
49	J. E. Stallmeyer
50	W. J. Hall
51	J. M. Massard
52	R. J. Mosborg
53	G. K. Sinnamon
54	W. H. Munse
55	J. L. Merritt
56	J. D. Haltiwanger
57	A. S. Veletsos
58	W. J. Austin
59-100	U. of I. Reserve